CZECH TECHNICAL UNIVERSITY IN PRAGUE

Faculty of Civil Engineering
Department of Building Structures

Sorption properties of clay materials

DOCTORAL THESIS

Ing. Jakub Diviš

Ph.D. Programme:	Civil Engineering
Branch of Study:	Building Engineering
Supervisor:	prof. Ing. Petr Hájek, CSc., FEng.
Supervisor specialist:	Ing. Jan Růžička, Ph.D.

Prague, 2021

ČESKÉ VYSOKÉ UČENÍ TECHNICKÉ V PRAZE

Fakulta stavební
Thákurova 7, 166 29 Praha 6

Prohlášení

Jméno doktoranda: Ing. Jakub Diviš

Název disertační práce: Sorption properties of clay materials

Prohlašuji, že jsem uvedenou disertační práci vypracoval samostatně pod vedením školitele prof. Ing. Petra Hájka, CSc., FEng. a školitele-specialisty Ing. Jana Růžičky, Ph.D.

Použitou literaturu a další materiály uvádím v seznamu použité literatury.

V textu jsou použity úryvky z autorských článků a konferenčních příspěvků, a to převážně v kapitolách popisující průběhy prováděných experimentů.

Disertační práce vznikla v souvislosti s řešením projektů:

- SGS14/113/OHK1/2T/11: "Analysis and optimization of properties of natural building materials effecting quality of interior microclimate of buildings";
- SGS16/129/OHK1/2T/11: "Hydrophobic modification of natural materials in order to preserve the original sorption and thermal-technical properties";
- SGS17/009/OHK1/1T/11: "Technological, Economical and Structural Evaluation of Environmentally Friendly Straw-bale Experimental Object Realisation and Analysis of its Fire Characteristics";
- SGS18/106/OHK1/2T/11: "Application of current experimental data for creating numerical models of rammed earth using a finite element method (FEM) to predict mechanical behaviour";

V Praze dne 30. dubna 2021 ……

podpis

Acknowledgements

Above all, I would like to thank my supervisor Petr Hájek and my supervisor specialist Jan Růžička for introducing me to the world of scientific research and passing on advice and experience during the entire study and course of research.

I would also like to thank Filip, who was a great advisor to me at the beginning of my doctoral studies and helped me with orientation in research, grants, publications, etc. Honza was also a great helper, always willing to consult with me on various hygrothermal issues. I must also mention the technicians Honza and Radim and thank them for their help with preparing some experiments.

A huge thank you also goes to my colleagues from the faculty and UCEEB, who have always created a pleasant friendly environment. Hopefully, the amount of coffee drunk will not affect our health!

Special thanks belong to Kateřinka for help in the statistical evaluation of the results, Káč for help with formatting and graphic editing of the text, and Robert for English proofreading of the thesis. It would simply not be possible without these three people.

In conclusion, I would like to express my gratitude and thanks to my family for their support during my very long studies. I probably would not have enjoyed it without their understanding, help, support, and the constant question "*When will you submit your dissertation?*". In less than eight years I managed to engender this thesis, but I am much prouder that I engendered two great offspring.

Abstract

Global solutions to the impact of human activity on the environment, slowing climate change, reducing CO_2 emissions, reducing the consumption of non-renewable energy, and saving strategic raw materials are also significantly reflected in the construction industry. Great pressure is beginning to be put on the use of low-carbon building materials and the reduction of embodied and operational energy in buildings. Similarly, in recent years, the society has focused on a healthy indoor environment in buildings because people spend most of the day indoors. Assessing the complex quality of buildings in terms of sustainable construction is becoming a common part of the design and implementation process in many developed countries.

The use of low-carbon materials can reduce the negative impact of construction on the environment. An appropriate combination of these materials and an optimized project solution will save non-renewable strategic raw materials and reduce primary energy consumption and CO2 emissions. And finally, a high-quality microclimate in the interiors of buildings can be ensured.

Materials and structures made of unfired clay are among the natural low-carbon materials. In this work, their influence on the quality of the interior environment of buildings with respect to the relative humidity of enclosed air was investigated. This is one of the important parameters of the quality of the indoor environment of buildings.

This thesis is divided into three consecutive parts. First, the sorption properties of selected building materials were investigated. Materials commonly available and used on the Czech market, as well as those from unfired clay and clay structure products were examined. Measurements were performed on small samples at steady state. The resulting sorption isotherms are one of the parameters for comparing the sorption properties and the parameters entering the mathematical modelling of humidity in the solid structure and open interior.

Materials with small dimensions, moreover measured at steady state, do not necessarily testify to the behaviour of entire building constructions in the real environment, as the influence of surface and surface treatments, structural joints, etc. are considered as well. Such an environment never reaches a steady state and all hygrothermal processes are dynamic over time. Therefore, a total of six building structures were selected on which further experiments were performed. It was a group of standard, commonly used building structures (exposed concrete wall; ceramic block wall with lime plaster; and gypsum board partition wall) and a group of structures made of clay materials (rammed earth wall; fair-face brickwork from unburned clay hollow blocks; and wall of unburned clay hollow blocks with clay plaster).

To determine the porous nature of these selected structures, another sorption analysis was performed according to the BET method. Subsequently, an experimental methodology for dynamic adsorption and desorption properties was proposed. Selected building structures were experimentally measured in a climatic chamber, and the humidity response of the indoor environment, to a sharp increase in relative humidity in the interior, was investigated. These measurements were repeated three times to obtain the necessary relevant data set for subsequent statistical evaluation.

Statistical analysis of the performed experiments consisted in determining the confidence interval of measuring dynamic sorption properties and their subsequent comparison. An analysis of the dynamics rate of adsorption and desorption processes was also performed.

The resultant conclusions took into account not only the measured and evaluated data but also a broader view of the use of clay materials in construction.

Keywords: clay materials, relative humidity, interior microclimate, sorption, moisture buffering

Abstract in Czech

Celosvětová tématika o dopadu lidských činností na životní prostředí, globální oteplování, snižování emisí CO_2, snižování spotřeby neobnovitelné energie, úspora strategických surovin aj. se samozřejmě výrazně promítá i do oboru stavebnictví. Začíná být velký tlak na využívání nízkouhlíkových stavebních materiálů a snižování svázané i provozní energie v budovách. Stejně tak se v posledních letech společnost zaměřuje na zdravé vnitřní prostředí v budovách, neboť lidé ve vnitřních prostorách tráví převážnou část dne. Hodnocení komplexní kvality budov z pohledu udržitelné výstavby se stává v řadě vyspělých zemí běžnou součástí projekčního a realizačního procesu.

Využíváním kvalitních nízkouhlíkových materiálů se může snížit negativní dopad stavebnictví na životního prostředí. Při vhodné kombinaci těchto materiálů, a optimalizovaným projektovým řešením, dojde k úspoře neobnovitelných strategických surovin, snížení spotřeby primární energie a vyprodukovaných emisí CO2. V neposlední řadě bude zajištěno kvalitní vnitřní mikroklima v interiéru budov.

Materiály a konstrukce z nepálené hlíny se řadí mezi přírodní nízkouhlíkové materiály. V této práci byl zkoumán jejich vliv na kvalitu vnitřního prostředí budov s ohledem na relativní vlhkost vnitřního vzduchu. To je jeden z významných parametrů kvality vnitřního prostředí v budovách.

Práce byla rozdělena na tři navazující části. Nejprve byly zkoumány sorpční vlastnosti vybraných stavebních materiálů. A to jak běžně dostupných a využívaných na českém trhu, tak i materiálů z nepálené hlíny a hliněných stavebních produktů. Tato měření probíhala na malých vzorcích v ustáleném stavu. Výsledné sorpční izotermy jsou jedním z parametrů pro porovnávání sorpčních vlastností a parametrů vstupujících do matematického modelování vlhkosti v konstrukci a interiéru.

Materiály o malých rozměrech, navíc měřených v ustáleném stavu, nemusí mít správnou vypovídající hodnotu o chování celých konstrukcí budov (vliv povrchu a povrchových úprav, konstrukční spáry, aj.) v reálním prostředí. Takové prostředí nikdy nedosáhne ustáleného stavu a všechny tepelně-vlhkostní procesy jsou v čase dynamické. Proto bylo vybráno celkem 6 stavebních konstrukcí, na kterých byly provedeny další experimenty. Jednalo se o skupinu standardních, běžně užívaných stavebních konstrukcí (stěna z pohledového betonu, stěna z keramických cihel omítnutá vápennou omítkou a sádrokartonová příčka) a skupinu konstrukcí z jílových materiálů (stěna z dusané nepálené hlíny, stěna z režného zdiva z nepálených hliněných cihel a stěna z nepálených hliněných cihel omítnutá hliněnou omítkou).

Pro stanovení porézní struktury těchto vybraných konstrukcí byla provedena BET analýza, jejíž výsledky upřesnily provedené sorpční experimenty. Následně byla navržena metodika experimentu dynamických adsorpčních a desorpčních vlastností. Zvolené stavební konstrukce byly experimentálně měřeny v klimatické komoře a byla zkoumána vlhkostní odezva vnitřního prostředí na prudké zvýšení relativní vlhkosti v interiéru. Tato měření byla třikrát opakována pro získání potřebné relevantní sady dat pro následné statistické vyhodnocení.

Statistická analýza provedených experimentů spočívala ve stanovení intervalu spolehlivosti měření dynamických sorpčních vlastností a jejich následné porovnání. Byla provedena také analýza samotné míry dynamiky adsorpčních a desorpčních procesů.

Následné vyhodnocení uvádí do kontextu nejen naměřená a vyhodnocená data, ale také širší pohled na využití jílových materiálů ve stavebnictví.

Klíčová slova: materiály z nepálené hlíny, jíly, relativní vlhkost, vnitřní prostředí, sorpce, tlumení vlhkosti

List of abbreviations

Abbreviation	Explanation
CTU	Czech Technical University in Prague
FCE	Faculty of Civil Engineering
UCEEB	University Centre for Energy Efficient Buildings
UCT	University of Chemistry and Technology, Prague
WHO	World Health Organization
IUPAC	International Union of Pure and Applied Chemistry
WHEAP	World Heritage Earthen Architecture Programme
CMS	Clay Minerals Society
SDG	Sustainable Development Goals
SBS	Sick Building Syndrome
BET	Brunauer-Emmett-Teller theory
RH	Relative Humidity
STP	Standard temperature and pressure
MBV	Moisture Buffer Value
AIC	Akaike Information Criterion
RMSE	Root Mean Squared Error
RSS	Residual Sum of Squares
SSR	Regression sum of squares
SSE	Error sum of squares
SST	Total sum of squares
R^2	Coefficient of determination
P	Probability
SGS	Student Grant Competition
C	Commercial clay mixture Claygar
S	Sand
W	Water
K	Kaolinite
Z	Zeolite
I	Illite
M	Montmorillonite
HPC	High performance concrete

Nomenclature

Symbol	Explanation	Unit
A	Area	m^2
a	Slope of the curve	-
MBV	Moisture buffer value	$kg \cdot (m^2 \cdot \%RH)^{-1}$
m	Degree of the polynomial	-
m	Weight	kg, *or* g
n	Number of observation/sample size	-
p	Partial water vapour pressure	Pa
p_{sat}	Saturation vapour pressure	Pa
R_V	Specific gas constant	$J \cdot kg^{-1} \cdot K^{-1}$
RH	Relative humidity	%, *or* -
r	Number of samples	-
S_{BET}	Specific surface area	$m^2 \cdot g^{-1}$
T	Temperature	°C, *or* K
t	Time	s, *or* min
u	Moisture content mass by mass	$kg \cdot kg^{-1}$
V	Volume	m^3
V_L	Langmuir maximum adsorption capacity	$cm^3 \cdot g^{-1}$
v	Vapour density/concentration	$kg \cdot m^{-3}$
v_{sat}	Saturation vapour density	$kg \cdot m^{-3}$
w	Moisture content mass by volume	$kg \cdot m^{-3}$
α	Confidence level/reliability factor	-
β	Regression coefficient	-
μ	Vapour diffusion resistance	-
v	Degree of freedom	-
ρ	Density	$kg \cdot m^{-3}$
ψ	Porosity	%

Contents

1 Introduction

1.1 Motivation

In recent years, investors, architects, designers, and also ordinary users have become more interested in the use of natural building materials in construction. Their applications can be both traditional proven technology of our ancestors and current thanks to modernization and research in the field. The main advantages of using natural materials include their low impact on the environment due to their renewable nature, their ability to increase user comfort, and their health benefits to the population.

Not only environmental activists, but also top officials are dealing with the impact of human activities on the environment. The world's most important documents / agreements are The Sustainable Development Goals and the European Green Deal. Responses to the current state of nature and society and goals for the future are set in these documents.

The Sustainable Development Goals

The Sustainable Development Goals (SDGs) represent the development agenda for the years (2015–2030) and follow the Millennium Development Goals (MDGs) agenda. The Sustainable Development Goals are the result of a three-year negotiation process that began in 2012 and was formulated by all UN member states, civil societies, businesses, academia and citizens from all continents. The Sustainable Development Agenda was officially endorsed by the UN Summit in 2015 in the document Transforming our World: The 2030 Agenda for Sustainable Development, which also includes 17 Sustainable Development Goals (SDGs), see Fig. 1. [1]

Fig. 1 The 17 Sustainable Development Goals [1]

The agenda is based on three pillars – economic, social, and environmental. These pillars are inextricably linked and complementary. The main topics are People, Planet, Prosperity, Peace and Partnership.

The goal of sustainable development in construction is to reduce the energy cost of buildings, use natural and environmentally friendly materials, use recycled and recyclable materials, use energy from renewable sources, protect biodiversity, and reduce the environmental impact of the building throughout its life cycle.

The European Green Deal

Another important document dealing with the impact of human activities on the environment is The European Green Deal (Fig. 2). The atmosphere is warming; the climate is changing; one million of the eight million species on the planet are at risk of being lost; forests and oceans are being polluted and destroyed.

The constructions and reconstructions of buildings require a considerable amount of energy and mineral resources (e.g., sand, gravel, and cement components). Obviously, these minerals are depletable and their reserves are declining sharply. Up to 40 % of the total world energy consumed is used for the construction, renovation, and operation of buildings.

The aim of this deal is to protect, conserve and enhance the EU's natural resources while reducing emissions and protecting the health and well-being of citizens from environment-related hazards. [2]

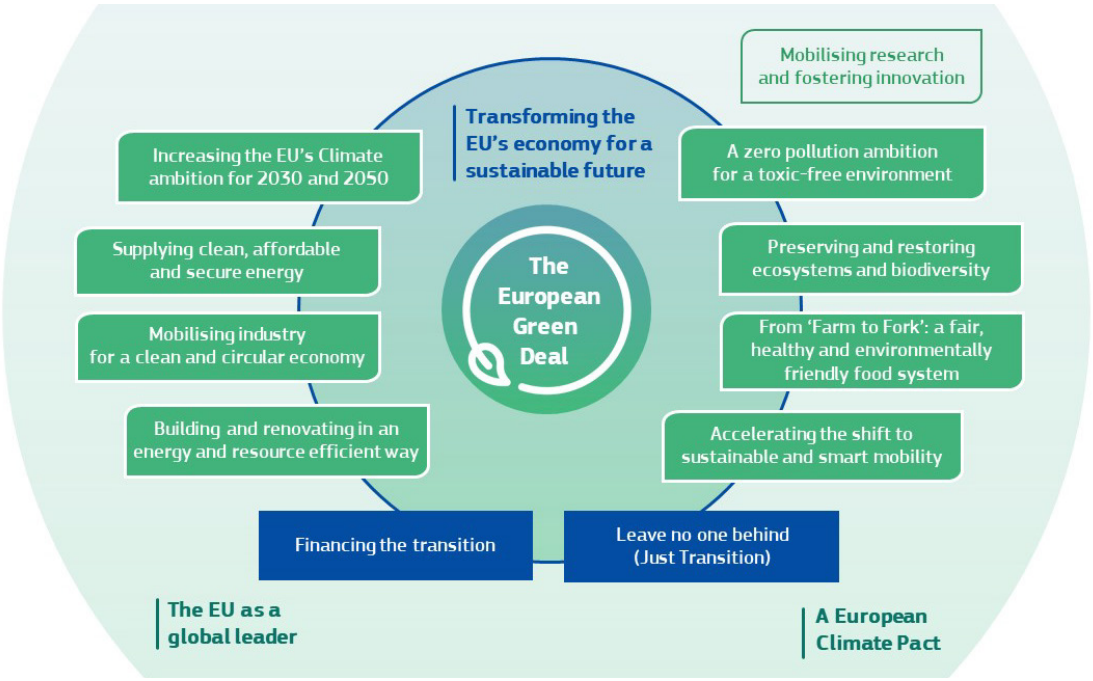

Fig. 2 The European Green Deal [2]

This dissertation thesis was created in accordance with these documents and the efforts to promote responsible and sustainable construction. It deals with natural materials (mainly clay materials), their impact on the quality of the indoor environment, and the potential for reducing energy consumption through the use of these materials as passive elements.

1.2 Thesis statement

The fundamental principles of sustainable building construction are based on three basic pillars: environmental, social and economic. One important indicator is the relative humidity of the indoor environment, a part of the social pillar dealing with the quality of the indoor microclimate. Low humidity

level can cause dry throat, nasal passages and skin, while high relative humidity level can lead to growth of moulds, multiplication of bacteria and can cause water condensation problems on cold surfaces.

Appropriate levels of relative humidity in the interior of buildings can be maintained by building service systems, however, this increases the operating energy in buildings and is sensitive to and dependent on proper operation, settings, control, and monitoring. Due to frequent climate fluctuations, the amount of energy consumed by technical equipment for humidity control in building interiors is also increasing significantly. The worldwide tendency is to reduce operational energy consumption, so it is appropriate to use passive principles to regulate internal relative humidity in buildings.

The relative humidity in the interior can be stabilized by the choice of suitable building structures and structural materials with no operational energy consumption. Unfired clay materials are said to have good sorption properties that are suitable for passive moisture control. Clay materials have superior sorption properties due to their pore system and the properties of inherent minerals. In addition, unfired clay materials have a far lower negative impact on the environment than standard building materials.

The primary aim of this thesis is to investigate the influence of clay building materials on the quality of the indoor environment and to verify the potential for reducing energy consumption when using these materials as passive elements. The thesis compares selected clay building materials with materials commonly used in construction. The goal then is to quantify the measured results and evaluate them on the basis of various analyses.

Relevant research questions include: Can the sorption properties of clay materials be suitably applied as a passive solution for internal relative humidity regulation? Are the existing moisture buffer experiments suitable for describing the dynamic behaviour of moisture transport in real conditions? How can the dynamic sorption behaviour of air humidity in the interior be appropriately presented? What are the measurement uncertainties with respect to the inhomogeneous structure of clay materials?

1.3 Methods

The thesis summarizes the latest research on the influence of building structures and structural materials on the relative humidity in the indoor environment of buildings (Fig. 3).

The first experiments focus on the sorption properties of materials in a steady state. Sorption isotherms are measured on various clay mixtures and clay products, other natural building materials, and typical standard building materials (reference values for comparison). Measurements of pore system parameters were performed on selected building structures. The results of the measurement describe the properties of the building materials (sorption isotherm and specific surface area).

The next set of experiments test the dynamic behaviour of building structures. Different structures were tested and their potential to influence humidity in the indoor environment were assessed. The key part is the statistical evaluation of the measured data. The performed analysis takes into account the measurement uncertainty and inhomogeneity of the selected building structures.

All measurements of clay materials and structures were compared with commonly used building materials and structures.

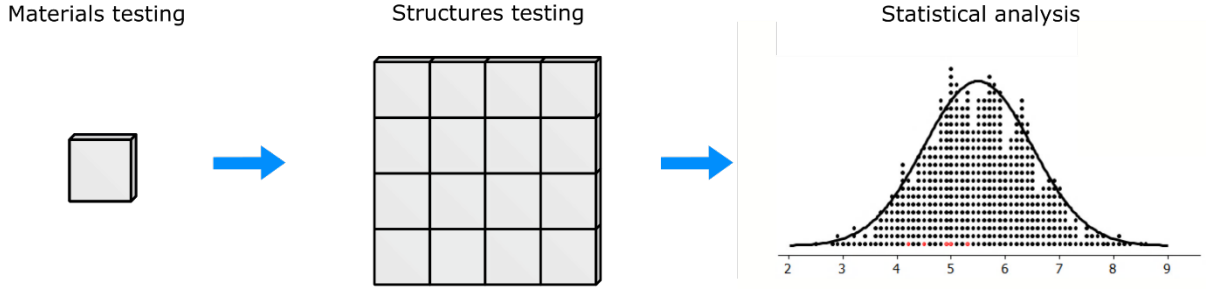

Fig. 3 Research structure

1.4 Follow-up to projects

This thesis follows the research and grants of researchers and students from the Department of Building Structures at the Czech Technical University in Prague which focus on natural materials. Connections are made with the following projects (divided according to the participation of the author of this thesis):

Principal Investigator:

- SGS14/113/OHK1/2T/11: "Analysis and optimization of properties of natural building materials effecting quality of interior microclimate of buildings";
- SGS16/129/OHK1/2T/11: "Hydrophobic modification of natural materials in order to preserve the original sorption and thermal-technical properties";
- SGS18/106/OHK1/2T/11: "Application of current experimental data for creating numerical models of rammed earth using a finite element method (FEM) to predict mechanical behaviour";

Co-Investigator:

- SGS17/009/OHK1/1T/11: "Technological, Economical and Structural Evaluation of Environmentally Friendly Straw-bale Experimental Object Realisation and Analysis of its Fire Characteristics";

Previous projects:

- SGS11/101/OHK1/2T/11: "Development and Experimental Verification of Mechanical-physical Properties of Pre-formed Rammed Earth Wall Panel";
- SGS13/010/OHK1/1T/11: "Influence of raw natural clays to indoor quality according to the mineralogical composition and boundary conditions of the mathematical model of the zone";
- Ministry of Industry and Trade of the Czech Republic, Program Efekt 122142 0507: "Selected Properties of Natural and Others Structural Materials, Structures and Buildings";
- MŠMT ČR 1M0579 – RIV/68407700:21110/07:01138078: „Prefabricated Load Bearing Wall Panels – Effective Technologies for Earth Structures;

Following the doctoral thesis:

- RŮŽIČKA, Jan. Influence of Way of Stabilization of Unburned Bricks on Mechanical Physical Properties. 2006 [3];
- HAVLÍK, Filip. Development and Experimental Verification of Mechanical-physical Properties of Pre-formed Rammed Earth Wall Panel. 2015 [4].

2 Problem description and current state of the solved topic

This work deals mainly with the sorption properties of clay materials and their effect on relative humidity in the indoor environment. The initial search was therefore divided according to individual subtopics dealing with the indoor air quality, the transport of water vapour in porous building materials, clay and its properties, and utilization of sorption properties in constructions and architecture.

In this chapter, some author's formulations published in journals or conference papers are used. These are listed in the references.

2.1 Indoor air quality

Modern people spend most of their time inside buildings. Many surveys show (Fig. 4) that nowadays people spend almost 90 % of the time in residential buildings, offices, schools, day-care centres, and other building facilities. For this reason, it is essential to focus on the quality of the internal environment. This also means that if occupants are unwell, they may suffer symptoms and discomfort while indoors, some of which may be related to the buildings they occupy.

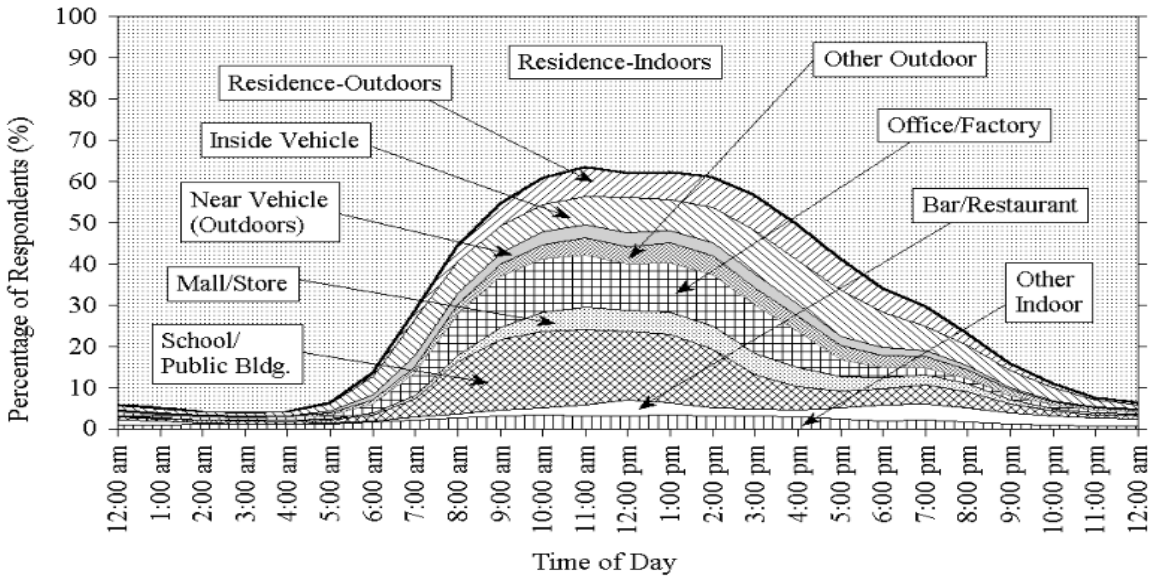

Fig. 4 Time spent in buildings [5]

An important topic at present is the quality of the indoor environment of buildings. Indoor air quality (IAQ) depends on many factors: outdoor air quality, amount of air pollutants, ventilation air volume, and the ventilation system. In most cases, the air quality in buildings is worse than the air quality in the

outdoor environment. Currently, there is an effort to make an energy-efficient building with a healthy indoor environment.

Of course, the quality of indoor air depends on the quality of outdoor air, as ventilation supplies outdoor air to buildings. Outdoor air ventilation removes pollutants generated in the building, but allows in pollutants from the outdoor air. Deteriorated ambient air quality is primarily the result of energy consumption in transportation and industry and in building construction. Pollutants associated with the operation of buildings account for about 40 % of the total pollutant production, of which ventilation accounts for up to 50 % of that amount. [6]

Ventilation of buildings requires air treatment for most of the year: heating, cooling, humidification, and dehumidification. In the case of forced ventilation, it requires energy to transport air. The total energy consumed in this way will cause a further increase in external pollution. Outdoor pollution can have various impacts depending on the extent to which it is reflected; regional (SO_2, NO_x) or global (CO_2). [7]

2.1.1 Sick Building Syndrome

A technical term describing the situation where people in buildings suffer from symptoms of illness or feel unwell for no apparent reason is described as Sick Building Syndrome (SBS). Symptoms often get worse with time when people spend time in buildings and improve or disappear when people are out of the building.

SBS leads not only to serious health issues but also to socio-economic problems. Job performance is compromised; productivity loss is significant. It causes reduced work performance and increased absenteeism resulting in a total cost which may well be in the range of 0.5–1.0 % of GNP [8]. In extreme cases, the personal relationships of inhabitants may also be compromised.

Sick building syndrome is widespread and may occur in all types of buildings – residential and office buildings, schools, etc. SBS problems are estimated at up to 30 % of new, rebuilt or refurbished buildings. The most common SBS symptoms are the following [8]:

- neurotic effects – lethargy, headaches, fatigue, lack of concentration, irritability, enhanced or abnormal odour perception;
- mucous-membrane irritation – throat and nose irritation, cough, shortness of breath, stuffy nose, dry throat, runny or blocked nose (sometimes described as congestion, nosebleeds, itchy or stuffy nose), dry or sore throat (sometimes described as irritation, upper airway irritation or difficulty swallowing);
- asthma and asthma-like symptoms – difficulty in breathing, wheezing, and chest tightness;
- irritated, dry or watering eyes (sometimes described as itching, tiredness, redness, burning, or difficulty wearing contact lenses);
- skin symptoms – dryness, pruritus, rash, itching, or irritation of the skin, occasionally with a rash, less specific symptoms such as headache, lethargy, irritability, and poor concentration;
- flu-like symptoms.

Typically, several of these symptoms are experienced simultaneously and they are often accompanied by complaints of stuffiness, poor air, dry air, noise, light, or temperatures which are too hot or too cold. The severity of these symptoms and their frequency depend on the quality of the design of the building, the indoor environment, and its equipment.

The SBS causes have been recognized in connection with inappropriate building design, influence of materials used in buildings and furniture, interior equipment (copiers, computers, etc.), insufficient air exchange and ventilation, and high concentrations of CO_2, VOC, and other gases. The quality of the indoor environment is degraded by the following [9]:

- unsuitable lighting, colour temperature, etc.;
- unsuitable heating: elevated indoor temperature, dry air;
- poor acoustics;

- unsuitable air exchange and ventilation: microbes and mites in air-handling units, toxic moulds, chemical and biological pollution, and accumulation of potentially dangerous gases.

2.1.2 Indoor microclimate

A building environment created for human occupation in enclosed spaces can be characterized as an indoor microclimate. It can be divided into the following constituents: hygrothermal microclimate; air quality (odor, toxic, aerosol, microbial); ionizing; electrostatic; electromagnetic; electronic; acoustic; lighting; and psychological microclimate.

Each constituent level is assessed on the basis of its physiological and psychological strain on humans, the effects being variable. The following figure (Fig. 5) shows the meaning of some selected components. [10]

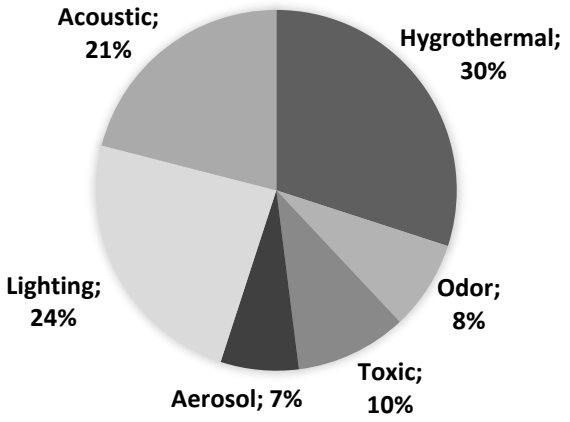

Fig. 5 Chosen constituents of the indoor microclimate and their influence

The **hygrothermal microclimate** is a component of the environment formed by heat and humidity fluxuations. It is the most important component for ensuring the internal environment of buildings, especially in terms of human health and happiness, but also in relation to the life of the building materials. Temperature and humidity in buildings closely interact and reinforce each other.

Thermal comfort is a traditional factor in assessing the state of the indoor environment. Thermal well-being can be characterized as a state where the environment deprives a person of his heat production in the range of his thermoregulation. The optimal thermal-humidity state of the indoor environment is important not only for human health but also for the proper functioning of the building itself. Due to the individual variations in the physiological functions of people, it is not possible to ensure a feeling of well-being in the room for all occupants. There is always about 5 % dissatisfaction rate due to thermal discomfort [11].

Factors determining the hygrothermal comfort of the environment:

- air temperature;
- thermal radiation;
- air velocity;
- air humidity;
- thermal insulating properties of clothing;
- human physical activity.

The **light microclimate** is created by the geometric dimensions of the space, method of lighting, type and location of luminaires, lighting levels and their uniformity in different planes, i.e. distribution of brightness in space, placement of necessary equipment, colour adjustment of space and all equipment objects and people in space. A suitable light microclimate is very important for human health and overall well-being [12].

The criteria used to describe the light microclimate are:

- daylight factor;
- illuminance;
- chromaticity temperature;
- colour rendering index;
- glare index.

The **acoustic microclimate** is formed by acoustic flows which act on the subject by their acoustic pressure. The optimal acoustic microclimate is achieved if sound is eliminated which adversely affects a person's well-being (i.e., disturbs calm, annoys, prevents the required sound intake, or endangers physical and mental health). The criteria used to describe the acoustic microclimate are [13]:

- sound intensity – sound pressure level;
- sound frequency;
- reverberation time.

The **odor microclimate** is a component of the environment formed by flows of odor substances in the air to which occupants are exposed. Odors, gaseous compounds perceived as good or bad smells, are produced by human bodies or activities or released from building structures. Odors enter buildings both from the outside and from the inside: via air conditioning equipment, building materials and fixtures, but mostly from human activity. In addition to the usual odors from smoking and food preparation, styrene, formaldehyde, and paint fumes (previously unknown to construction) can also be found in the interior today. People produce CO_2 and body odors while indoors. The level of these "anthropotoxins" are generally an indicator of indoor air quality. Only a sufficient supply of fresh air can increase the quality of the odor microclimate in buildings. [7]

2.1.3 Relative humidity in buildings

Relative indoor humidity is one of the crucial indicators for the quality of the internal microclimate. The air mixture is composed of dry air and water vapour (Fig. 6). The amount of water vapour in the air determines the partial pressure of water vapour p [Pa], or the vapour density v [kg · m^{-3}].

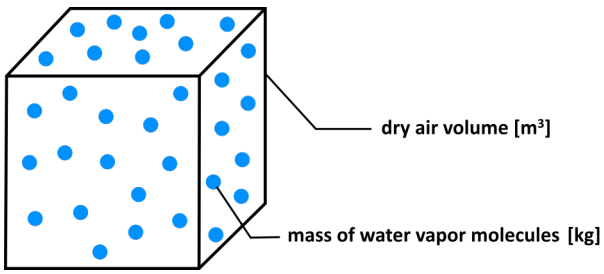

Fig. 6 Water molecules in dry air

Relative humidity (RH) is defined as the ratio of the partial pressure (or density) of water vapour in the air to the saturated partial pressure (or density) of water vapour at a given temperature and same total pressure. Relative humidity depends on the temperature and pressure of a system. Relative humidity is normally expressed as a percentage, with a higher percentage meaning the air mixture is more humid. At 100% relative humidity, the air is saturated and is at its dew point. [14]

$$RH = \frac{p}{p_{sat}} \cdot 100 = \frac{v}{v_{sat}} \cdot 100 \quad [\%] \tag{1}$$

where
RH ... relative humidity [%];
p ... partial water vapour pressure [Pa];

p_{sat} ... saturation vapour pressure [Pa];
v ... vapour density [kg · m^{-3}];
v_{sat} ... saturation vapour density [kg . m^{-3}];

The amount of water vapour in the interior is determined by the concentration of water vapour in the exterior, paths of ventilation, and sources of water vapour within the building.

The sources of water vapour in the interior could be, for example, from having a shower (700–2600 g · h^{-1}), cooking (600–1500 g · h^{-1}), drying clothes (50–500 g · h^{-1}), flowers (5–20 g · h^{-1}), or the occupant themselves (30–300 g · h^{-1}) [15].

During summer the content of water vapour in the outdoor air is high. Once the air is brought into the interior and cooled, the resulting air is damp and the RH can rise above 70 %. However, in winter there is a small amount of water vapour in the outdoor air, so once brought into the interior and heated (without further adjustment), the resulting air is dry and the RH may fall below 30 %. The dependence of the relative humidity and temperature of the air supplied to the interior in summer and winter is shown in Fig. 7 in the part of Mollier diagram. Red line: warm outdoor air with a temperature of 26 °C is supplied to the interior and cooled to 22 °C (cooling by wall surfaces, furniture, etc.). Blue line: cold outdoor air with a temperature of −2 °C is supplied to the interior and heated to 22 °C. The risks caused by this condition are described below.

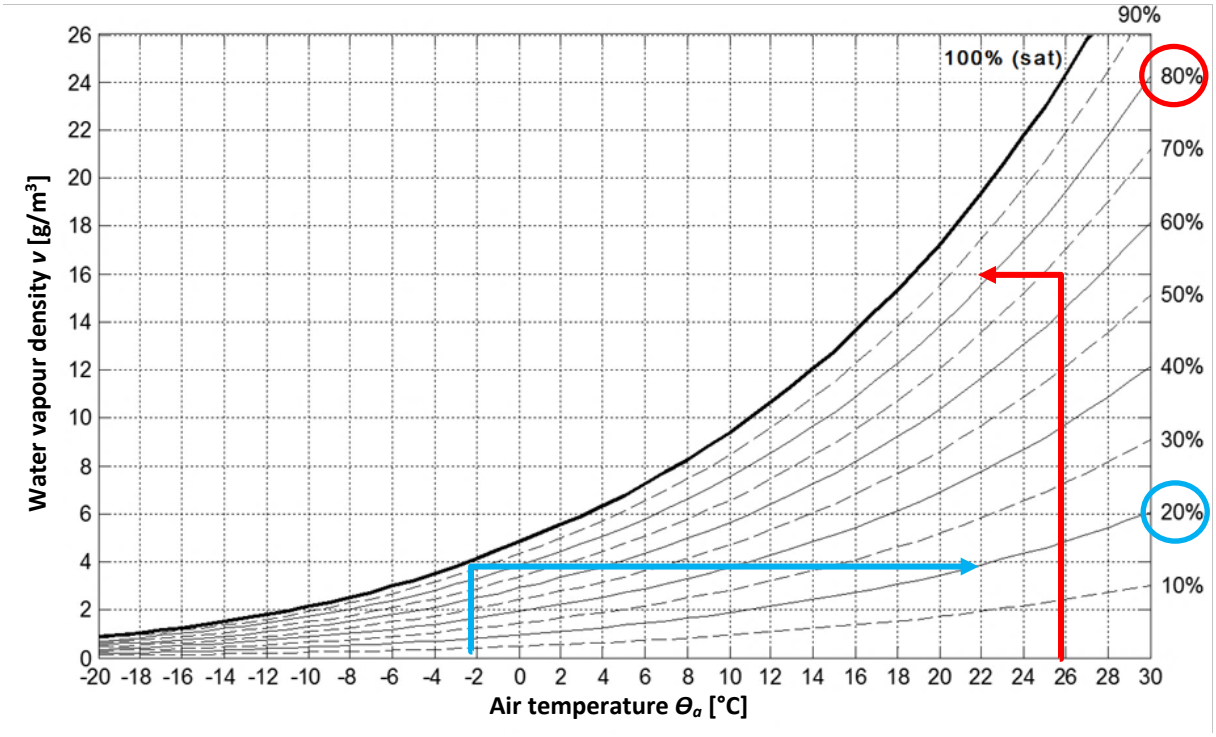

Fig. 7 Temperature and RH of the air supplied to the interior in summer (red) and winter (blue)

Thermal and humidity comfort is the condition that expresses satisfaction with the hygrothermal environment. The comfort zone for humans is described by the hygrothermal microclimate of the interior through a combination of air temperature and relative humidity.

International standards such as the American ASHRAE standard 55 [16] recommend a comfort zone of temperature 66 to 84 °F (18.9–28.9 °C) and relative humidity of 30–80 %; European authors such as M. V. Jokl [15] recommended optimal indoor humidity in the range of 30–70 % with a temperature 19–24 °C. Korjenic [17] states the optimal levels of indoor humidity for human beings are in Austrian climates in the range of 40–60 %, of which the upper limit is preferred in winter and the lower limit in summer. The passive house center in the Czech Republic [18] recommends values for

residential buildings as follows: winter air temperature 18–24 °C, in summer 20–28 °C; values of relative humidity of indoor air between 40–60 %. Fig. 8 illustrates the dependence of the quality of the internal microclimate on relative humidity and internal temperature.

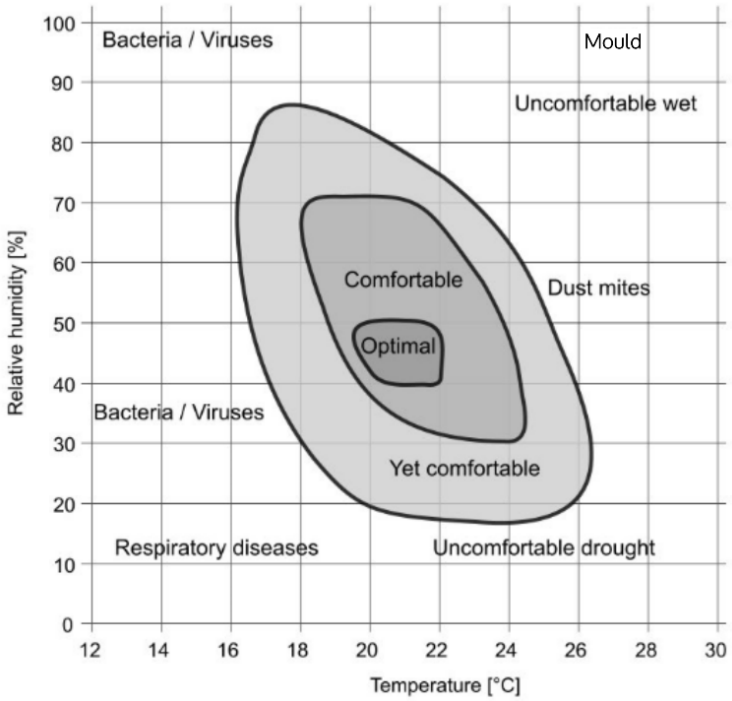

Fig. 8 IAQ in the context of hygrothermal microclimate [10]

The optimum humidity of the internal environment fluctuates from 40 to 60 %. The relative humidity in the range of 30 to 70 % is still considered a comfortable indoor environment (Fig. 9).

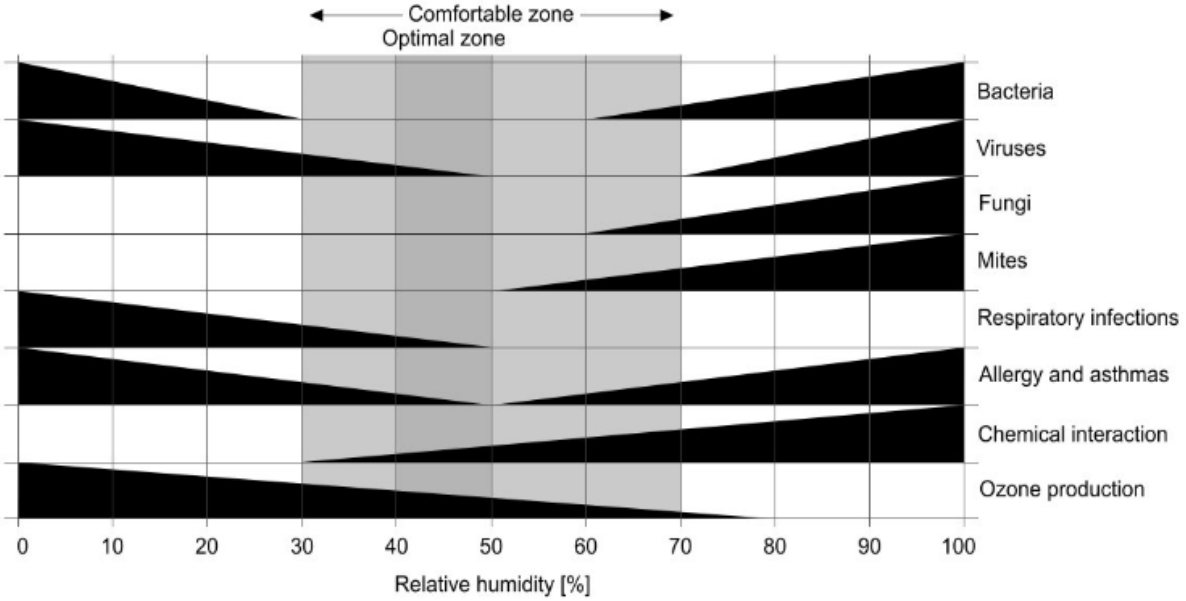

Fig. 9 Problems caused by high / low relative humidity [19]

Low relative humidity in the interior (below 30 %) is a common problem in winter. The cold air supplied from the outside heats up and its relative humidity drops sharply. With low relative humidity, people

often suffer from drying out. The airway mucosa is dried, and dust, dirt, and disease cannot be quickly removed from the airways. Longer breathing of the respiratory tract increases the risk of respiratory tract illness. Typical ailments include cough, bronchitis, runny nose, and sinusitis. Dry skin, lips, and eyes are also a frequent consequence of low RH. Plastics are electrically charged and collect additional dust particles in dry air. At relative humidity below 40 % (and especially below 30 %), the probability of static charge increases for some materials [15].

High values of relative humidity in the interior (above 70 %) are usually a problem in summer. Outside warm air is supplied to the interior where it is cooled, for example, by walls or furniture surfaces, and the relative humidity of the air increases. High humidity levels can lead to the growth of mould, bacteria and mites and can cause condensation problems on cold surfaces. As a result, they can lead to increased respiratory problems, frequent sore throats, headaches, runny nose, and nervous behaviour in children. Adults are more likely to suffer from nausea, vomiting, shortness of breath, constipation, back pain, runny nose, and nerve problems. Humidity in the internal environment also affects the durability of structures. High humidity leads to the degradation of finishes and deterioration of thermal insulation [15].

From the above, it is clear that the value of relative humidity in the interior plays an important role in IAQ. Therefore, the properties of the indoor air or air supply are currently being refined.

However, altering relative humidity in air-conditioning units is energy intensive and cost-consuming. This is not in line with the global push to reduce energy consumption and increase energy efficiency in all aspects of life, including construction and the buildings indoor microclimate.

Relative humidity can also be regulated, without any operating energy, by choosing building structures and structural materials with moisture buffering properties.

Materials that absorb and desorb moisture can be used to accumulate and reduce extreme values of air moisture and supply saved moisture to the interior during dry periods. The main advantage of using building structures to moderate the indoor environment is they have usable mass and reduce operating energy.

Clay minerals, compared to other building materials, can more effectively use their mineralogical composition as a storage for indoor humidity. At the same time, clay materials and earthen structures are considered environmentally friendly due to lower values of embodied CO_2 and SO_2 emissions. The embodied energy can be fully and easy recycled at the end of the life span of the building and into the future.

It is these principles of passive regulation of relative humidity in building interiors that this thesis deals with.

2.2 Transfer of water vapour in porous building materials

The moisture balance of porous building materials is determined by moisture transport (liquid and gas states) within the material (Fig. 10), moisture storage characteristics, and the material's properties.

Water vapour is an integral part of indoor air quality and building structure integrity. Under certain boundary conditions, too much or too little moisture can pose a risk to human health and to the service life of structures.

In the case of poor design or implementation of the exterior building structure or incorrect use of the building, condensation of water vapour may occur inside the structure. Under certain conditions of surface temperature, air temperature, and its relative humidity, water vapour can also condense on the surface of the material.

Air is a mixture of gases (dry air) and water vapour. The composition of the homogeneous dry mixture is as follows (by volume): N (78.09 %), O_2 (20.95 %), Ar (0.93 %), CO_2 (0.033 %) and Ne, He, CH_4, Kr, H, Xe (all less than 0.002 %). [20]

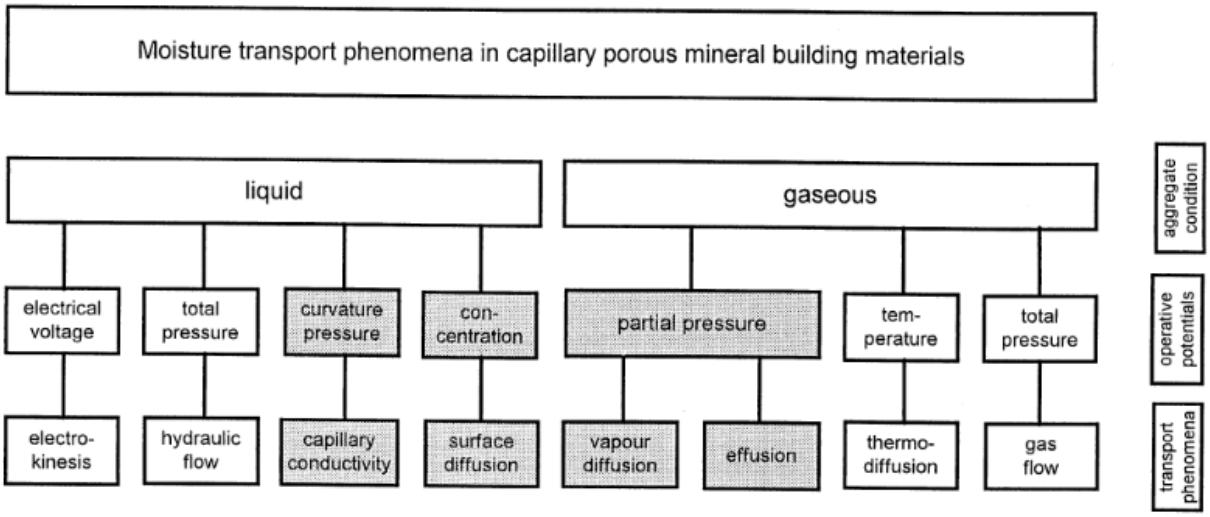

Fig. 10 Moisture transport phenomena in porous building materials [21]

2.2.1 Water vapour transport based on diffusion

2.2.1.1 Water molecule

The water molecule is composed of hydrogen and oxygen, in a ratio of two parts hydrogen for each part oxygen, giving the molecular formula H_2O. In all forms, water is a polar molecule with electron-poor hydrogen atoms and electron-rich oxygen. It is this that leads to the hydrogen bonding interaction between water molecules. Attractive and repulsive forces act between the water molecules over short distances. [22]

The water molecule does not have a regular shape, so its size cannot be easily determined. The molecular diameter is about 2.75 angstroms. The water molecule is still the same size, regardless of its state of mater [23]. Here is the conversion of units of dimension of one water molecule:

$$2.75\ \text{Å} = 0.275\ \text{nm} = 2.75 \cdot 10^{-10}\ \text{m} \quad .$$

The size of the H_2O molecule is important for understanding the principles of water vapour transport by building materials.

The behaviour of water molecules in building materials varies: [24]

- free water (fills large pores and cavities)
- physically bound (Van der Waals force)
- capillary water (forms the filling of small pores and capillaries)
- adsorbed water (fills the smallest pores and covers the walls of the porous space)
- chemically bound water (forms part of the basic grid of materials)

2.2.1.2 Transport of water vapour through building structures

In a system that is not in a state of thermodynamic equilibrium, spontaneous processes occur under constant external conditions, ultimately leading to the establishment of equilibrium.

A transport process is one in which the value of a monitored quantity changes at a certain point in the system with time. The monitored quantity can be an amount of substance, energy, or momentum. [25]

Convection

Convection or air flow is the movement of air caused by differences in atmospheric pressure, which is the result of differing temperatures and air densities. The air flows from places of higher pressure (lower temperature) of air to places of lower pressure (higher temperature) of air. The flow rate depends on the magnitude of this difference.

Convection in building structures can occur in poorly designed or executed structures (Fig. 11). Depending on the size of the pressure drop, the concentration of water vapour in individual environments, and the permeability of the structure (leaks in the airtight layer), the flowing air can also transport water vapour. This can accumulate in poorly designed structures and subsequently condense. Enabling convection is therefore a major problem that affects the properties and durability of the materials used in a structure. Convection transfers far more moisture to the structure than does diffusion. It is assumed that no convection occurred in the experiments below.

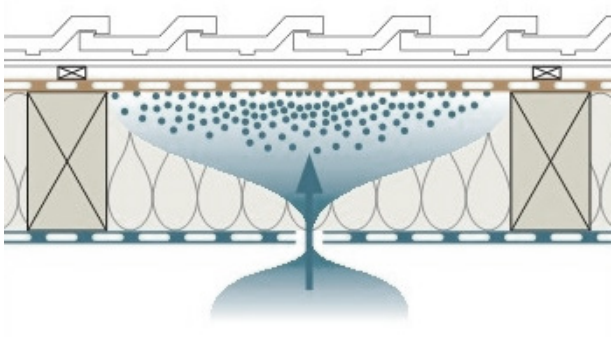

Fig. 11 Convection in building structure [26]

Diffusion

Diffusion is a process in a concentration-inhomogeneous system in which concentrations self-equilibrate to a steady state. During diffusion, the mass is transported from one part of the system to another. Diffusion flow is the driving force in the transport of gas through porous material (Fig. 12).
Flow of a substance is caused by local variance in its concentration. The change in the concentration of the component with the position, or more precisely, the derivation of the concentration according to the position is described by Fick's law. [25]

Diffusion of water vapour molecules in air is a well investigated and described phenomenon but is a complex problem with porous building materials. In the porous space of materials, water vapour is transported in the air; however, transport is limited by the cross-section of the pores, the adsorption phenomena occurring on the walls of the pores, and the curvature of the pore pathways. Diffusion does not occur in capillaries that have a diameter of less than 10^{-7} m, because capillary condensation prevents the transport of gas by diffusion. [27]

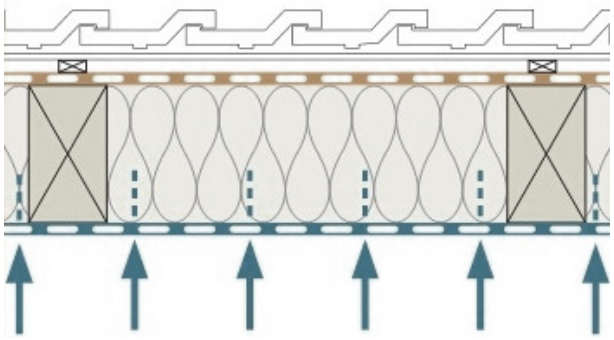

Fig. 12 Diffusion in building structure [26]

Other specific transport phenomena are: effusion, transfusion, self-diffusion, thermodiffusion, etc. Liquid water can also be transported in the structure, e.g. by water adsorption, or capillary action. These phenomena are not the subject of this thesis.

Sorption

Sorption is a general term for absorption, adsorption, and chemisorption. Absorption is the assimilation of one substance into another throughout its volume. Adsorption is the binding of a gaseous or liquid substance to the surface of another substance. Chemisorption is a type of adsorption in which a chemical bond is formed on a surface. Only adsorption and its reverse process, desorption, are discussed below.

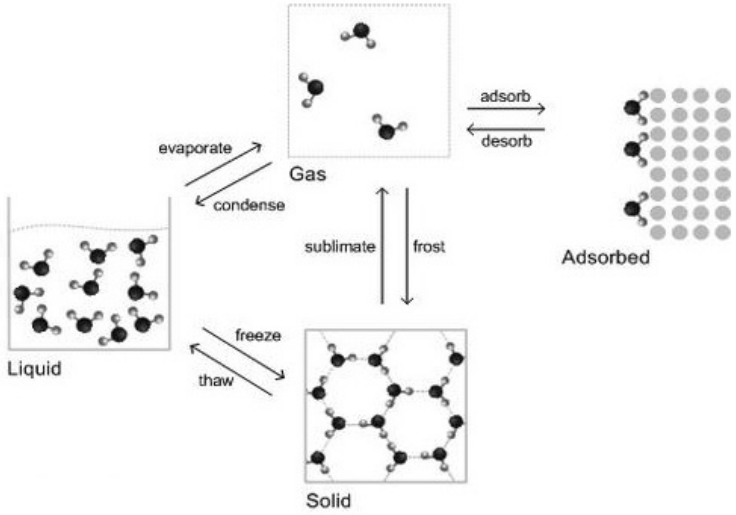

Fig. 13 Moisture states and phase change processes [28]

Moisture sorption occurs through diffusion, which transports water vapour through the pore system of materials. Surfaces of hydrophilic porous solids in contact with water vapour molecules in humid air have the tendency to attract and capture these water molecules because of the polar nature of the water molecule (Fig. 13).

This process is called **adsorption**; physical forces are applied here (Van der Waals); there is no chemical change; it is a reversible process. The opposite process, **desorption**, requires the supply of energy to release the appropriate physical bonds between the absorbate and the absorbent. The term gas/moisture sorption includes both adsorption and desorption. The substance on the surface of which adsorption has occurred is called the adsorbent, and the gas used is the adsorbate. The equilibrium between the gas phase and the adsorbed layer is called the adsorption equilibrium and the equilibrium gas pressure. A gas molecule that adheres to the surface of the adsorbent (sample) is said to be adsorbed.

The moisture content of the material therefore affects, among other things, the relative humidity of the air in the environment. By monitoring and controlling adsorption and desorption, useful information and properties of the solid can be obtained. The dependence of equilibrium moisture of a material on the relative air humidity at constant temperature is called a **sorption isotherm** (Fig. 14). For each RH value of the ambient air, a moisture balance of the given material is experimentally created (mass of water content per mass of dry soil or mass of water content per volume of dry soil). The connecting line between these values is the so-called sorption isotherm. The difference between the adsorption and desorption isotherm is called hysteresis.

The adsorption of gases is usually described through isotherms, that is, the amount of adsorbate on the adsorbent as a function of its pressure at constant temperature. The amount adsorbed is nearly always normalized by the mass of the adsorbent to allow comparison of different materials. Adsorption and desorption isotherms are curves describing the retention/release of gases and ultimately the mobility of a substance from the transported media to a solid phase at a constant temperature and pressure. There

are currently several different models of isotherms (Langmuir, Freundlich, Dubinin–Radushkevich, Temkin, Flory–Huggins, Hill, Redlich–Peterson, Sips, Toth, Koble–Corrigan, Khan, Radke–Prausnitz, or Brunauer–Emmett–Teller isotherm model) [29]. The BET theory of multimolecular adsorption, which is suitable for porous building materials, will continue.

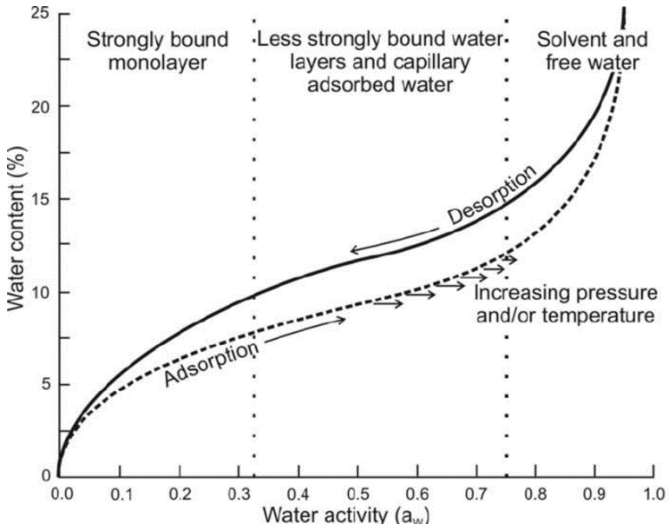

Fig. 14 Typical adsorption and desorption curve of building materials [30]

Physisorption is characterized by the fact that the adsorption equilibrium between the adsorbed and free molecules is established very quickly, both when the gas pressure increases and when it decreases. Physisorption is therefore referred to as a reversible process which can be achieved, for example, by changing the pressure or temperature. The range of action of attractive intermolecular forces is such that several layers of adsorbed molecules can be formed during physisorption, a phenomenon which is then referred to as multilayer adsorption. Adsorption at constant temperature depends on the relative pressure $RH = p/p_{sat}$, which is defined as the ratio of a given equilibrium partial pressure and the saturation pressure of the adsorption gas.

During adsorption from a fully dried adsorbent ($p/p_{sat} = 0$) with increasing pressure, gas molecules typically gradually surround the sample surface and occupy one thin layer, a monolayer, which with a certain number of molecules, covers the entire sample surface. With further addition of gas molecules (increasing partial pressure), there is a gradual accumulation of other layers, so-called multilayers, the formation of which arises in parallel with capillary condensation in the pores of the substance. [31]

The following figures (Fig. 15, Fig. 16, Fig. 17) show the adsorption mechanism: The porous solid has completely unsaturated surface forces at RH = 0. When the material comes into contact with water vapour in air a monomolecular adsorption process forms a single layer of water molecules on the surface of the pores. As RH increases, additional layers of water molecules form by the polymolecular adsorption process. When the opposing molecules on the pore walls join, capillary condensation occurs.

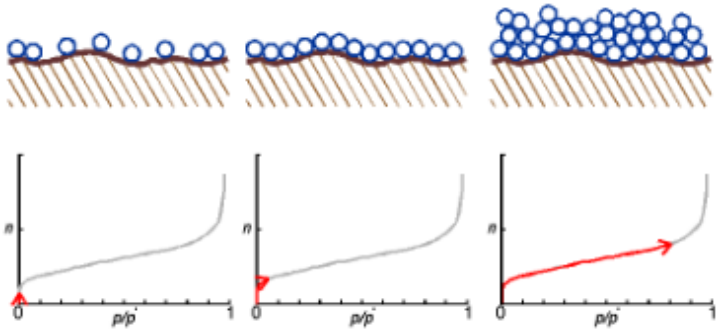

Fig. 15 Gas adsorption process and isotherm formation: nonporous material [32]

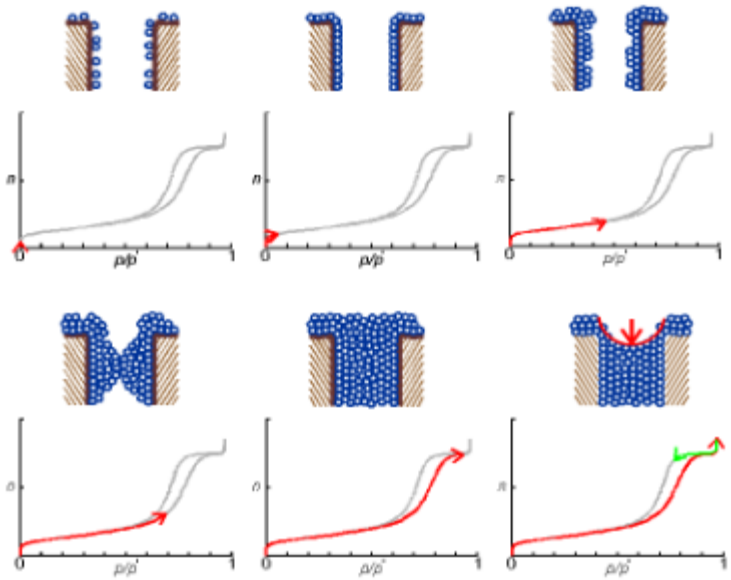

Fig. 16 Gas adsorption and desorption process and isotherm formation: mesoporous material [32]

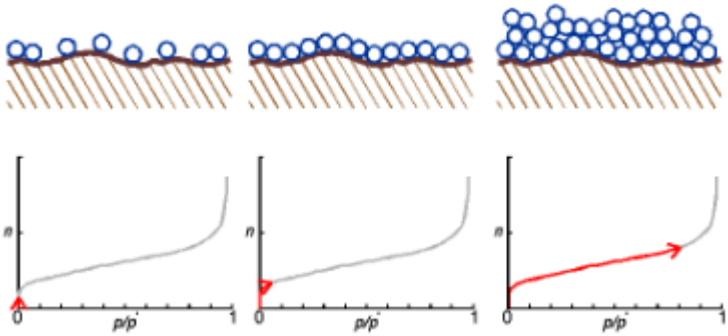

Fig. 17 Gas adsorption process and isotherm formation: microporous material [32]

The adsorbed amount of gas (water molecules) n_a at the weight of the sample m depends on the equilibrium pressure p, the temperature T, and the nature of the gas-sample system. If it is measured at a constant temperature and if the gas is below its critical temperature [32], it applies:

$$\frac{n_a}{m} = f\left(\frac{p}{p_{sat}}\right)_T \quad , \tag{2}$$

where
n_a … amount of gas;
m … weight of the sample;
p … equilibrium partial pressure;
p_{sat} … saturated pressure;
T … constant temperature of the system.

This equation represents the adsorption isotherm, which is determined experimentally and generally expressed graphically. All experimental isotherms can be assigned their shape by one of the six basic shapes that characterize the system. This is (Fig. 18) the classification according to the International Union of Pure and Applied Chemistry (IUPAC, 1985) for types marked *Type I* to *Type VI* [33].

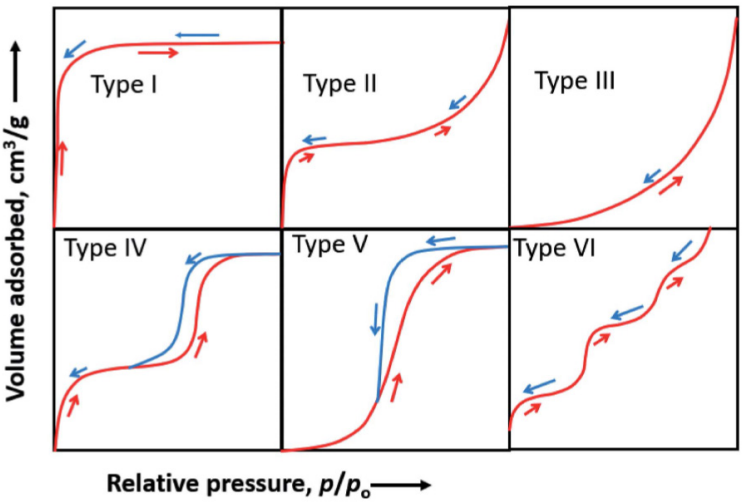

Fig. 18 Different types of sorption isotherms as classified by IUPAC [34]

Type I isotherms are typical of microporous solids having small external surfaces. A Type I isotherm is concave to the p/p_{sat} axis, and the amount adsorbed approaches a limiting value. This limiting uptake is governed by the accessible micropore volume rather than by the internal surface area. A steep uptake at very low p/p_{sat} is due to enhanced adsorbent-adsorptive interactions in narrow micropores (micropores of molecular dimension), resulting in micropore filling at very low p/p_{sat}.

Type II reversible isotherms are given by the physisorption of most gases on nonporous or macroporous adsorbents. The shape of the isotherm is concave to the p/p_{sat} axis, then almost linear, and finally convex to the p/p_{sat} axis. The shape is the result of unrestricted monolayer and multilayer adsorption up to high p/p_{sat}. If "the knee" is sharp (the beginning of the middle almost linear section), this usually corresponds to the completion of monolayer coverage. A more gradual curvature (a less pronounced break into the linear part) is an indication of a significant amount of overlap of monolayer coverage and the onset of multilayer adsorption.

Type III isotherms have no identifiable monolayer formation; the adsorbent-adsorbate interactions are now relatively weak, and the adsorbed molecules are clustered around the most favourable sites on the surface of a nonporous or macroporous solid.

Type IV isotherms are typical of mesoporous adsorbents. The adsorption behaviour in mesopores is determined by the adsorbent-adsorptive interactions and also by the interactions between the molecules in the condensed state. In this case, the initial monolayer-multilayer adsorption on the mesopore walls, which takes the same path as the corresponding part of a Type II isotherm, is followed by pore condensation.

In this case capillary condensation is accompanied by hysteresis. This occurs when the pore width exceeds a certain critical width, which is dependent on the adsorption system and temperature. With adsorbents having mesopores of smaller width, completely reversible isotherms are observed without hysteresis. In principle, these isotherms are also given by conical and cylindrical mesopores that are closed at the tapered end.

Type V isotherms are typical that the low p/p_{sat} shape is very similar to that of Type III, and this can be attributed to relatively weak adsorbent–adsorbate interactions. At higher p/p_{sat}, molecular clustering is followed by pore filling. This isotherm exhibits a hysteresis loop which is associated with the mechanism of pore filling. Type V isotherms are observed for water adsorption on hydrophobic microporous and mesoporous adsorbents.

Type VI reversible stepwise isotherm is representative of layer-by-layer adsorption on a highly uniform nonporous surface. The step height now represents the capacity for each adsorbed layer, while the sharpness of the step depends on the system and the temperature. Amongst the best examples of Type VI isotherms are those obtained with argon or krypton at low temperature on graphitised carbon black. [35] [36]

Hysteresis

The hysteresis loop is associated with the filling and emptying of the mesopores and macropores by capillary condensation. The lower branch represents measurements obtained by progressive addition of gas to the adsorbent, and the upper branch represents measurements by progressive withdrawal. Hysteresis is a phenomenon in porous materials, where the emptying of the pores by the adsorbed gas occurs differently than their filling. The adsorption and desorption curves do not overlap in this area. Hysteresis loops occur at isotherms in the multilayer adsorption region and are usually associated with capillary condensation (liquefaction of the adsorbent due to limited space in mesopores at pressures below saturated pressure) on the adsorption curve and pore emptying (evaporation of adsorbate and condensate from mesopores) on the desorption curve. Macropore filling occurs only at high relative pressures p/p_{sat}. [35]

Hysteresis loops can have a wide variety of shapes (Fig. 19). Their shape and location in the isotherm depend on the size and shape of the pores. For hysteresis loops, a classification was adopted distinguishing four types of loops (marked H1–H4):

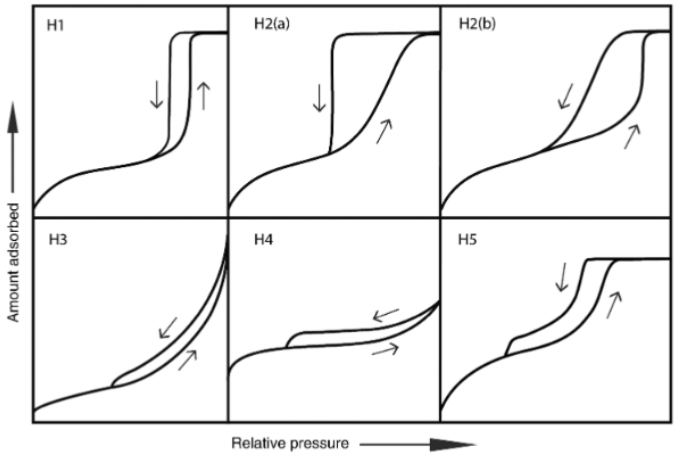

Fig. 19 Classification of hysteresis loops [35]

The hysteresis loop H1 is characterized by very steep, almost perpendicular steps that are almost parallel in adsorption and desorption. Such a hysteresis loop is characteristic of well-defined cylindrical pores.

The hysteresis loop H2 is typical of disordered porous materials with a wide pore size and shape distribution. This loop shape is related to so-called bottle-shaped pores, i.e. pores having narrow inlet necks behind which the pores expand or a porous material whose cylindrical pores have different sizes and intersect with each other, thus creating larger free volumes at the intersection.

The hysteresis loop H3 shows no limit at high pressures. It is characteristic of agglomerates of plate-like particles forming slit pores in the interparticle space.

The hysteresis loop H4 is characteristic of narrow slit pores but, in contrast to loop H3, contains micropores, exhibiting the character of a type I isotherm before condensation. [37]

2.2.2 Influence of porosity on material properties

Because the storage and transport of moisture in building materials occur in the pores of these solids, it is necessary to take into account their porous system when evaluating the sorption properties of materials. The porosity of building materials also directly affects the following: bulk density, mechanical strength, thermal conductivity, sound insulation properties, and fluid and gas transport.

This chapter describes the division of the pore system, the porosity of building materials, and their specific surface.

The pore system

According to the Oxford English Dictionary, a pore means: *a minute opening, aperture, or hole (usually one imperceptible to the unaided eye) in a surface, through which gases, liquids, or microscopic particles pass or may pass*.

In fact, not all pores are accessible from external surfaces. According to IUPAC (1994), pores in porous solids can be divided according to their availability to an external gas or fluid into [38]:

- Closed pores (not connected to the surface and do not participate in transport processes)
- Open pores (connected to the surface and do participate in transport processes)
  - One side open (ink-bottle shaped and cylindrical)
  - Two sides open (cylindrical and funnel shaped through-pores)

Accessible surfaces for adsorption of the water molecule are only via the open pores. Fig. 20 shows the different types of pores in the material. This division is only schematic; for porous materials the density of the matrix is key. It is necessary to add information about which medium and under what conditions (open or closed) these pores are available. For example, pores that are closed to water molecules may still be accessible to helium atoms.

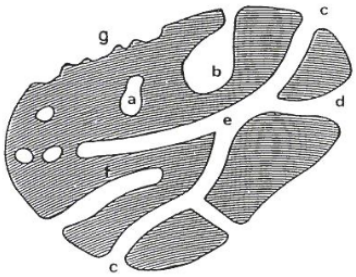

Fig. 20 Schematic picture of a porous solid [38]: (a) closed pore; (b) one side open ink-bottle pore; (c) two open sides cylindrical pore; (d) two open sides funnel shaped pore; (e) two open sides through pore; (f) one side open cylindrical pore; (g) external surface

The pore-size

There are a number of categories of pore size. For example, "nano-, micro-, and millipores", or "submicroscopic-, capillary-, and macropores", or "sub-, ultra-, super-". [39]–[41] In chemical engineering, the established classification of pore size into three categories according to IUPAC (1985) is used (Tab. 1).

Tab. 1 Pore-size standard classification of materials according to IUPAC

Type of pore	Size [nm]
Micropore	0–2
Mesopore	2–50
Macropore	> 50

Source: [33]

This scale divides the pores according to their width, i.e. the diameter of a cylindrical pore, the distance between two sides of a slit-shaped pore, or the smallest dimension in the fissure pore. Pores are classified into the following groups: macropores, mesopores, and micropores. It may be desirable to subdivide micropores into the finer division. However, this is not necessary with building materials. Macropores and mesopores are a key part of the pore system.

There is mainly simple adsorbate-adsorbent interaction on the surfaces of large pores and on external surfaces in macroporous systems. In mesopores, there are cooperative adsorbent-adsorbent interactions across medium-sized pores leading to capillary condensation. For micropores, it is typical that there is an overlap of adsorption forces from opposite walls of pores.

Fig. 21 gives an idea of the size of the water molecule relative to the size of a porous system.

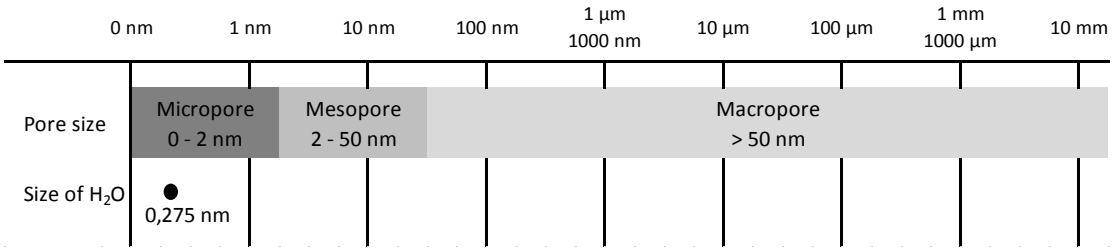

Fig. 21 Size of the water molecule and the pore-size classification of materials

Porosity

The porosity of a material is defined as the ratio of the volume of the pores to the total volume of the material:

$$\psi = \frac{V_0}{V} \ [-], [\%] \quad , \tag{3}$$

where
ψ … the porosity;
V_0 … the volume of opened and closed pores;
V … is the total volume of material.

The description of the pore system is essential. Porous solids with the same apparent porosity, but with pores of different geometry, size and openness react in a different way under the same conditions.

The value of the porosity of a building material alone tells us very little about its sorption potential. Tab. 2 shows the porosity values for different materials. It is clear from the porosity values that the materials have a huge scatter. In addition, individual sources indicate different ranges.

Tab. 2 Approximate values of porosity of selected materials

Material	Porosity [%]
Fire brick	20–37
Limestone	31
Cement mortar	32
Lime mortar	41
Gypsum	51–66
Sandstone	0,5–25
Sand	25–38
Loam	36–44
Clay loam	40–48
Clay	46–55
Bentonite	65

Source: [42]

The specific surface area

The complexity and diversity of the porous structure of materials has led to the application of many experimental techniques for their better characterization. One of them is also a specific surface area measurement. Gas adsorption measurements are used for determining the surface area and pore size distribution of different solid materials. The measurement of adsorption at the gas/solid interface also gives essential information to the nature and behaviour of solid surfaces. The specific surface area of adsorbents depends on their structure; the number of pores and the size of the surface area has a great influence on surface reactions. The large accessible surface area of the material increases the adsorption capacity. [43]

The standard ISO 9277:2010 [44] specifies the determination of the overall specific external and internal surface area of dispersed or porous solids by measuring the amount of physically adsorbed gas, according to the method of Brunauer, Emmett and Teller (BET method) [45]. It takes into account the International Union for Pure and Applied Chemistry (IUPAC) recommendations of 1984 and 1994. The BET method is applicable only to adsorption isotherms of type II (disperse, nonporous or macroporous solids) and type IV (mesoporous solids, pore diameter between 2 nm and 50 nm). Inaccessible pores are not detected. The BET method cannot reliably be applied to type I isotherms or to solids which adsorb the measuring gas.

Various methods (volumetric, gravimetric, calorimetric, or spectroscopic) are used to measure the amount of adsorbed gas. The most common volumetric methods (Fig. 22) are generally designed to measure nitrogen or krypton isotherms at 77 K and argon isotherms at 87 K. The term "volumetric" means that the amount adsorbed is derived from measuring the change in gas pressure as the gas volume changes. The isotherm is usually recorded point by point by discreetly adding and removing a known amount of gas at the time intervals required to reach equilibrium at each point. In the static (gradual) volumetric method for the determination of the adsorption isotherm, known amounts of gas are introduced into the sample space. Each step waits until the pressure inside the sample burette stabilizes. The amount of gas adsorbed is the difference between the amount of gas received and the amount of gas filling the dead volume (burette volume minus sample volume). For accurate measurement of the adsorption isotherm, it is necessary to remove all adsorbed gas from the sample by degassing (vacuuming) before starting the measurement. Degassing can also be supported/accelerated by increasing the sample temperature. At higher temperatures, more molecules desorb faster, so it is recommended to heat the sample at the same time as degassing but, with respect to the maximum temperature, to avoid permanent changes in the sample. The specific surface area is then related to the weight of the degassed sample. The most commonly used adsorbate for determining specific surface and pore size distribution is nitrogen (N_2); the measurement temperature is 77 K; the area of the occupied molecular site is 0.162 nm. [32]

The output of the experimental measurement includes:

- Specific surface area S_{BET} [$m^2 \cdot g^{-1}$], defined as the accessible surface area of a substance per unit mass.
- The pore size distribution of the material describes the representation of pores of different sizes. The distribution function/curve is expressed by deriving the area or volume of the pores according to the pore size.

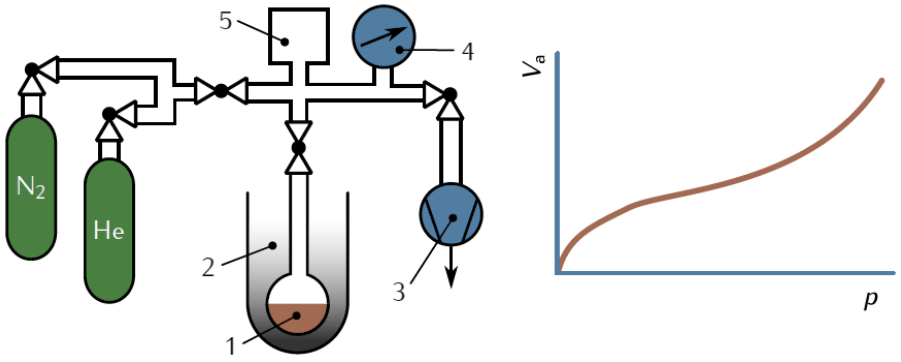

Fig. 22 Principle of volumetric method [32]

2.2.3 Sorption properties in steady state – literature review

In steady state, the relationship between the water content in the porous structure of the material and the relative humidity of the environment can be displayed graphically by a curve, called the sorption isotherm. At a constant temperature, the sorption isotherm shows the corresponding water content of the material at a given value of air humidity.

Due to the complexity of sorption processes, isotherms cannot be determined explicitly by calculation; it is necessary to record them experimentally for each product. If the composition or structure of the material changes then its sorption behaviour and also its sorption isotherm changes.

The presentation of sorption isotherms may differ in units on individual axes. When determining isotherms according to BET, the vertical axis is indicated by moles of gas adsorbed divided by the moles of the dry material and the horizontal axis by the ratio of the partial pressure of the gas divided by its partial pressure at saturation. Another way to express this is by the amount of adsorbed water molecules.

On the vertical axis is the ratio (or percentage) of the weight of adsorbed water molecules divided by the weight or volume of the dry sample. On the horizontal axis there is the relative humidity of the closed steady environment.

The ability of the material to bind air humidity (hygroscopicity) is unambiguously determined by the course of the so-called sorption isotherm. The difference between the adsorption and desorption branch (hysteresis) is given by the specific behaviour of water in the pore system of the material and is significant for capillary porous materials, which include clays and clay mixtures.

Below is a selection from the literature that deals with the determination of sorption isotherms of clay building materials:

Fig. 23 shows the sorption isotherms of four different types of clay materials compared to other building materials. Measurements have been performed at the FEB Laboratory in Kassel [46]. The results clearly show that the higher amount of clay minerals in the clay materials, the higher absorption capacity of the materials is expected. This is further influenced by the content of various types of clayey minerals.

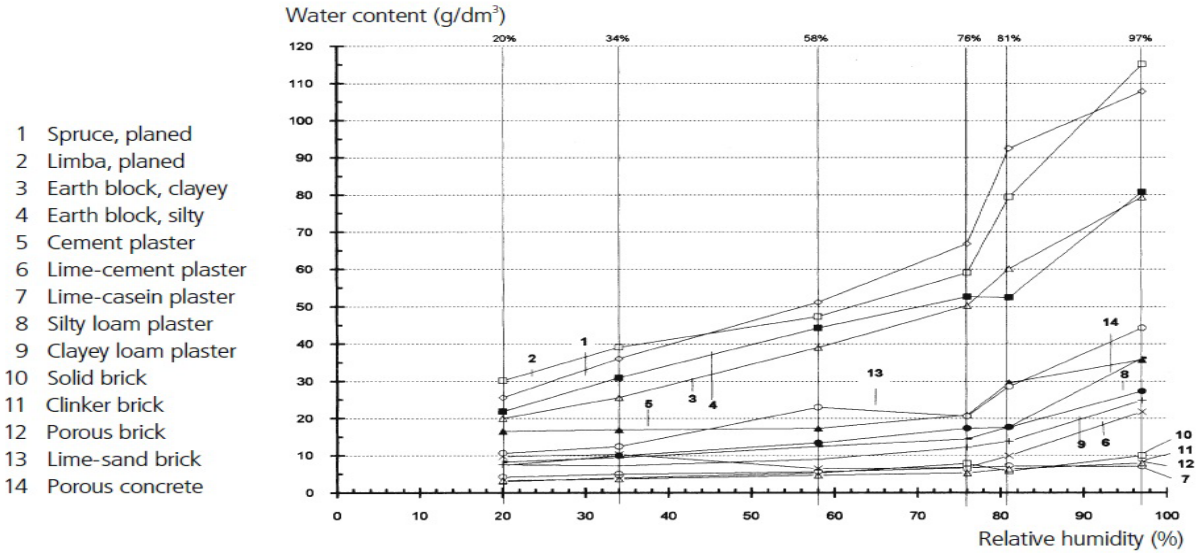

Fig. 23 Comparison of sorption isotherms for typical building materials [46]

The hygrothermal properties of clay materials were also measured at the "Institute for Sustainable Energy Technology" at the University of Nottingham. The following graph (Fig. 24) shows the sorption isotherms of chemically stabilised rammed earth. The mixture contains a stabilizer in the form of Portland cement powder. [47]

Another experimental measurement was created in collaboration with the Polytechnic University of Bari (Italy) and the University of Nottingham (UK) [48]. The results in Fig. 25 show that the addition of 5 % by wt. lime increases the absorbed water content of all mix types, in particular mix C, which correlates with the increase in bulk porosity. These results are surprising because, in our experiments, chemical stabilization reduces the sorption potential. Saidi et al. (2018) confirm that the stabilization of unfired clay (with cement or lime) not only worsens the thermal conductivity of the material but also worsens the sorption properties [49].

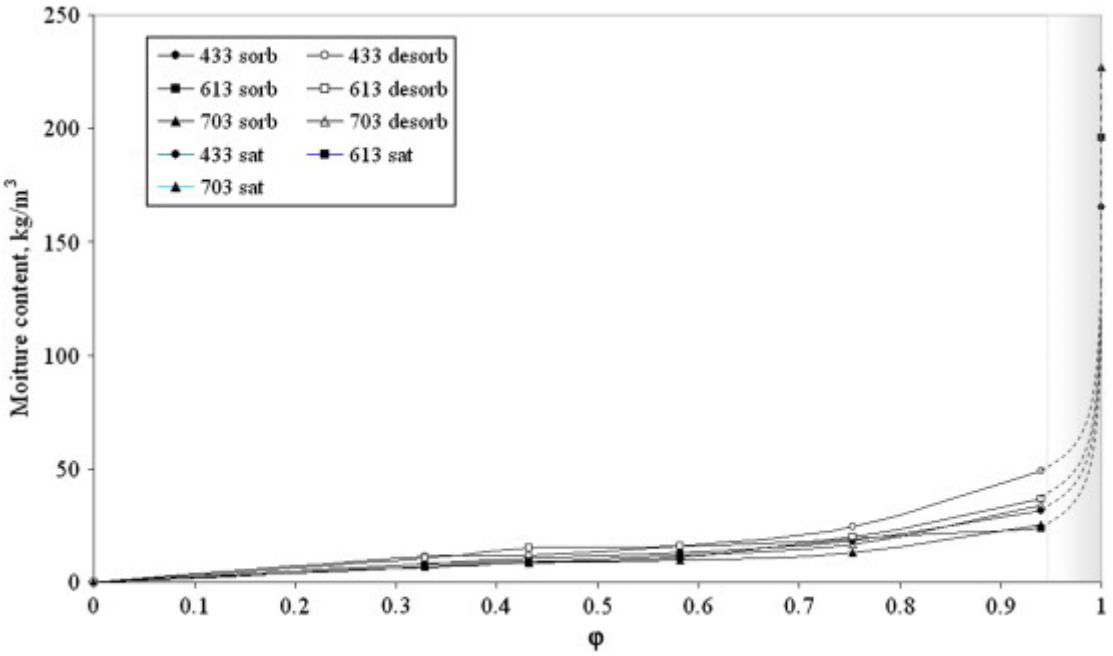

Fig. 24 Sorption isotherm of adsorption and desorption curves for three SRE materials [47]

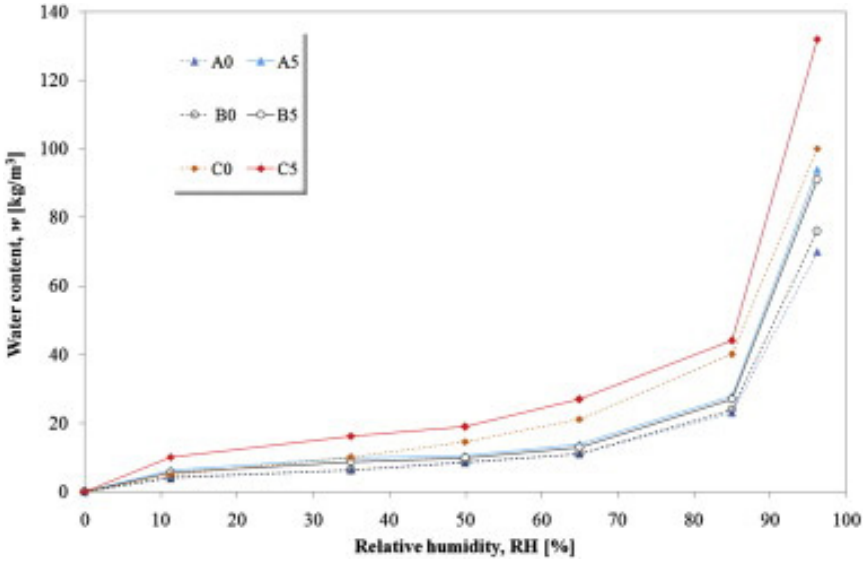

Fig. 25 Moisture adsorption isotherms for clay mixes [48]

Cagnon et al. (2014) examined the hygrothermal properties of earth bricks. The result of the experiments was, among other things, the difference between desorption isotherms of earth bricks (produced at five brickworks in the neighbourhood of Toulouse in southern France) measured by two different methods: the DVS method and the saturated salt solution method [50].

For example, Randazzo et al. (2016) [51] or Liuzzi et al. (2018) [52] dealt with the sorption properties of clay plasters in steady state. The results vary according to the type of material examined, the clay mineral used, and also according to the various admixtures. Ashour et al. (2015) presented the results [53] of the equilibrium moisture content of earth block materials with different compositions. They were fabricated from cohesive soil, cement, and gypsum combined with two kinds of natural fibres (wheat and barley straw).

The work of El Fgaier et al. (2016) concern the effect of sorption capacity on the mechanical and thermal properties of unfired clay bricks that were industrially produced in the north of France. The

study [54] has demonstrated that this clay material has a high sorption capacity, compared to other building materials such as concrete block or fired clay bricks.

At the University of Bath (UK), they also studied the sorption properties of unfired clay materials. McGregor et al. (2014) presented the results of static and dynamic tests on 114 unfired clay samples [55]. Samples were prepared as Compressed Earth Blocks (CEB) or clay plasters. The influence of clay mixture on the moisture buffering capacity, water vapour permeability, and sorption isotherms was determined. Further work [56] was focused on the measurement of MBV and steady state sorption properties (water vapour permeability and sorption isotherms). Experiments were performed on samples of Compressed Earth Blocks (CEB) and Stabilised Compressed Earth Blocks (SCEB), see Fig. 26.

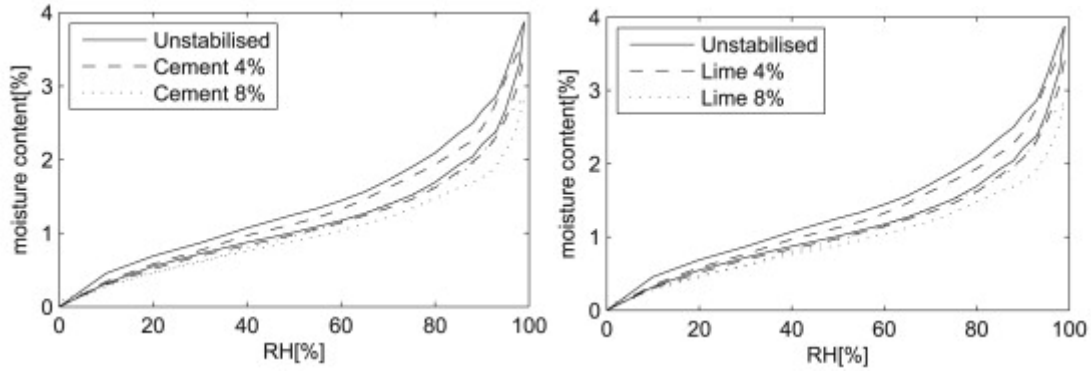

Fig. 26 Sorption isotherms of CEB and SCEB with cement or lime [56]

Individual results cannot be directly compared. The mixtures were measured under different boundary conditions. The properties of the porous moisture transfer material show that the sorption properties change with variations in ambient temperature and therefore, the sorption isotherm measured at 21 °C cannot be compared with the sorption isotherm measured at 23 °C. The differences in the sorption curves at different temperatures are shown in Fig. 27.

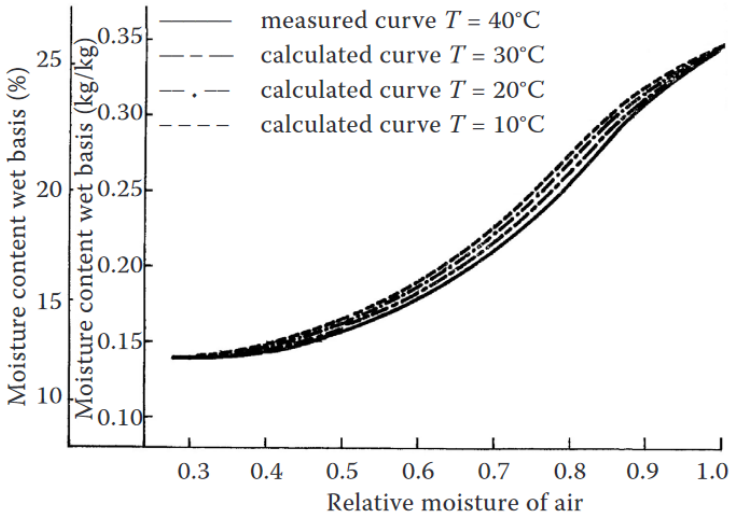

Fig. 27 The effect of ambient temperature on the equilibrium humidity of the material [57]

The result of the search shows that a large number of experimentally measured sorption isotherms of clay materials can be traced. The sorption isotherm is understood as a hygrothermal property of the material, but it itself has little informative value for construction practice. However, a significant application can be found in dynamic calculations (e.g., WUFI) and in mathematical zone moisture models. It is also part of the MBV calculation below.

The type and amount of clay mineral used, the chemical stabilization, the ratio of clays and sands in the mixture, etc. have a fundamental effect on the sorption isotherms of clay materials. Part of this research was to verify these properties.

2.2.4 Sorption properties in dynamic state – literature review

The main disadvantage of comparing the sorption potentials of individual building materials by way of sorption isotherms is that they say nothing about the actual building structure, which typically consists of various materials in several layers.

Already in his doctoral thesis [58], Carsten Rode Pedersen devoted himself to the hygrothermal behaviour of composite building structures and the theory of combined heat and moisture transport. Rode et al. in the Nordic project [59] defined the characterization of the moisture buffering capability of building materials, the NORDTEST method. The Moisture Buffer Value is the figure that has been developed in the project as a way to appraise the moisture buffer effect of materials. Described is also a test protocol which explains how materials should be tested for determination of their Moisture Buffer Value. The test protocol proposes climatic exposures which vary in 8 h and 16 h cycles: 8 h of high humidity and 16 h of low humidity. The timing comes from the usual daily cycle of 8 h sleeping time, working hours, etc. and other practical reasons during the test. Low humidity is proposed at 33 % RH and the high level at 75 % RH however, other humidity levels are proposed according to saturated salt solution. Furthermore, test specimen size is recommended. The minimum of exposed surface area is 0.01 m^2 and the thickness should be at least the moisture penetration depth for daily humidity variations or 10 mm. A minimum of 3 cycle tests must be carried out. This test also describes the sorption properties of single materials. The MBV values of materials can be classified into five different categories (Fig. 28). It is obvious that the optimum moisture buffering response should be as high and fast as possible. The MBV level 2 g/(m^2 % RH) @ 8/16h represents a very high efficiency moisture buffering material.

$MBV_{practical}$ class	Minimum MBV level	Maximum MBV level
	[g/(m^2 % RH) @ 8/16h]	
Negligible	0	0.2
Limited	0.2	0.5
Moderate	0.5	1.0
Good	1.0	2.0
Excellent	2.0	...

Fig. 28 Ranges for practical Moisture Buffer Value classes [59]

Roels and Janssen (2006) from Catholic University of Leuven compared the Nordtest and Japanese test methods for the moisture buffering performance of building materials [60]. A numerical study on four different materials (wood fibre board, plywood, gypsum plaster, and aerated cellular concrete) compared these two methods. Both test methods turned out to be very similar in measurement principles and also objectives. The specimen thickness was shown to be important. For samples with a thickness below the *1/e* penetration depth, the JIS and Nordtest protocols gave similar results; for samples with a thickness above the *1/e* penetration depth, different results were obtained.

McGregor et al. (2014) in their article [56] presented the results of measuring the potential to regulate indoor humidity by various building materials using the Moisture Buffering Value (MBV) concept. Measurements of MBV and steady state properties (water vapour permeability and sorption isotherms) were performed on 18 samples of clay materials (compressed earth blocks and stabilised compressed earth blocks). It also showed how the variability of experimental conditions in the dynamic measurement can change the obtained MBV. The results of other paper [55] indicate unfired clay material has a much higher potential to regulate the indoor humidity than conventional construction materials previously reported in the literature. The clay mixture selection (clay minerals and particle

size distribution) is more determinate for moisture buffering than from changes to soil density, preparation or stabilisation.

Liuzzi et al. (2013) dealt with dynamic sorption properties and zone moisture modelling. The subject of the research [48] was various clay mixtures without chemical stabilization or with the addition of lime. Cascione et al. (2020) presented results [61] of moisture buffering capacity of three hygroscopic plasters (clay, gypsum, and lime) and compared with the numerical simulations of a single-zone room space.

Other dynamic experiments of clay materials were performed by Maskell, D. Thomson, A., Walker, P., Lemke, M. (2018) in order to determination of the optimal plaster thickness for moisture buffering of indoor air [62]. In the case of non steady state, the water molecules penetrate only to a certain depth of the building structure during dynamic adsorption and desorption. This paper presents a method for determining the optimal thickness from experimentation on specimens of varying thickness. In this paper it is demonstrated that there is a thickness of material beyond which there is no increase in moisture buffering capacity. The importance of determining the depth of moisture buffering penetration results in the possibility of optimizing the final layer structure (thickness, topcoats, etc.) for an effective internal moisture buffering performance.

Several experimental methods trying to describe the influence of building materials on indoor relative humidity have been introduced. Several full-scale measurements of moisture buffering in building materials have been carried out. Some of them have been proposed by Padfield, T. (1998) [63], or by Mitamura et al. (2001) [64]. Salonvaara et al. (2004) performed dynamic experiments of sorption properties of building structures [65]. The moisture capacity of building materials in dynamic conditions was tested in small-scale laboratory tests, followed by a full-scale structural test. The results showed that building materials exposed to interior air can have a strong effect on the indoor air humidity level.

An interesting full-scale test (Fig. 29) of moisture buffer capacity of walls of a surface area of approx. 15.38 to 20.24 m^2 was carried out by Mortensen et al. (2005) [66]. Plasterboard structure and cellular concrete walls were tested. The idea was to mimic the exposure of moisture variations to interior surface materials. To measure the moisture buffering effect of the structures, the room was subjected to controlled moisture variations. The results proved that the moisture buffer capacity of materials can be used to reduce humidity fluctuations of the indoor environment.

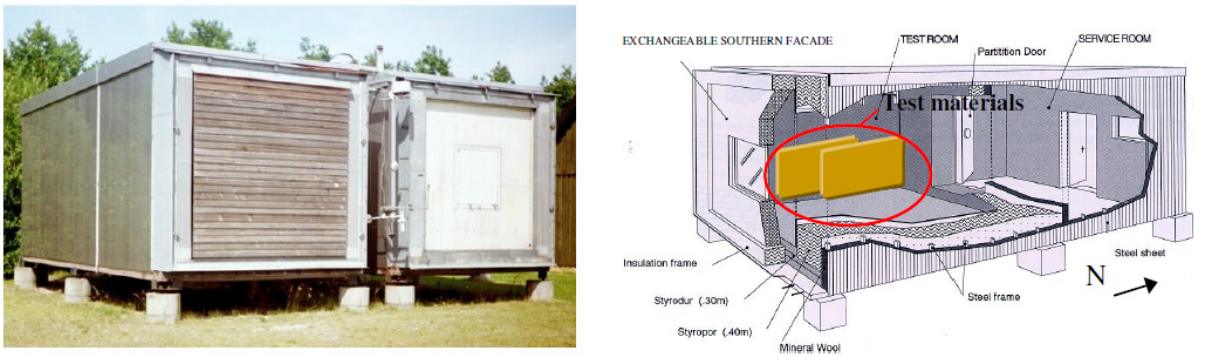

Fig. 29 The test rooms at DTU [66]

Cascione et al. (2019) are the authors of a review of moisture buffering capacity: From laboratory testing to full-scale measurement [67]. The challenges related to moisture buffering measurement, the approaches adopted by researchers, and the discrepancies between existing methods in the evaluation of the dynamic adsorption properties were investigated.

Brenton K. Kreigera and Wil V. Srubar (2019) performed an extensive search [68] for dynamic measurements of sorption properties. This work presents a comprehensive meta-analysis of experimental studies and a review of numerical approaches concerning the moisture buffering capacity of common building materials from more than 180 published experiments. There is a historical development of

dynamic sorption measurements from the first German Standard DIN (1968), through The Padfiled method (1998), the Japanese Industrial Standard JIS (2002), The NORDTEST method (2005) to ISO 24353 standard. The most commonly employed NORDTEST method is currently used as the primary standard for material characterization of moisture buffering value (MBV). Fig. 30 illustrates how widely MBV varies across individual studies and measurement methods, as well as variations within identical building materials.

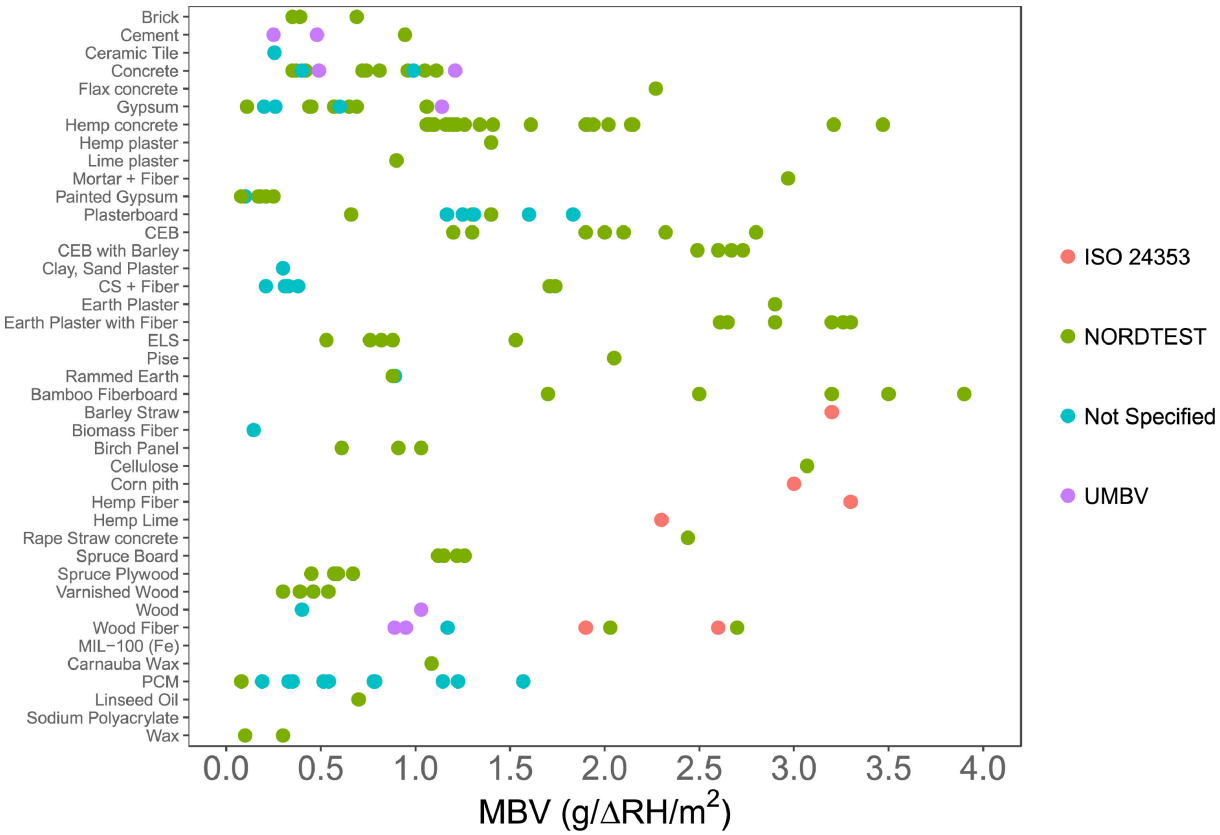

Fig. 30 Reported MBV of building materials [68]

To gather reliable and valid results of the behaviour of the complete building structures, the appropriate testing method has to be developed. The aim of this research was to investigate the humidity response of the indoor environment to the sorption properties of building structures during a jump in relative humidity in the interior.

Full scale experiments have a high informative value provided the experiment is properly demarcated and not affected by unexpected ambient conditions. However, it should be noted that full-scale tests are very financially and materially demanding and labor intensive. Therefore, a medium scale test method was proposed for the purpose of this thesis. The main idea of the dynamic sorption test is to simulate real situations in the building and the behaviour of real building structures in real world conditions.

2.3 Clay and its properties

Many institutions around the world deal with the use of clay in building construction. Among the best known are the Earth Architecture, Earth Building UK & Ireland, the Earth Building Association of Australia EBAA (Australia), Dachverband Lehm e.V. (Germany), CRAterre (France) and in the Czech Republic the Association of Clay Building.

They deal mainly with the application of clay products in construction, vocational training, gathering information about clay materials and completed buildings. This information is also given in many publications dealing with clay plasters, rammed earth, adobe, and other clay technologies. These are, for example:

- Building with Earth: Design and Technology of a Sustainable Architecture (Minke, G.) [46];
- Rammed Earth: Design and Construction Guidelines (Walker, P.; Keable, R.; Martin, J.; Maniatidis, V.) [69];
- Upscaling Earth: Material, Process, Catalyst (Heringer, A.; Howe, L. B.; Rauch, M.) [70];
- Building with Cob: A Step-by-Step Guide (Weismann, A.; Bryce, K.) [71];
- Essential Rammed Earth Construction: The Complete Step-By-Step Guide (Krahn, T.) [72];
- Der Lehmbau und seine praktische Anwendung (Niemeyer, R.) [73];
- Rammed earth (Rauch, M.; Kapfinger, O.) [74];
- Lehmwellerbau: Konstruktion, Schäden und Sanierung (Ziegert, Ch.) [75]
- Earth Architecture (Rael, R.) [76]
- Earth Construction: A Comprehensive Guide (Houben, H.; Guillard, H.) [77]
- Hliněné stavby (Žabičková, I.) [78]
- Hlinené domy novej generácie (Suske, P.) [79]

2.3.1 Composition of clay mixture

Unfired clay as a raw material for construction is a hygroscopic, water-absorbing, and an inhomogeneous material. The inhomogeneity of the material is given by its composition, in particular, the type and amount of clay minerals that significantly affect the properties of the product. Also, the way the mixture is processed significantly affects its properties.

Unfired clay materials usually consist of solids (gravel, sand, silt, organic matter, and clay minerals) and pore space where there is air and water molecules (Fig. 31). Gravel, sand and silt form the filler and clay minerals the binder.

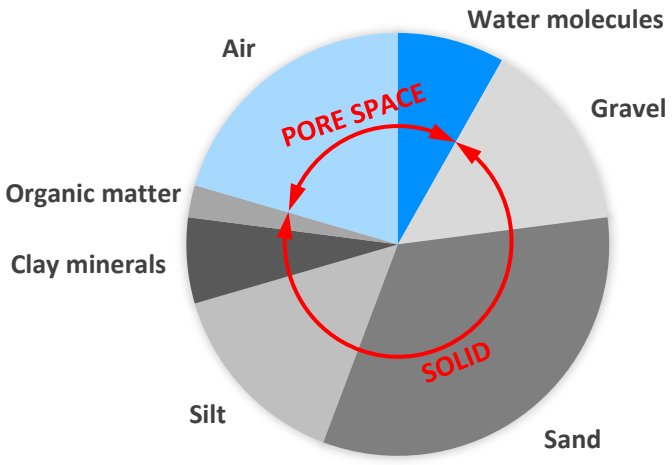

Fig. 31 Composition of clay mixture

Particle characteristics, including size, shape and mineral composition, are important to consider when establishing the properties of earth materials. There are several classifications of solid particles by size, e.g. according to Unified Soil Classification System (USCS), American Association of State Highway and Transportation Officers (AASHTO), American Geophysical Union (AGU), U.S. Department of Agriculture (USDA), Udden-Wentworth classification system, or Massachusetts Institute of Technology (MIT) [80]. The deviations of these individual classifications are small and unimportant for this research. The classification of solid particles according to ISO 14688-1:2002 is given in Tab. 3.

Tab. 3 Soil grain sizes according to ISO 14688-1:2002

Soil type	Symbol	Grain size range [mm]
Gravel	Gr	2–63
Sand	Sa	0.063–2
Silt	Si	0.002–0.063
Clay mineral	Cl	< 0.002

Source: [81]

The proportion of individual components of the material grains can be expressed using the grain-size curve. A sieve analysis is used in civil engineering for its determination. This procedure serves to assess the particle size distribution (PSD) of the granular material by allowing the material to pass through a series of sieves of gradually smaller mesh size and measuring the amount of material stopped by each sieve as a fraction of the total mass. The PSD is often of critical importance to a material's properties and it can help to understand its physical and chemical properties. The PSD affects the strength and load-bearing characteristics of a material and affects the reactivity of solids participating in physical and chemical reactions (the adsorption of atmospheric moisture for example). Fig. 32 shows the particle size distribution as a graph of percent material passing versus the logarithmic sieve size. There are examples of different ratios of the individual components in the mixture.

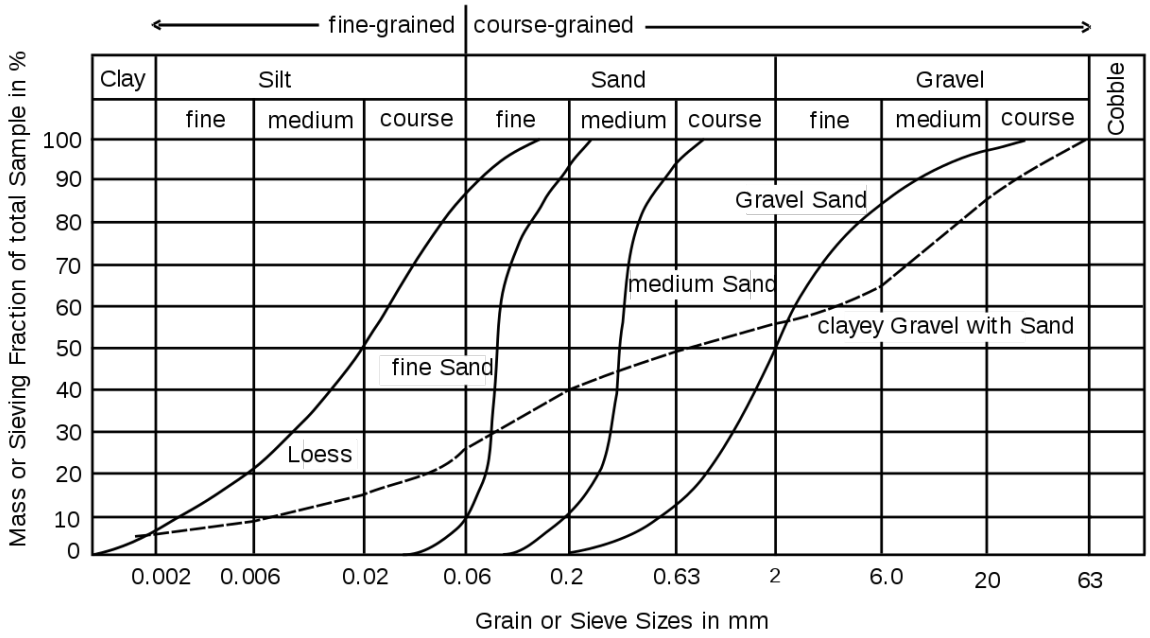

Fig. 32 Graph of percent passing versus the logarithmic sieve size [82]

Another possible description of the soil mixture is soil texture. The texture of the soil is an indication of the relative content of particles of various sizes in the soil. It will indicate the percentage of sand (size 0.063–2 mm), silt (size 0.002–0.063 mm), and clay (size less than 0.002 mm) present in the soil. A soil textural triangle diagram is used to classify the texture of soil particles.

The equilateral triangle according to USDA (black lines and description in Fig. 33) has ten zones, where each zone of the triangle represents one type of soil. The term "loam" also appears here. Loam is usually used to describe a mixture of sand, silt, and clay in various proportions. It is more of a slang term and not used in soil engineering. Therefore, a modified triangular diagram "Shepard Sediment Classification Diagram" (red line and description in Fig. 33) is also used.

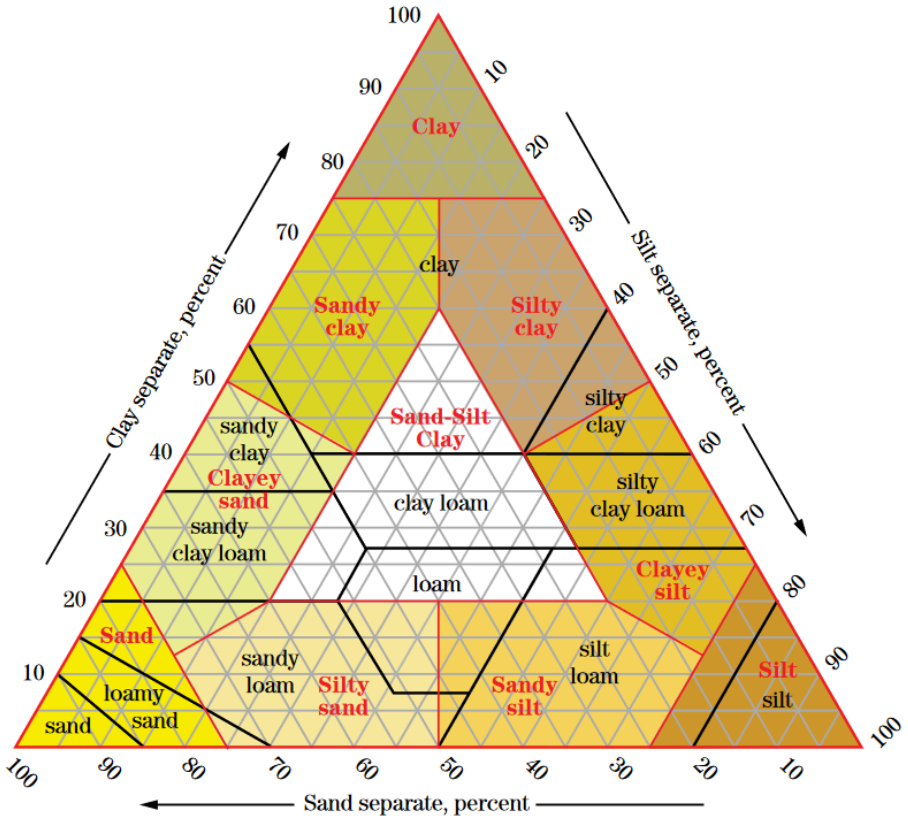

Fig. 33 A soil textural triangle diagram according to USDA (black) and Shepard (red) [80]

2.3.2 Clay minerals

Clay minerals are formed by soil-forming and biochemical processes in the soil with the contribution of soil microorganisms. This involves the decomposition of primary silicates or the synthesis of products that are released during mineral weathering. The main components of clay minerals are Si, Al, O, H, with smaller amounts of Ca, Mg, Fe, K, Zn, etc.

The basic structural unit of clay minerals consists of a tetrahedral (Si–O) layer and an octahedral (Al–O) layer (Fig. 34). The existence of hydrogen bonding interaction between silica and alumina layers holds them together strongly.

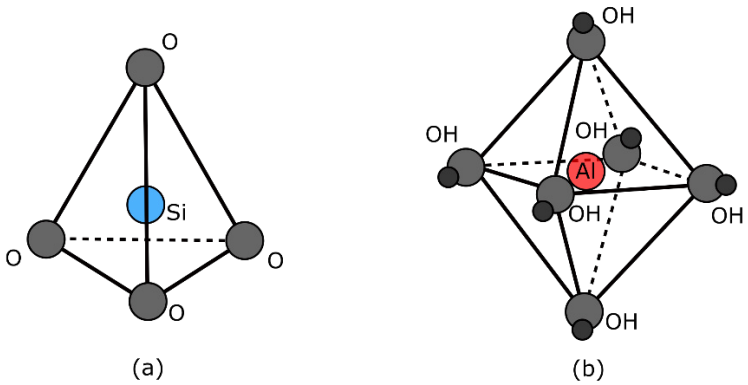

Fig. 34 Scheme of silica tetrahedral (a) and alumina octahedral (b)

Clay crystals are very small (below 2 microns). Each crystal is composed of a series of several hundred wafers. Each wafer is composed of two or three layers – silica (one or two layers) and alumina (one

layer). The division of clay minerals varies in the literature, however, for the purposes of this thesis, clay minerals are divided into groups according to the arrangement of the crystal lattice (Fig. 35):

- Kaolinite (1:1) – one layer of silica and one layer of alumina
- Illite (2:1) – two layers of silica and one layer of alumina, without expanding grid
- Montmorillonite (2:1) – two layers of silica and one layer of alumina, with expanding grid

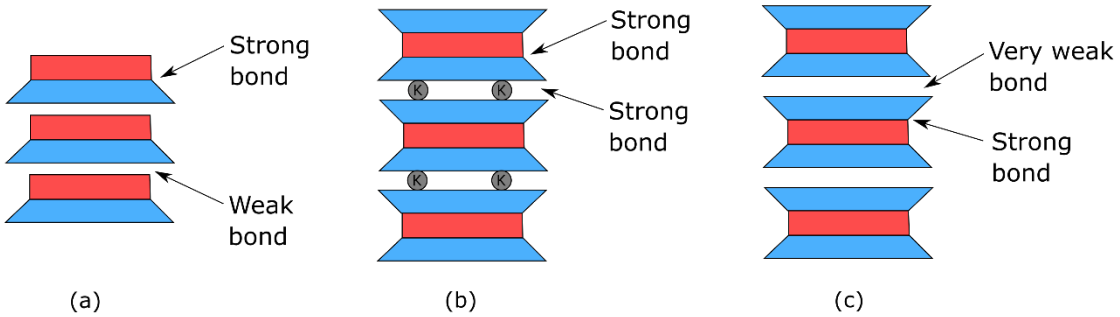

Fig. 35 Schematic diagrams of the structure: kaolinite (a); illite (b); montmorillonite (c) [83]

"The wafers carry hydroxy (-OH) groups and negative charges, due to the presence of impurities (e.g., iron) which are able to take the place of silicon and aluminium even if they have fewer positive charges. As a consequence positive ions, like sodium in montmorillonite, are frequently trapped between wafers, and water is able to penetrate the crystal as it is attracted by the hydroxy groups.

The access of water results in the increase of the distance between wafers and causes swelling of the clay. In a dry atmosphere, the water is lost and the clay contracts.

Illite contains calcium between wafers, and this ensures a stronger attraction between them. The swelling of illite is therefore smaller.

Kaolin is a very pure clay which contains no iron. As a result, the wafers have no negative charge, and there are no ions trapped between them. The wafers are kept together by relatively strong hydrogen bonds, and water is unable to separate them.

A little swelling also takes place in kaolin as water is attracted to the surface of the thin, flat crystals and is able to separate them.

All clays are plastic when wet because the thin crystals slide easily over one another under slight pressure. If more water is added to wet clay, it is completely dispersed." [84]

From the above, it is clear that the chemical composition and bonds directly affect the sorption properties of clay minerals. This is due to the strength of the bonds, the possibility of free bonds, and the resulting specific surface.

Tab. 4 compares selected clay minerals by Specific surface area (S_{BET} in $m^2 \cdot g^{-1}$) and by Langmuir maximum adsorption capacity (V_L in $cm^3 \cdot g^{-1}$).

Tab. 4 Adsorption capacity and specific surface area of clay minerals

Clay mineral	V_L [$cm^3 \cdot g^{-1}$]	S_{BET} [$m^2 \cdot g^{-1}$]
Kaolinite	3.88	15.7
Illite	2.22	11.2
Montmorillonite	6.01	56.5

Source: [85]

The chemical bonding of additional elements (iron, magnesium, potassium, etc.) and their quantities determine the resulting mechanical and sorption properties as well as their final colour.

Clay minerals are the binding material in soil as cement is in concrete. Often, clay crystals in soil are arranged in a flocculated form that is not very plastic. If it remains under water long enough, the arrangement changes to a dispersed form that is more plastic. This process is accelerated by mixing of the soil with a sufficient amount of added water. [86]

Dunoyer de Segonzac (1970) assumes the beginning of the conversion of kaolinite already at temperatures of 70–90 ° C, according to Šuch (2001) and Segonzac (1970) the conversion of smectites already occurs at 50–80 ° C to mixed-layered mineral illite-smectite [86], [87]. This has a fundamental effect on the direction of selected laboratory measurements. In order not to change the structure of the clay material, the sample must not be dried at higher temperatures, as for concrete, before performing the experiment.

2.4 Utilization of sorption properties in construction and architecture

The principles of passive moisture buffering have been used in many examples. Natural clays in the form of clay plasters, clay boards, unburned bricks, or rammed earth structures are used to keep appropriate level of relative humidity in the internal environment.

Below are four important examples of the different types of buildings and the different technologies used.

2.4.1 Buildings for industry

Ricola Herb Center (Switzerland)

- Herzog & de Meuron Architects
- Year of construction: 2013
- Technology: rammed earth panels

One shining example of rammed earth is the Ricola Herb Centre in Laufen (Basel), designed by the architects Herzog & de Mueron with a facade constructed by Martin Rauch, see Fig. 36 and Fig. 37.

The building is a long high-volume building with flat roof and façade of rammed earth. Façade elements were made of compacted local clay sourced from the Laufen valley.

To achieve a stable thermal-humidity microclimate, walls made of prefabricated rammed earth panels with a thickness of 0.5 m are used, which surround the entire warehouse with dimensions of approximately 30 × 50 m and a height of 10 m.

Fig. 36 Ricola Herb Centre, Laufen
(source: photo J. Růžička)

Fig. 37 Ricola Herb Centre, Laufen
(source: pohoto J. Růžička; [88])

In the stocking part, earthen panels keep a stable microclimate for storing and processing of herbs without any other ventilation system. This decreases the energy demand for the operation phase of the building, making it energy efficient and decreasing negative environmental impact.

2.4.2 Service buildings

Depository for the East Bohemian Museum in Pardubice (Czech Republic)

- Adam Rujbr Architects
- Year of construction: 2019
- Technology: unburned brick covered by clay plaster

Unfired clay material is used in this building to mitigate the effects of heat and moisture. Also it is a recyclable material, see Fig. 38 and Fig. 39.

Fig. 38 Depository for the East Bohemian Museum in Pardubice [89]

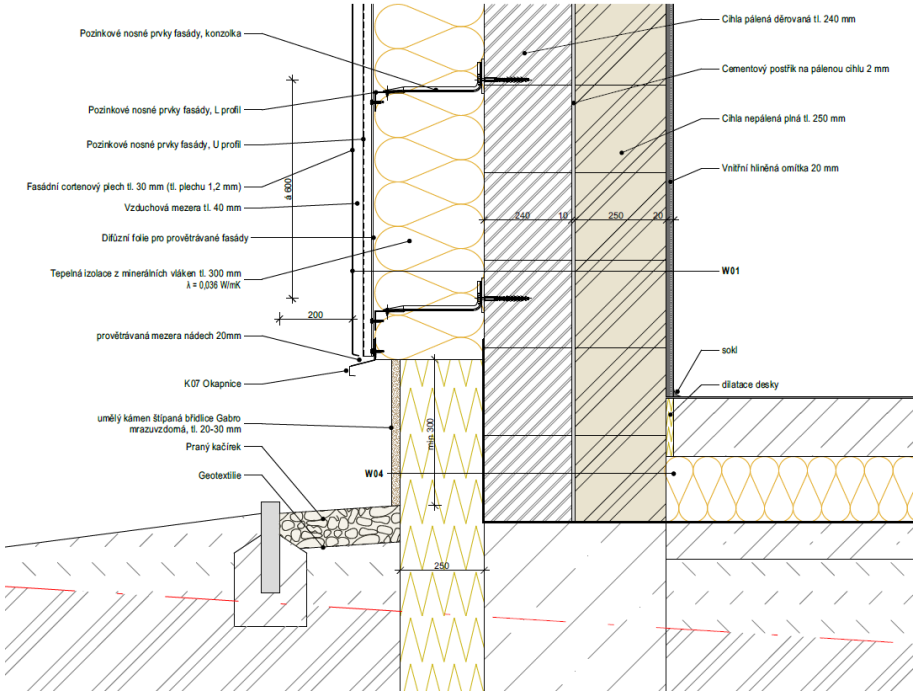

Fig. 39 Plinth detail – use of unburned brick and clay plaster in the interior [89]

The building is extremely energy efficient. It has modern technologies such as recuperation and a heat pump located on an extensive green roof. The structure itself is a reinforced concrete skeleton with a panel ceiling on composite steel-concrete beams. The envelope then consists of a cor-ten facade, a ventilated gap, a layer of mineral thermal insulation of 300 mm thick, and fired bricks interwoven with unfired brick with clay plaster. The combination of these bricks brings a large storage capacity of heat and humidity and thus can help reduce temperature and humidity fluctuations.

Unfired bricks form the inner layer of the perimeter shell which, in this case, amount to about 350 tons of material.

During the project, the authors tried to design an object that is economical, not only operationally but, from environmentally friendly materials which are either recycled or recyclable. [89]

2.4.3 Office buildings

Office building for UNFCCC, Bonn (Germany)

- RKW, Rhode Kellermann Wawrowsky
- Year of construction: 2013
- Technology: clay boards covered by clay plaster

The renovation of this house, built in 1953, proves that clay is not just used in the reconstruction and conversion of historical buildings. The requirements of the refurbishment and renovation of the building for the Secretariat of the United Nations Framework Convention on Climate Change (UNFCCC) were high: the client placed high priority on the use of sustainable building materials and consistent compliance with ecological building guidelines in order to meet the requirements of climate protection both in production and in maintenance, see Fig. 40 and Fig. 41.

Building boards made of clay and reeds were installed on the metal posts of the inner walls, with cellulose insulation panels as filling. They ensure the best room climate and have excellent soundproofing properties. Finally, the clay building boards were covered with clay plaster and painted by the final white silicate coat. [90]

Fig. 40 Office building for UNFCCC, Bonn [90]

Fig. 41 Use of clay boards [90]

2.4.4 Buildings for education and residence

Sluňákov – Centre for ecological activities (Czech Republic)

- Projektil architects
- Year of construction: 2007
- Technology: uncovered unburned brick

Unfired clay material is used in this building as an environmentally friendly material.

The building is designed for energy efficiency using modern alternative energy sources and general principles of sustainable construction. The form of the proposed object is the result of a process to create an ecological house which integrates into the surrounding nature using solar energy and protecting itself from bad weather by using earthen wall (Fig. 42).

The materials used are mostly traditional and have been selected with regard to ecological acceptability. Wood, glass, concrete, and stone in gabions are used for facades. The interior is mostly wood, glass and/or brick walls, fired and unfired, plastered or bare.

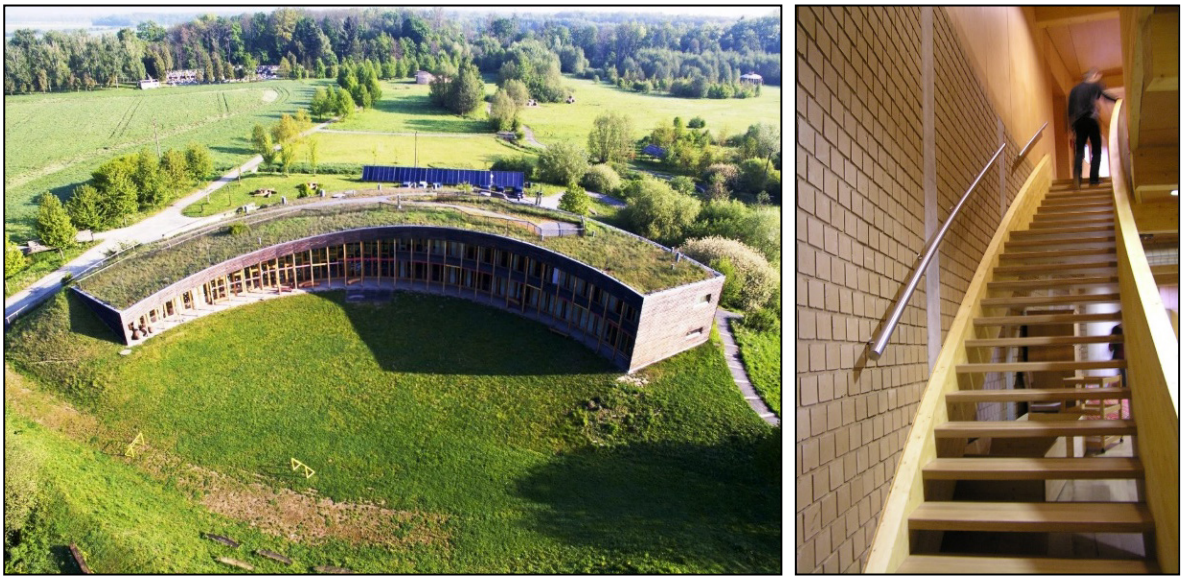

Fig. 42 Centre for ecological activities Sluňákov [91]

3 Sorption properties of materials in steady state

In this chapter, some author's formulations published in journals or conference papers, which are listed in the references, are used.

Measurement of sorption properties is part of a long-term research on the use of clay materials in modern structures, from the Faculty of Civil Engineering, CTU in Prague, Department of Building Structures. It follows projects dealing with the development and use of load-bearing prefabricated panels of rammed earth.

Although the sorption properties of clay materials have been documented many times (see chapter 2.2.2), each clay mixture has its own specific properties due to the different ratios of clay minerals, fillers and other components. In the research, the sorption curve of a specific clay mixture had been determined, from which rammed earth panels were made. At the same time, sorption curves for other specific clay mixtures and materials and other standard building materials were determined.

This part of the thesis deals with the experimental measurement of sorption properties of selected materials in a steady state. Determination of hygroscopic sorption properties of porous building materials and products were performed according to the ISO 12571:2013 standard.

The aim of the experiments was to measure the sorption isotherm as one of the properties of porous building materials and, furthermore, to compare these properties with data reported in the literature and compare the sorption properties of individually selected and tested materials. A total of 31 different materials were measured and divided into the following categories: rammed earth panels, clay products, and standard building materials (Fig. 43).

Rammed earth panels

The research [4] at Department of Building Structures of the CTU in Prague focused on, among other things, the mechanical properties of rammed earth panels. The mechanical properties of prefabricated structures of various compositions were investigated. This thesis follows this research in measuring the sorption properties of identical mixtures.

Various mixtures were tested. The first and most determinate test was the effect of different types of clay minerals. The pure clay minerals montmorillonite, illite, kaolinite and zeolite were used. Another major raw material for the performed tests was obtained from the resources of Claygar, a Czech company which produces unburned clay commercially. It is a soil mixture of hydromicas and kaolinite with minor addition of montmorillonite.

The effect of the amount of added sand, which affects the mechanical and sorption properties of the product, was investigated. The composition of the mixture was optimized on the basis of a series of experiments with respect to shrinkage, cracking, and mechanical properties. Another topic was the addition of a chemical binder to the mixture, the resulting product being a “stabilized rammed earth”. Cement and lime were added to the selected mixtures. The influence on the resulting mechanical and sorption properties of the structure was monitored. The effect of different methods of drying the sample was also investigated.

Clay products

Other clay materials and structures were also selected as test specimens: clay undercoat and finishing plaster from the company Picas, clay panel from Lemix, unburned brick Nature Energy from Heluz and adobe (unburned brick from earth and organic materials) from a historical building from the end of 19th century in Western Bohemia.

Standard building materials

Some samples were selected to compare the sorption properties of natural materials and standard commercial building materials: lime plaster, concrete, HPC, gypsum board, spruce wood, OSB, and ceramic block.

Tab. 5 shows an overview of all measured materials.

Tab. 5 Tested samples and their mixture compositions

Groups of samples		Sets of samples	Mixture composition / description
Rammed earth panel	variant of the sand stabilization	C_W10	soil C, 10 % water
		C_S10/W10	soil C, 10 % sand, 10 % water
		C_S30/W10	soil C, 30 % sand, 10 % water
	variant of clay minerals	M_W20	montmorillonite, 20 % water
		I_W10	illite,10 % water
		K_W20	kaolinite, 20 % water
		M_S30/W20	montmorillonite, 30 % sand, 20 % water
		I_S30/W10	illite, 30 % sand, 10 % water
		K_S30/W20	kaolinite, 30 % sand, 20 % water
		Z_W22	zeolite, 22 % water
	variant of the chemical stabilization	C_W12_lim	soil C, 12 % water, 5 % lime
		C_S30/W15_lim	soil C, 30 % sand, 15 % water, 5 % lime
		C_S10/W12_lim	soil C, 10 % sand, 12 % water, 5 % lime
		C_W12_cem	soil C, 12 % water, 5 % cement
		C_S30/W15_cem	soil C, 30 % sand, 15 % water, 5 % cement
		C_S10/W12_cem	soil C, 10 % sand, 12 % water, 5 % cement
	variant of the drying method	C_S10/W10 110 °C	soil C, 10 % sand, 10 % water – dried at 110 °C
		C_S10/W10 60 °C	soil C, 10 % sand, 10 % water – dried at 60 °C
		C_S10/W10 sun	soil C, 10 % sand, 10 % water – sun-dry
		C_S10/W10 air	soil C, 10 % sand, 10 % water – air-dry
Clay product	clay plaster	Clay undercoat plaster	clay undercoat plaster – Picas Econom
		Clay finishing plaster	clay finishing plaster – Picas Econom
	clay commercial product	Unburned brick	unburned brick – Heluz Nature Energy 12/25
		Clay panel	clay panel – Lemix
		Adobe	adobe – old unburned brick
Other	standard building materials	Spruce wood	Spruce wood
		OSB	OSB 3 – Kronospan
		Gypsum board	Gypsum board – Rigips RB (A) 12.5
		HPC	High-performance concrete
		Concrete C30/37	Concrete of the strength class C30/37
		Lime plaster	Lime plaster – HASIT 160 Fein-Kalkputz
		Ceramic block	Ceramic block – Heluz 8

Note: The explanation of marks: M (montmorillonite); I (illite); K (kaolinite); Z (zeolite); C (commercial clay mixture Claygar); S (sand); W (water); Cem (cement); Lim (lime).

The reference material for comparison

As a reference material, the mixture **C_S10/W10** was determined. The reason for this is the connection with the above thesis (Havlík, F.). This reference material is permanent for the entire research.

The raw material for the reference material was acquired from the resources of Claygar (C), a Czech company who manufacture unburned clay products. This clay consists mainly of hydromicas and kaolinite with minor additions of montmorillonite. The amount of added sand (S) is 10 %, determined from the clay part of mixture. The amount of added water (W) is 10 %, determined from the weight of mixture. This mixture is without the addition of chemical stabilization (cement or lime).

Other reference materials are **Concrete C30/37** and **Gypsum board** – Rigips RB (A).

3.1 Sorption isotherms – methodology

To compare sorption isotherms of building materials, a sorption test according to the European Standard EN ISO 12571:2013 is recommended. [92]

The experimental measurement of sorption properties is carried out in the glass desiccator at a constant temperature and atmospheric pressure. Prescribed relative humidity in the desiccator is achieved by saturated salt solutions (see below). The test samples are exposed to the relevant environment until reaching the equilibrium weight. This state is achieved when the weight change during 24 hours is less than 0.1 %. The sorption curve of the tested material which describes the potential to accumulate air humidity, is the result of the experiment and can be compared to other single materials. The formula of sorption curve can be used for further mathematical simulations.

Preparation of test samples

To determine the sorption properties, it was necessary to choose a suitable size and shape of the samples. For large samples, the equilibrium state process takes a long time. Conversely, for a sample that is too small (light), it would not be possible to determine its equilibrium weight accurately enough (to 0.1 % of the sample weight).

Production of samples for rammed earth panels occurred by mixing a predefined mixture of individual components (clay, sand, water, admixtures). The samples were made by a pneumatic tamper into a metal mould in four layers. The 40 × 40 × 160 mm blocks were then cut with a hand saw to the required sample size. Concrete samples and plasters (clay and lime) were also produced by casting into a mould (40 × 40 × 160 mm) and subsequent cutting. Samples of other materials were made by cutting from the original formats to the required size (Fig. 44).

A sorption curve was created for test specimens of the size approx. 40 × 40 × 15–25 mm and of the weight about 50–60 g. All materials were measured in sets of 3 samples.

Samples made with mixed water (concrete samples, rammed earth samples, and plasters) were first air-dried for 28 days under controlled conditions at temperature 18–23 °C; 30–60 % RH).

Drying of the samples

The drying of the samples in the drying room was performed differently for each material. Standard building materials were oven dried at 105 °C. Clay samples were dried at 60 °C because higher drying temperature could lead to chemical changes in the structure of clay minerals, potentially affecting the resulting sorption properties. [86]

Drying was continued until the equilibrium weight of test samples was achieved.

Description of measurements

Each sample was placed in its closable plastic box. The box prevented material loss during sample handling, ensuring the weight of the sample and non-exposure to laboratory conditions during weighing.

After reaching mass equilibrium during drying, the samples were placed in a glass desiccator (Fig. 45). There was a prepared environment with the given RH, which was formed by saturated salt solution LiCl (see Tab. 6).

A PC fan was placed in the desiccator, guaranteeing air circulation and improving the transfer of moisture by convection, thus speeding the stabilization of the weight of the samples. There is also the data logger (Comet S3120) that reads the temperature and relative humidity hourly within the desiccator (Fig. 46). The temperature in the laboratory was constant during the measurement.

The change in the weight of the sample corresponds to the increase/decrease of the physically bound, atmospheric moisture in the pore system of the material. After stabilizing the weight of the sample, the material was exposed to the next step of the selected RH (Tab. 6).

After the gradual completion of the entire scale (adsorption), the opposite process occurred (desorption). Finally, the samples were allowed to dry at 105 °C and then weighed. The adsorption and desorption curves of individual samples are determined from the measured values.

Measured points of sorption isotherm

Aimed RH levels in the desiccator were created by saturated aqueous salt solution (Tab. 6) and present the particular points on the sorption curve. These saturated solutions were chosen since some of them were recommended as fixed points for forming a calibration scale of the relative humidity of moist air. The RH values of the selected solutions form an equal scale and cover the interval between 10 % and 100 % relative humidity.

The method of saturated solutions is based on chemical systems in steady state, which allow a known and constant value of relative humidity to be maintained in sealed surroundings. The moist air in a chamber/desiccator is characterized by a relative humidity value dependent on the temperature and atmospheric pressure.

For saturated solutions, it is necessary to follow best practices in their preparation and use to avoid significant deviations from the expected RH value. These uncertainties can be even greater than 5 % RH, which is unacceptable. The values of the relative humidity for saturated solutions reported in the literature differ from each other by about 1–2 % RH at 20 °C. [93]

The currently available relative humidity sensors have high uncertainty and are not always metrologically satisfactory for the determination of RH value. Comparatively, the chemical equilibrium methodology based on saturated aqueous salt solutions is reliable when the fundamental requirements are met.

RH values determining sorption isotherms were determined from measurements using data-loggers placed in the desiccators.

Tab. 6 Equilibrium relative humidity of selected saturated salt solutions at 20 °C and 25 °C

Saturated solution	LiCl	$KC_2H_3O_2$	K_2CO_3	NH_4NO_3	NaCl	KCl	KNO_3	K_2SO_4
RH [%] at 20 °C	11.3	23.1	43.2	61.8	75.5	85.1	94.6	97.6
RH [%] at 25 °C	11.3	22.5	43.2	61.8	75.3	84.3	93.6	97.3

Source: [94]

Determination of dry bulk density

Determination of dry bulk density was carried out according to the European Standard EN 772-13 (2001) [95]. At the end of the experiment, all materials were placed in a drying room at 105 °C at constant weight to get the correct value of dry bulk density. The linear dimensions of the samples were measured with an electronic digital calliper with a precision of ± 0.005 mm. A sample's volumes were calculated from these dimensions.

Used equipment

Dataloggers (Comet S3120) were used to measure temperature and relative humidity in glass desiccators. The accuracy ranges of the Comet S3120 are ± 2.5 % RH and ± 0.4 K for condition 23 °C. [96]

The laboratory balance AND GX-4000 was used to measure the weight of the samples. The accuracy of balance is: readability 0.001 g; repeatability (standard deviation) 0.001 g; linearity 0.002 g. [97]

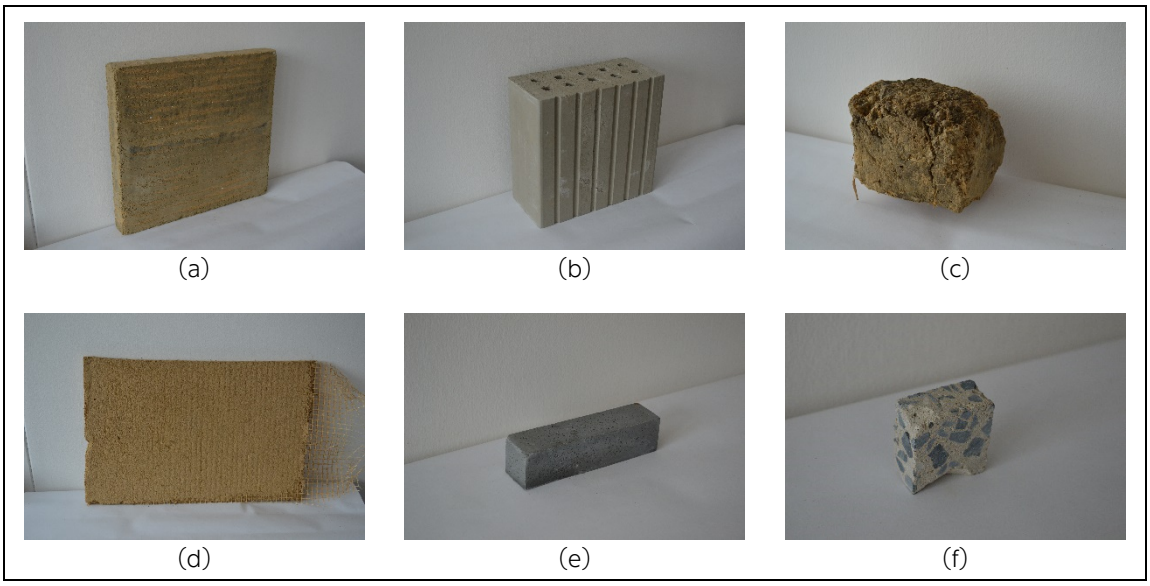

Fig. 43 Some tested materials: (a) rammed earth panel, (b) unburned brick, (c) adobe, (d) clay panel, (e) high-performance concrete, (f) concrete C30/37

Fig. 44 Samples preparation

Fig. 45 Test samples

Fig. 46 Measurement of samples

3.2 Sorption isotherms – measurements and results

The sorption isotherm is usually expressed as the dependence of the *moisture content mass by mass* (u) in kg · kg^{-1} on the relative humidity of the environment. The moisture content mass by mass is the ratio between the weight of the sorbed water molecules to the weight of the dry sample. The sorption isotherms expressed in this way characterize the properties of the material independent of its bulk density, i.e. independent of the method of processing and the amount used in the construction.

The results below show that 1 kg of spruce wood absorbs two times more moisture than 1 kg of clay material. However, in the case of a building structure, it is necessary to take into account the actual volume of material used and thus consider the *moisture content mass by volume* (w) in kg · m^{-3}. From

this analysis it is clear that, for example, a rammed earth wall with a thickness of 200 mm is able to absorb almost twice as much moisture as a solid wooden wall of the same thickness. The two times lower sorption potential of the clay material is compensated by four times higher bulk density compared to spruce wood.

Moisture content is calculated as:

$$u = \frac{m_w}{m_{dry}} \quad [\mathrm{kg \cdot kg^{-1}}] \quad \text{, or} \quad w = \frac{m_w}{V_{dry}} \quad [\mathrm{kg \cdot m^{-3}}] \quad . \tag{4}$$

Since this thesis focuses mainly on building materials, sorption isotherms are given with respect to their bulk density, i.e. in units of moisture content mass by volume w in $\mathrm{kg \cdot m^{-3}}$.

Tab. 7 shows the determined bulk densities of the tested materials.

Tab. 7 Dry bulk density of tested samples

Groups of samples		Sets of samples	Dry bulk density [kg · m⁻³]
Rammed earth panel	variant of the sand stabilization	C_W10	2 026.8
		C_S10/W10	2 033.6
		C_S30/W10	2 039.6
	variant of clay minerals	M_W20	1 672.2
		I_W10	1 995.1
		K_W20	1 476.2
		M_S30/W20	1 685.0
		I_S30/W10	1 885.1
		K_S30/W20	1 684.5
		Z_W22	1 319.6
	variant of the chemical stabilization	C_W12_lim	1 728.5
		C_S30/W15_lim	1 849.7
		C_S10/W12_lim	1 760.5
		C_W12_cem	1 882.1
		C_S30/W15_cem	1 815.3
		C_S10/W12_cem	1 897.8
	variant of the drying method	C_S10/W10 110 °C	1 927.6
		C_S10/W10 60 °C	1 967.7
		C_S10/W10 sun	1 954.3
		C_S10/W10 air	1 960.5
Clay product	clay plaster	Clay undercoat plaster	1 853.0
		Clay finishing plaster	1 669.3
	clay commercial product	Unburned brick	1 626.8
		Clay panel	1 352.2
		Adobe	1 643.2
Other	standard building materials	Spruce wood	500.0
		OSB	466.1
		Gypsum board	720.0
		HPC	2 216.0
		Concrete C30/37	2 132.0
		Lime plaster	1 625.2
		Ceramic block	1 259.4

Note: The explanation of marks: M (montmorillonite); I (illite); K (kaolinite); Z (zeolite); C (commercial clay mixture Claygar); S (sand); W (water); Cem (cement); Lim (lime).

3.2.1 Rammed earth panels

The sorption isotherm of a specific clay mixture, from which rammed earth panels were made, was determined in the following: (F. Havlik's research on the mechanical properties of rammed earth). It is believed that due to the small amount of filler (10 %) the hygroscopic properties of the panels can be very good and could significantly help maintain a constant relative humidity in the interior.

At the same time, sorption isotherms were determined for other clay mixtures, which were processed as rammed earth. A total of 16 different mixtures were compared.

The basis of all samples was a clay raw material: pure clay minerals (M, I, K, Z) or clay raw material (C) from the company Claygar s.r.o., which consists mainly of hydromicas and kaolinite with minor addition of montmorillonite. The particle size distribution of this material is shown in Fig. 47.

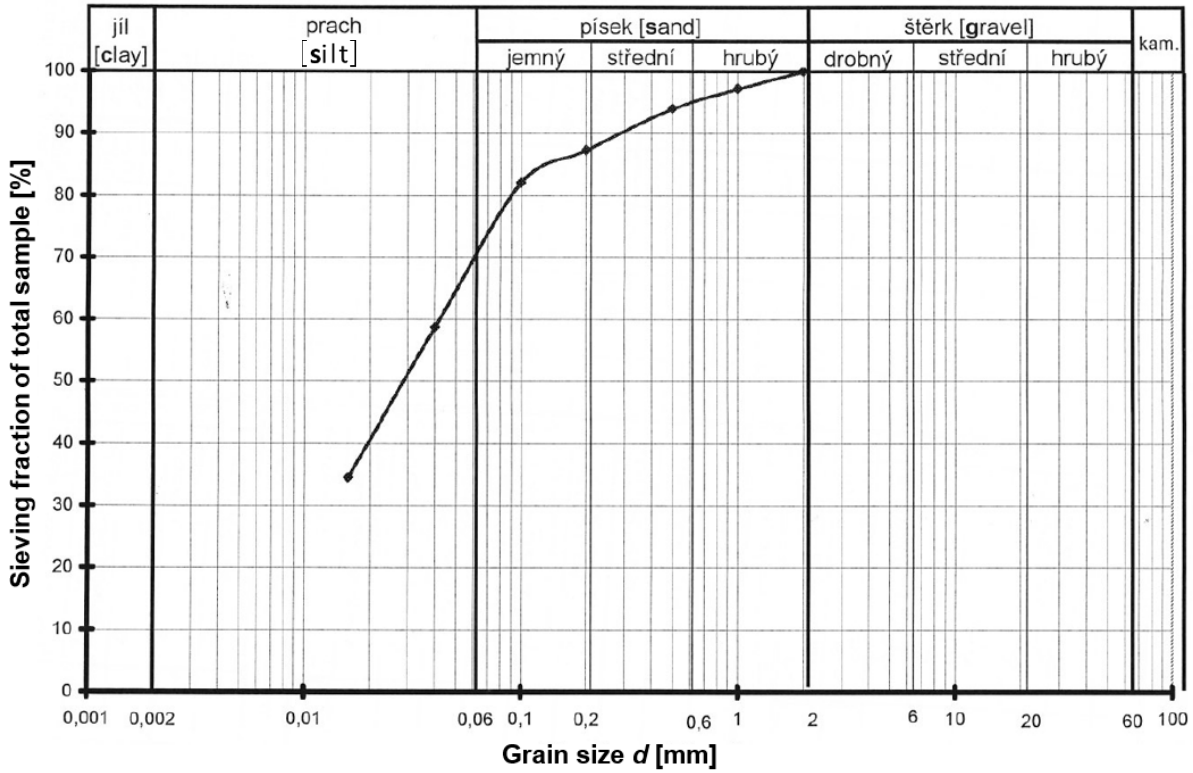

Fig. 47 Particle size distribution of clay raw material Claygar (C)

The composition of the individual clay mixtures for the production of test specimens determines their designation. The first letter indicates the main clay component, followed by information on the amount of sand fraction 0–4 (S) and water (W).

3.2.1.1 Influence of mineralogical composition

Fig. 48 shows the expected results of the difference in mineralogical composition. As described many times in the literature, montmorillonites have the best sorption properties, followed by illites and zeolites, with kaolinites having the worst properties. This disparity is due to the construction of the wafers from the individual minerals.

Montmorillonites (M) have about 53 % better sorption properties than illites (I) and zeolites (Z), and up to 80 % better properties than kaolinites (K). It should be noted that while it is necessary to consider sorption properties, it is more important to consider the mechanical properties.

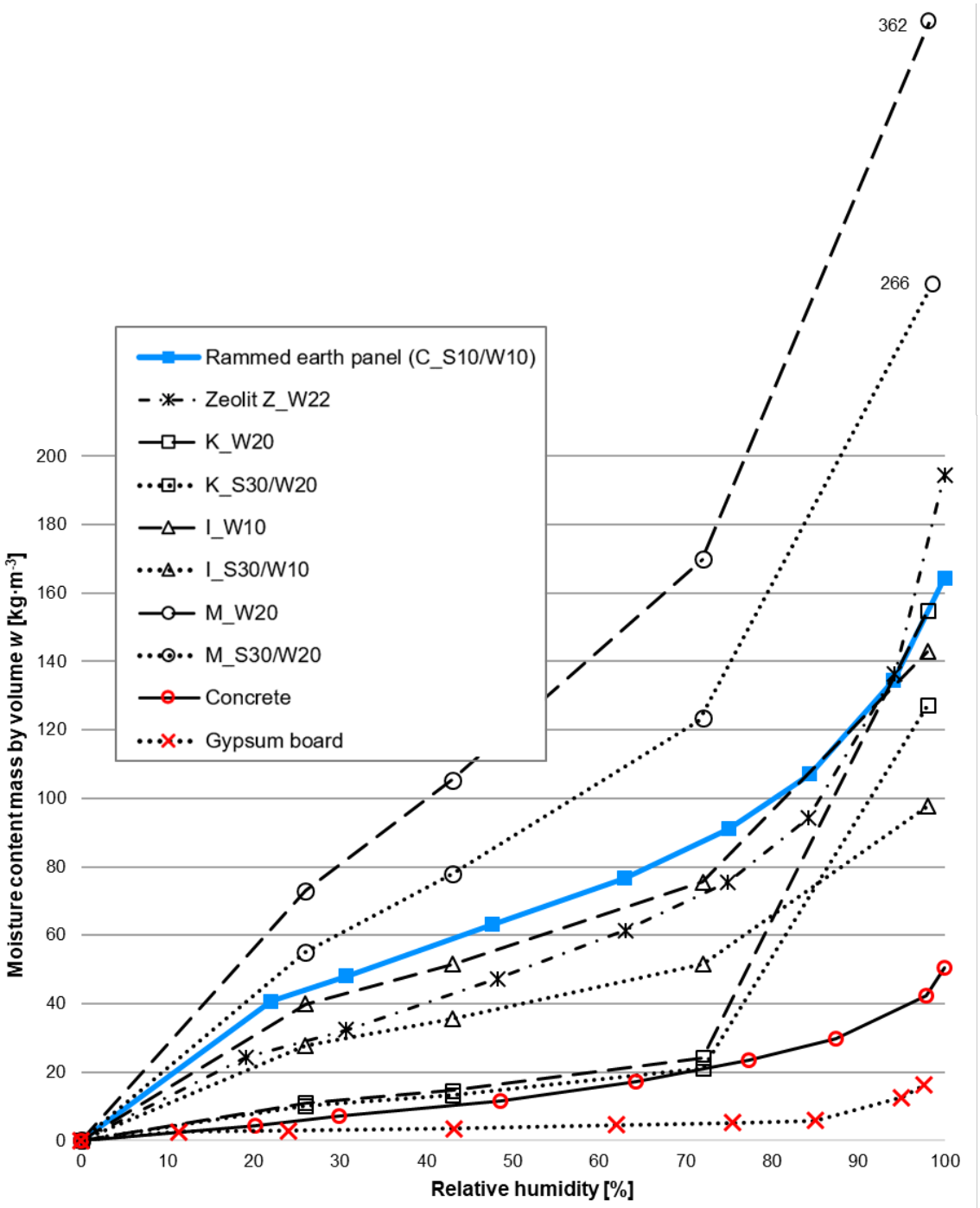

Fig. 48 Adsorption isotherms – different mineralogical composition

3.2.1.2 Influence of sand sharpening

Furthermore, the effect of the amount of sand added was investigated. The effect of the sand additive (so-called shrinkage-reducing sharpening) is evident from graphs Fig. 48 and Fig. 49. The more sand contained in the clay mixture, the worse its sorption properties are. The reason is the low ability of sand grains to bind air humidity, due to their minimal porosity and specific surface area.

In previous research [4], the composition of the mixture was optimized based on a series of composition experiments. Optimal mechanical properties were sought.

The addition of 10 % sand lessens the sorption ability of the clay mixture by 12 %. Adding 30 % sand will lessen it by up to 25 %, for illite by up to 30 %, but for kaolinite by only 11 %.

In Fig. 49 are shown two measurements of the C_S10/W10 mixture. The measurement of the "Rammed earth panel (C_S10/W10)" is newer and was performed in more steps of increasing relative humidity. The measurement difference is approximately 1.6 %, which can be considered a statistical error.

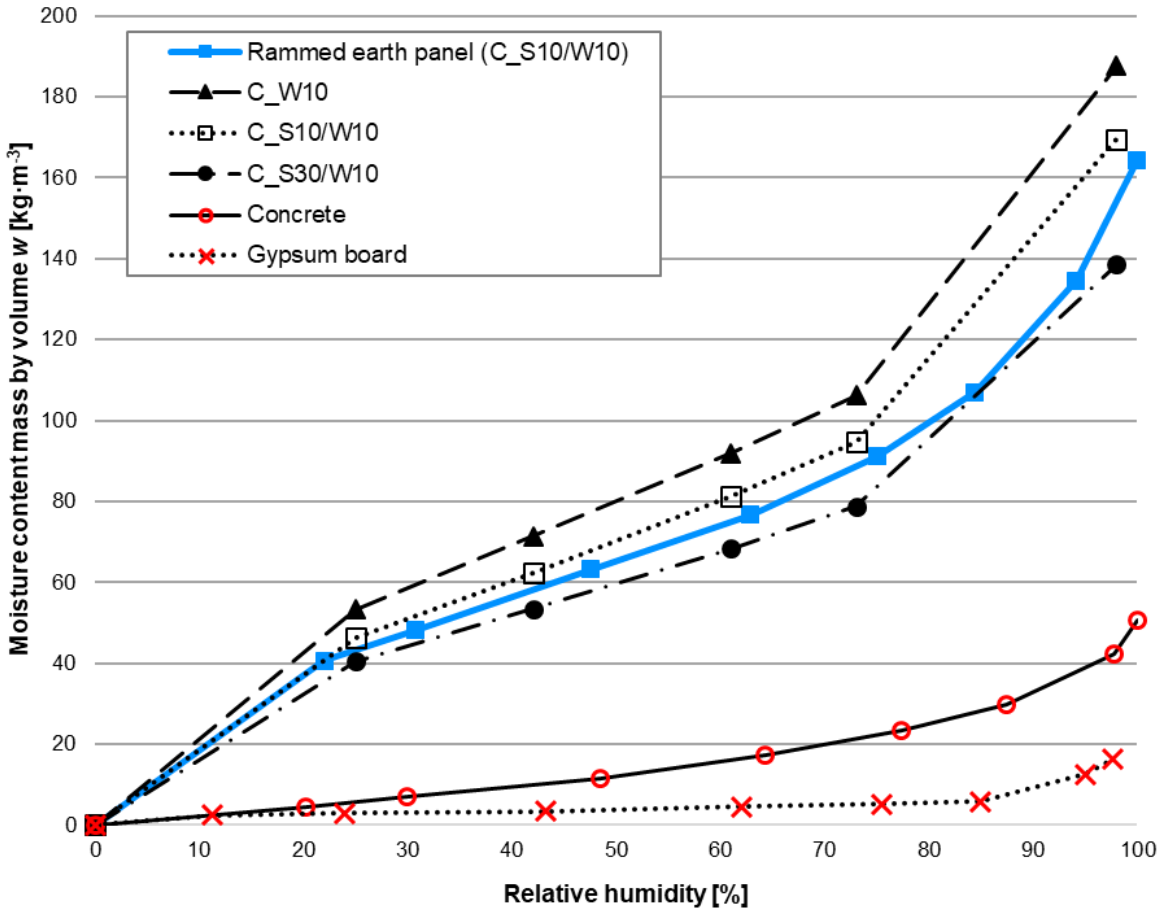

Fig. 49 Adsorption isotherms – different amount of sand in the mixture

3.2.1.3 Influence of chemical stabilization

Chemical stabilization of the clay mixture (by adding lime or cement) will improve its mechanical properties but, at the same time, significantly worsen its sorption properties. This is due to chemical bonds inside the material.

The addition of 5 % lime to the clay mixture lowers the sorption potential by up to 43 % as compared to the original composition without chemical stabilization. When stabilizing 5 % of cement, the reduction in sorption capacity is about 40 %.

The sharpening of an already chemically stabilized clay mixture shows smaller differences in sorption properties than with mixtures without lime or cement. By adding 10 % sand to the mixture, the sorption potential is reduced by 8 %. By adding 30 % sand to the mixture, the sorption potential is reduced by 20 % (lime), and by 32 % (cement).

The results show (Fig. 50) that the addition of 10 % of sand and of 5 % of cement or lime (mixture C_S10/W10_cem and C_S10/W10_lim) still gives > 2 times the sorption potential of concrete and up to 8 times better than gypsum board.

3.2.1.4 Influence of drying method

The literature states that chemical changes in the structure of clay materials can occur as early as 60 °C. This part was focused on the comparison of measured values of rammed earth C_S10/W10 processed, respectively dried by various technological procedures.

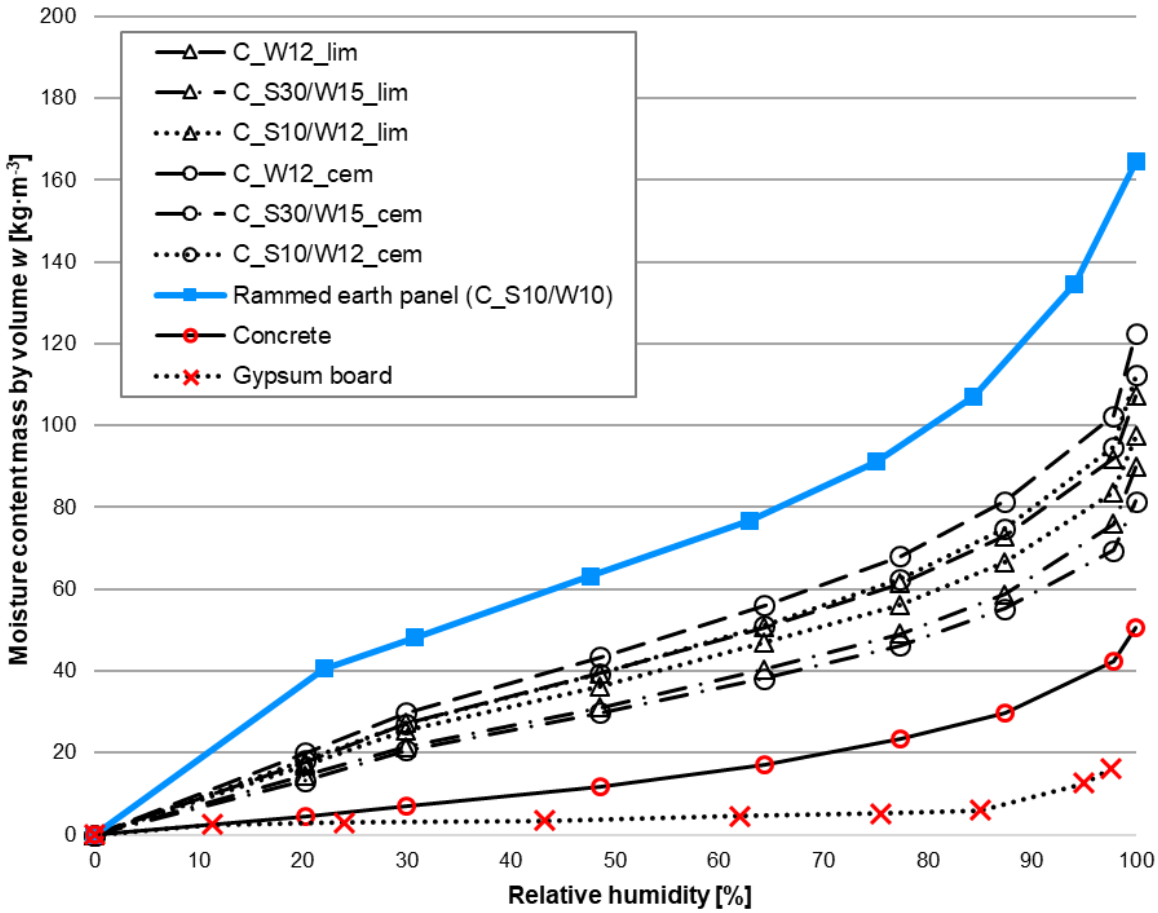

Fig. 50 Adsorption isotherms – stabilized rammed earth with lime and cement

The adsorption curves of the individually measured materials show (Fig. 51) a similar shape. From the measured values it can be read that rammed earth dried after mixing at 110 °C absorbs the least air moisture compared to other sets (up to 10 % less sorption potency compared to air-dried samples). In contrast, most water vapour from air is absorbed by mixtures dried in the sun (approx. 40 °C) and indoors at the temperature of 20 °C, the mixture C_S10/W10 air (Rammed earth panel). The difference between drying at 60 °C and drying in indoor air is about 3.5 %.

The differences in the measured values are not high, but they show a certain tendency. It is important to realize that this is one identical mixture, so the ratio of individual raw materials in the compared sets is the same. The technological process of production differs only in the method of drying the samples. The order of the adsorption curves corresponds to the drying temperature: the higher the drying temperature, the lower the adsorption capacity. The „air“ and „sun“ curves are almost identical in terms of statistical deviation.

3.2.2 Clay products

Although natural clay has excellent sorption properties, in practical use clay materials contain a certain amount of sand, primarily to minimize shrinkage. Typical clay plasters contain 60–75 % of sand, decreasing the sorption ability. Such a high amount of sand means that the sorption properties of clay plaster are at the same level as traditional building materials. When using rammed earth technology (amount of sand 0–30 %), the content of the clay component is higher, and with it the sorption potential increases.

The expected result (Fig. 52) is that rammed earth has a much higher sorption potential than other clay products.

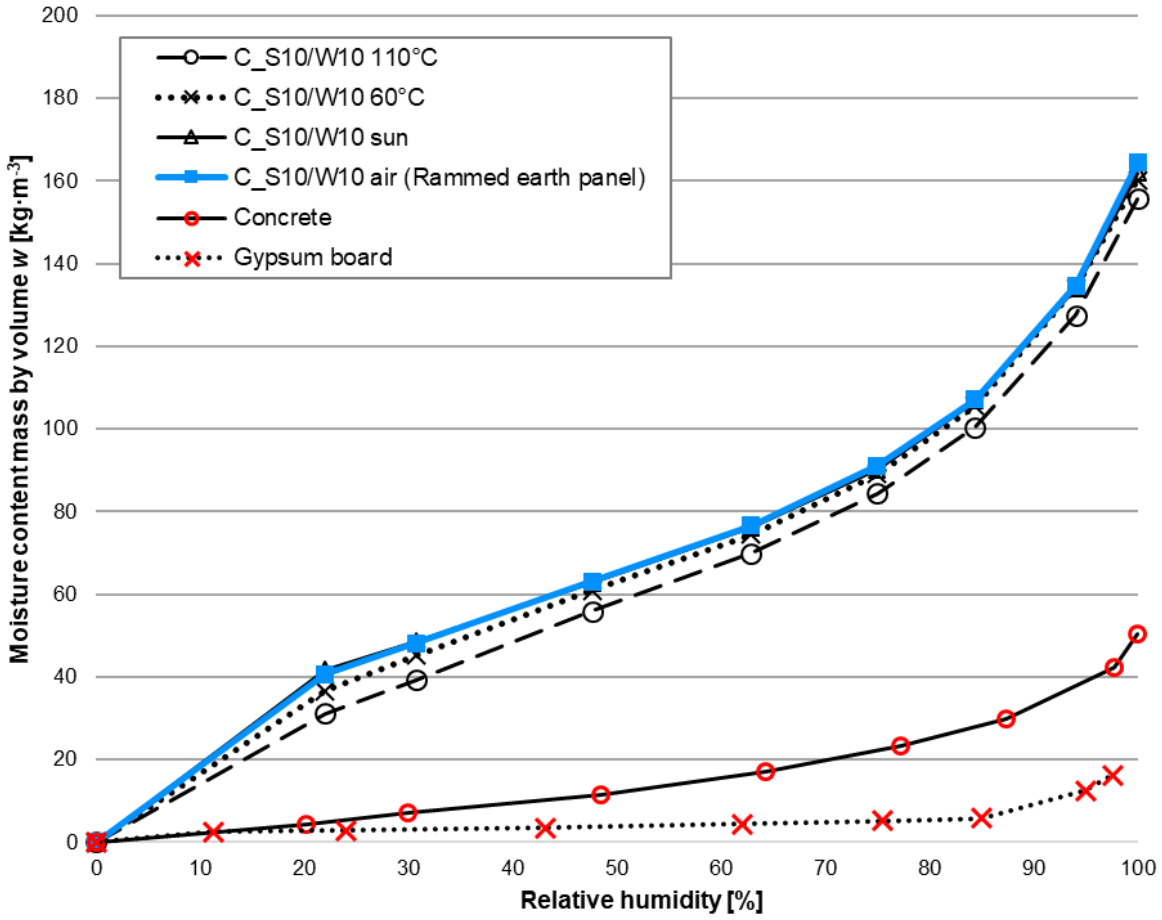

Fig. 51 Adsorption isotherms – different types of drying

Selected clay products can be divided into three groups according to the results of sorption capacity. As expected, rammed earth samples have the highest sorption potential. Compared to the selected reference material from rammed earth C_S10/W10, adobe brick and unfired brick (commercial product) have a 40–45 % lower sorption potential. The third group includes clay plasters and clay panels, which have an 80–85 % lower ability to accumulate air humidity. As mentioned above, clay plasters contain a large amount of sand, and the tested clay panel had a large proportion of silt.

Experiments show (Fig. 52) that clay plasters and clay panels have about 20–35 % less adsorption potential versus concrete. On the other hand, adobe or unburned bricks have a 2.5–2.8 times higher sorption capacity.

3.2.3 Standard building materials

One of the expected results was a comparison of clay materials with standard building materials (most used in building construction). The results are shown in Fig. 53.

Wood materials, spruce wood, and OSB, have a 20 % lower sorption potential than the reference clay mixture C_S10/W10. It should be noted here that wood materials have a significantly lower bulk density. Thus, if the results were expressed as moisture content mass by mass u [kg · kg^{-1}], wood materials would be presented as better adsorbents.

Other selected materials, such as lime plaster, ceramic block, HPC concrete, or gypsum board, have a very low adsorption potential, up to 90–98 % lower than the rammed earth panel.

Moisture content values at RH > 80 % for lime plaster tend to be observed as outliers.

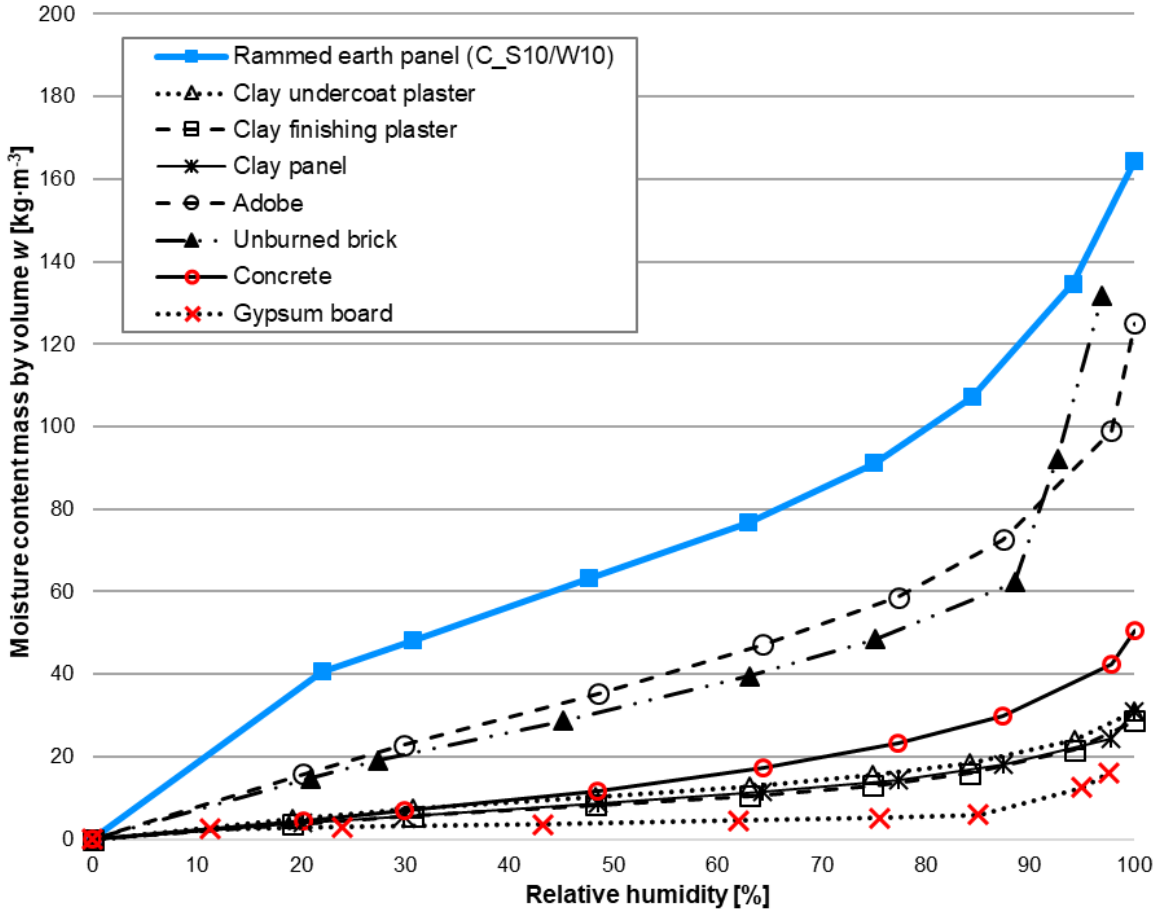

Fig. 52 Adsorption isotherms – different clay products

3.2.4 Partial conclusions

Adsorption isotherms of the tested materials which describe the potential to accumulate air moisture are the results of experiment and can be compared to other single materials. The formula of sorption isotherm can be used for further mathematical simulations and modelling. The main disadvantage of the outputs from this experiment is that it does not say anything about actual building structure, which typically consists of several materials in several layers.

However, the sorption curve is a basic quantity or description of the sorption potential of the material. The following is an evaluation of the six selected materials that were used for further experiments (dynamic sorption properties).

3.2.4.1 Materials used for dynamic sorption

This is the set of test samples used in the walls tested for dynamic sorption: concrete, lime plaster, and gypsum board as standard building materials and rammed earth, clay plaster, and unburned hollow block as clay materials.

Differences in sorption potential among the chosen materials are expected. The sorption curves are shown in Fig. 54.

Not surprisingly, the rammed earth panel has the highest sorption potential of selected materials. In the second place, 45 % lower capacity, is the unburned brick. A little startlingly concrete follows with about 5 times lower adsorption potential compared to the clay mixture C_S10/W10. Clay plasters have an 86 % lower potential for moisture sorption from air compared to a reference material made of steamed clay. The worst absorbency, according to the results of the experiment, are lime plasters and gypsum board.

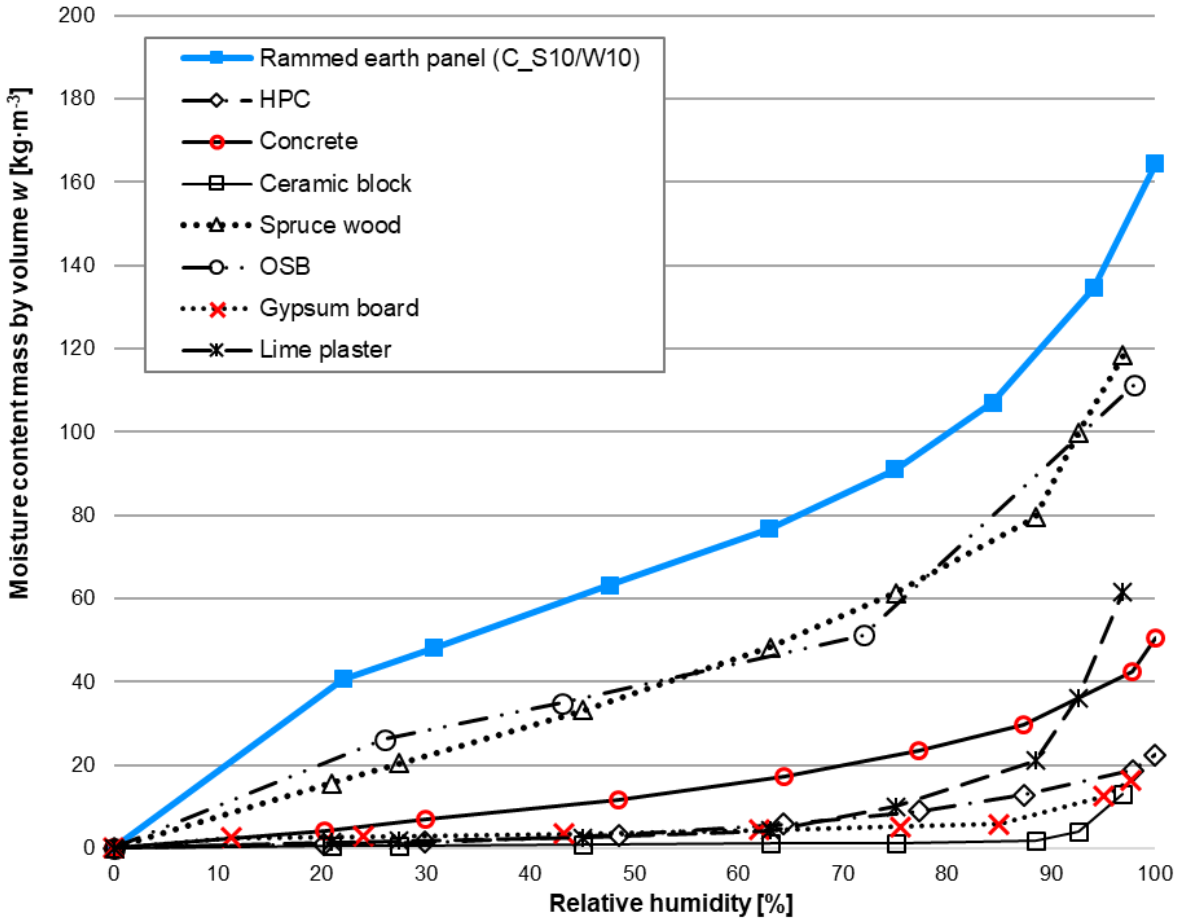

Fig. 53 Adsorption isotherms – different standard building materials

The comparison of clay materials with commonly used materials was quite surprising and showed that the potential of sorption properties of some clay materials is sometimes overrated. Low potential of tested clay plasters due to the high amount of sand for decreasing shrinkage is obvious. Their sorption potential is slightly lower compared to concrete mixtures.

3.2.4.2 BET method

From the experimental samples of the structural walls, which were used for the test of dynamic sorption properties (chapter 5), small samples were taken for measuring the specific surface area. Values were determined based on the BET method (chapter 4). One output is also the determination of the adsorption and desorption isotherm (Fig. 55).

The exact values given by the BET method and those from EN ISO 12571:2013 cannot be compared because, in the first case, nitrogen was absorbed into the sample and, in the second case, water molecules. However, it is possible to compare the shape of the sorption curves, the order of the absorption potential, and the mutual absorbed ratios.

It can be said that the shapes of the adsorption curves correspond to each other. Nevertheless, the gypsum board shows different results. Its value for sorption potential falls between unburned brick and concrete. This may be because the sample in the desiccator was pure gypsum, but the sample using the BET method also contained surface cardboard.

According to the results of the BET method, compared with the rammed earth panel C_S10/W10, the adsorption potential of unburned brick is less by 58 %, that of gypsum board by 76 %, that of concrete by 81 %, that of clay plaster by 89 %, and that of lime plaster by 92 %.

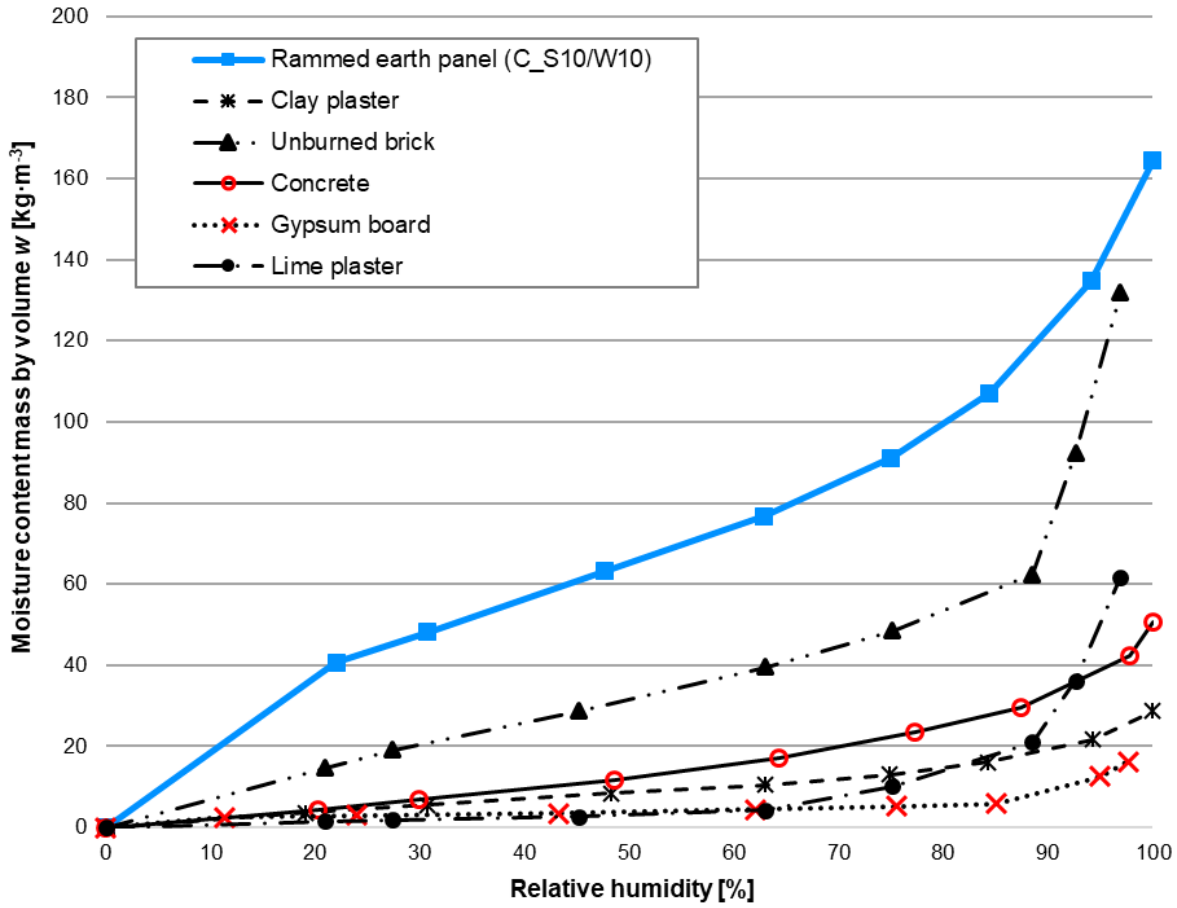

Fig. 54 Adsorption isotherms – comparison of materials used for dynamic sorption

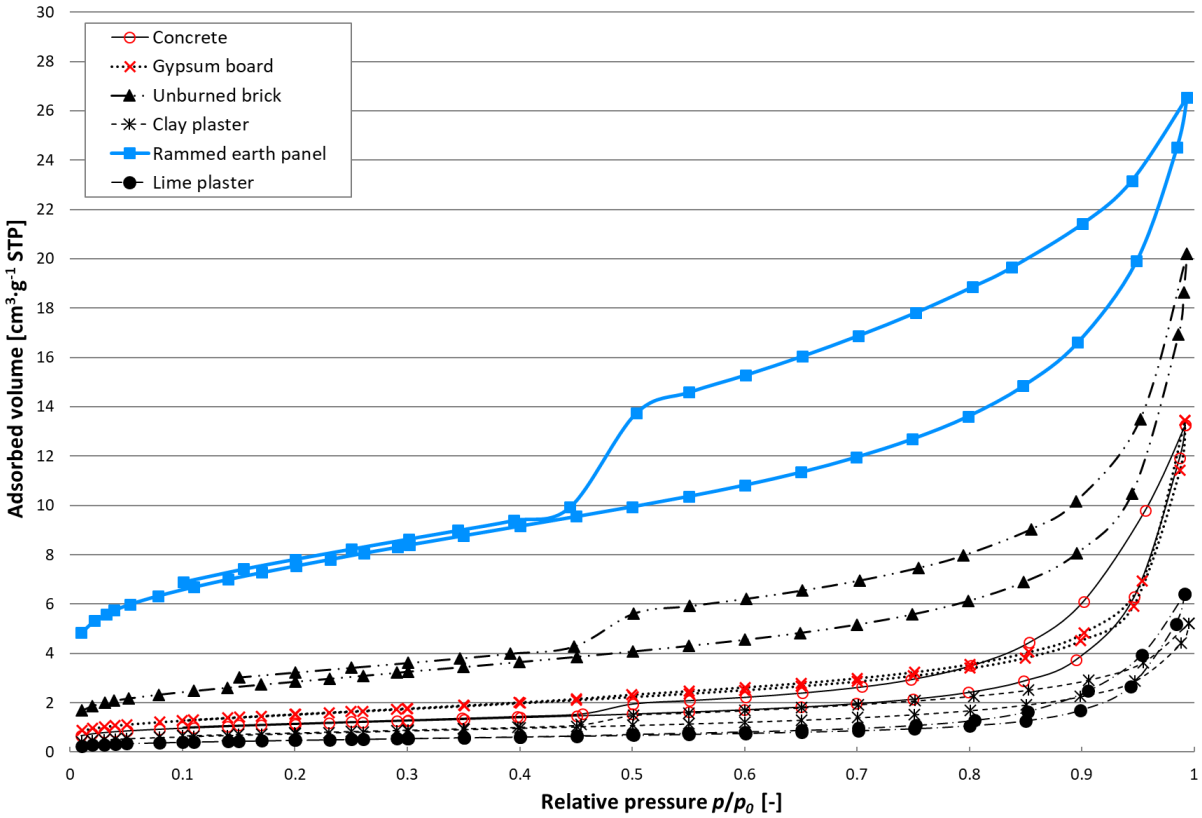

Fig. 55 Adsorption isotherms by BET method – comparison of materials used for dynamic sorption

Fig. 56 shows the adsorption and desorption isotherms of the selected materials used for the dynamic evaluation of sorption properties. Further evaluations of the experimental measurements are given in chapters 4 and 5.

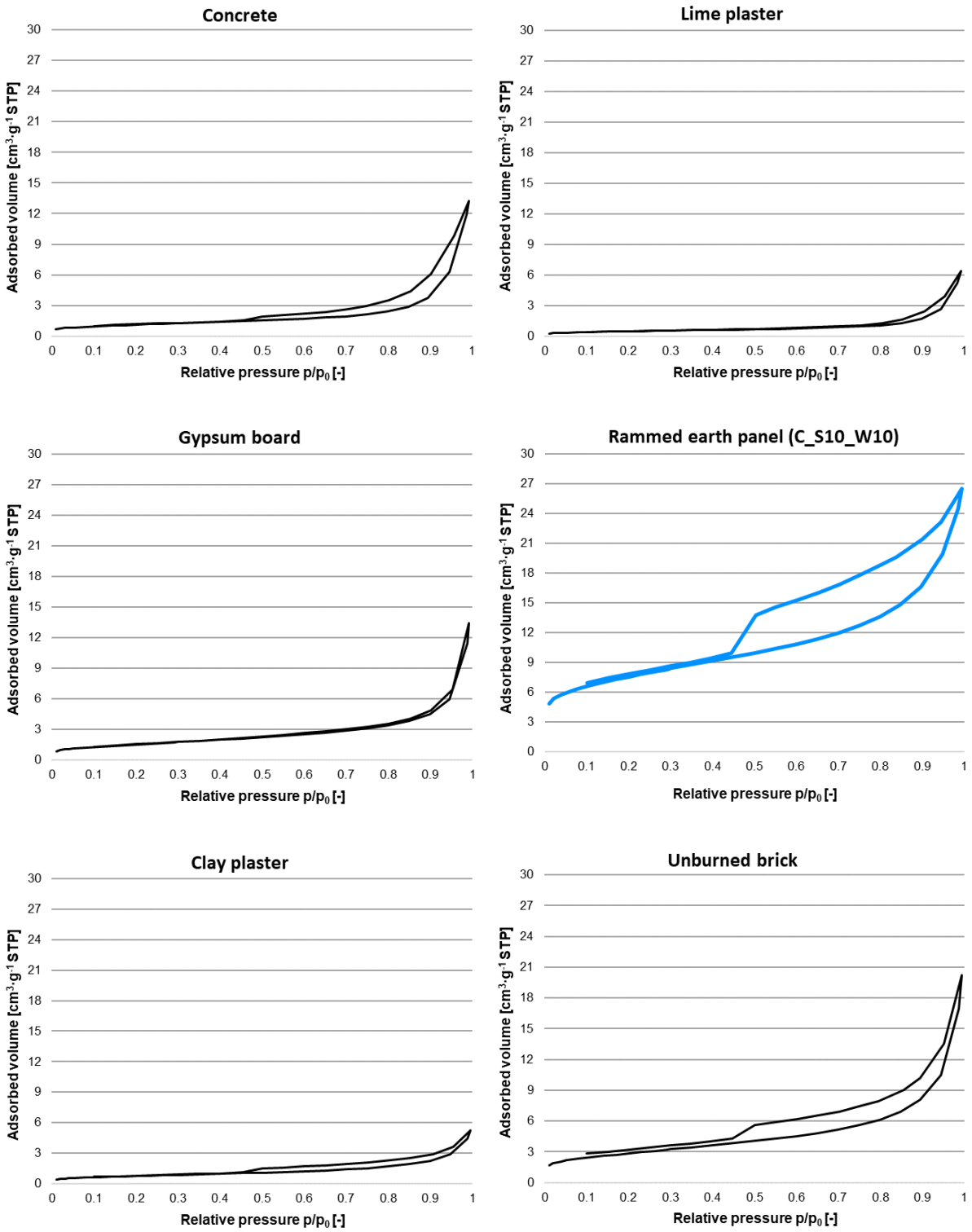

Fig. 56 Adsorption and desorption isotherm of tested structures

4 Specific surface area of materials

For a better interpretation of the results, it is also useful to know the specific surface area of the investigated materials. The pore system of the defined samples will thus be better described.

This measurement was performed at the University of Chemistry and Technology Prague at the Department of Inorganic Technology in cooperation with Mr. Miroslav Lhotka.

4.1 Surface area – methodology

The specific surface area of the structures was measured using a Micromeritics 3Flex Surface Characterization Analyzer device. The 3Flex is a fully automated, high-performance instrument for mesopore and micropore analyses and delivers superior accuracy, resolution, and data reduction. The results from this device include the BET surface area, isotherm, t-Plot, etc. Detailed specifications of the device are given here: [98].

Tested samples

BET analysis was performed on the same samples as the Dynamic Sorption experiment. Samples were taken from the surface of individual structures. A small amount of surface was removed, about 10 g. The samples were dried in a desiccator with molecular sieve desiccant for 1 week. They were then transferred to the UCT Prague laboratory.

Explanation of output

Here the 'cm^3 STP' is a standard cubic centimetre, which is a unit of quantity of gas rather than a unit of volume. It represents the amount of gas (nitrogen N_2) molecules or moles that would occupy one cubic centimetre at standard temperature and pressure, as calculated by the ideal gas law.

Standard temperature and pressure (STP) are standard sets of conditions for experimental measurements to be established so comparisons can be made between different sets of data. International Union of Pure and Applied Chemistry (IUPAC) standards are often used. Here STP is defined as a temperature of 273.15 K (0 °C) and an absolute pressure of exactly 100 kPa (1 bar) [99].

4.2 Surface area – measurements and results

BET analysis was performed on samples taken from the dynamic sorption experiment: concrete, lime plaster, and gypsum board (as a standard building structure) and rammed earth, clay plaster, and unburned brick (as a clay structure). The samples were dried with a molecular sieve desiccant for 1 week and then in a chemical laboratory degassing station by heating the samples under vacuum at 60 °C for 3 days to suction off the bound water molecules.

4.2.1 BET analysis report

Tab. 8 shows the summary results of all measured structures. The pore size distribution from the measured isotherms of the selected structures is also included (Fig. 57 and Fig. 58). It describes the representation of pores of different sizes for the adsorption and desorption process.

Tab. 8 BET analysis report

	Sample	BET Specific surface area [$m^2 \cdot g^{-1}$]	t-Plot external surface area [$m^2 \cdot g^{-1}$]	Single point adsorption total pore volume [1] [$cm^3 \cdot g^{-1}$]	t-Plot micropore volume [$cm^3 \cdot g^{-1}$]
C1	Concrete	4.07	3.49	0.014	0.000 227
C2	Lime plaster	1.76	1.70	0.006	0.000 002
C3	Gypsum board	5.49	5.51	0.010	-0.000 053
C4	Rammed earth panel	26.97	20.87	0.036	0.002 554
C5	Clay plaster	2.72	2.78	0.005	-0.000 049
C6	Unburned brick	10.24	9.48	0.020	0.000 280

[1] Single point adsorption total pore volume of pores less than 40.3 nm diameter at p/p° = 0.950

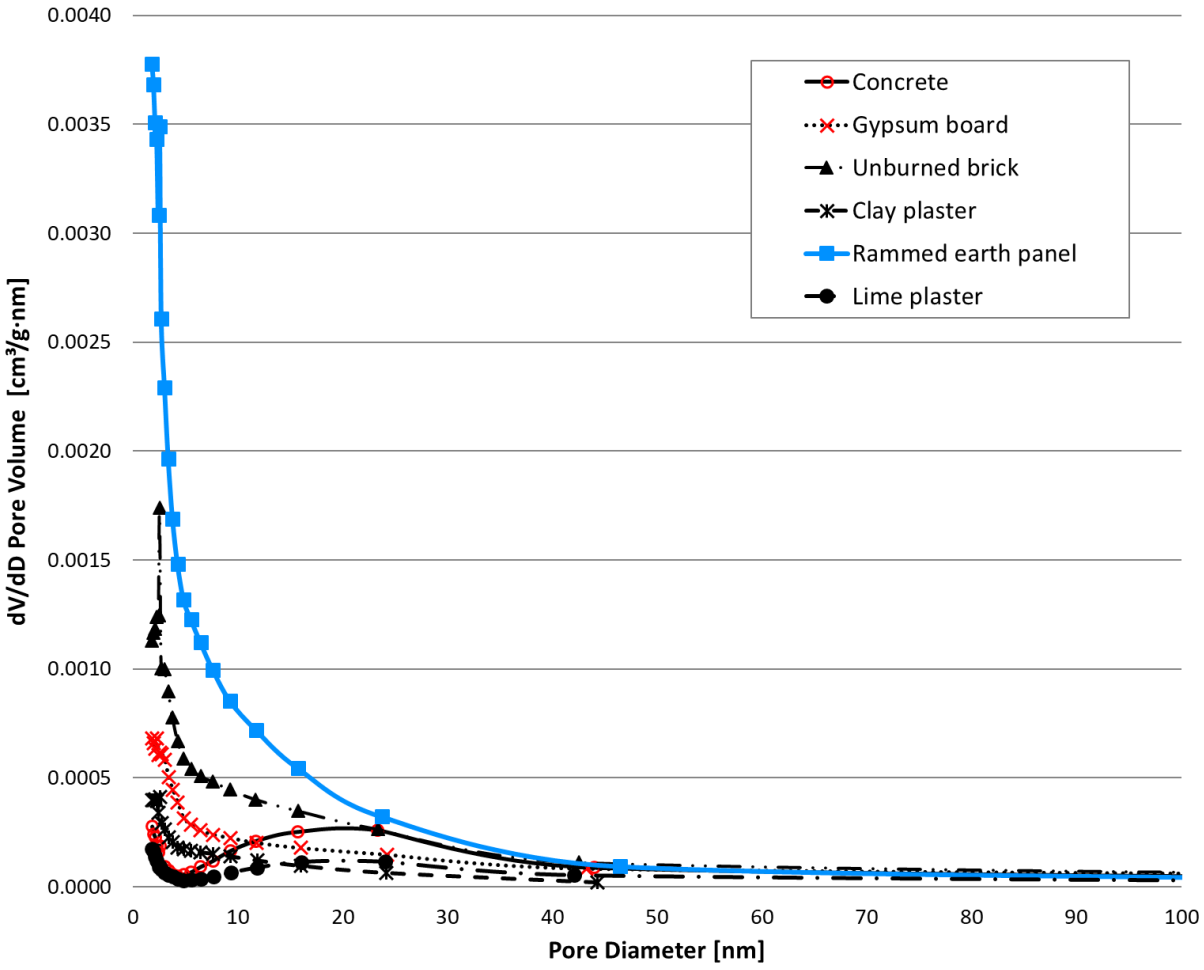

Fig. 57 Pore size distribution – adsorption

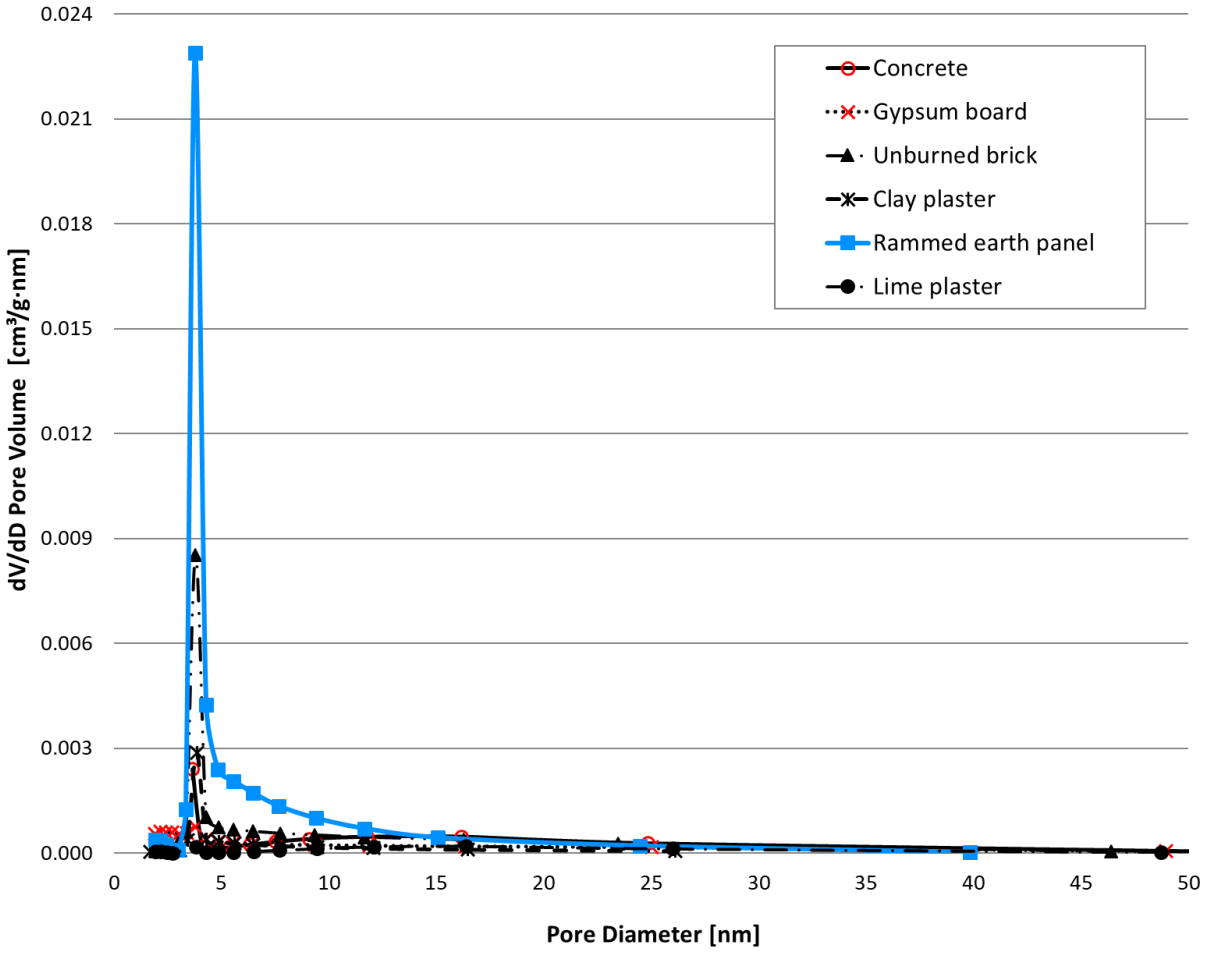

Fig. 58 Pore size distribution – desorption

4.2.2 Partial conclusions

BET analysis is an advanced but also expensive test of the sorption properties of a material. A lot of useful information can be read from it to understand the moisture dependencies in clay materials. The following conclusions can be drawn from the above results of experimental measurements.

Adsorption and desorption isotherms are given in Chapter 3.2.4 in Fig. 56. From their shape, it can be concluded that lime plasters and gypsum board are non-porous materials with a sorption curve Type 2 according to IUPAC. Clay plasters and concrete have a similar shape of sorption isotherms. Their shape corresponds to Type 2 or Type 4. Hysteresis is negligible. These materials can be declared as macroporous or non-porous, or there is a minimum number of mesopores. The sorption curve of unburned brick is classified as Type 4 with clear hysteresis. It is a partially mesoporous material. Material from the rammed earth panel has a clear character: a very porous material with high hysteresis. According to IUPAC, it is a Type 4 isotherm, typical of mesoporous adsorbents. The pores of the material are open on both sides. The shape of the hysteresis loop corresponds to Type H3, which corresponds to slit pores.

Based on the measured data, it can be stated that the material made of rammed earth also contains micropores, i.e. pores with a diameter of less than 2 nm. Micropores can make up to 7 % of the total pore volume, which is less than 40.3 nm.

For this thesis, it is important to compare the specific surface area of selected materials. The measured values are given in Tab. 8. Interestingly, the percentage differences in adsorption potential given in Chapter 3.2.4.2 correspond to the percentage difference in BET Surface area. Thus, compared

to the rammed earth panel C_S10/W10, the specific surface area of unburned brick is smaller by 62 %, of gypsum board by 80 %, of concrete by 82 %, of clay plaster by 90 %, and of lime plaster by 94 %.

Single point adsorption total pore volume of pores less than 40.3 nm diameter at p/p° = 0.95 of clay mixture C_S10/W10 is equal to 0.0365 $cm^3 \cdot g^{-1}$. This is 1.8 times more than the volume of unburned brick, 2.6 times more than concrete, 3.7 times more than gypsum board, and approx. 6 times more than clay and lime plaster.

5 Sorption properties of building structure in dynamic state

In this chapter, some author's formulations published in journals or conference papers (listed in the references) are used.

The relative humidity of the interior is variable during the day. It depends mainly on the relative humidity of the exterior and the intensity of ventilation, as well as indoor contributions. In typical housing units, the main sources of moisture are human activities (washing, ironing, cooking, showering), plants, and human respiration and transpiration. The average apartment produces 4–15 kg of water vapour per day (see Tab. 9). Porous materials react to these fluctuations in humidity – they can adsorb or desorb air humidity.

This process is dynamic, however, so a sorption isotherm that only describes the steady state will not suffice.

Chapter 2.2.4 deals with the search of dynamic sorption properties of porous materials. However, the tests performed do not always reflect the real operation of the building. Another essential reason for determining this test is to be able to compare individual materials and structures. It is always necessary to use the same materials in the experiments and much more important for clay materials, as these are materials with inhomogeneous properties.

The aim of this chapter is to describe the influence of dynamic sorption properties of clay materials on the relative humidity of the indoor environment during changes in the relative humidity in the interior.

Full scale test of dynamic sorption for building structures was developed and tested by Diviš, Růžička (2016) [100]. The main idea of the dynamic sorption test was to simulate real situations in the building and the behaviour of real building structures in “real” conditions.

The partial goal of this chapter is to compare the influence of sorption properties of selected structures and to monitor the humidity response of the indoor environment. The evaluation will take into consideration both the results of this chapter and the relationship with the sorption isotherm and the specific surface area of the materials used.

Tab. 9 Indicative values of water vapour source in the interior according to Gertis and Erhorn (1985)

Source of water vapour	Amount [g · h^{-1}]
Person in light activity	30–60
Having a bath	ca. 700
Having a shower	ca. 2 600
Cooking	ca. 100
Drying clothes	0–200
Room plants	5–20

Source: [101]

5.1 Dynamic sorption – methodology

The subject of the research is a detailed description of the sorption properties of materials based on unburnt clay. These materials are generally known for their ability to control the relative humidity in the interior.

The preceding step described the sorption properties of building materials at steady state. For this purpose, a sorption isotherm determined according to the prescribed standards was used. Nevertheless, the informative value of this parameter for real structures and real environments is limited. It is necessary to compare these values with the dynamic behaviour of real structures loaded with real operations in buildings. However, there is no standard procedure for this test, so it was necessary to define a methodology.

The test results should show the potential of unfired clay structures. The test deals with the moisture response of the internal environment to the dynamic sorption properties of selected building structures with changes in relative humidity in the interior. The goal of the full-scale test of dynamic adsorption and desorption is to simulate real situations in the interior microclimate and the behaviour of real building structures in real conditions.

5.1.1 Building structure

Dynamic sorption properties of real structures were tested in the climatic chamber on specimens from structural parts. The dimension of the exposed area A (test specimen without wooden frame) of all test specimens is the same, 820 × 750 mm, i.e. $\boldsymbol{A = 0.615\ m^2}$. The thickness of the sample corresponds to the composition of the individual structures (see below).

The test specimens were installed in a wooden frame with the rear side covered by OSB board of thickness 12 mm. The rear and perimeter sides of the test samples were covered by PE foil Gutta to avoid side moisture transfer. The joints were sealed with aluminium adhesive tape and the sealant Isocell Airstop Sprint. Samples produced in this way were inserted into the test frame of the climatic chamber.

The rest of the test space between the sample and the steel frame of the test chamber was filled with 6 mm thick plexiglass. This space was necessary for the installation of the sample. The vapour-tight connection of the plexiglass and the steel frame is secured by the sealant Terostat-IX, the connection of the PE foil from the sides of the sample and the plexiglass is ensured by the ISOCELL AIRSTOP Sprint sealant and the aluminium adhesive tape or adhesive tape ISOCELL AIRSTOP Flex.

These vapour barrier measures ensured the transmission of only 1D lines between the area of the test sample A and the volume of the climatic chamber V. Fig. 59 shows the fitting of the test specimen to the test frame of the chamber and the vapour tightness measures taken.

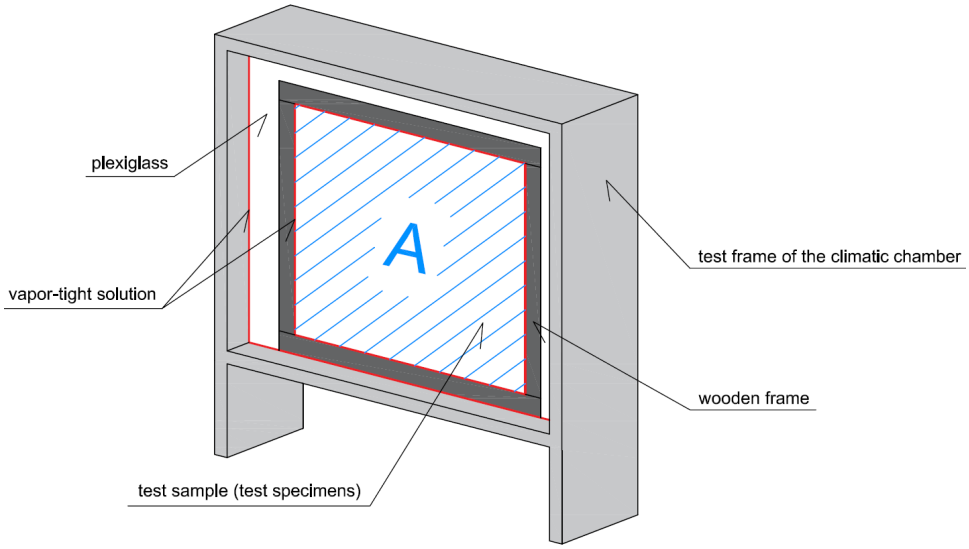

Fig. 59 Vapour-tight solution: attaching the test specimen to the test frame

The used airtight sealing materials:

- quick-drying sealant ISOCELL AIRSTOP Sprint (in Fig. 59 in red);
- adhesive tape ISOCELL AIRSTOP Flex (in Fig. 59 in red);
- aluminium adhesive tape (in Fig. 59 in red);
- rubber sealant Teroson Terostat-IX (in Fig. 59 in red);
- PE foil thickness 0.1 mm, manufacturer Gutta International; vapour diffusion resistance number is approx. μ =144 000;
- Plexiglass, thickness 6 mm, manufacturer PLEXIPLAST (in Fig. 59 in white).

After assembling, the test samples were conditioned in the laboratory at 45 ± 10 % RH and a temperature of 23 ± 2 °C for 2.5 months. The Dynamic sorption properties experiment of real structural parts was performed at UCEEB CVUT in Prague, in Hygrothermal laboratory.

The following test samples were tested: plexi board, concrete, lime plaster, gypsum board, rammed earth panel, clay plaster, and unburned brick (Fig. 60, Fig. 61, and Fig. 62).

5.1.1.1 Plexi board

Plexiglass board is a reference material. However, the structure is mainly used to verify the experiment, as the material is diffusion-impermeable and the airtightness of the experimental measuring device and apparatus can be verified with it.

Plexiglass XT, extruded, thickness 6 mm, 6/000/XT – from company PLEXIPLAST s.r.o. is used including a protective foil.

5.1.1.2 Concrete

Structure S1 is a mixture of common concrete C30/37 developed and optimized at UCEEB CTU in Prague. The mixture consists of cement CEM I 42.5 R (ČM, Mokrá), aggregate fraction 4–16 mm, aggregate fraction 0–4 mm, and water. The construction thickness is 70 mm.

5.1.1.3 Lime plaster

Structure S2 was made of ceramic hollow blocks Heluz 8 of thickness 80 mm. The masonry mortar was from Cemix 5. The structure was covered by lime plaster HASIT 160 Fein Kalkputz, without additional surface treatment (coating).

The composition is according to the manufacturer's recommendations:

- Ceramic block Heluz 8 (375 × 80 × 238 mm); the thickness 80 mm [102]
- Masonry mortar Cemix 5 [103]
- Lime undercoat plaster HASIT 666 Kalkputz; the thickness 20 mm [104]
- Lime finishing plaster HASIT 160 Fein-Kalkputz; the thickness 2 mm [105]

5.1.1.4 Gypsum board

Structure S3 is a partition wall, it was made by gypsum board Rigips RB (A) thickness 12.5 mm without surface treatment (coating). The supporting structure consists of a metal stud CW 75, which is filled with thermal insulation of mineral fibers.

The composition is designed especially for dry construction of interior building structures.

5.1.1.5 Rammed earth panel

Structure S4 was made of rammed earth. The mixture C_S10/W10 is made of a mixture of raw clay material from the Czech company Claygar (90 %), sand of fraction 0–4 (10 %), and water (10 %). The height of the compacted layers was 40–50 mm. The rammed earth panel has the thickness 100 mm.

5.1.1.6 Clay plaster

Structure S5 was made of unburned clay hollow blocs Heluz Nature Energy 12/25 of the thickness 120 mm. The masonry mortar was from the clay mixture Picas Econom. The surface layer is made of clay plaster PICASS ECONOM of the total thickness 22 mm (10 + 10 + 2).
The composition is according to the manufacturer's recommendations:

- Unburned clay brick HELUZ NATURE Energy 12/25; the thickness 120 mm [106]
- Adhesion coating Picas Econom [107]
- Clay undercoat plaster Picas Econom in two layers; total thickness 20 mm [108]
- Clay finishing plaster Picas Econom; total thickness 2 mm [109]

5.1.1.7 Unburned brick

Structure S6 was made of fair-face brickwork from unburned clay hollow blocks Heluz Nature Energy 12/25 of thickness 120 mm. The masonry mortar was from the clay mixture Picas Econom.

The composition is according to the manufacturer's recommendations:

- Unburned clay brick HELUZ NATURE Energy 12/25; the thickness 120 mm [106]
- Clay masonry mortar Picas Econom [108]

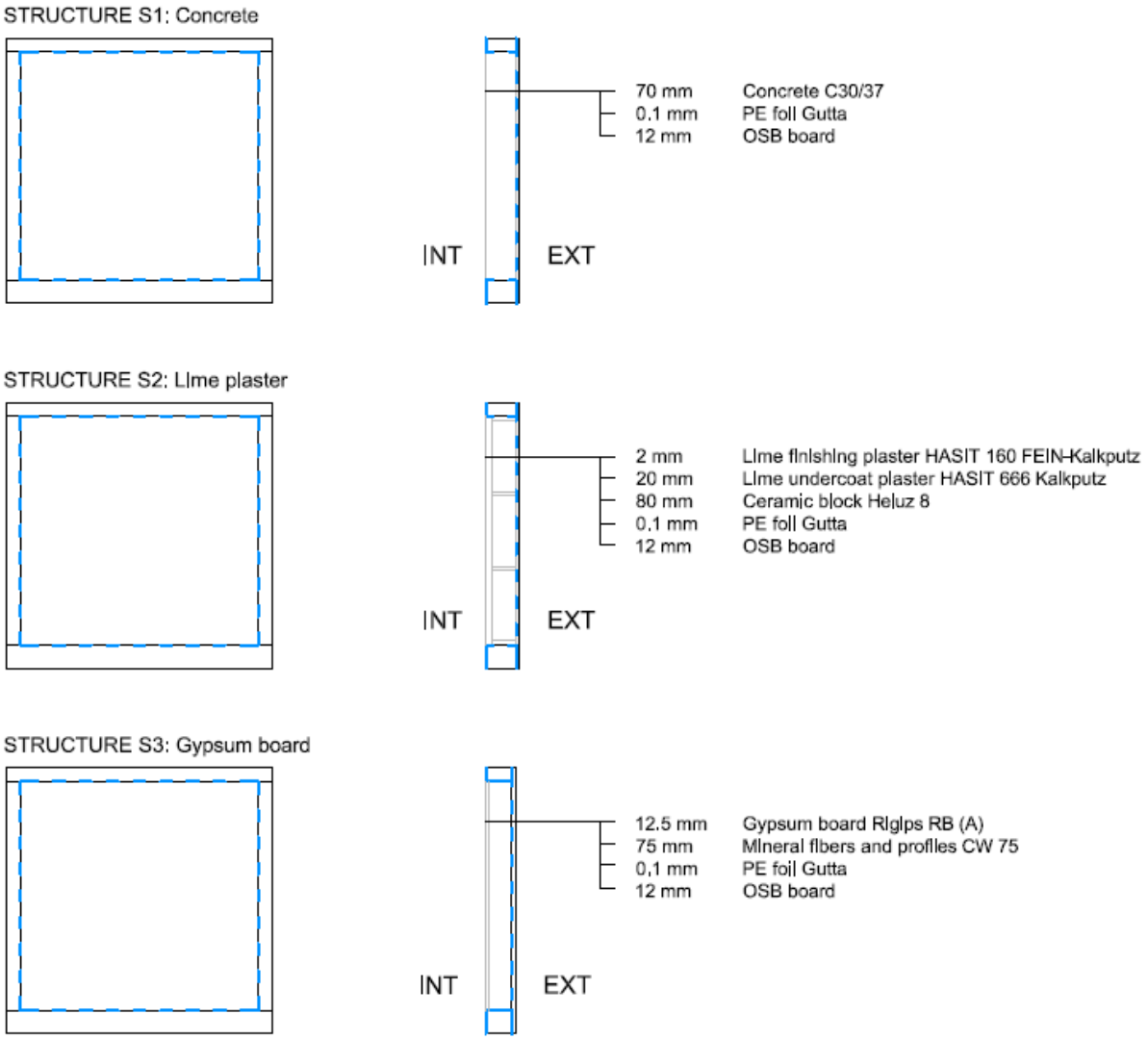

Fig. 60 Test samples S1–S3

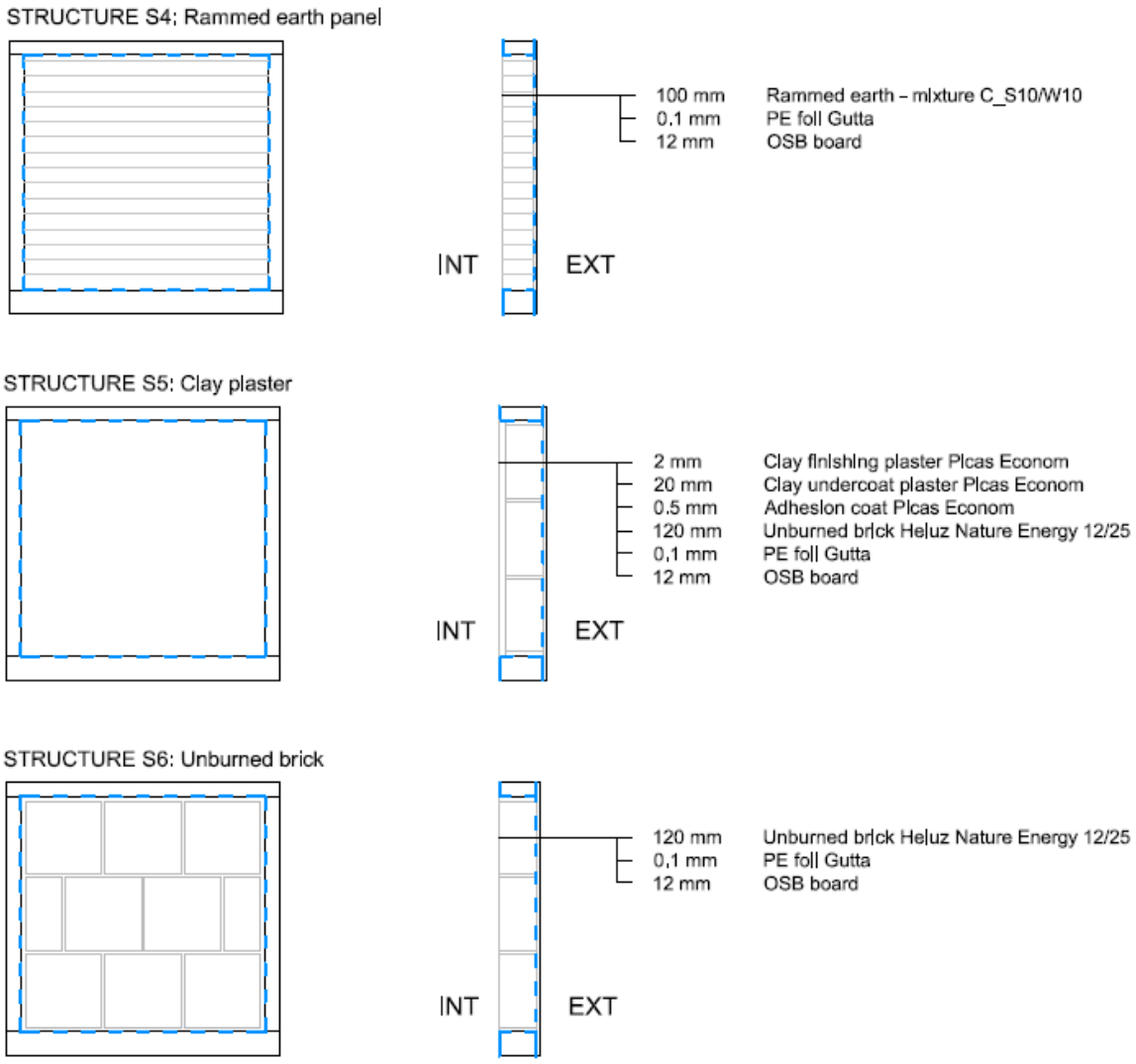

Fig. 61 Test samples S4–S6

5.1.2 Measured quantities

The aim of the experimental tests was to prove the proposed testing methodology and to verify the different behaviour of the test samples.

The following were measured: temperature T [°C], relative humidity RH [%], and amount of water consumed m [g]. The individual quantities were measured in a minute step.

The following were monitored: dynamic change of relative humidity in the environment, the amount of water supplied to the environment, and ambient air temperature. All these factors directly affect the rate of dynamic sorption.

The measurement of relative humidity and temperature occurred in three places: outside the chamber (the lab), in the middle of the climatic chamber, and at the front surface of the chamber.

Relative humidity in the climatic chamber, either adjusted by the device or as a response of previous steps, was measured continuously during the test. Moreover, the amount of water used by the device to keep the adjusted RH level in the chamber was measured.

5.1.3 Description of measuring apparatus

Actual structural parts have been tested in the climate chamber WEISS WK3-1000/0-S with the test space dimensions approx. 950 mm (height), 1 100 mm (width), 950 mm (depth). The material of the inner surface of the test chamber is polished stainless steel.

Fig. 62 Testing structures in the climatic chamber: a) concrete wall; b) ceramic hollow blocks with lime plaster; c) partition wall from gypsum board; d) rammed earth panel (C_S10/W10); e) unburned clay hollow blocks with clay plaster; f) fair-face brickwork from unburned clay hollow blocks

Relative humidity within the climatic chamber and in the laboratory was measured continuously during the test. Temperatures in the climatic chamber and in the laboratory and the amount of water used by the device to keep the adjusted RH level in the chamber was measured as well.

The measuring apparatus:

- climate test chamber WEISS WK3-1000/0-S;
- laboratory balance AND GX-4000 for measuring water consumption;
- datataker DT85 Series3 for data recording;
- temperature and humidity measurement sensors Rotronic HC2-S+E2-05XX (TRHa_008, TRHa_036, TRHa_047).

The volume of the test chamber according to the manufacturer is approx. 993 litres. This, however, is only the usable space; installation space is not included (Fig. 63). For the experiments described below, it is necessary to know the entire volume of air that is regulated in the chamber. The total volume of the test space is $V = 1.3\ m^3$.

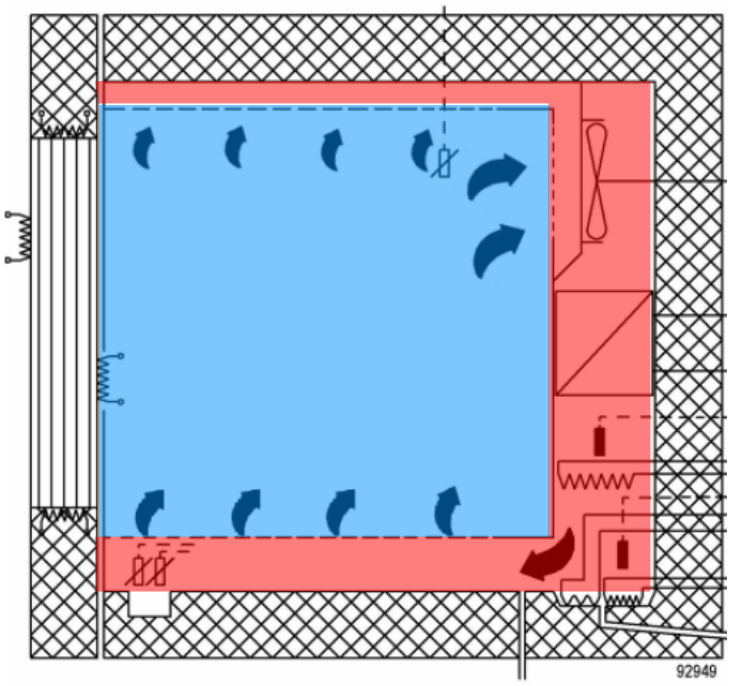

Fig. 63 Cross-section of test chamber: usable space (blue), installation space (red)

Fig. 64 represents the instrumentation scheme, which indicates the climatic chamber, the location of the measurement sensors, and the test sample in the wooden frame.

The pictures in Fig. 65 show the Measuring apparatus – the climate chamber, the location of the sensors, the datataker, and the balance. The experiment process was controlled by PC and SW of the climate chamber.

Accuracy of used measuring instruments

The sensors Rotronic HC2-S+E2-05XX were used to measure temperature and relative humidity. The accuracy of the Rotronic humidity and temperature probes is highest at the adjustment points. HygroClip2 (HC2) probes are adjusted according to international standards with a volume flow of $10\ l \cdot min^{-1}$. and 1 m/s at 23 ± 5 °C (Fig. 66). The accuracy ranges are ± 0.8 % RH and ± 0.1 K for conditions 23 ± 5 °C. The accuracies specified for probes relate to reference probes traceable to the national standard. [110]

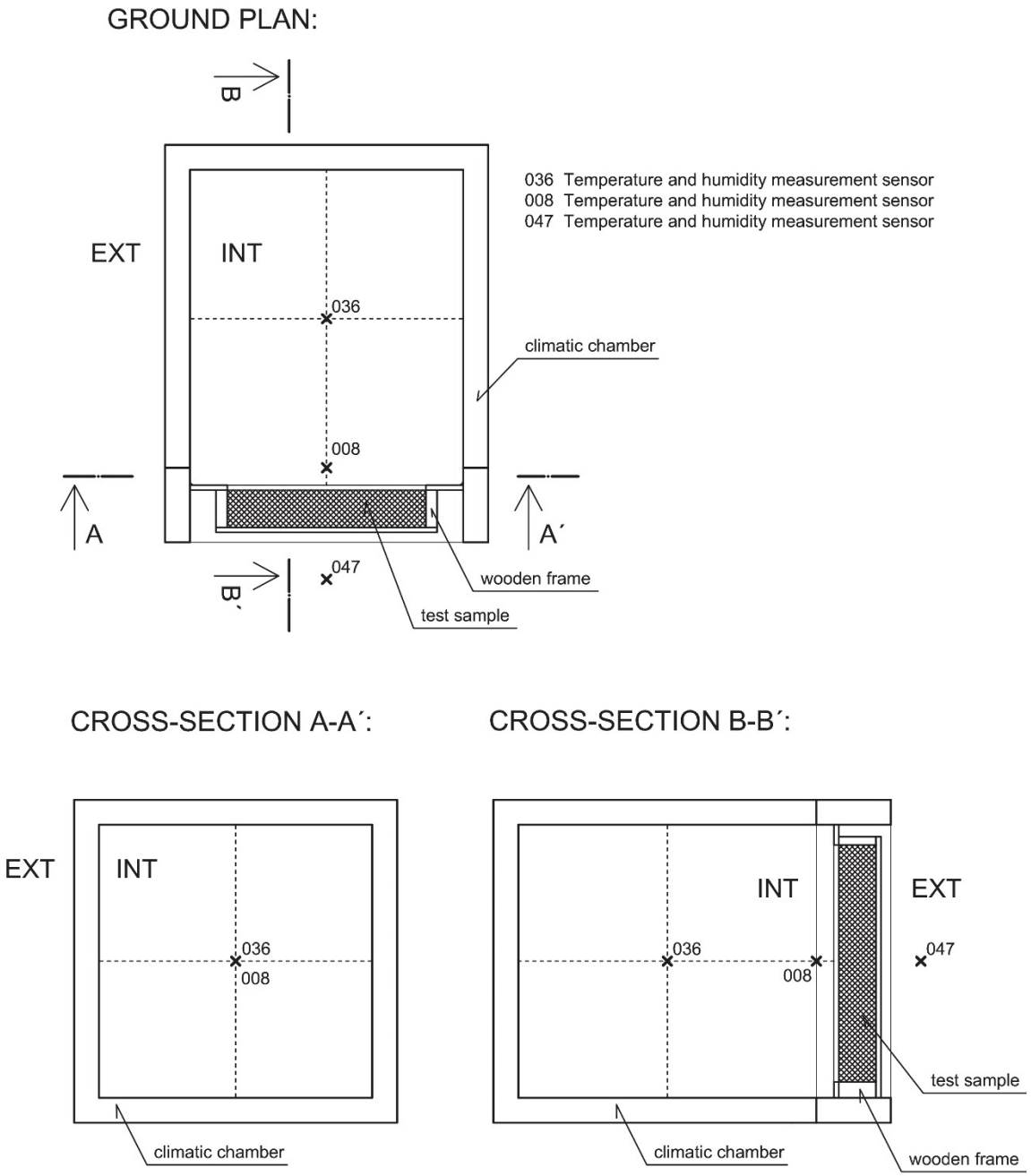

Fig. 64 Diagram of the instrumentation scheme – climatic chamber, test sample, location of the sensors

The laboratory balance AND GX-4000 was used to measure water consumption during the 60-minute wetting process. The RH in the chamber space was increased in steps and maintained from 45 % to 95 %. The accuracy of balance is: readability 0.001 g; repeatability (standard deviation) 0.001 g; linearity 0.002 g. [97]

The climate chamber is controlled by its own sensors. The humidity constancy in time is ± 1 to ± 3 % RH, the temperature homogeneity in space is ± 0.5 to ± 1.0 K. [111]

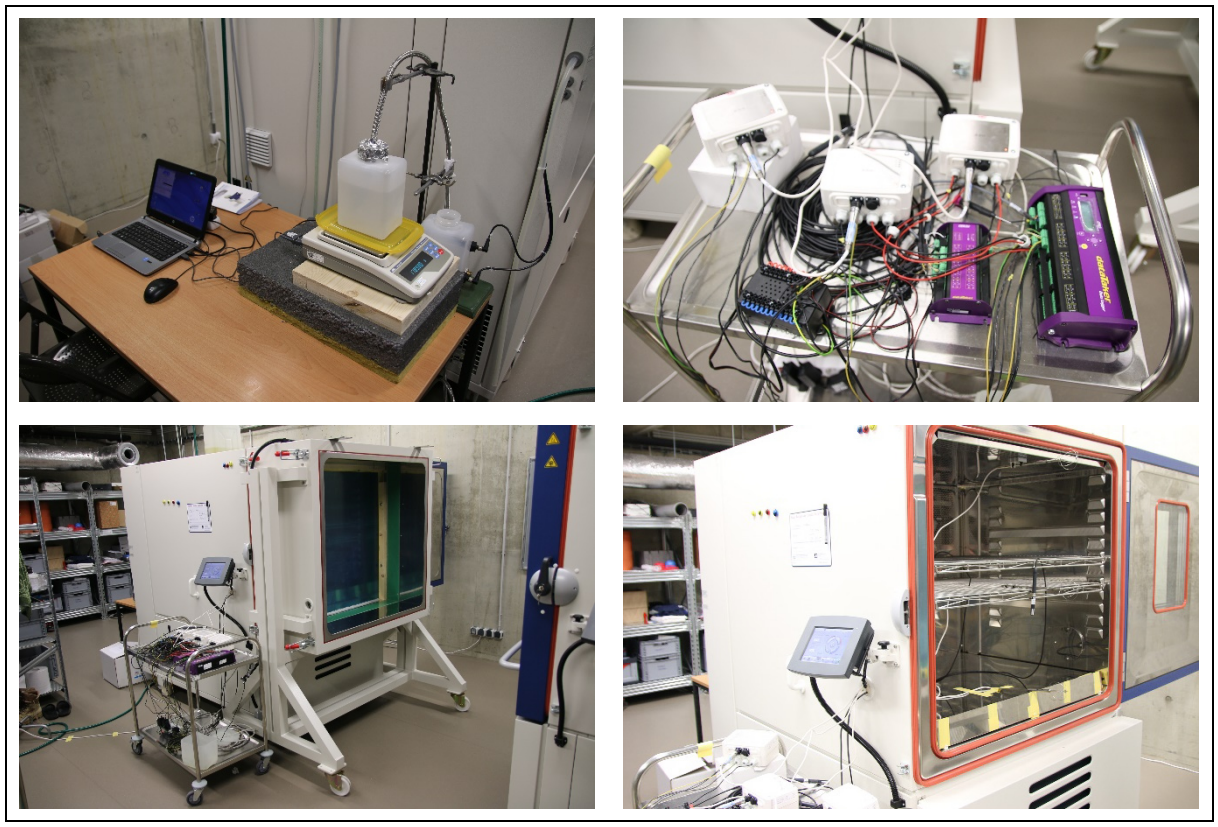

Fig. 65 Measuring apparatus

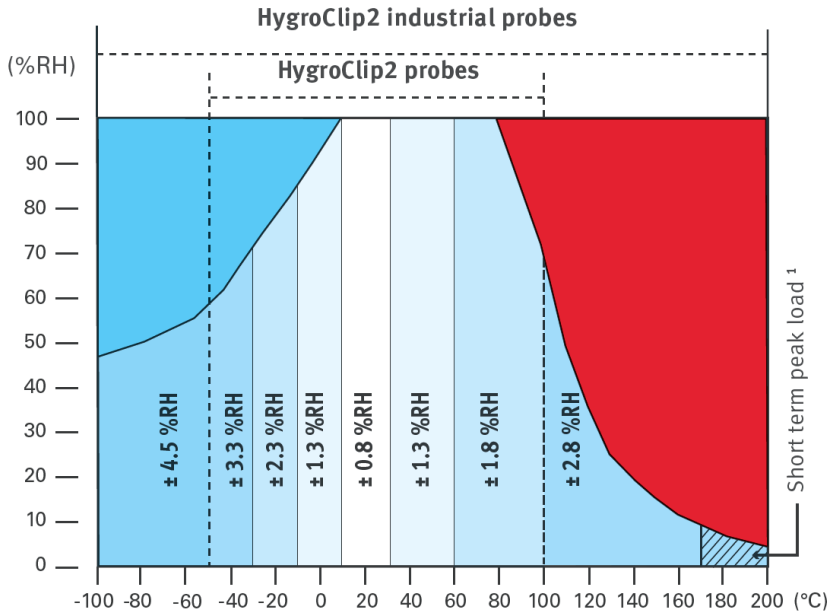

Fig. 66 Accuracy of humidity measurements over the measuring range [110]

5.1.4 Description of the experiment

The test specimens were conditioned in laboratory conditions at 45 ± 10 % RH and laboratory temperature of 23 ± 2 °C for 2.5 months. Subsequently, the test sample was placed in a climatic chamber, where it was conditioned at a temperature of T = 23 °C, and a relative humidity of RH = 45 %. This conditioning lasted 4–7 days. The whole test was isothermal (constant chamber temperature).

The goal of the full-scale test of dynamic adsorption and desorption is to simulate realistic situations in the interior microclimate and the behaviour of actual building structures in real conditions. The proposed test method for climatic chamber is based on the following two situations: 1) the internal environment and the tested structure are in an equilibrium state and 2) the internal environment is facing an intensive increase of relative humidity for a specific period (i.e., someone is taking a shower or bath, cooking, drying clothes, etc.). After that, two scenarios are possible:

- var I: the climatic chamber is ventilated for a specific time period to reach a starting level of internal humidity. Then it is observed how much moisture is absorbed in the structure – how the internal humidity in the chamber increases (desorption potential of the building structure), or
- var II: at the end of the high humidity period, it is observed how the relative humidity in the climatic chamber decreases – that determines the potential of the tested building structure to moderate the moisture peaks and to absorb the moisture from the environment (adsorption potential of the building structure).

Var I – *Dynamic desorption test*: This part of the test describes the behaviour of the test sample after the high humidity period finishes and the relative humidity in the environment drops down to the starting moisture level due to ventilation, open windows, etc. The ability of the tested structure to accumulate moisture in a short time period and to increase relative humidity gradually in the environment is observed. The test was carried out at a constant temperature of 23 °C in the climatic chamber and the testing of dynamic desorption consisted of the following steps (also shown in Fig. 67):

1. conditioning of the test sample and internal environment to an equilibrium state at T = 23 °C and RH = 45 % for 48 hours;
2. fast increased of relative humidity at 95 % RH for 60 minutes;
3. ventilation of the environment to the starting humidity level 45 % RH for 15 – 20 minutes;
4. monitoring of RH changes in the climatic chamber for 8 hours.

Var II – *Dynamic adsorption test*: This situation describes the behaviour of the test sample after the high humidity period finishes and moisture from the environment has accumulated on the tested wall. The test was carried out at a constant temperature of 23 °C in the climatic chamber and the testing of dynamic adsorption consisted of the following steps (also shown in Fig. 67):

1. conditioning of the test sample and internal environment to an equilibrium state at T = 23 °C and RH = 45 % for 48 hours;
2. fast increased of relative humidity at 95 % RH for 60 minutes;
3. monitoring of RH changes in the climatic chamber for 8 hours.

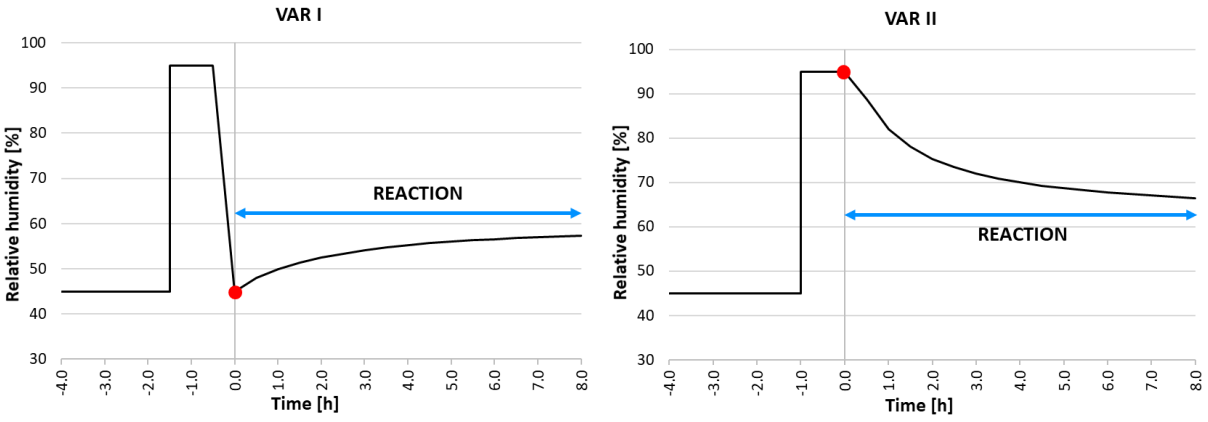

Fig. 67 Dynamic desorption test (var I) and Dynamic adsorption test (var II)

This ratio parameter is significant:

$$\frac{A}{V} \qquad \left[\frac{\mathrm{m}^2}{\mathrm{m}^3}\right], \tag{5}$$

where A/V is the ratio between the area A [m^2] of the sample that can sorb air humidity and the volume V [m^3] of the experimental chamber.

In this case, the ***A/V* ratio is 0.473 $\mathbf{m^2 \cdot m^{-3}}$**. This ratio is the same for all experimental structures. Changing the ratio would change the results. The higher the ratio, the more the structure can adsorb/desorb air humidity from the environment. Conversely, the smaller the ratio, the smaller the amount of water vapour the structure can absorb from the air.

5.2 Dynamic sorption – measurements and results

The following building structures were tested according to the proposed measurement methodology: concrete wall, ceramic hollow blocks covered by lime plaster, gypsum board partition wall, rammed earth panel, unburned clay hollow blocs covered by clay plaster, and fair-face brickwork from unburned clay hollow blocks. As a reference test sample, a plexi glass board was chosen. It was used to prove the air and humidity tightness of the climatic chamber.

Each building structure was experimentally tested according to Var I (Dynamic desorption test) and Var II (Dynamic adsorption test). All measurements on all building structures were repeated three times.

Dynamic desorption test: This part of the test describes the behaviour of the test sample after the high humidity period finishes and the relative humidity in the environment drops down to the starting moisture level due to ventilation, open windows, etc. The ability of the tested structure to accumulate moisture in a short time period and to increase relative humidity gradually in the environment is observed. The test was carried out at a constant temperature of 23 °C in the climatic chamber.

Dynamic adsorption test: This part of the test describes the behaviour of the test sample after the high humidity period finishes and moisture from the environment is accumulated to the tested wall. The test was carried out at a constant temperature of 23 °C in the climatic chamber.

Relative humidity in the climatic chamber, either adjusted by the device or in response to previous steps, was measured continuously during the test. Furthermore, the amount of water used by the device to keep the adjusted RH level in the chamber was measured.

Tab. 10 explains the labelling of the experimental results reported in this document.

Tab. 10 Signage mentioned in this document

Signage	Explanation
var I	Var I – Dynamic desorption test
var II	Var II – Dynamic adsorption test
1/3	1st repeated measurement
2/3	2nd repeated measurement
3/3	3rd repeated measurement

Fig. 68 explains the description of the results of sorption properties in the dynamic state presented in this thesis. On the left vertical axis is the value of relative humidity in the climate chamber, showing the state of the indoor environment. On the right vertical axis is the value of the amount of water consumed when controlling the chamber at RH 95 % for one hour.

On the horizontal axis is the time (in hours) with the beginning of the observation at the point 0:00. In var I the beginning is after ventilation from RH 95 % to RH 45 %, and in var II it is after switching off the one-hour humidification. To the left of this limit is the conditioning of the sample to RH 45 % (for the sake of clarity, the entire conditioning time is not displayed) and subsequent wetting for one hour at the level of RH 95 % and, for var I, an additional 15–20 minutes of ventilation to the original value of RH 45 %.

The amount of water consumed is shown in the graph as a function of time. It is located below the RH curve at the stage of humidification (to RH 95 % for 60 minutes).

Fig. 68 Description of the graph showing the measurement results

5.2.1 Verification of the airtightness of the chamber

The surfaces of the climate chamber are made of sheet metal and all joints should be tight. The critical point is the connection between the experimental sample and the test frame of the chamber. A reference test sample of plexiglass was used to verify the air and humidity tightness of the climatic chamber. The sealing materials used are listed above.

Results of var I

According to the results in Fig. 69, after reaching RH 95 %, switching off the humidification and ventilation system to RH 45 %, the relative humidity in the interior does not change significantly. There is a tendency for a slight increase in RH consistent with the order of the error rate of the sensors.

It can be said that the chamber is tight and only slightly affects the results of the following experiments.

Amount of water consumed: measurement no. 2/3 shows outliers from other measurements. A measurement error or system error (water leak) has occurred. This result was excluded from the evaluation, see chapter 5.2.8.1 section Evaluation of water consumption. Other results correspond to the expected course and the expected behaviour based on the laws of physics.

Results of var II

Fig. 70 shows that, after reaching RH 95 % and switching off the humidification, the relative humidity in the interior does not decrease significantly. This means that there is no convection between the interior of the climate chamber and the laboratory environment.

The measured relative humidity fluctuates between 90–95 %, indicating fluctuations in the information from the sensor. This is confirmed by locations with a slight increase in RH, which is physically unrealistic, so it is an error caused by the measuring range of the sensors.

Again, the chamber is tight and affects the results of the following experiments only slightly.

Amount of water consumed: approximately 33 g of water was consumed to increase the RH from 45 % to 95 % (in the form of water vapour in the chamber air). To maintain this value for one hour and overcome the effect of leaks, the system consumed about 3–5 g of additional water.

The charts in Fig. 69 and Fig. 70 show that there are minor leaks in the climatic chamber or around the sample. This must be considered during evaluation of the results.

The set values of relative humidity in the climate chamber were 45 % (conditioning) and 95 % (increased humidity). These values were inaccurately indicated by measuring sensors in the chamber. As part of the experiment, more accurate sensors were installed in the chamber, which showed corresponding values of about 43 % and 93 %. These values are used in the statistical evaluation of the experimental data.

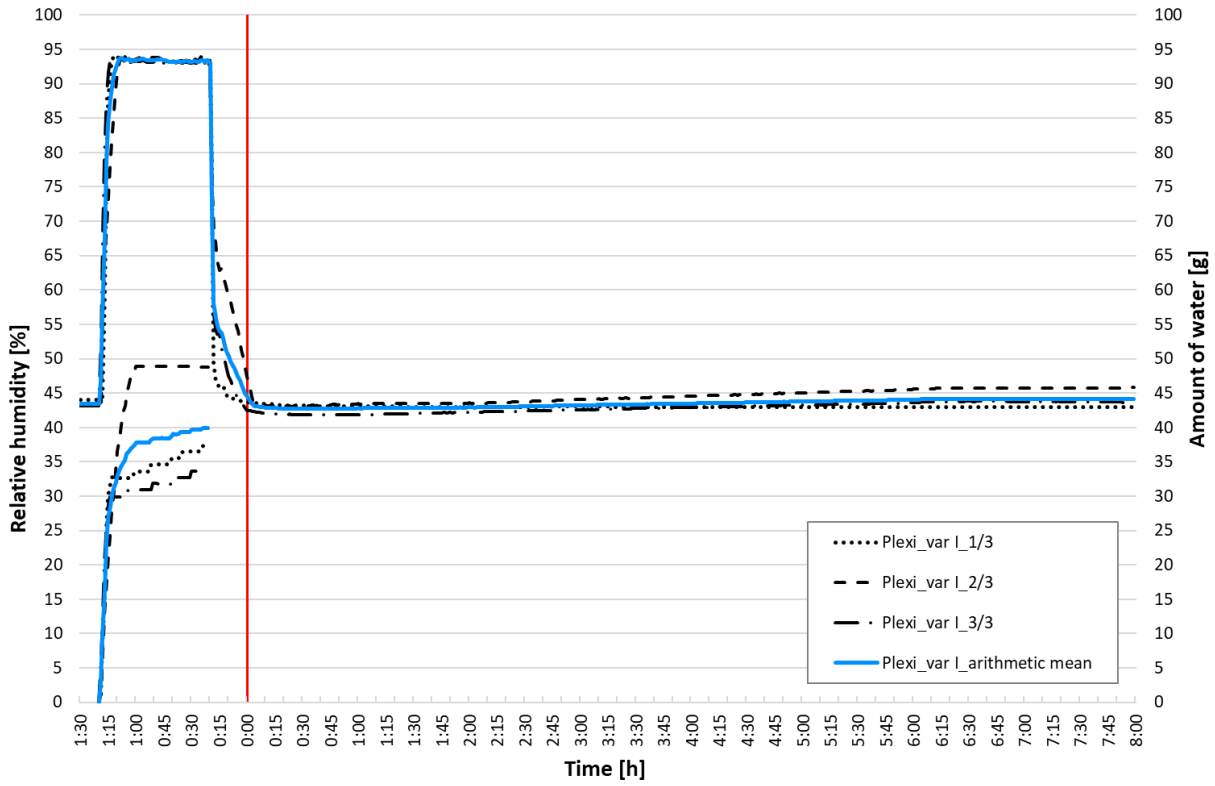

Fig. 69 Dynamic sorption – verification of the airtightness of the chamber – var I

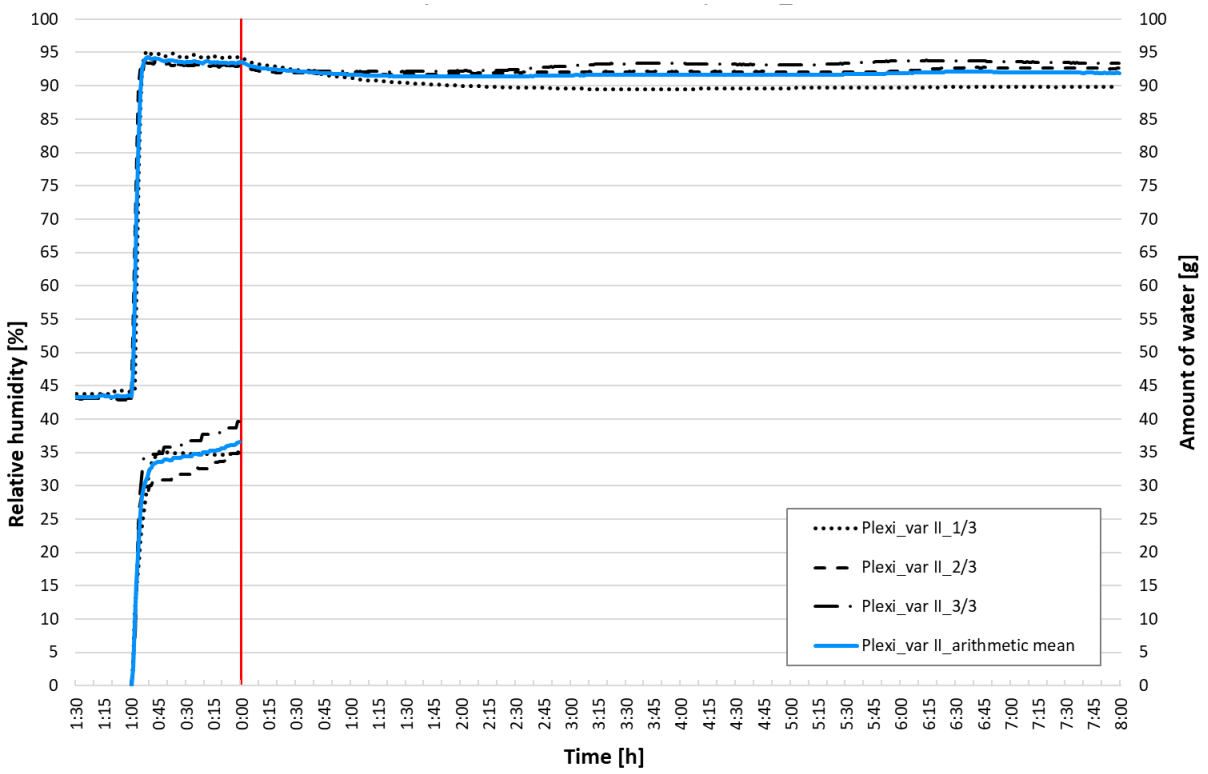

Fig. 70 Dynamic sorption – verification of the airtightness of the chamber – var II

5.2.2 Concrete

Results of var I

The measurement of relative humidity (Fig. 71) shows fundamental inaccuracies. Probably an error occurred in experiment 1/3. The readings of RH in the interval of eight hours does not correspond to prediction and is also different from RH readings of other materials with similar properties.

This situation may be caused by a poorly sealed chamber or a system error in the chamber, resulting in distorted values.

In contrast, the water consumption measurement shows almost identical values, i.e. approximately 54 g, for the RH 95 % remaining in the chamber for 60 minutes.

Results of var II

The influence of relative humidity on the adsorption dynamic properties of concrete (Fig. 72) are almost identical during repeated measurements. The course of relative humidity in the climate chamber of repeated measurements is almost identical and indicates the high homogeneity of the tested material.

Amount of water consumed: The values of repeated measurements are again almost identical. The total water consumption after 60 minutes is about 55 g.

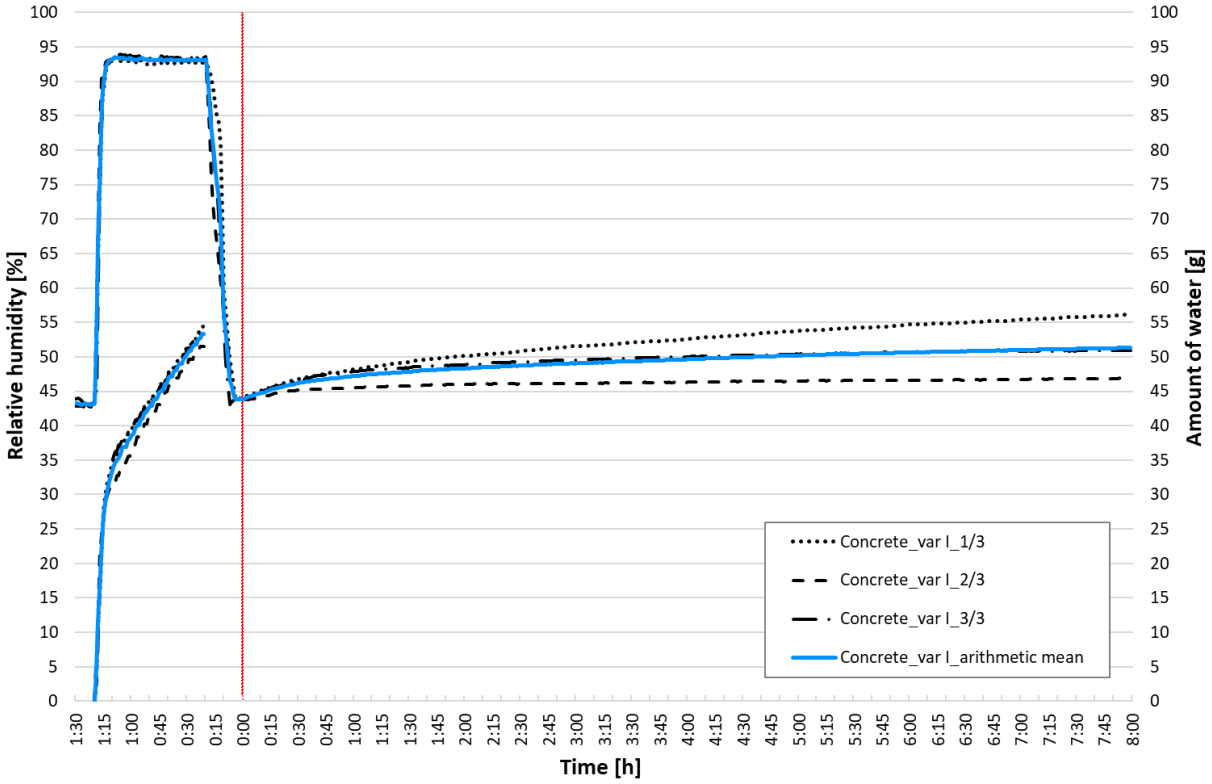

Fig. 71 Dynamic sorption – concrete – var I

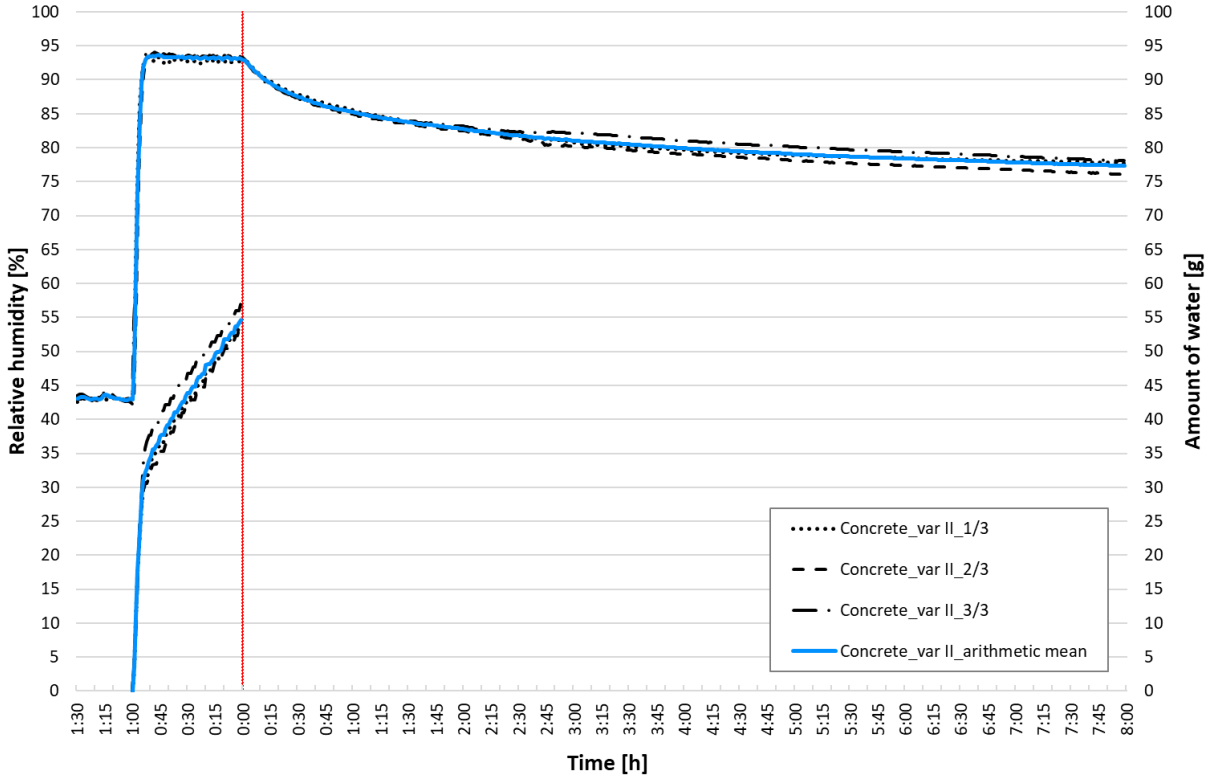

Fig. 72 Dynamic sorption – concrete – var II

5.2.3 Lime plaster

Results of var I

The results (Fig. 73) of the relative humidity measurements are almost identical. After 1.5 hours the RH increases from 45 % to 50 %, then for another 6.5 hours the RH value is kept constant at 50 %.

Amount of water consumed: data from measurement 2/3 appear as outliers. The explanation for this deviation is not clear. However, this result was not excluded from the evaluation, see chapter 5.2.8.1 section Evaluation of water consumption.

Results of var II

Repeated measurements (Fig. 74) again have homogeneous results. After eight hours, the air relative humidity drops from 93 % to 75 %. The dynamic course in the first minutes is not as noticeable as with the clay structures described below.

The water consumption in the experiment again indicates similar rate and volume values. The total average water consumption was about 52 g.

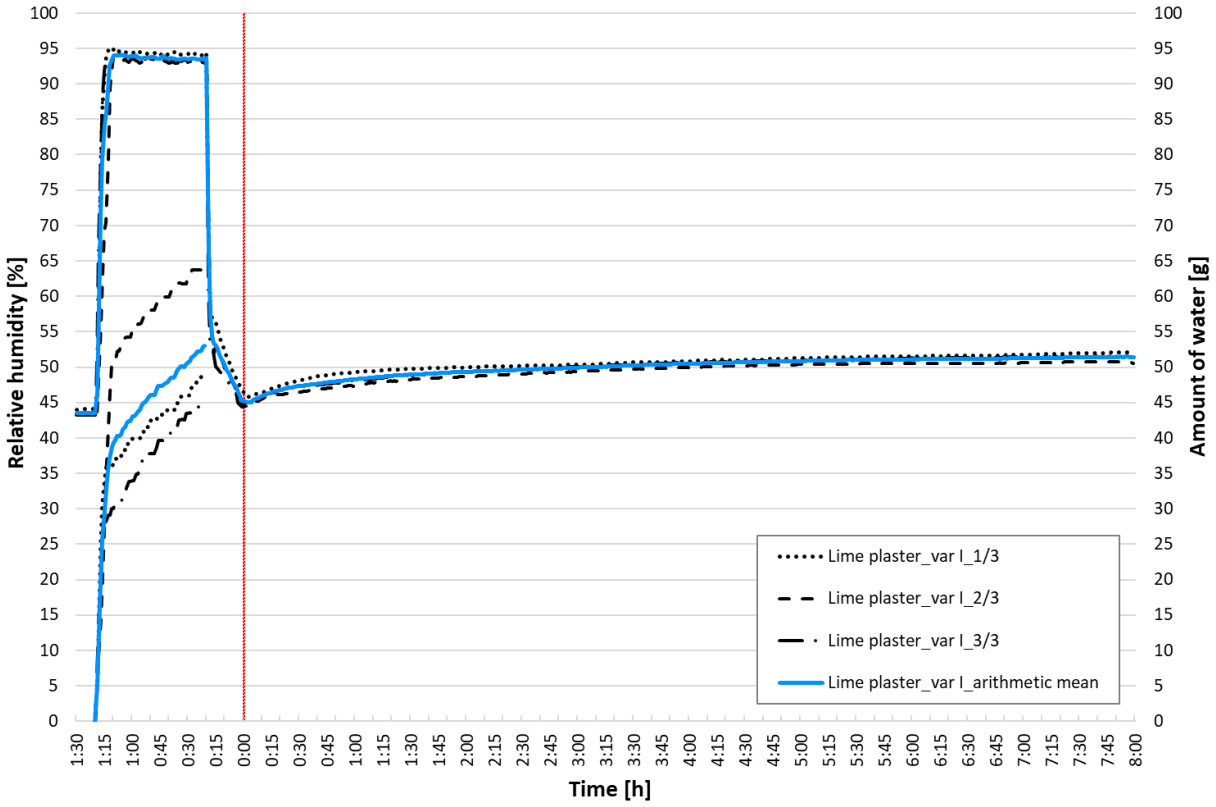

Fig. 73 Dynamic sorption – lime plaster – var I

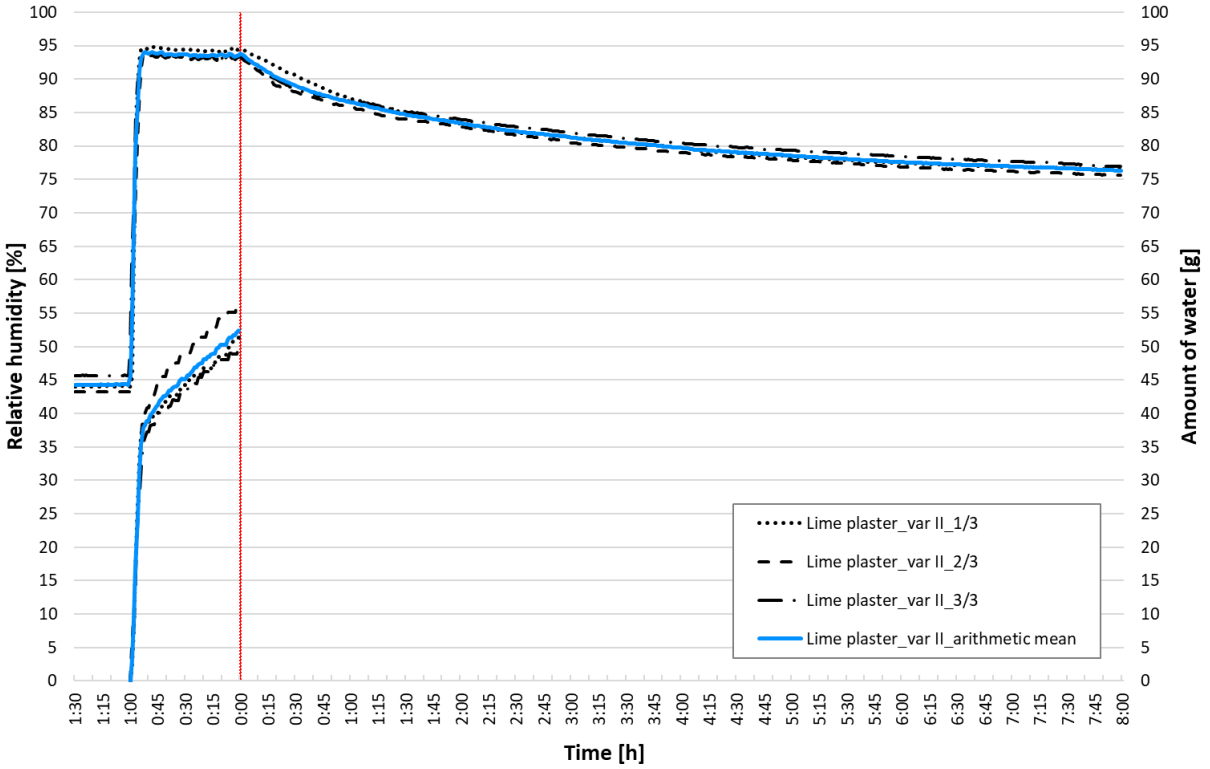

Fig. 74 Dynamic sorption – lime plaster – var II

5.2.4 Gypsum board

Results of var I

Repeating of the experiment (Fig. 75) yielded similar data without outliers. The relative humidity rises from 43 % to 50 % in 1.5 hours and remains constant at this value for the remaining 6.5 hours of observation.

The water consumption in the climate chamber during repeated measurements follows a similar path. Total consumption is 55 g.

Results of var II

Repeated measurements of gypsum board structure (Fig. 76) have similar results as structure with lime plaster – homogeneous results of repeated measurements with a gradual decrease of RH up to 75%.

Water consumption in 60 minutes was on average 54 g. This parameter is also similar to the results of the lime plaster structure.

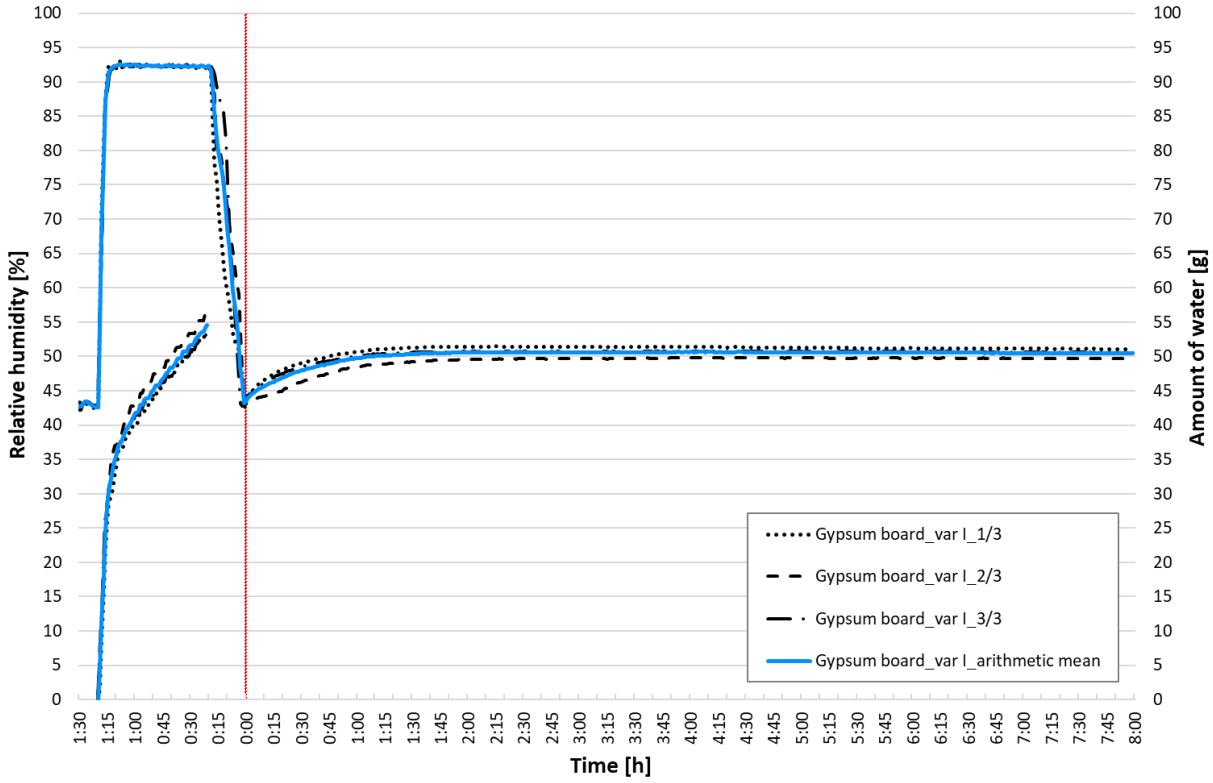

Fig. 75 Dynamic sorption – gypsum board – var I

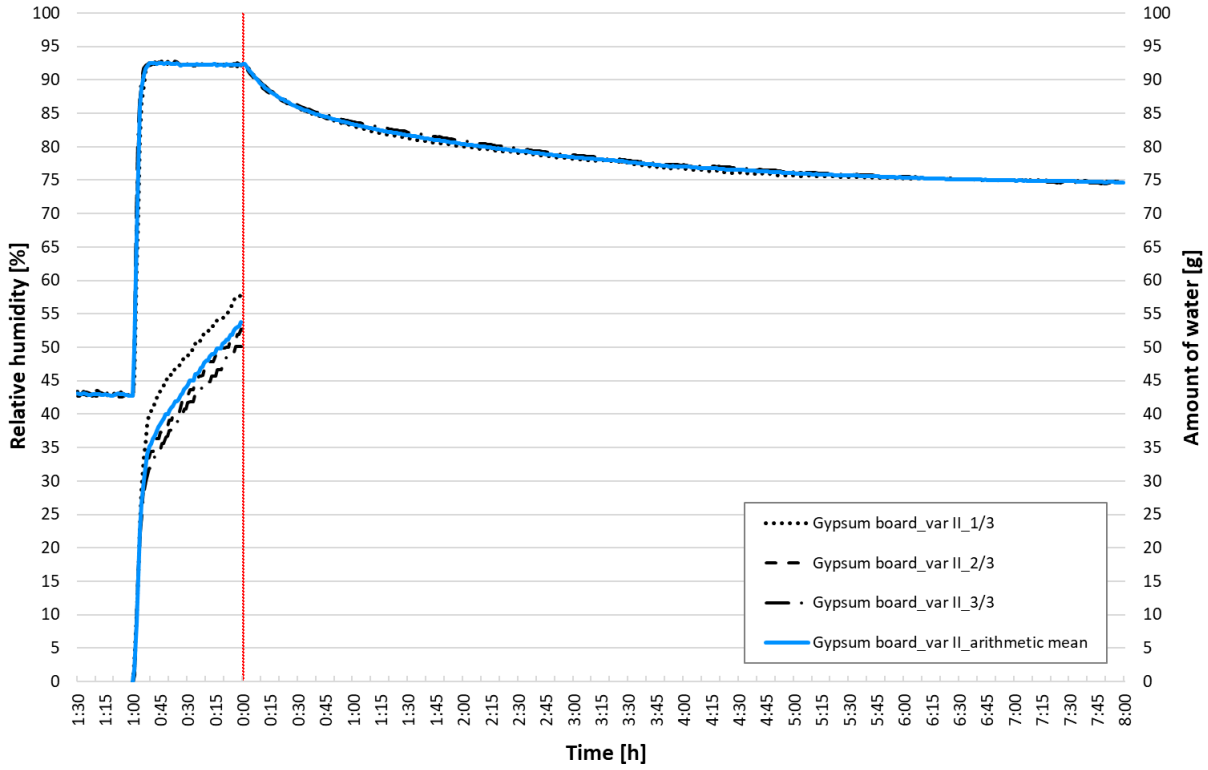

Fig. 76 Dynamic sorption – gypsum board – var II

5.2.5 Rammed earth panel

Results of var I

Rammed earth panel is the first in a set of clay structures. Repeated measurements of relative humidity in an experiment with dynamic desorption (Fig. 77) show that the RH in the interior increases sharply after ventilation. The adsorbed water molecules quickly return from the material to the interior. This rapid dynamic process takes about an hour. This is followed by a very slight decrease when the porous structure apparently re-absorbs the water vapour.

The water consumption during the experiment is significantly higher than in previous structures. Measurement 3/3 shows an unknown error, as the total amount of water consumed was 135 g (to maintain the scale, the resulting value is not visible in the graph). The remaining two measurements achieve the same values and curves of water consumption, i.e. 83 g. The result of measurement 3/3 was excluded from the evaluation, see chapter 5.2.8.1, section Evaluation of water consumption.

The conditioning values correspond to the proposed experimental procedure, so the measurement error obviously occurred in the climatic chamber system.

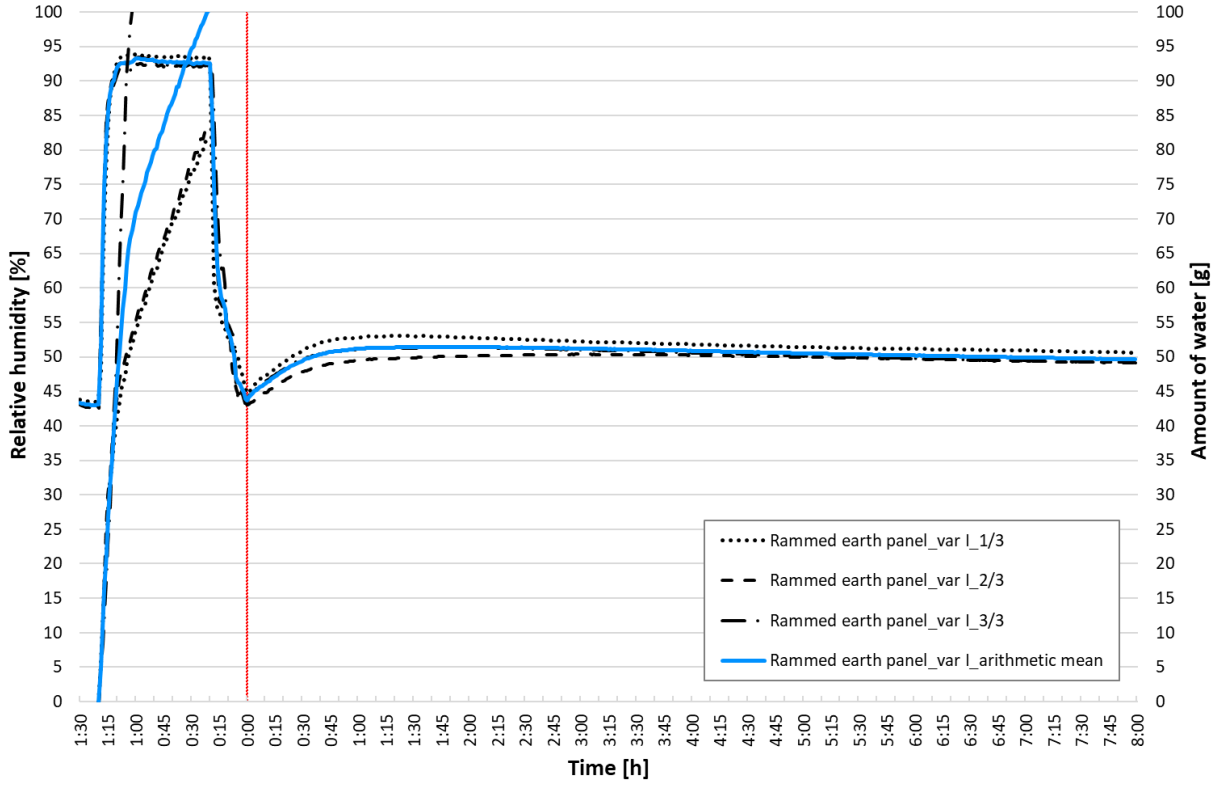

Fig. 77 Dynamic sorption – rammed earth panel – var I

Results of var II

According to Fig. 78, sample 1/3 was apparently wetter during conditioning (RH 46 %); conditioning was not an inaccuracy of the system to the same value (43 %). More water molecules have accumulated in the structure. This also reduced the need for humidification (lower water consumption). Because the sample was more saturated, it had less sorption potential when the moisture source was turned off.

Samples 2/3 and 3/3 have a similar relative humidity reaction profile.

The course of RH curves is similar. In the first minutes of rapid decrease in relative humidity, water vapour is absorbed into the porous structure of the material. After eight hours, the RH decreased to 60 %, i.e. by 35 %.

Amount of water consumed: measurement 1/3 shows outliers (consumption only 53 g). This result was excluded from the evaluation, see chapter 5.2.8.1, section Evaluation of water consumption. The remaining measurements had a water consumption of about 80 g after one hour of wetting.

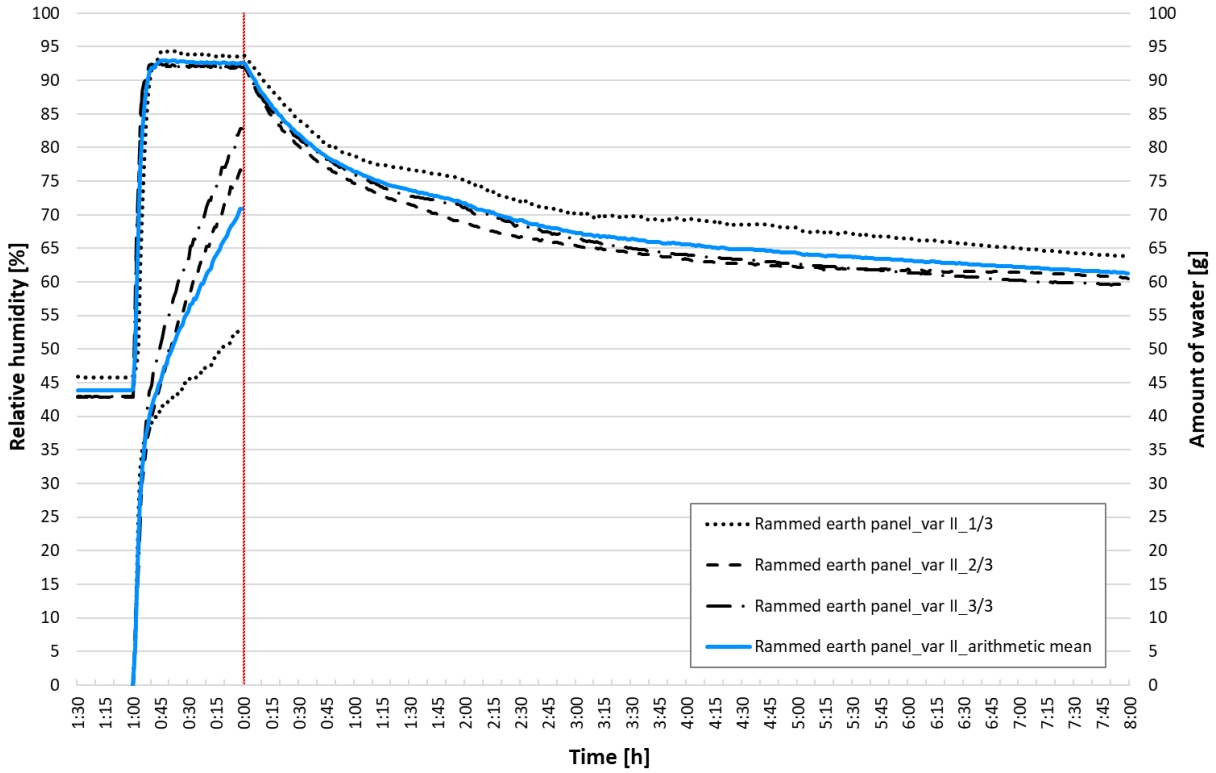

Fig. 78 Dynamic sorption – rammed earth panel – var II

5.2.6 Clay plaster

Results of var I

As with the concrete structure, the clay plastered wall (Fig. 79) has slightly different results with repeated measurements. Measurements 1/3 and 2/3 have a different rate, and measurement 3/3 corresponds to the total average of the measured values.

In the first minutes of observation, the clay plaster quickly desorbs water vapour from the structure and thus increases the RH in the adjacent indoor environment.

The water consumption of the experiment has the same results. In total, about 52 g were consumed on average, less than expected.

Results of var II

The results of this experiment (Fig. 80) are similar to those of the rammed earth panel. Measurement 1/3 absorbed more moisture (higher RH value in the hourly humidification interval), so it probably cannot sorb water molecules from the air as much after turning off the humidification system. Measurements 2/3 and 3/3 follow an almost identical path. The relative humidity drops in 8 hours to an average relative humidity of 67 %.

The water consumption is regular and corresponds to the var I experiment. The total average water consumption during wetting is more than 50 g.

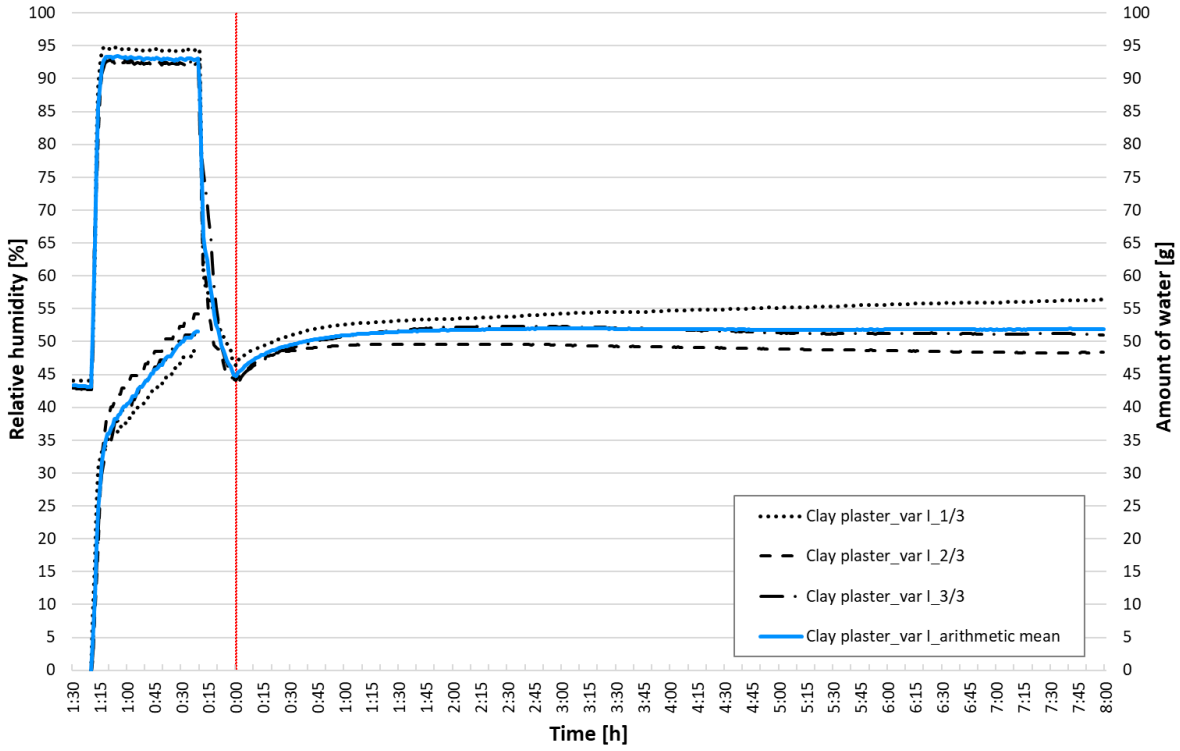

Fig. 79 Dynamic sorption – clay plaster – var I

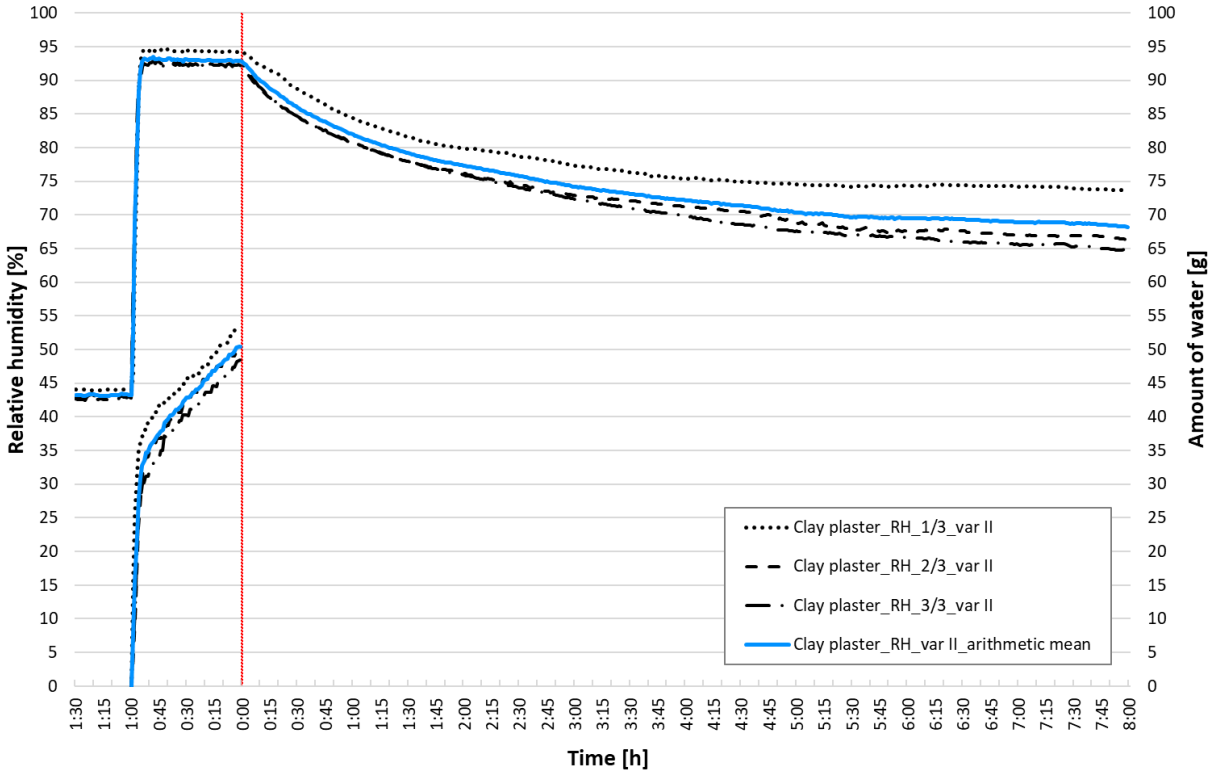

Fig. 80 Dynamic sorption – clay plaster – var II

5.2.7 Unburned brick

Results of var I

Fig. 81 shows that the difference in the location of the measured curves is given by a slightly different initial value after ventilation (at 0:00). However, the path of the observation curves is parallel. A common feature is a rapid increase in RH in the first minutes, then an almost constant maintenance of the RH value.

The water consumption during the experiment is almost identical with an average total of about 58 g.

Results of var II

The results of the 1/3 measurement are again slightly higher, for the same reason as for other clay structures. The value of relative humidity drops by 30 % in 8 hours to an average value of around RH 65 % (Fig. 82).

The total water consumption during the experiment has the same shape of curves and the total amount is again about 58 g.

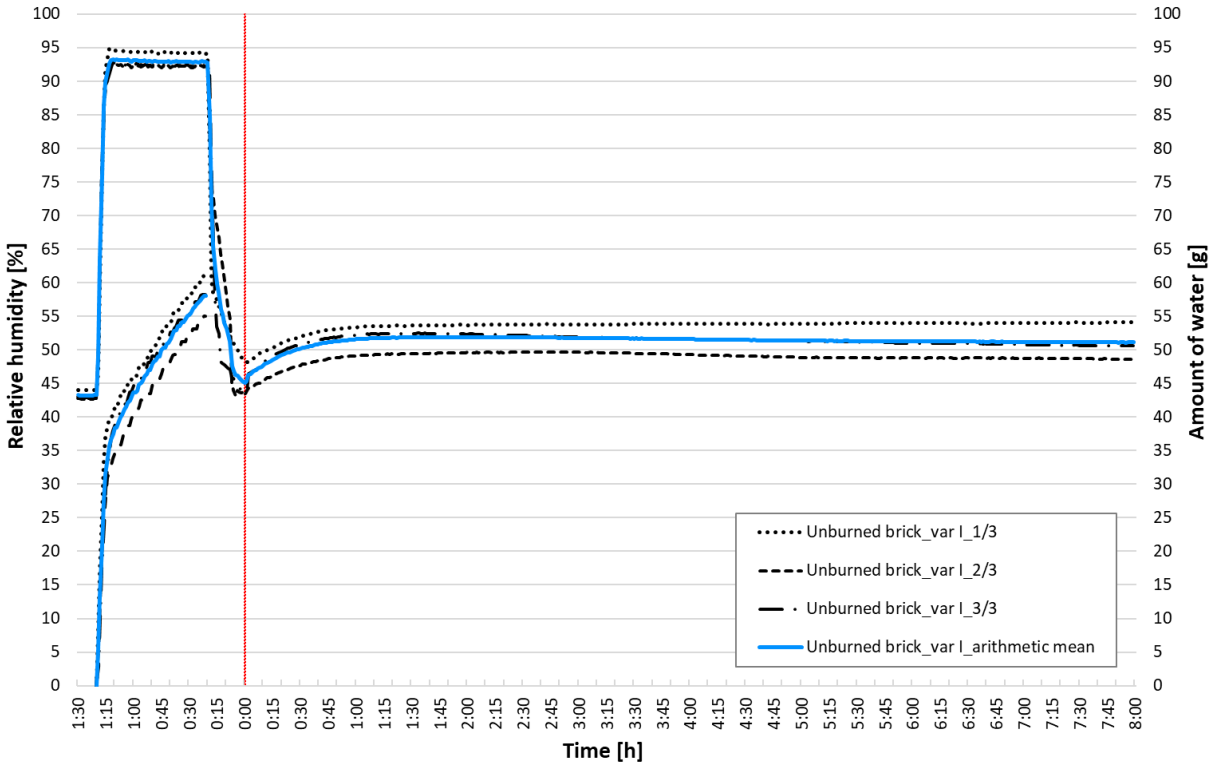

Fig. 81 Dynamic sorption – unburned brick – var I

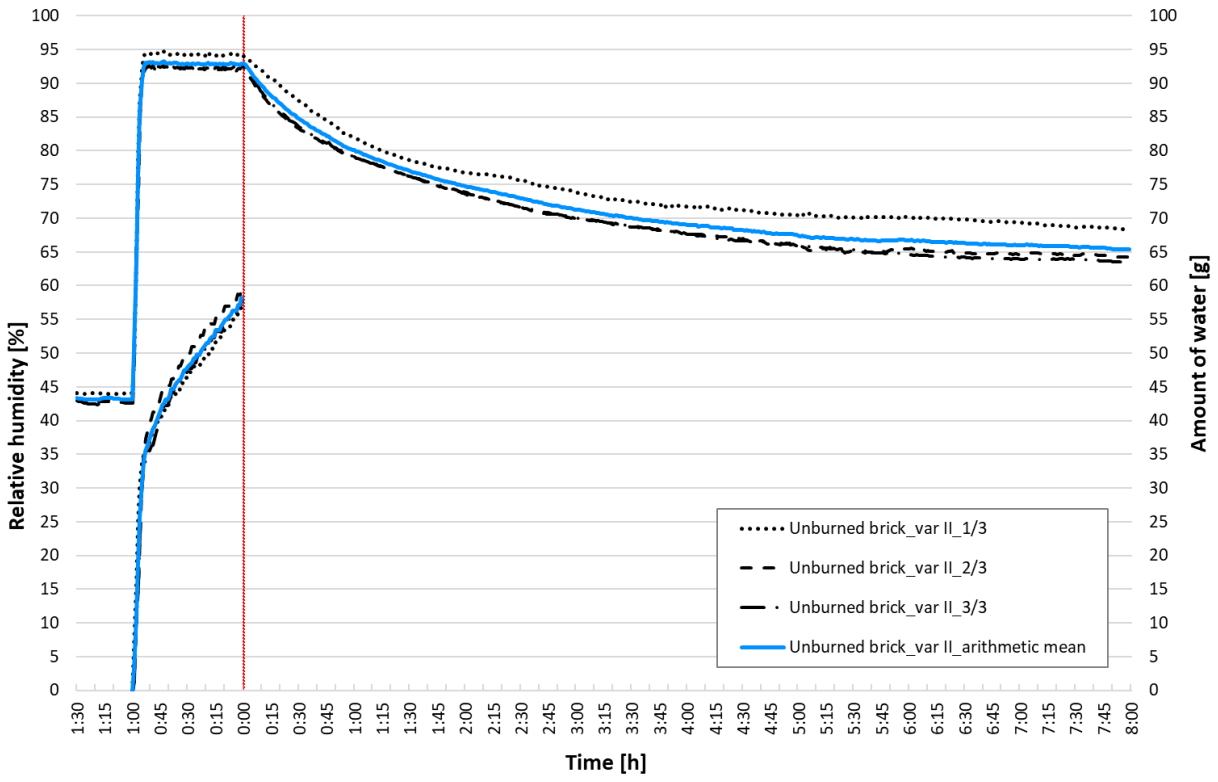

Fig. 82 Dynamic sorption – unburned brick – var II

5.2.8 Partial conclusions

The results of experimental measurements of dynamic sorption properties of building structures are summarized in this chapter. The experiment was performed in two variants, the so-called adsorption dynamic test (var I) and desorption dynamic test (var II).

A total of six structures were examined; three were conventional building structures and three based on clay minerals. Each measurement was repeated three times. The primary measurements were relative humidity and temperature, but water consumption in the system was recorded as well.

5.2.8.1 Water consumption

Computational water consumption

In this section the amount of water in the experiment is calculated.

There are many empirical relationships to conclude from calculating the concentration of water vapour at the saturation limit. The concentration (density) of water vapour in the air is calculated, for example, as:

$$v = RH \cdot v_{sat} \qquad [\mathrm{kg \cdot m^{-3}}] \quad , \tag{6}$$

where RH $[-]$ is the relative humidity of the air and v_{sat} $[\mathrm{kg \cdot m^{-3}}]$ is the density of saturated water vapour in the air at temperature T [°C].

The following empirical relationship applies to the concentration of saturated water vapour in the air:

$$v_{sat} = \frac{a \cdot \left(b + \frac{T}{100}\right)^{n}}{R_V \cdot (T + 273.15)} \qquad [\mathrm{kg \cdot m^{-3}}] \quad , \tag{7}$$

where a, b, n are constants, and R_V $[\mathrm{J \cdot kg^{-1} \cdot K^{-1}}]$ is specific gas constant for water vapour.

For temperature $T = 23\ °C$ the following applies:

$$a = 288.68\ \text{Pa}, \qquad b = 1.098, \qquad n = 8.02, \qquad R_V = 461.5\ \text{J} \cdot \text{kg}^{-1} \cdot \text{K}^{-1},$$

therefore, after calculation, the concentration of saturated water vapour in the air at temperature $T = 23$ °C is $v_{sat} = 0.020\ 55\ \text{kg} \cdot \text{m}^{-3}$. Then the values of water vapour concentration at 23 °C and relative humidity 45 % and 95 % are $v_{45\,\%} = 0.009\ 25\ \text{kg} \cdot \text{m}^{-3}$ and $v_{95\,\%} = 0.019\ 52\ \text{kg} \cdot \text{m}^{-3}$.

The difference between these values Δv [kg · m^{-3}] calculates the amount of water vapour [kg] needed to increase the RH in the interior from 45 % to 95 % at constant temperature and pressure and air volume of 1 m^3. If the actual volume of the climatic chamber V [m^3] is considered, the amount of water m [kg] needed to increase the RH from 45 to 95% is obtained.

$$\Delta v = 0.010\ 27\ \text{kg} \cdot \text{m}^{-3}, \qquad V = 1.617\ \text{m}^{-3}, \qquad m = 0.016\ 61\ \text{kg}$$

The expected water consumption in the climate chamber with a step increase in relative humidity from 45 % to 95 % is ***16.61 grams***.

Dixon's Test

The evaluation of the measurement of water consumption during humidification from 45 % to 95 % can be performed together for variant I and variant II. Thus, a total of six identical experiments are analysed.

It is clear from the obtained data, that some measurements show outliers. These anomalies, if left in the data set, will affect the overall results of the observation. These gross errors can be caused by a system error which is discussed below. Statistical proof of outliers was performed using the Dixon's test.

Dixon (1951) described statistics methods for identification and rejection of outliers in simple data sets. Dixon's tests are used for the file with a small number of observations ($n \leq 30$). For a set of n observations x_i, ordered such that $x_1 \leq x_2 \leq \ldots \leq x_n$, the statistics are defined by:

$$r_{j,i-1} = \frac{x_n - x_{n-j}}{x_n - x_i} \quad , \tag{8}$$

where j indicates the number of outliers suspected at the upper end of the data set, and i-1 indicates the number of outliers suspected at the lower end. Dixon gave analytic formulas for the density and cumulative distribution functions for r_{10}, r_{11}, r_{12}, r_{20}, r_{21}, and r_{22}. The r_{10} is also called Q value, so the outlier rejection test is therefore called the *Q-test*.

For r_{10}, the test criterion Q is calculated for the 1^{st}, or last (n^{th}) value of the series:

$$Q_1 = \frac{x_2 - x_1}{x_n - x_1} \quad , or \quad Q_n = \frac{x_n - x_{n-1}}{x_n - x_1}. \tag{9}$$

In the statistical table, there is a critical value Q_α, that is a reference value corresponding to the sample size n and confidence level α. The selected values are in Tab. 11.

The test criterion is compared with the critical value. If $Q_1 \geq Q_\alpha$, or $Q_n \geq Q_\alpha$, it can be stated that at the confidence level α, the test value x_1, or x_n is the outlier. This outlier can be excluded from the data set and the procedure can be repeated. If $Q_1 < Q_\alpha$, or $Q_n < Q_\alpha$, the value of the variation series cannot be excluded, the value belongs to the data set.

Tab. 11 Critical value Q_α for Dixon's test for confidence level $\alpha = 0.05$

Number of observations n	Critical value Q_a [-]
3	0.941
4	0.765
5	0.642
6	0.560

Evaluation of water consumption

The Dixon's test was performed on all six experimental structures and on a reference plexiglass. The test was performed on the whole measured series (60 minutes), and the confidence level was chosen to be $\alpha = 0.05$.

From the performed measurements, it is observed that the rate of water consumption is the same in all performed experiments during the first five minutes from the beginning of the gusty humidification (from RH 45 % to RH 95 %). There is considerable water consumption to supply water molecules to the interior air of the chamber and increase the relative humidity from 45 % to 95 %. According to weight measurement, this amount is about 30 g. However, this does not correspond to the calculated water consumption required for this change in relative humidity in the experimental space, i.e. 16.61 g (see above). The calculated value is approximately half as much as the measured value. It is assumed that there is a regular loss of water on route (in the system). This loss is about 14 g of water. As this is a periodic loss, it does not affect the comparison of the experimental results.

The consumed water between the 5th and 60th minute was fed into the system by leakage of water vapour in the experimental set (see the structure of the reference plexiglass) and mainly due to the sorption properties of the compared structures. The higher the water consumption, the more the structure absorbs moisture during the wetting process. The difference between the amount of water consumed by the reference plexiglass and the selected building structures is the amount that is adsorbed in the porous structure of these materials.

Fig. 83, Fig. 84, and Fig. 85 show the course and amount of water consumption depending on the observation time in the span of 60 minutes, when the structure was exposed to RH 95 %, simulating a sudden impact source of moisture in the interior.

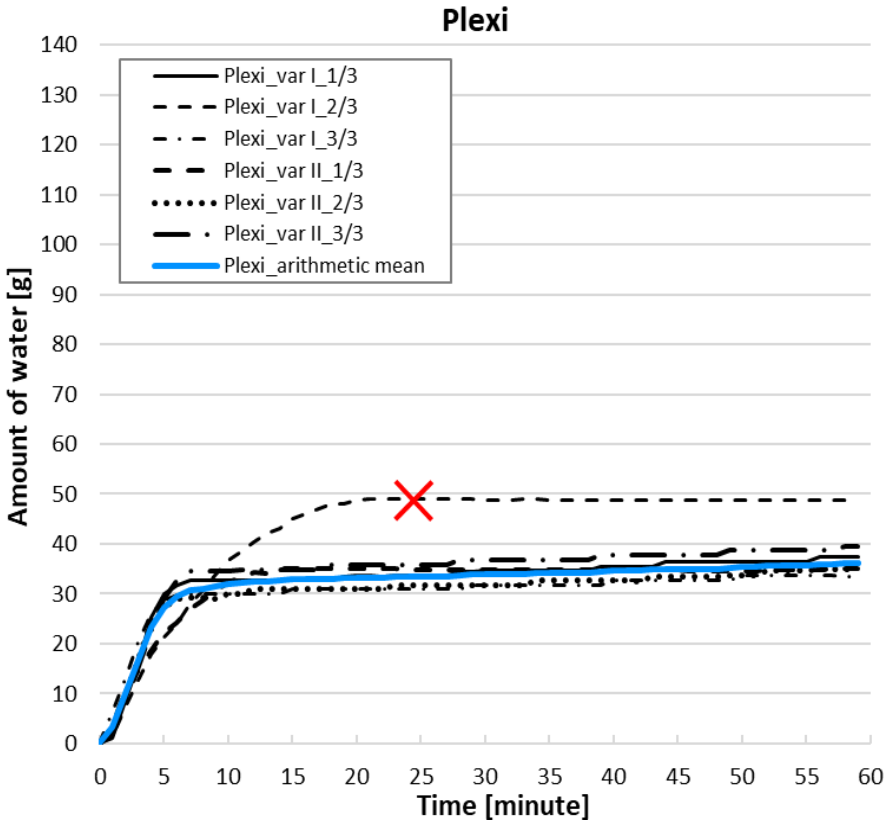

Fig. 83 Water consumed by the system during the experiment: reference material for verification of the airtightness of the chamber

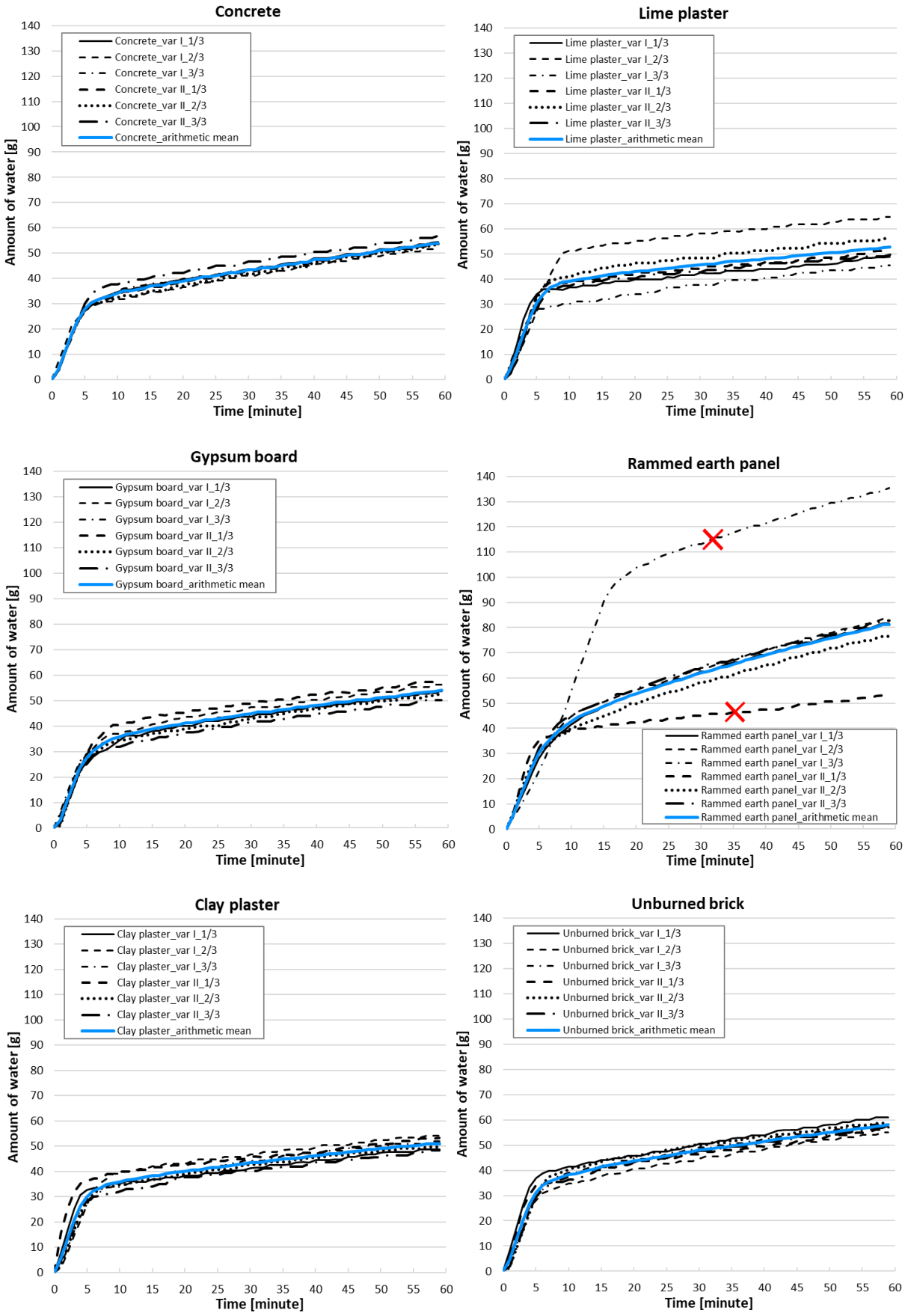

Fig. 84 Water consumed by the system during the experiment by individual structures: concrete, lime plaster, gypsum board, rammed earth panel, clay plaster, and unburned brick.

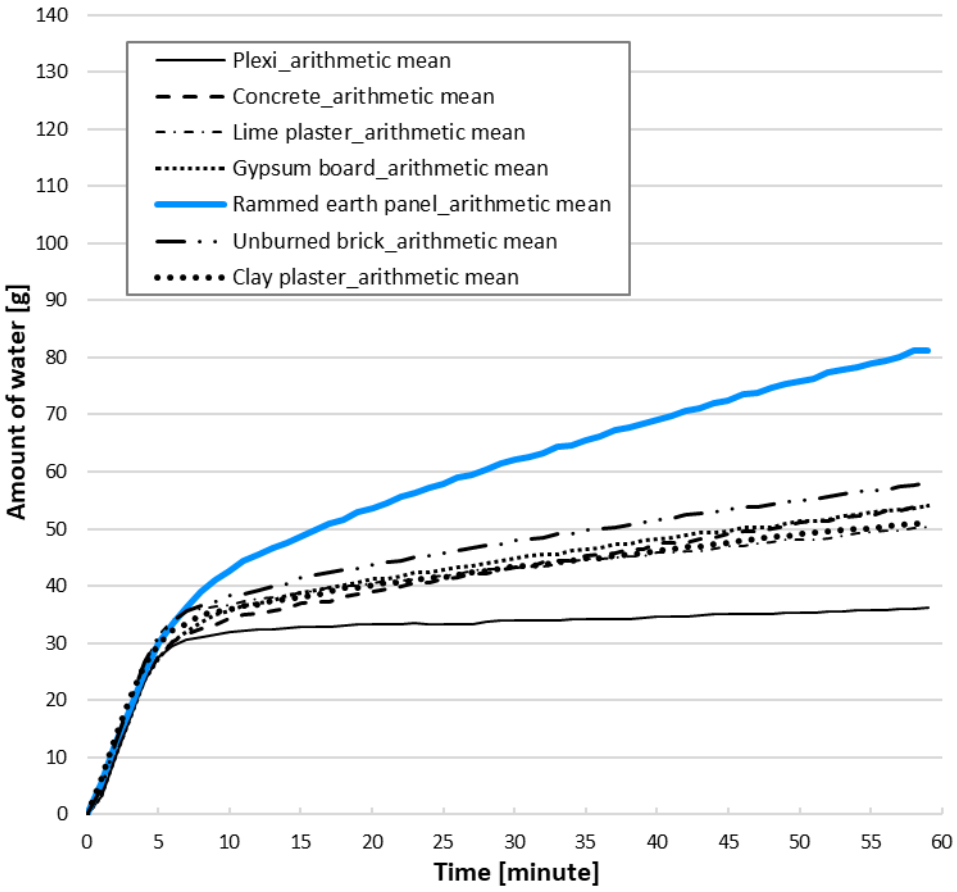

Fig. 85 Water consumption during the experiment

Water consumption curves (Fig. 85) show a linear increase from about the 15 minute mark, so gradients can also be compared. The slope on the interval from 20–60 minutes is calculated as a linear function $y = ax + b$, where the slope determines the parameter a. According to this parameter (Tab. 12), the selected structures can be divided into four groups arranged from the smallest to the largest sorption potential: Lime and Clay plasters; Gypsum board and Concrete; Unburned brick; and Rammed earth panel.

Tab. 12 Slope of the water consumption curve in the interval of 20–60 minutes

Tested structure	Slope of the curve a [-]
Plexi	0.07
Concrete	0.39
Lime plaster	0.26
Gypsum board	0.34
Rammed earth panel	0.71
Unburned brick	0.38
Clay plaster	0.28

5.2.8.2 Response of relative humidity

The following graphs (Fig. 86, Fig. 87) summarize the results of the performed experiments. The courses of relative humidity over time are given as the humidity response of the indoor environment depending on the type of adjacent building structure and its sorption properties.

The arithmetic means of measurements of individual building structures in the performed experiments Dynamic desorption properties (var I) and Dynamic adsorption properties (var II) are shown.

Results of var I

Clay materials quickly desorb the adsorbed moisture back into the interior. The most pronounced dynamic event occurs in the first hour of the observation. The course of RH is very similar for all clay materials. The RH value peaks in about 90-120 minutes, depending on the ratio of the exposed area of material A and the volume of the experimental space V.

In the case of rammed earth, after a peak of approximately RH 52 %, there is a tendency in the following 6 hours to reduce the relative humidity by 2 %. This can be the subsequent sorption of moisture into deeper places of the pore system. This experiment, however, certainly does not prove it.

Non-clay structures (concrete and lime plaster) have the least dynamic response with a slight rise to about 50 % relative humidity.

Gypsum board shows characteristics between clay and non-clay materials with peak RH occurring after about 2–3 hours.

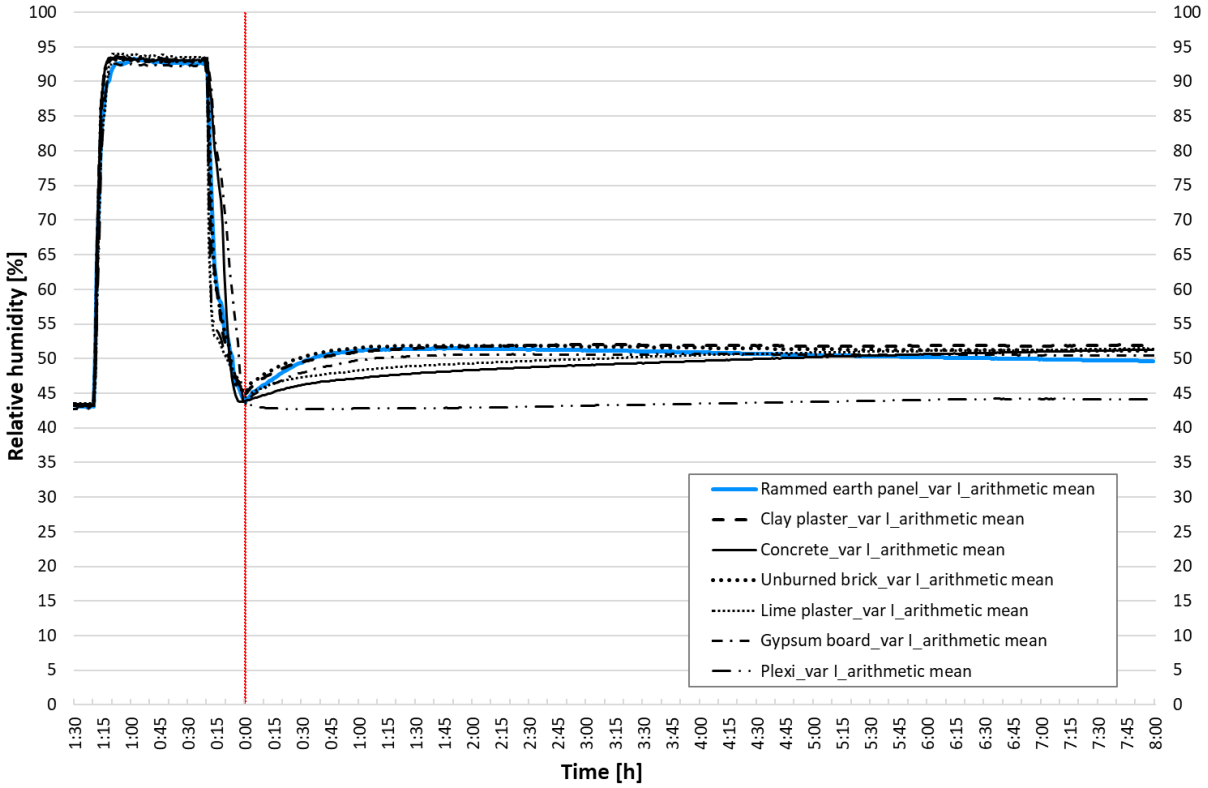

Fig. 86 Dynamic adsorption – arithmetic mean – var I

Results of var II

The Dynamic adsorption properties (var II) experiment provides easily communicated results on the dynamic sorption properties of selected structures.

The structure made of rammed earth clearly has the greatest potential for adsorption of moisture from the air, followed by unburned brick and clay plaster. The lowest results are shown by non-clay materials. This trend is evident throughout the eight hour observation period.

After eight hours of observation at a given A/V ratio, the rammed earth panel will reduce the relative humidity in the interior by 34 %, unburned brick by about 30 %, and clay plaster by 27 %. The decrease in relative humidity of non-clay structures after eight hours is 17–20 %.

The graph also shows the rate of decrease in relative humidity as indicated by the slope of the RH curve. The steeper the slope of the curve, the higher the adsorption rate. In the case of rammed earth, the decrease in RH in 60 minutes is up to 18 % (interestingly, this same reduction of RH takes non-clay materials 8 hours to achieve).

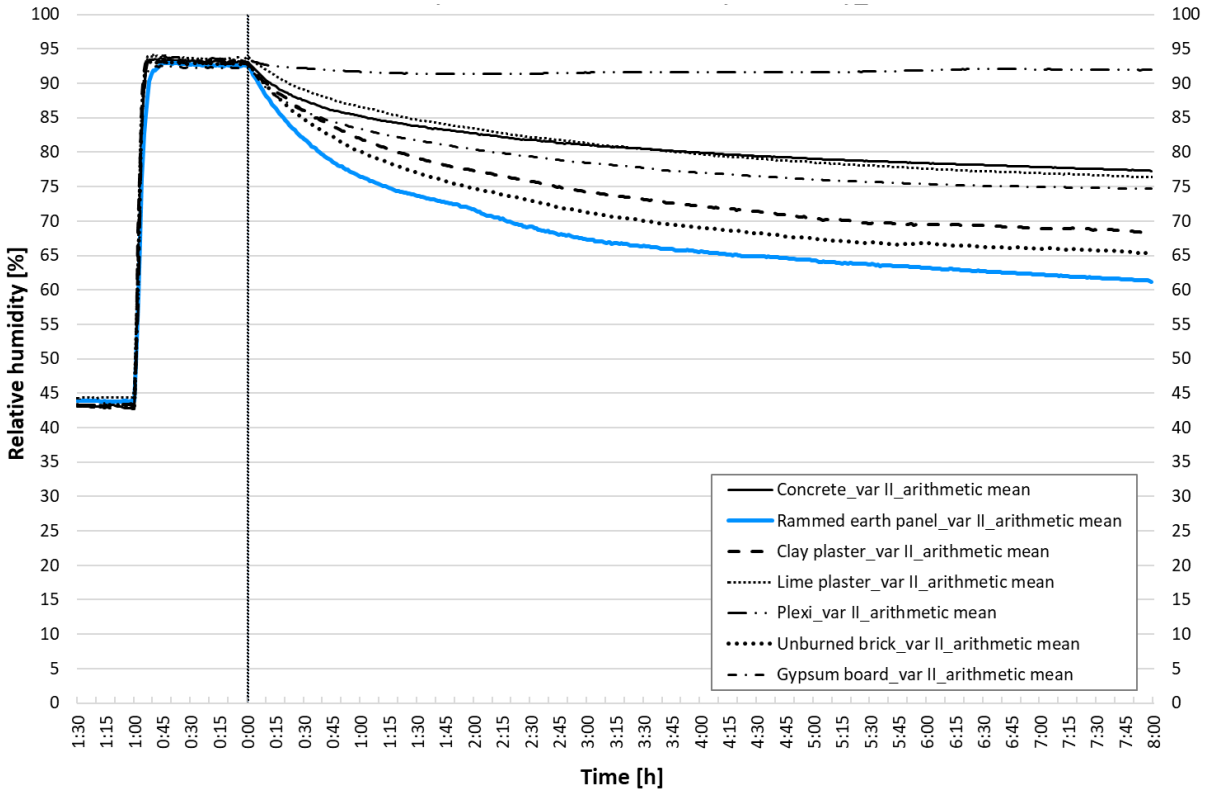

Fig. 87 Dynamic desorption – arithmetic mean – var II

6 Analysis of sorption properties of building structure

For a correct evaluation of the measured experimental results, it is necessary to perform mathematical analysis based on standard statistical methods. Without such analysis, the measured results cannot be correctly compared with each other. Clay products are inhomogeneous materials, thus it is necessary to evaluate the measured data accordingly and take into account the measurement uncertainties.

Described theories, definitions, and formulas were taken from the literature [112], [113], [114].

The definitions of some basic general statistics terms relevant to this thesis are taken from International Standards ISO 3534-1 to 3 [115], [116], [117].

6.1 Mathematical analysis

In order to use any method of data analysis, it is necessary to be aware of the data structure. The measured data have a functional dependence. According to the type of experiment, a continuous decreasing or continuous increasing function is evaluated. The result of the experiment is loaded with errors (see below), therefore the measured data are not deterministic values, but stochastic values, so stochastic statistics to evaluate the results is used. Experimental data obtained by repeated measurements of a selected quantity should be considered as independent random variables, uniformly distributed with the distribution function.

Def: n independent random variables $\boldsymbol{X} = (X_1, \dots, X_n)^T$, uniformly distributed with the distribution function, are called random sampling [112], where n is the number of measurements and $\boldsymbol{X}$ is the vector of random variables.

6.1.1 Measurement errors

In general, there are imperfections in a measurement that give rise to an error in the measurement result. The error has two components: a random component, and a systematic component.

"**Random error** presumably arises from unpredictable or stochastic temporal and spatial variations of influence quantities. The effects of such variations, hereafter termed random effects, give rise to variations in repeated observations of the measurand. Although it is not possible to compensate for the random error of a measurement result, it can usually be reduced by increasing the number of observations; its expectation or expected value is zero.

Systematic error cannot be eliminated but it can often be reduced. If a systematic error arises from a recognized effect of an influence quantity on a measurement result, the effect can be quantified and if it is significant in size relative to the required accuracy of the measurement, a correction or correction factor can be applied to compensate for the effect. It is assumed that, after correction, the expectation or expected value of the error arising from a systematic effect is zero." [113]

6.1.2 Assumptions of measurement

The experimental measurement was repeated three times; $r = 3$.

The following assumptions are considered for statistical evaluation:

- repeated measurements were performed according to the same methodology, using the same aids and equipment (airtight sealing materials, climate test chamber, etc.);
- the same measuring instruments were used during all measurements (sensors, balance, etc.);
- the measured data are without outlying observations (verified by the graphical method);
- the measured data are not determinative values, but stochastic random variables;
- the measured points create a continuous decreasing or continuous increasing function (depending on the type of experiment);
- there is a functional relation $Y = f(X)$ between the measured quantities, where X is an independent random variable;
- n pairs $[x_i, y_i]$ of quantities were obtained from the measurements, where
  i = 1, …, n;
  x_i … time;
  y_i … relative humidity;
- systematic measurement errors have not been identified, so only random errors are considered.

6.1.3 Steps of analysis

The statistical evaluation of the dynamic sorption properties measured on the six building structures was performed in the following three steps:

- In the first step, it is necessary to smooth individual observations by use of regression analysis. The regression curves were determined using the least squares method.
- Then the accuracy of the regression model was evaluated by testing hypotheses. Suitable regression curves were chosen.
- The last step is to determine the confidence interval. It is established by using the Student's distribution.

6.1.4 Regression analysis

The regression analysis is one of the most important and widely used statistical tools that attempts to determine the strength and character of the relationship between one dependent variable Y and a series of other independent variables X. A common form of regression analysis is a polynomial. Polynomial regression is a special case of multiple regression, with only one independent variable X. One-variable polynomial regression model can be expressed in matrix notation as:

$$\boldsymbol{Y} = \boldsymbol{X\beta} + \boldsymbol{\epsilon} \quad , \tag{10}$$

where $\boldsymbol{Y}$ is a response vector of a dependent variable; $\boldsymbol{\beta}$ is a vector of coefficient of regression, $\boldsymbol{X}$ is a design matrix of independent variable and $\boldsymbol{\epsilon}$ is a random error vector.

This model can be rewritten as:

$$Y_i = \beta_0 X_i^0 + \beta_1 X_i^1 + \beta_2 X_i^2 + \cdots + \beta_m X_i^m + \epsilon_i \quad , \; i = 1, \ldots, n, \tag{11}$$

where
m … degree of the polynomial – the highest power of $\boldsymbol{X}$ appearing in the equation;
Y_i … dependent variable for the i-th article;
X_i … independent variable for the i-th article;

β_j … j-th regression coefficient, $j = 0, \dots, m$;
ϵ_i … i-th random regression error;
n … number of measured values.

The assumptions of regression model are:

- $m < n$;
- $E\boldsymbol{Y} = \boldsymbol{\beta X}$;
- $E\boldsymbol{\epsilon} = 0$;
- $var\boldsymbol{Y} = \sigma^2 \boldsymbol{I}_n$.

It is necessary to estimate the unknown values of $\boldsymbol{\beta}$ and $\boldsymbol{\epsilon}$. The aim of the regression is to interpolate the values $(X_i;Y_i)$; $i=(1,\dots, n)$ with the *m-th* degree polynomial $\beta_0 X_i^0 + \beta_1 X_i^1 + \beta_2 X_i^2 + \cdots + \beta_m X_i^m$ so that for the coefficients $\beta_0, \beta_1, \dots, \beta_m$ it holds that the sum of the squares of the deviations of the original values from the obtained polynomial is minimal (Fig. 88).

A polynomial regression model of the *m-th* degree was chosen for stochastic analysis. A model of the relationship is hypothesized and estimates of the parameter values are used to develop an estimated regression equation. The regression parameters of the model were estimated using the least squares method based on minimizing the sum of squares of deviations.

$\hat{\beta}_0, \hat{\beta}_1, \dots, \hat{\beta}_m$ are obtained by finding the values of $\beta_0, \beta_1, \dots, \beta_m$ that minimize the sum of squares differences between Y_i and $\hat{Y}_i$ for observation i:

$$\widehat{\boldsymbol{\beta}} = \arg\min_{\boldsymbol{\beta}} \sum_{i=1}^{n} (Y_i - \boldsymbol{X}_i^T \boldsymbol{\beta})^2 \quad , \tag{12}$$

$$\hat{Y}_i = \boldsymbol{X}_i^T \widehat{\boldsymbol{\beta}} \quad , \tag{13}$$

where
$\widehat{\boldsymbol{\beta}}$ … estimation of parameter $\boldsymbol{\beta}$;
$\hat{Y}_i$… estimation of the mean value of Y_i, i.e. EY_i for observation i; $\hat{Y}_i$ is the Y_i value lying on the fitted regression line for a given X_i;
$\boldsymbol{e}$ ... observed errors, i.e. the distance the data set of n points from the fitted regression line.

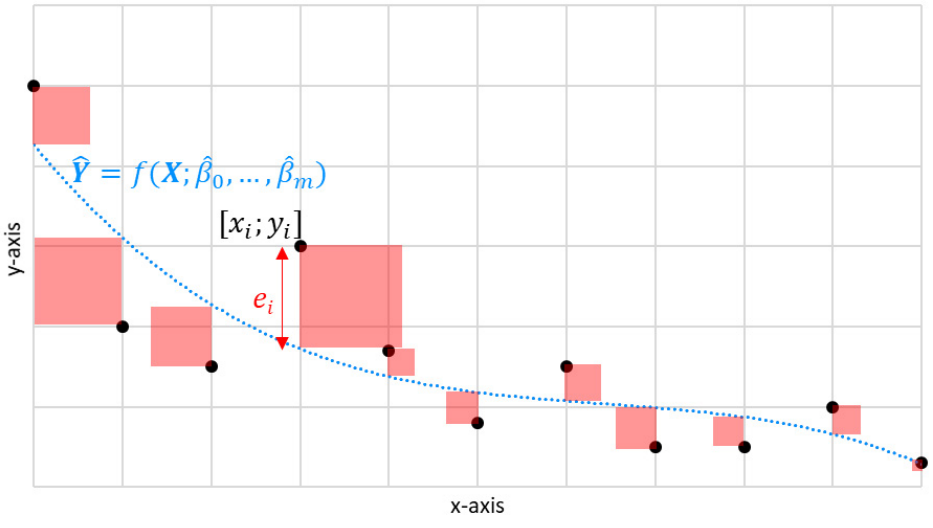

Fig. 88 The method of least squares

Process of evaluation of measured data

The regression parameters are estimated by the method of least squares. It is an extension of the procedure used in a simple linear regression. First, the sum of the squared errors is calculated, and then a set of estimators is found that minimize the sum. After setting the parameters, the accuracy of the model is evaluated. Various tests are employed to determine if the regression model is satisfactory (see below).

Data obtained from the repeated measurements (repetition $r = 3$) were first subjected to analysis based on regression models, in which the observation time was represented as the fixed independent variable $\boldsymbol{X}$, and the relative humidity in the interior was the dependent variable $\boldsymbol{Y}$. Based on the analysed data and the assumed course of the functional relationship $\boldsymbol{Y} = f(\boldsymbol{X})$, a polynomial regression was chosen. Regression parameters were determined for polynomial functions of degree: $m = 3$, 4, and 5. A polynomial regression function of the 1st degree ($m = 1$) (the linear regression function) and a polynomial regression function of the 2nd degree ($m = 2$) (the quadratic regression function) were not considered because they do not correspond to the course of the measured data.

Using the add-in program Solver in MS Excel, the parameters of the regression curves were estimated. Thus, a total of three polynomial functions of different degrees were determined for each measurement. This was followed by testing the quality of the regression models and evaluating which curve best corresponds to the measured data.

Parameter β_0 was fixed to evaluate data from experimental measurements of dynamic sorption properties as:

$\hat{\beta}_0 = 43$ or 93,

because it is the starting point for observing the response of building structures to changes in internal humidity described in the Dynamic desorption test (var I) and Dynamic adsorption test (var II) methodologies, chapter 5.1.4. The methodology considers relative humidity of 45 % and 95 %, but the actual measured values were on average just the 43 % (RH value for var I) and 93 % (RH value for var II).

The following tables and figures show the results of the regression analysis for the structure rammed earth panel. Tab. 13, Tab. 14, and Tab. 15 show the parameters of the 3rd, 4th, and 5th degree of the polynomial regression curves for 3 repeated measurements in var II of the dynamic sorption experiment and Fig. 89, Fig. 90, and Fig. 91 show the measured data and their respective regression curves for the different degrees of the polynomial.

It shows how the data are evaluated. Parameters for further measurement of the remaining structures (concrete, lime plaster, gypsum board, rammed earth panel, clay plaster, and unburned brick in var I and var II of the dynamic sorption experiments) are stored in the author's archive.

The next step was to evaluate the suitability of the regression model.

Tab. 13 Set of regression analysis estimates for rammed earth panel (3rd degree)

Measurement	var II_1/3	var II_2/3	var II_3/3
m	3	3	3
n	480	480	480
$\hat{\beta}_5$	0	0	0
$\hat{\beta}_4$	0	0	0
$\hat{\beta}_3$	-8.456E-07	-1.131E-06	-9.733E-07
$\hat{\beta}_2$	7.663E-04	1.045E-03	9.057E-04
$\hat{\beta}_1$	-2.378E-01	-3.133E-01	-2.850E-01
$\hat{\beta}_0$	93	93	93

Tab. 14 Set of regression analysis estimates for rammed earth panel (4th degree)

Measure-ment	var II_1/3	var II_2/3	var II_3/3
m	4	4	4
n	480	480	480
$\hat{\beta}_5$	0	0	0
$\hat{\beta}_4$	2.662E-09	4.102E-09	3.677E-09
$\hat{\beta}_3$	-3.244E-06	-4.827E-06	-4.286E-06
$\hat{\beta}_2$	1.425E-03	2.060E-03	1.815E-03
$\hat{\beta}_1$	-2.906E-01	-3.945E-01	-3.578E-01
$\hat{\beta}_0$	93	93	93

Tab. 15 Set of regression analysis estimates for rammed earth panel (5th degree)

Measure-ment	var II_1/3	var II_2/3	var II_3/3
m	5	5	5
n	480	480	480
$\hat{\beta}_5$	-8.356E-12	-2.065E-11	-1.786E-11
$\hat{\beta}_4$	1.229E-08	2.791E-08	2.427E-08
$\hat{\beta}_3$	-7.103E-06	-1.436E-05	-1.253E-05
$\hat{\beta}_2$	2.043E-03	3.587E-03	3.136E-03
$\hat{\beta}_1$	-3.224E-01	-4.732E-01	-4.258E-01
$\hat{\beta}_0$	93	93	93

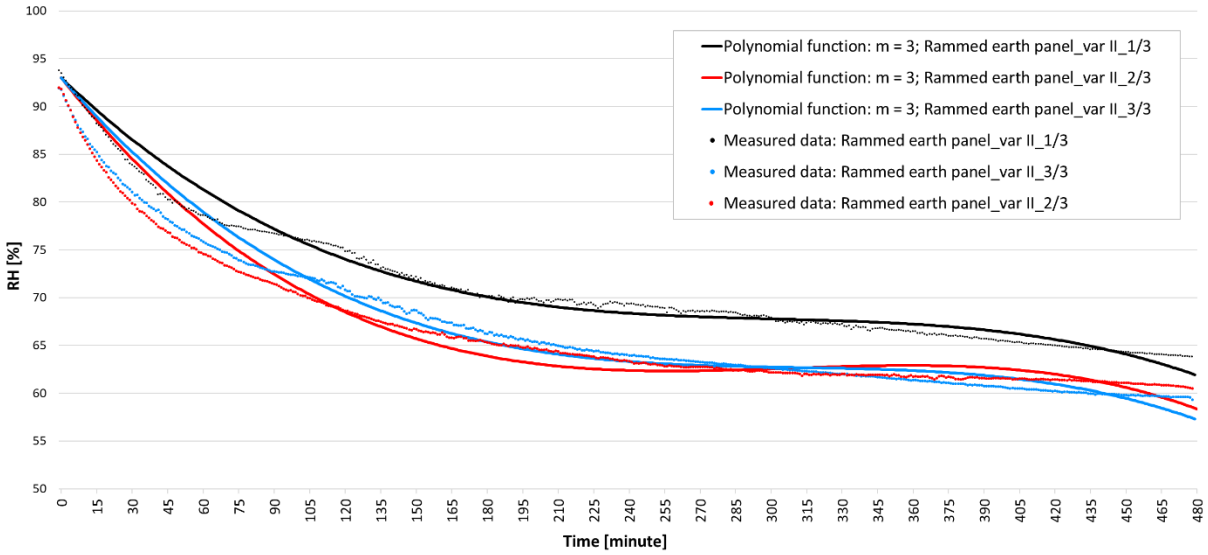

Fig. 89 Regression analysis for Rammed earth panel (polynomial function of the 3rd degree)

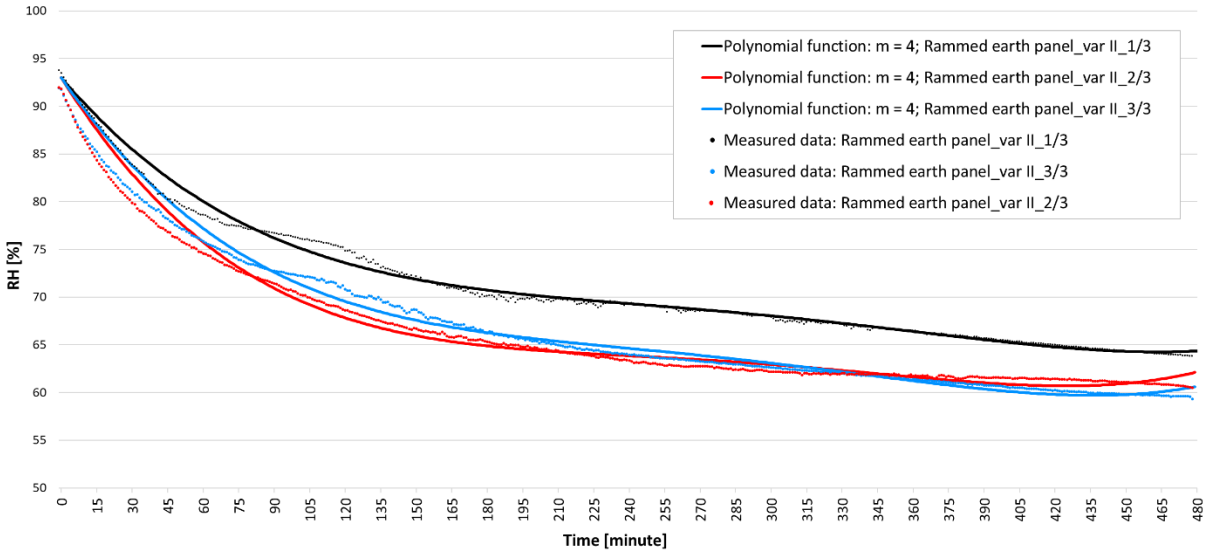

Fig. 90 Regression analysis for Rammed earth panel (polynomial function of the 4th degree)

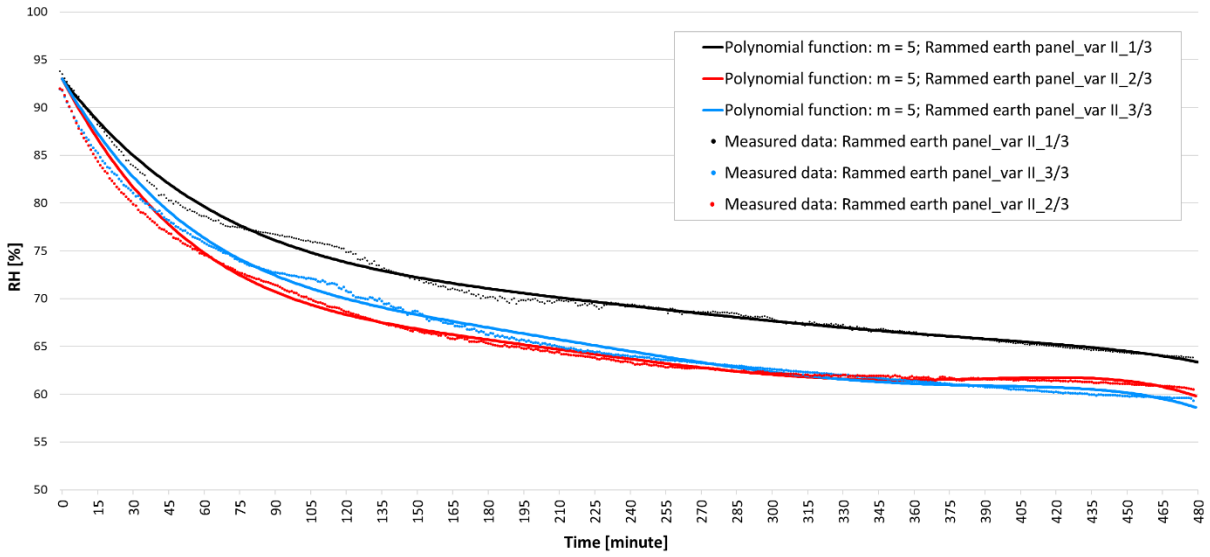

Fig. 91 Regression analysis for Rammed earth panel (polynomial function of the 5th degree)

6.1.5 Evaluation of the accuracy of the regression model

Model validation is an important step in the modelling process and it helps to assess the reliability of models. Based on this, the data can be used for comparison and decision making.

Two tests were performed to evaluate the accuracy of the regression model parameters. The first was the so-called "Akaike Information Criterion" (AIC), which evaluates the relative quality of the model. AIC is used to compare the quality of multiple selected models. The second evaluation was performed by using "the coefficient of determination", which analyses the quality measure of the regression model which, in its basic form, expresses what proportion of the variance in the dependent variable is predictable from the independent variable.

Akaike Information Criterion

"*Akaike's information criterion (AIC) compares the quality of a set of statistical models to each other. It estimates models relatively, meaning that AIC scores are only useful in comparison with other AIC scores for the same dataset.*

The AIC score rewards models that achieve a high goodness-of-fit and penalizes them if they become overly complex. The model with the lower AIC score is expected to strike a superior balance between its ability to fit the data set and its ability to avoid overfitting the data set. Therefore, the desired result is to find the lowest possible AIC, which indicates the best balance of model fit.

Although the AIC will choose the best model from a set, it won't say anything about absolute quality, only the quality relative to other models. Consequently, after selecting a model via AIC, it is necessary to validate the absolute quality of the model. Such validation commonly includes checks of the model's residuals." [118]

AIC formula for least squares regression analyses for normally distributed errors:

$$AIC = n \cdot ln\left(\frac{SSE}{n}\right) + 2m \quad , \tag{14}$$

$$SSE = \sum_{i=1}^{n} \left(Y_i - \hat{Y}_i\right)^2 \quad , \tag{15}$$

where
m … number of model parameters;
n … number of measured values;
SSE … error sum of squares, also called the residual sum of squares;
$\hat{\boldsymbol{Y}}$ … fitted value of $\boldsymbol{Y}$ for the given $\boldsymbol{X}$ value;
$\boldsymbol{Y}$ … observed value of the dependent variable.

Coefficient of determination

The R-squared (R^2, coefficient of determination) of the multiple regression is a statistical measure of how close the data are to the fitted regression line (Fig. 92, Fig. 93). It is the same as for a simple linear regression; the coefficient of determination R^2 is defined as:

$$R^2 = \frac{SSR}{SST} = 1 - \frac{SSE}{SST} \quad , \tag{16}$$

$$SSE = \sum_{i=1}^{n} \left(Y_i - \hat{Y}_i\right)^2 = \sum_{i=1}^{n} e_i^2 \quad , \qquad SST = \sum_{i=1}^{n} (Y_i - \bar{Y})^2 \quad , \qquad SSR = \sum_{i=1}^{n} \left(\hat{Y}_i - \bar{Y}\right)^2 \quad , \tag{17}$$

$$\bar{Y} = \frac{1}{n} \sum_{i=1}^{n} Y_i \quad , \tag{18}$$

where
SST … total sum of squares;
SSE … error sum of squares, also called the residual sum of squares;
SSR … regression sum of squares, also called the explained sum of squares;
$\bar{Y}$ … arithmetic mean of the observed data, i.e. variable $\boldsymbol{Y}$;
$\hat{\boldsymbol{Y}}$ … fitted value of $\boldsymbol{Y}$ for the given $\boldsymbol{X}$ value;
$\boldsymbol{Y}$ … observed value of the dependent variable;
$\boldsymbol{e}$ … difference between predicted and observed value.

Note: in MS Excel (2019) the designation is different: ESS is the Explained sum of squares and RSS is the Residual sum of squares.

The R^2 value shows the percentage of variation in the response variable Y explained by the explanatory variable X. Thus, it is an important measure of how well the regression model fits the data. The value of R^2 is always between zero and one, $0 \leq R^2 \leq 1$. The R^2 value of 0.9 or above is very good. A lower value may be satisfactory in some applications, but it should be noted that in such cases the prediction errors may be relatively high. [119]

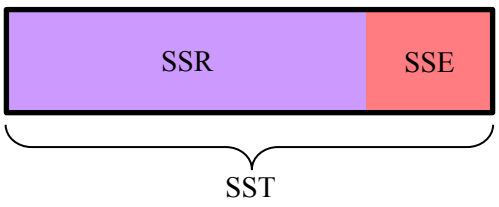

Fig. 92 Graphical description of the relationship of the total, error and regression sum of squares

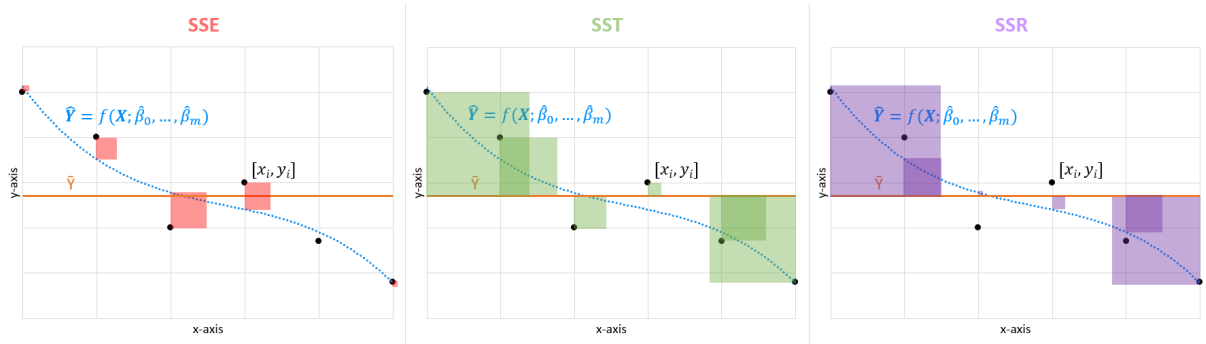

Fig. 93 Graphical representation of the decomposition of the sum of squares in multiple regression

Process of evaluation

Quality testing of the regression model was performed using the least squares method. Two independent methods were used for evaluation: Coefficient of determination (R^2), and Akaike's information criterion (AIC). The purpose of testing individual models using different test methods was to determine which degree of the polynomial better suited the data set. The evaluation of the quality of the model was performed in such a way that the smaller the AIC, the more suitable the statistic model, and the larger the R^2, the more suitable the statistic model (Tab. 16, Tab. 17, Tab. 18).

Tab. 16 Results of quality testing of the regression models (3rd degree)

Measurement	var II__1/3	var II__2/3	var II__3/3
m	3	3	3
n	480	480	480
$\hat{\beta}_5$	0	0	0
$\hat{\beta}_4$	0	0	0
$\hat{\beta}_3$	-8.456E-07	-1.131E-06	-9.733E-07
$\hat{\beta}_2$	7.663E-04	1.045E-03	9.057E-04
$\hat{\beta}_1$	-2.378E-01	-3.133E-01	-2.850E-01
$\hat{\beta}_0$	93	93	93
SST	20 916	22 096	25 823
SSE (RSS)	580	1319	1121
SSR (ESS)	20 336	20 777	24 702
R^2	0.972	0.940	0.957
AIC	96.915	491.331	412.975

Tab. 17 Results of quality testing of the regression models (4th degree)

Measurement	var II__1/3	var II__2/3	var II__3/3
m	4	4	4
n	480	480	480
$\hat{\beta}_5$	0	0	0
$\hat{\beta}_4$	2.662E-09	4.102E-09	3.677E-09
$\hat{\beta}_3$	-3.244E-06	-4.827E-06	-4.286E-06
$\hat{\beta}_2$	1.425E-03	2.060E-03	1.815E-03
$\hat{\beta}_1$	-2.906E-01	-3.945E-01	-3.578E-01
$\hat{\beta}_0$	93	93	93
SST	20 916	22 096	25 823
SSE (RSS)	210	458	429
SSR (ESS)	20 706	21 638	25 394
R^2	0.990	0.979	0.983
AIC	-388.744	-14.334	-46.257

Tab. 18 Results of quality testing of the regression models (5th degree)

Measurement	var II_1/3	var II_2/3	var II_3/3
m	5	5	5
n	480	480	480
$\hat{\beta}_5$	-8.356E-12	-2.065E-11	-1.786E-11
$\hat{\beta}_4$	1.229E-08	2.791E-08	2.427E-08
$\hat{\beta}_3$	-7.103E-06	-1.436E-05	-1.253E-05
$\hat{\beta}_2$	2.043E-03	3.587E-03	3.136E-03
$\hat{\beta}_1$	-3.224E-01	-4.732E-01	-4.258E-01
$\hat{\beta}_0$	93	93	93
SST	20 916	22 096	25 823
SSE (RSS)	155	154	201
SSR (ESS)	20 761	21 942	25 622
R^2	0.993	0.993	0.992
AIC	-531.314	-534.611	-407.356

Test evaluation and selection of regression parameters

For the structure of the rammed earth panel in var II of the proposed experiment (the dynamic adsorption test), it is obvious that the lowest AIC show regression models of the 5th degree. The second test for this material, according to the coefficient of determination, shows that the highest values of R^2, i.e. the most accurate model, are again for the polynomial curves of 5th degree.

Such an analysis was performed for all structures in both proposed variants (dynamic adsorption and desorption tests). As expected, the results of the remaining analyses were identical to the results described above.

Both AIC and R^2 indicate a fifth-degree regression polynomial as the most suitable; this curve best follows the measured values. Based on stochastic methods, it can be stated that the polynomial of the 5th degree is the most suitable.

6.1.6 Confidence interval

For more accurate data evaluation, it is necessary to determine the confidence interval (CI) of the measured data. A confidence interval is a range of values believed to include an unknown measured parameter. The interval has an associated confidence level that the true parameter is in the proposed range. The lower limit and the upper limit of the confidence interval are sought.

According to Dupač, V., and Hušková, M. [112], the measurement is assumed to have a normal distribution $N(\mu, \sigma^2), \mu \in R^1, \sigma^2 > 0$. However, its parameters of the mean (μ) and variance (σ^2) are not known. Therefore, the mean value is estimated using the so-called Student´s distribution (also called t-distribution). This statistical approach is suitable for a small data set. The Student's distribution converges to a Normal distribution with an increasing number of degrees of freedom (for values $n > 30$).

The interval B is called the confidence interval of the parameter θ with confidence $1 - \alpha$, for $\alpha \in (0;1\rangle$, just when

$$P[B \ni \theta] = 1 - \alpha \quad , \tag{19}$$

this is the probability that B will cover the actual parameter θ and α is the reliability factor.

To evaluate the measured data, a two-sided confidence interval is required:

$$B(\boldsymbol{Y}) = \left(C_L(\boldsymbol{X}), C_U(\boldsymbol{X})\right) \quad , \tag{20}$$

where $C_U(\boldsymbol{X})$ is the upper limit and $C_L(\boldsymbol{X})$ is the lower limit. Since a symmetric interval is required, therefore

$$P[\theta < C_L(\boldsymbol{X})] = P[\theta > C_U(\boldsymbol{X})] = \frac{\alpha}{2} \quad . \tag{21}$$

In practice, table distribution values of the t-distribution are used and the lower and upper limits of the confidence interval of the confidence $1 - \alpha$ are estimated by these equations:

$$\hat{C}_L(\boldsymbol{X}) = \bar{X} - t_{1-\frac{\alpha}{2},\mathrm{r}-1}\frac{S_r}{\sqrt{r}} \qquad and \tag{22}$$

$$\hat{C}_U(\boldsymbol{X}) = \bar{X} + t_{1-\frac{\alpha}{2},r-1}\frac{S_r}{\sqrt{r}} \quad . \tag{23}$$

Therefore, the estimate of confidence interval is:

$$\hat{B} = \left(\bar{X} - t_{1-\frac{\alpha}{2},r-1}\frac{S_r}{\sqrt{r}}; \bar{X} + t_{1-\frac{\alpha}{2},r-1}\frac{S_r}{\sqrt{r}}\right) \quad , \tag{24}$$

where

$$\bar{X} = \frac{1}{r}\sum_{i=1}^{r} X_i \quad , \tag{25}$$

$$S_r{}^2 = \frac{1}{r-1}\sum_{i=1}^{r}(X_i - \bar{X})^2 \quad , \tag{26}$$

and

$\hat{C}_L(\boldsymbol{X})$ … estimate of the lower limit of the confidence interval;
$\hat{C}_U(\boldsymbol{X})$ … estimate of the upper limit of the confidence interval;
$\hat{B}$… the estimate of the confidence interval;
$\bar{X}$ … sample mean;
$S_r{}^2$ … sample variance;
X_i … individual value of samples (random selection);
r ... number of samples (repeated measurements);
α … reliability factor;
v … degree of freedom, where $v = r - 1$
$t_{1-\frac{\alpha}{2},r-1}$ … $1 - \frac{\alpha}{2}$% quantile of $r - 1$ degrees of freedom (i.e. table value).

Tab. 19 gives the table values of $t_{1-\frac{\alpha}{2},v}$, where $P[B \ni \theta] = 1 - \alpha$, with v degrees of freedom.

Tab. 19 t-distribution quantiles

$\boldsymbol{v}$	$\mathbf{1-\frac{\alpha}{2}}$					
	0.800	0.900	0.950	0.975	0.9875	0.995
1	1.376	3.078	6.314	12.706	25.452	63.657
2	1.061	1.886	2.920	4.303	6.205	9.925
3	0.978	1.638	2.353	3.182	4.176	5.841
4	0.941	1.533	2.132	2.776	3.495	4.604
5	0.920	1.476	2.015	2.571	3.163	4.032
P	60 %	80 %	90 %	95 %	97.5 %	99 %
α	0.4	0.2	0.1	0.05	0.025	0.01

Process of evaluation

The reliability factor α is usually chosen small, most often 0.05 or 0.1; then the probability is 0.95 or 0.90, respectively. This is often stated as a percentage, i.e. 95 % or 90 %, respectively.

The experiment was repeated three times on each test sample ($r = 3$). Therefore, three repetitions of measurements of the same sample are performed. Each measurement was interpolated with a polynomial function of the 5th degree (previous chapter). A sample mean of these three regression curves was calculated. Then the sample variance was determined, followed by the lower and upper confidence intervals using the Student´s distribution:

- the number of samples is $r = 3$;
- the degree of freedom is $v = 2$;
- the reliability factor is $\alpha = 0.1$.

A 90 % confidence interval was determined.

To compare the results, it is suitable to express the confidence interval with non-fluctuating limits for the interval (increasing or stagnating with time). For the purposes of the thesis, it is appropriate to introduce an adjusted confidence interval as:

$$\left(t_{1-\frac{\alpha}{2},r-1}\frac{S_r}{\sqrt{r}}\right)_{i-1} \leq \left(t_{1-\frac{\alpha}{2},r-1}\frac{S_r}{\sqrt{r}}\right)_{i} \quad , where\ i = 2, \dots n. \tag{27}$$

This rule will make it easier to compare the results described in this thesis and at the same time it guarantees a probability at the 90 % level or higher (because the original interval may extend at some points).

Fig. 94 shows the sequential determination of the adjusted confidence interval. The grey dotted lines show the measured data; the black solid curves show the interpolated 5th degree regression curves for each measurement; the blue solid curve indicates the mean value of these polynomial curves; the red solid curves delimit the adjusted confidence interval (P ≥ 90 %).

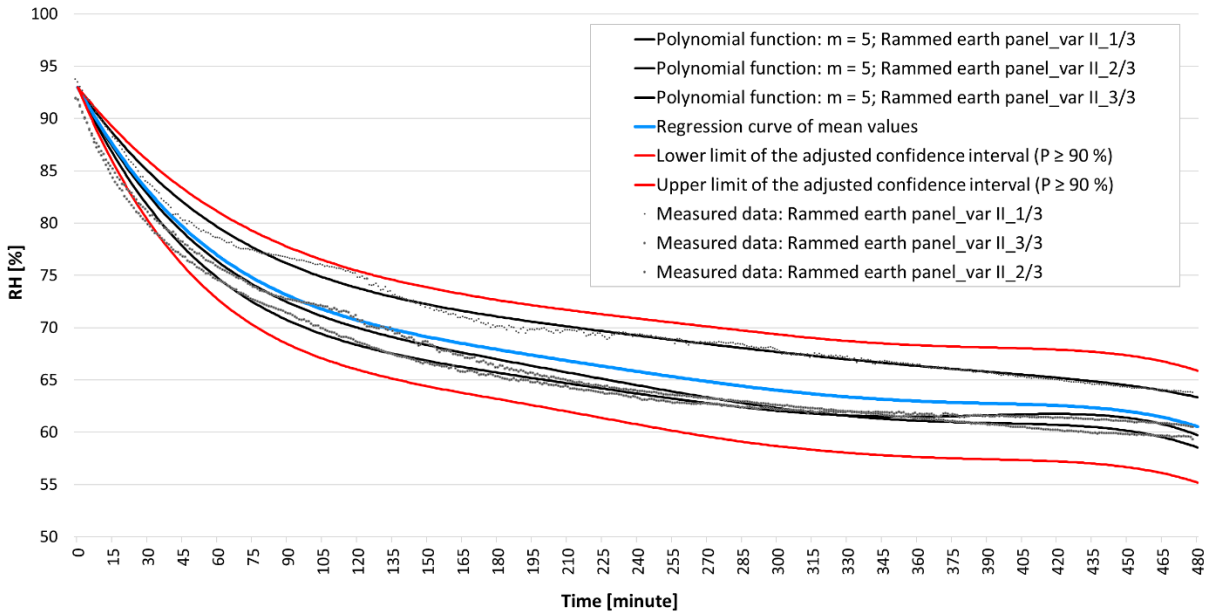

Fig. 94 Adjusted confidence interval of rammed earth panel in the var II

6.2 Confidence interval of dynamic sorption

The purpose of this thesis was to determine the relationship between selected building construction materials with respect to their dynamic sorption properties. As it was necessary to take into consideration their composition, often inhomogeneous, the regression analysis of the measured data described above was performed. All analyses were performed using MS Excel.

For each sample, three measurements were carried out to determine the dynamic sorption curves. The number of samples was $r = 3$; the degree of freedom was $v = 2$; the observation time was eight hours (480 minutes), i.e. the number of measured values $n = 480$; reliability factor $\alpha = 0.1$. The adjusted confidence interval (P ≥ 90 %) was sought. Below are the results of individual structures, the resulting comparison of adjusted confidence intervals, and the analysis of dynamic behaviour.

6.2.1 Adjusted confidence interval of individual structures

Concrete

The measured data of the var I experiment have an increasing variance with increasing observation time (Fig. 95). The expanding confidence interval corresponds to this. The results show that some of the measurements were erroneous. It would be appropriate to repeat this measurement, to exclude the erroneous measurement from the analysed data, and perform the analysis again.

On the other hand, in var II (dynamic adsorption experiment, Fig. 96), the measured data have a small variance of values and therefore the confidence interval is very narrow.

Lime plaster

Repeated measurements of the lime plaster structure are without significant differences, so the confidence interval is small throughout the observation period (Fig. 97 and Fig. 98).

The same can be said for the experiment in var I and in var II. Lime plaster has a small dynamic potential, which is better seen below when mutually comparing structures.

Gypsum board

The confidence interval of gypsum board measurement in a dynamic desorption experiment is relatively narrow. This is due to similar results in repeated measurements.

Repeated measurements in var II are almost identical, so the confidence interval is minimal. This can be interpreted in the sense that gypsum boards have a homogeneous course of dynamic sorption and the measurement deviation is negligible. The stability of the results is, of course, more suitable for the interpretation of the properties of the structure in comparison with structures made of inhomogeneous materials.

Rammed earth panel

Compared to previous structures, rammed earth generally has a wider confidence interval for the measured data. This was expected from an inhomogeneous building material.

The sorption potential of rammed earth is considerable. This is most evident when comparing individual structures, cf. below.

Clay plaster

The measured data show a relatively wide variance. In addition, the confidence interval tends to broaden as a fan-shape. This could be interpreted as high inhomogeneity of sorption properties or as an erroneous measurement. It would be useful to repeat the measurement to see which interpretation is more likely.

A wide confidence interval places the position of this material between standard commercial products (concrete, lime plaster, gypsum board) and the clay building products (rammed earth) when evaluating sorption properties.

Unburned brick

The last examined structure, unburned brick, has expected results similar to clay materials. In both variants var I and var II, the confidence interval is relatively wide, which indicates a greater inhomogeneity of the material, but also a greater potential for handling air humidity.

The results most closely match that of the rammed earth. A detailed comparison is given below.

The following figures (Fig. 95 to Fig. 106) show how the relative humidity in the experimental chamber increases or decreases with different building structure. It is the potential of dynamic sorption determined by statistical evaluation.

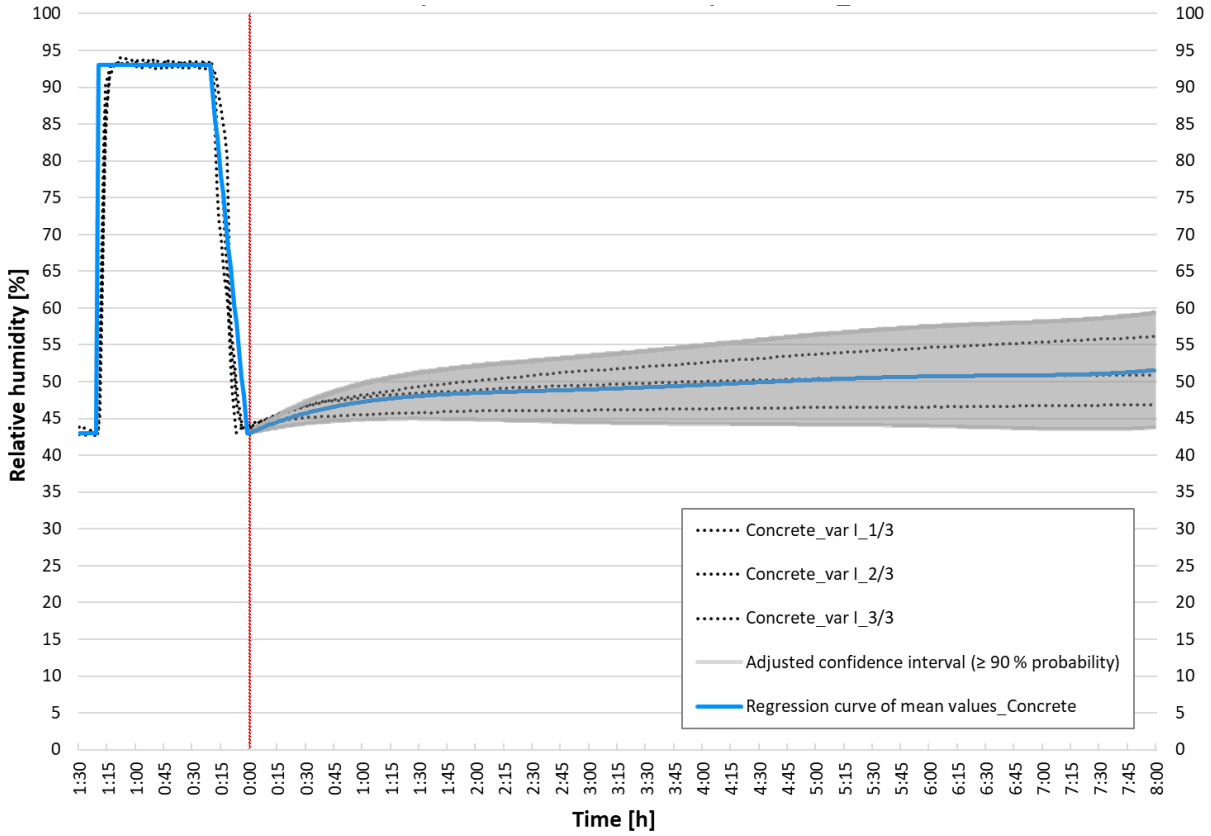

Fig. 95 Adjusted confidence interval of Concrete in var I

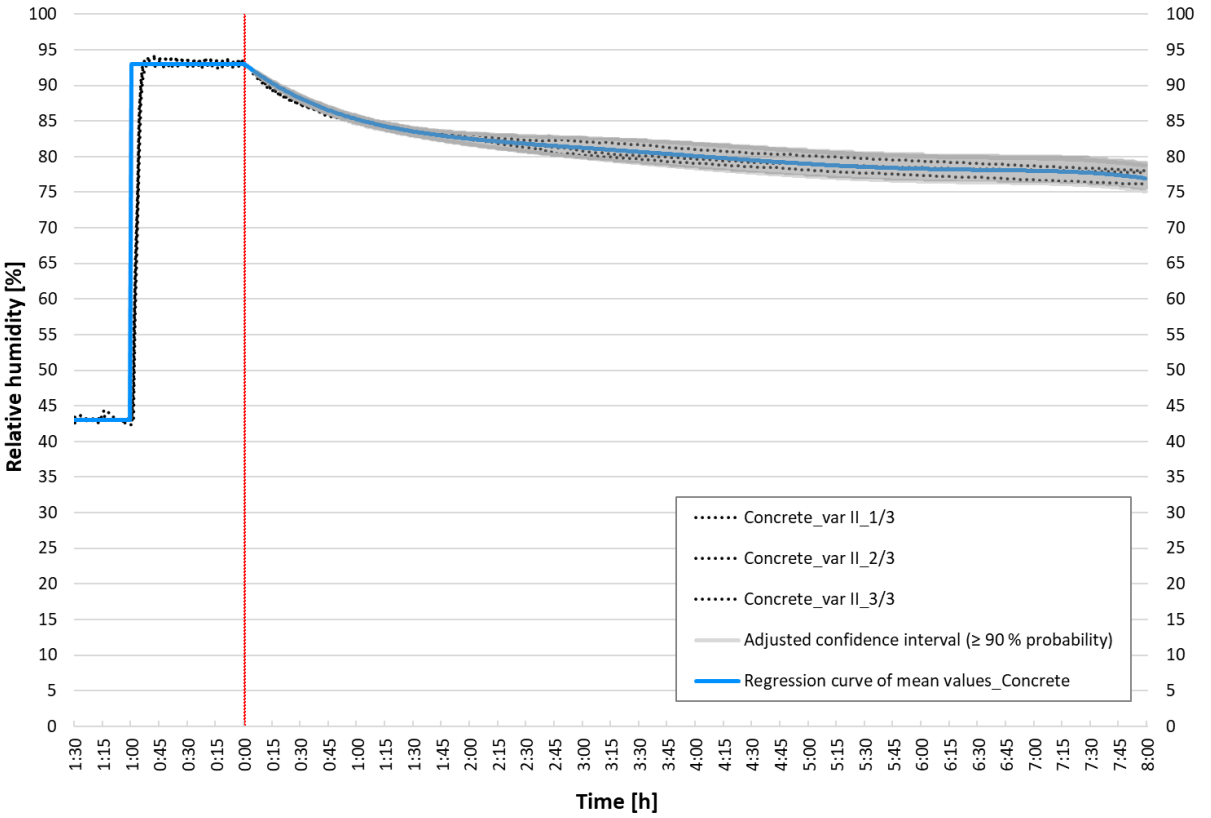

Fig. 96 Adjusted confidence interval of Concrete in var II

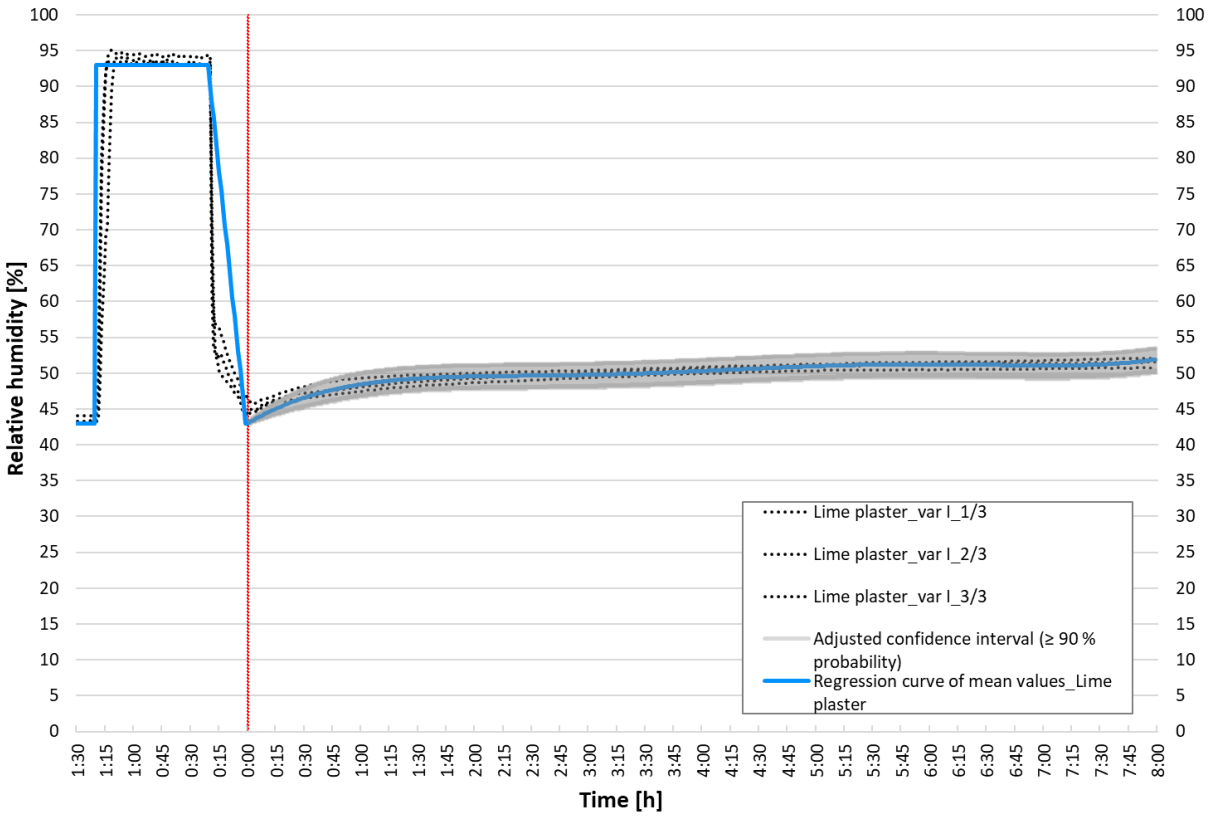

Fig. 97 Adjusted confidence interval of Lime plaster in var I

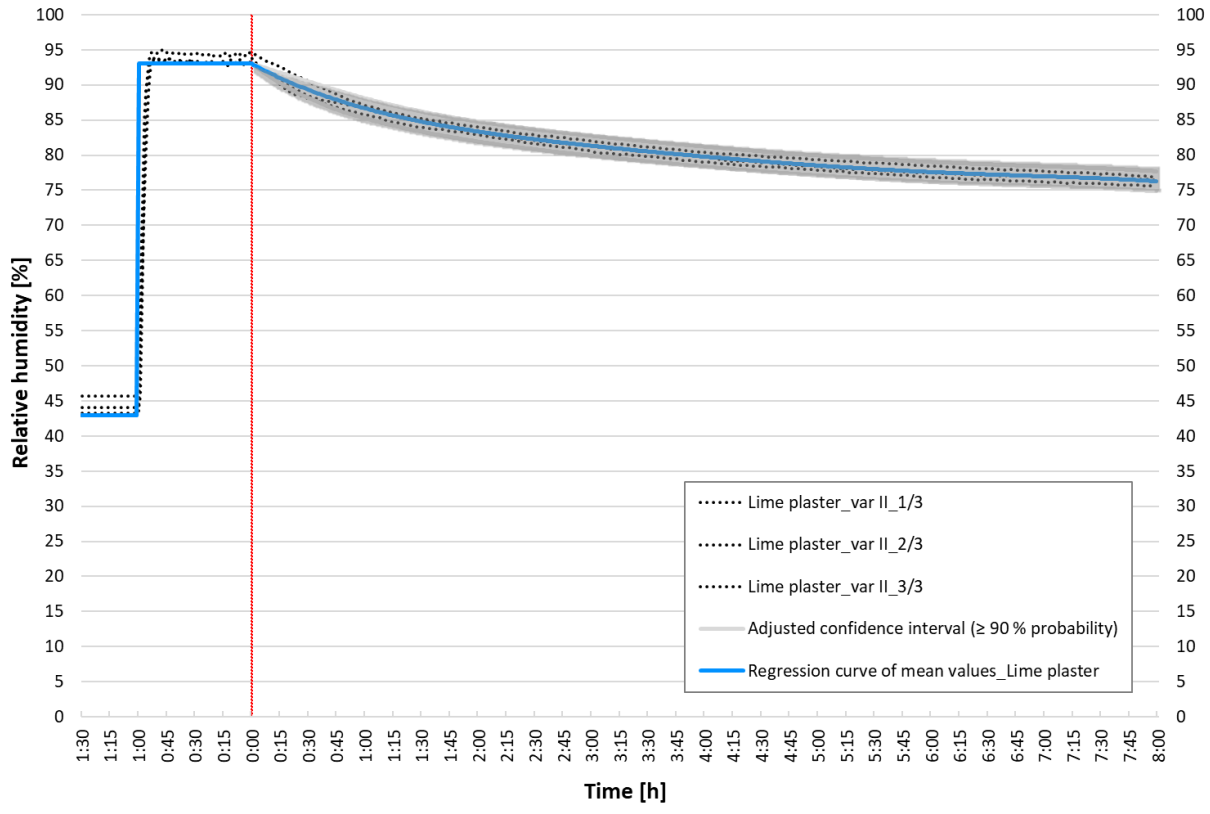

Fig. 98 Adjusted confidence interval of Lime plaster in var II

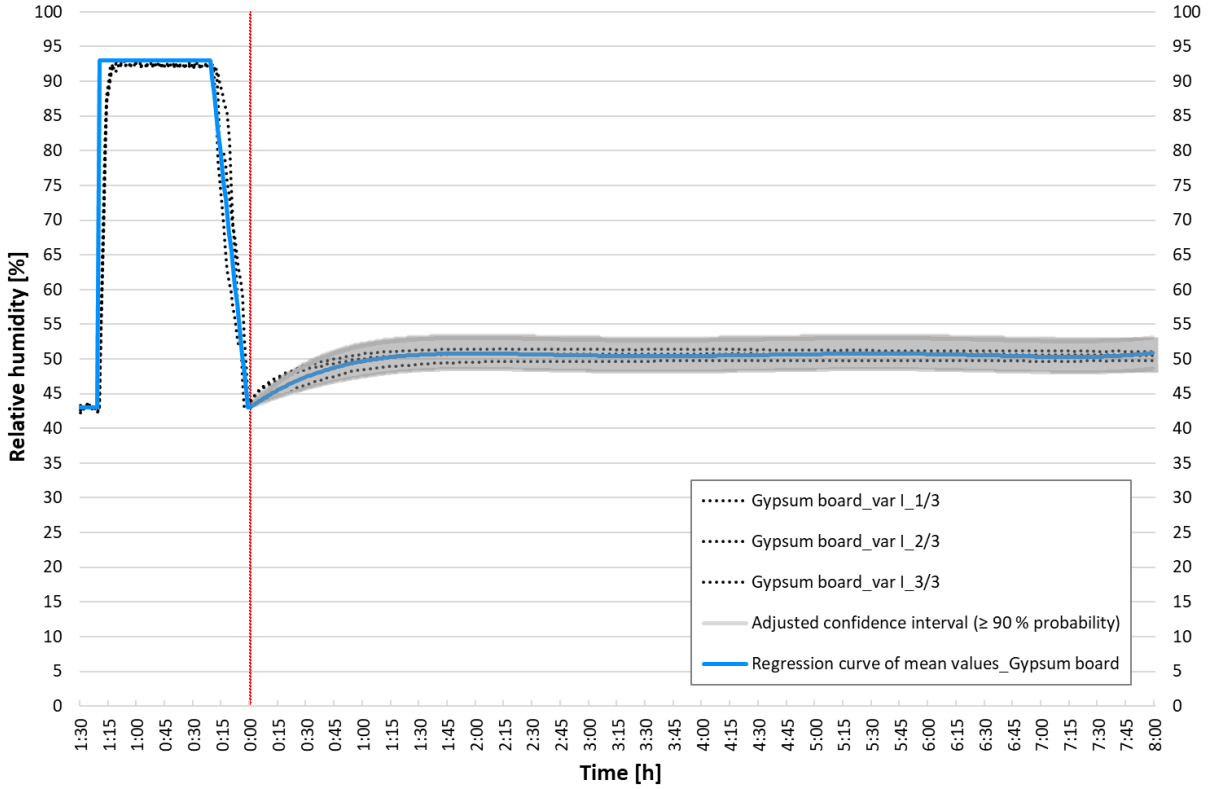

Fig. 99 Adjusted confidence interval of Gypsum board in var I

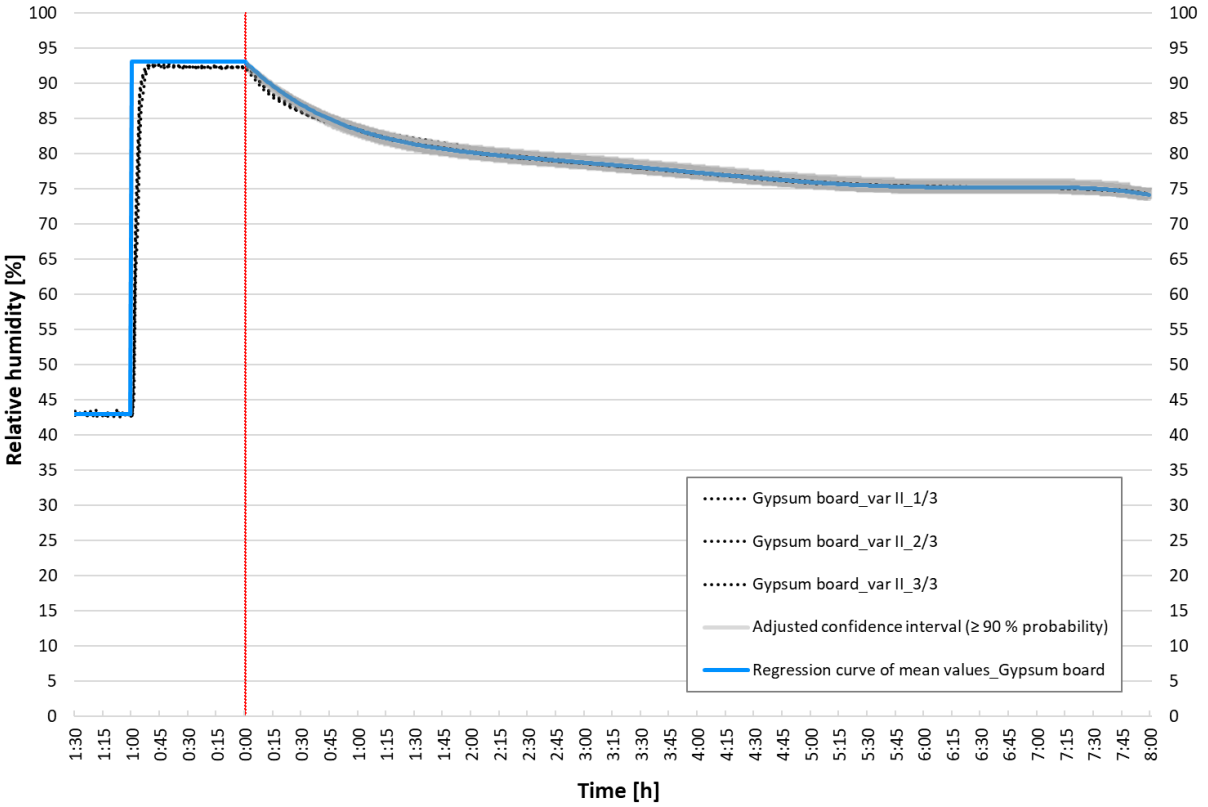

Fig. 100 Adjusted confidence interval of Gypsum board in var II

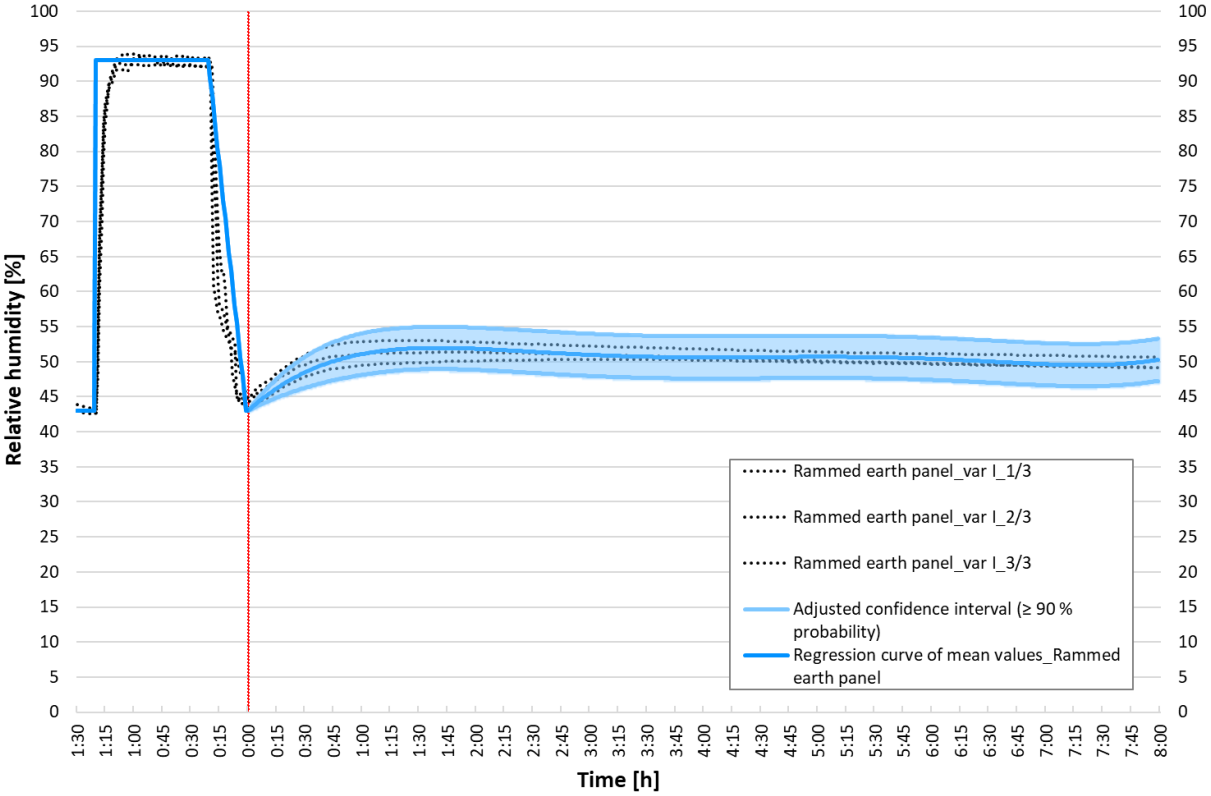

Fig. 101 Adjusted confidence interval of Rammed earth panel in var I

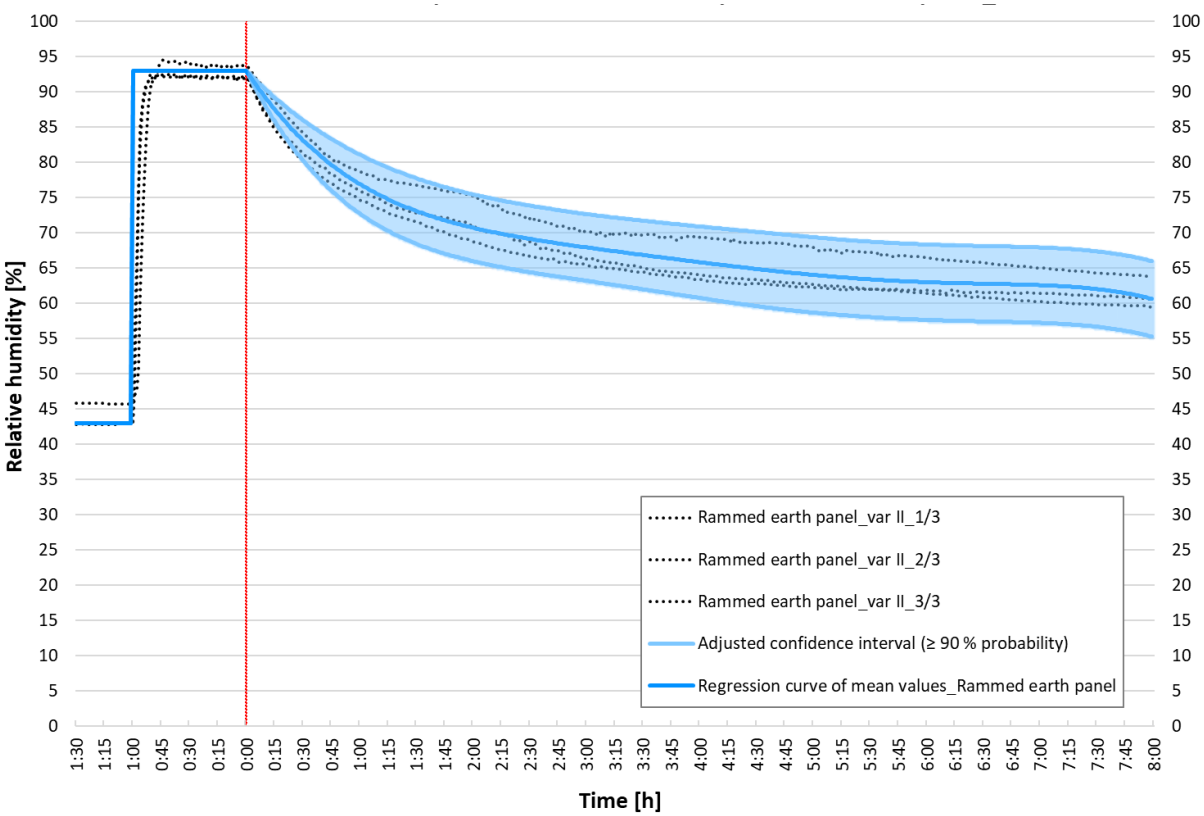

Fig. 102 Adjusted confidence interval of Rammed earth panel in var II

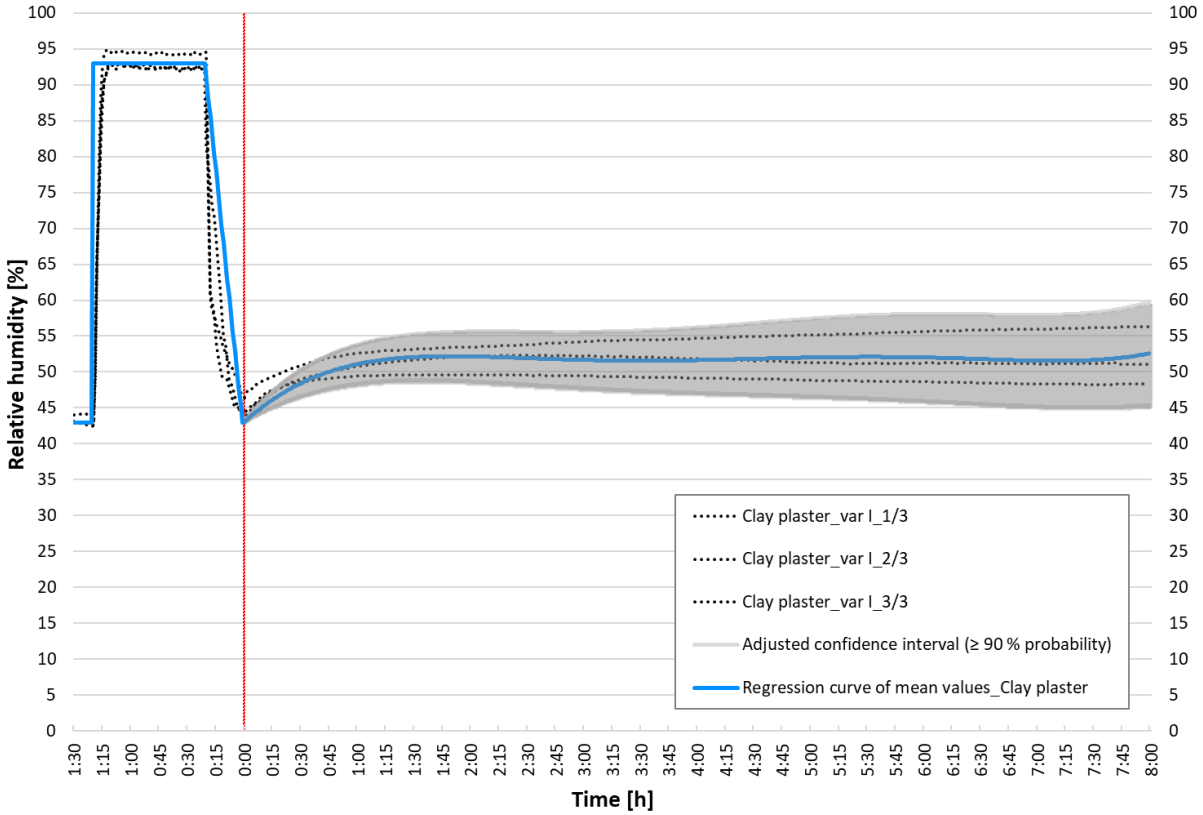

Fig. 103 Adjusted confidence interval of Clay plaster in var I

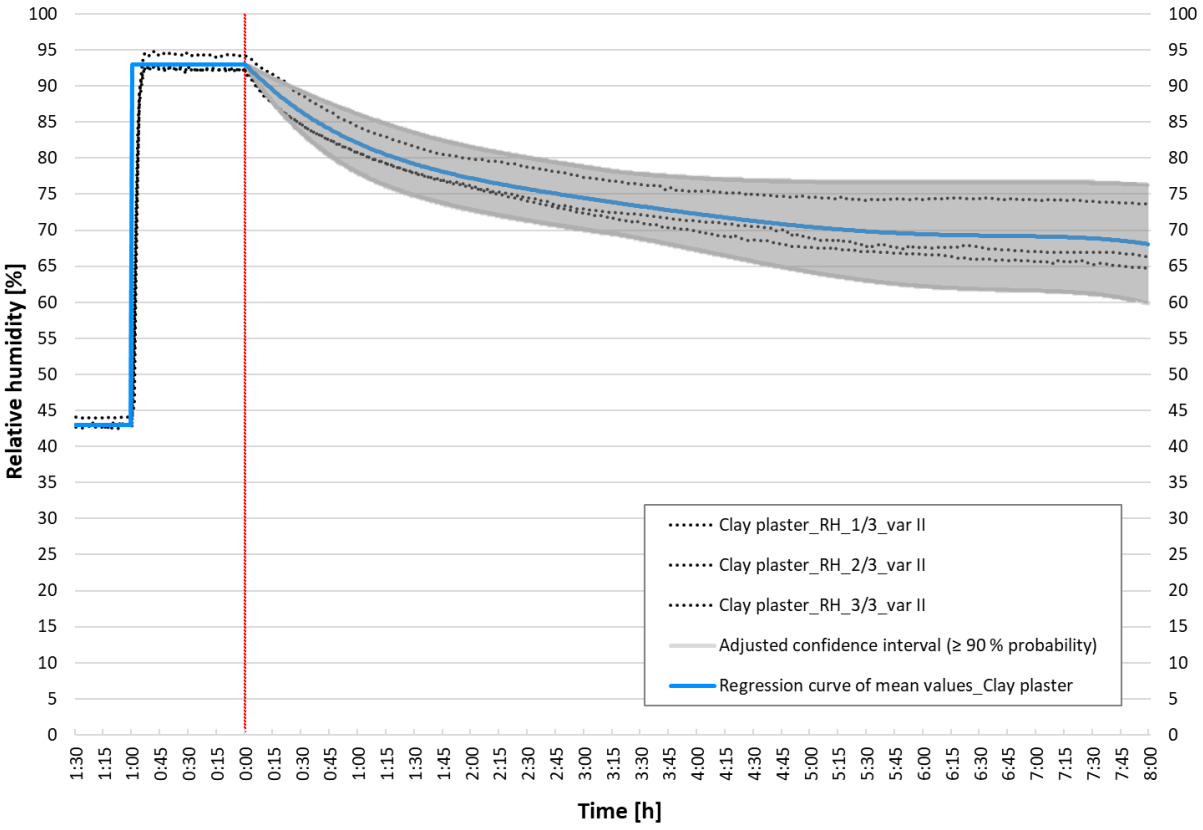

Fig. 104 Adjusted confidence interval of Clay plaster in var II

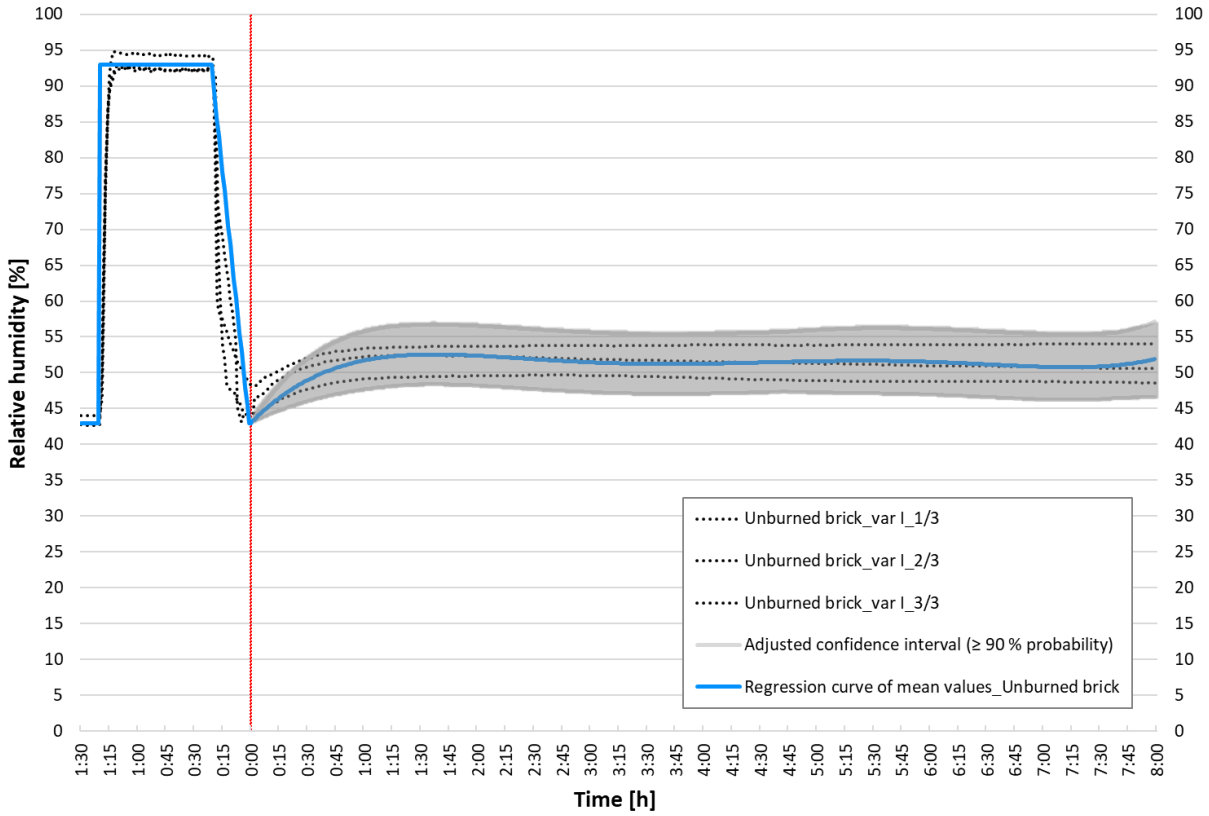

Fig. 105 Adjusted confidence interval of Unburned brick in var I

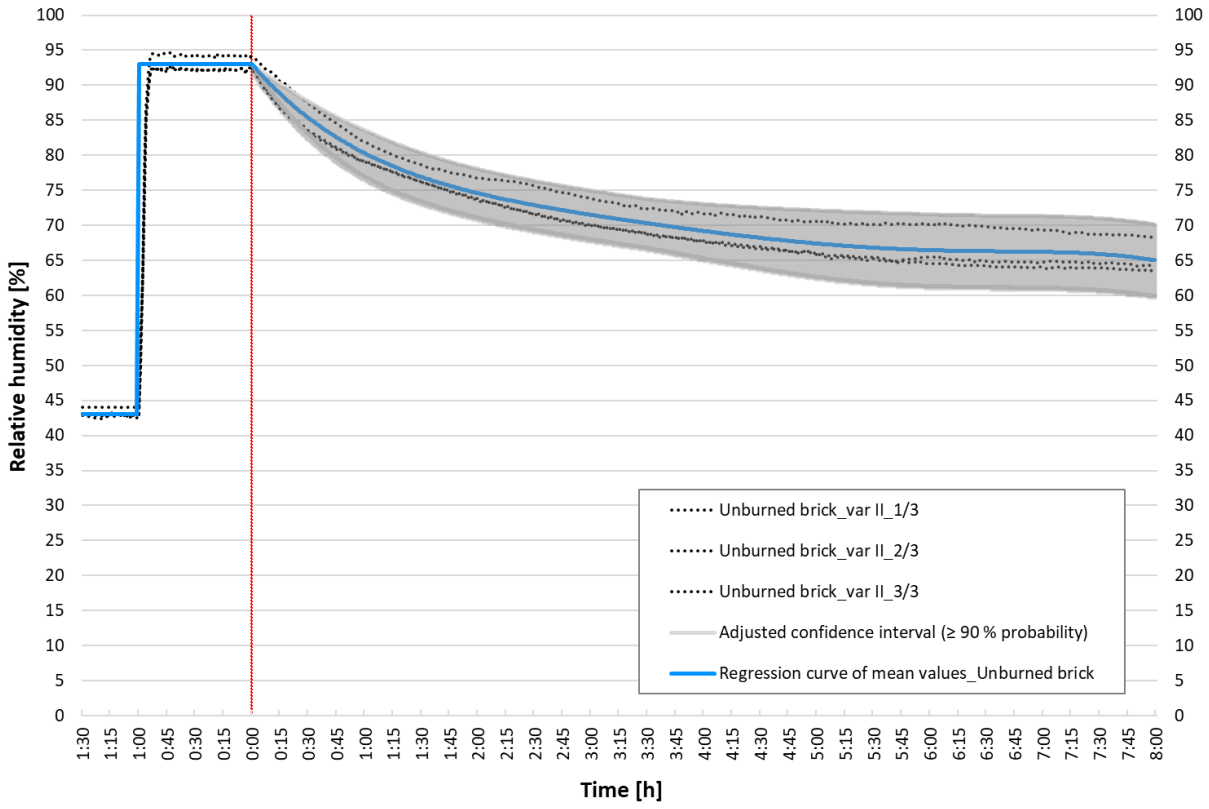

Fig. 106 Adjusted confidence interval of Unburned brick in var II

6.2.2 Comparison of adjusted confidence intervals

In this chapter, there is an essential graphical comparison of the adjusted confidence intervals of the moisture response results of selected building structures. This is the main conclusion of the dynamic experiments performed.

The adjusted confidence intervals of the dynamic desorption (var I) and adsorption (var II) experiments, which were performed on six structural compositions: concrete; lime plaster; gypsum board; rammed earth panel; clay plaster; and unburned brick, are shown and compared.

The statistical deviations of the regression curve of mean values are shown. The trend of the results is obvious with the usual building structures having homogeneous properties and confidence intervals very narrow. In contrast, clay structures have inhomogeneous dynamic sorption properties with wider confidence intervals.

It is not appropriate to analyse the results of the dynamic desorption test (var I) in this way. The methodology of this experiment is not adapted for such data analysis. The individual intervals overlap, and there is no clearly definable conclusion. In contrast, the dynamic adsorption experiment (var II) is very apt and well shows the measured results.

The following tables (Tab. 20, Tab. 21) compare the size of the confidence interval at different observation times. The selected times correspond to the evaluation in chapter 6.2.3, which determined the boundaries of the selected intervals.

Results of var I

The results of concrete structure show that some of the measurements were erroneous. It would be appropriate to repeat this measurement, to exclude the erroneous measurement from the analysed data, and perform the analysis again. The accuracy of the clay plaster results is questionable.

Differences in the size of the interval after 30 minutes are minimal; with increasing observation time the adjusted confidence interval between clay and non-clay structures increases.

Tab. 20 The size of the adjusted confidence interval (in %) var I

Structure	Observation time [minute]		
	30	90	420
Concrete	2.9	6.2	14.6
Lime plaster	2.3	3.1	3.1
Gypsum board	3.4	4.5	4.5
Rammed earth panel	4.4	6.0	6.0
Clay plaster	3.6	6.4	12.7
Unburned brick	5.9	8.3	9.1

As mentioned above, the confidence interval of concrete does not correspond to the expected tendency of the desorption experiment for building structures. This is evident from the comparison of the adjusted confidence interval of concrete and rammed earth (Fig. 107).

When comparing rammed earth panel with other common building materials (lime plaster and gypsum board), it can be stated that the clay material has a wider confidence interval. The main difference is evident in the first 90 minutes, when it is shown that the clay material has the greatest sorption potential (Fig. 108).

When comparing clay structures, the narrowest confidence interval is that of rammed earth, the thickest clay plaster. However, the course of the intervals is almost identical and, apart from the larger scatter of data, no significant differences can be observed from this output (Fig. 109).

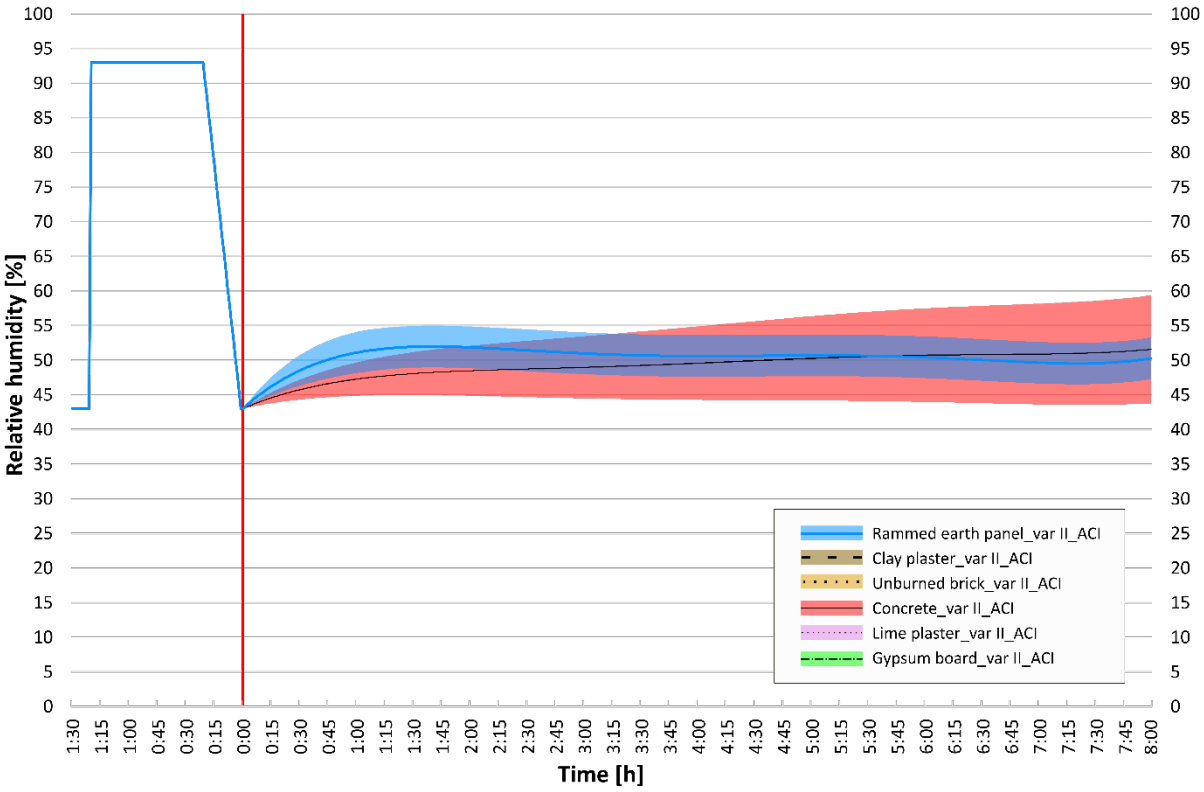

Fig. 107 Comparison of adjusted confidence intervals var I: rammed earth panel, concrete

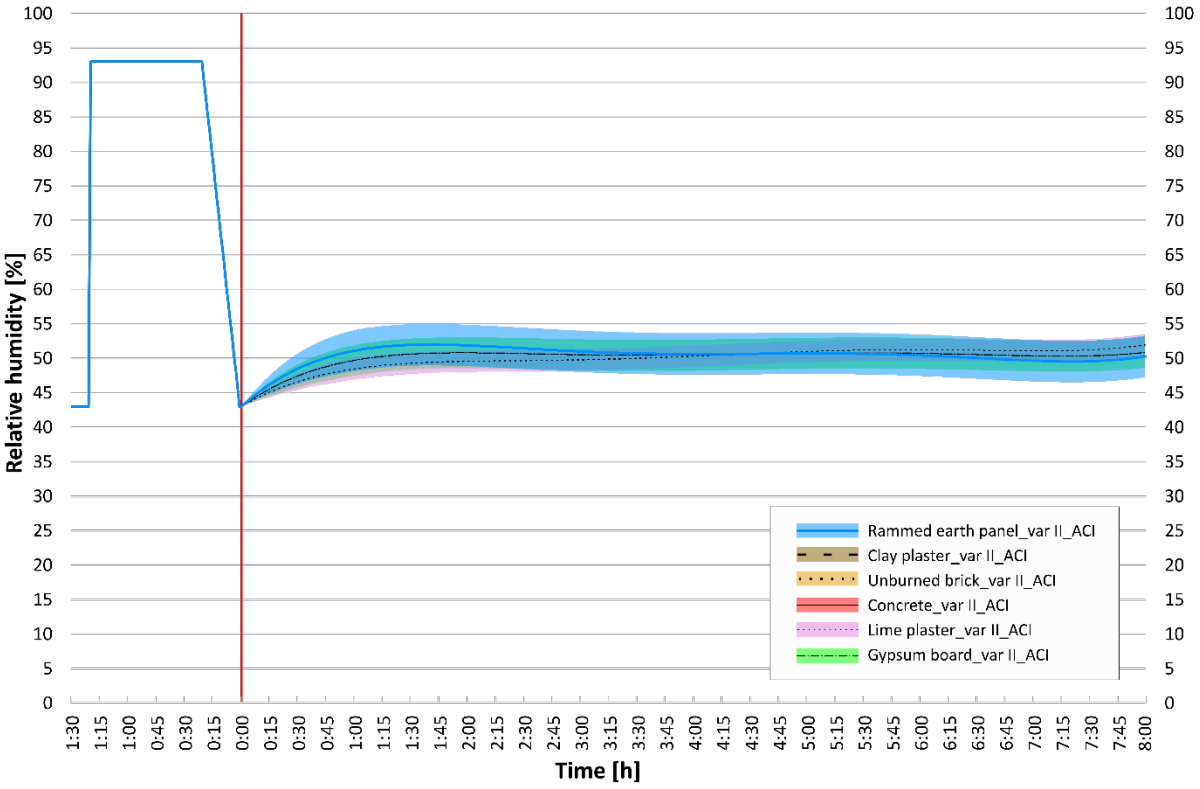

Fig. 108 Comparison of adjusted confidence intervals var I: rammed earth panel, gypsum board, lime plaster

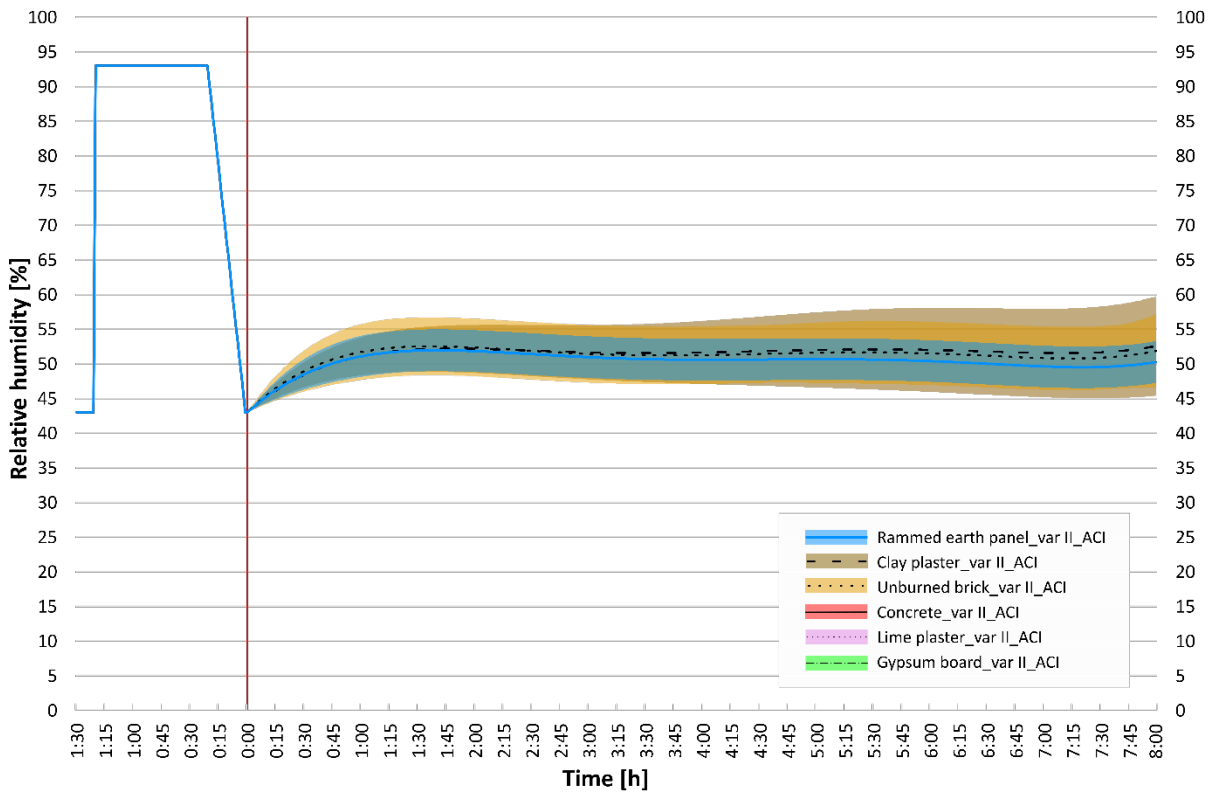

Fig. 109 Comparison of adjusted confidence intervals var I: rammed earth panel, unburned brick, clay plaster

Results of var II

If the measurement of the clay plaster was incorrect is a question in this case as well. At the end of the observation, it has a significantly longer confidence interval than with other clay materials.

The confidence interval of clay structures is similar over time. And it is also substantially larger than the range of non-clay materials.

Tab. 21 The size of the adjusted confidence interval (in %) var II

Structure	Observation time [minute]			
	60	120	300	420
Concrete	0.9	1.5	3.5	3.5
Lime plaster	2.9	2.9	2.9	2.9
Gypsum board	1.3	1.3	1.3	1.3
Rammed earth panel	8.4	9.4	10.7	10.7
Clay plaster	8.1	8.6	12.5	15.0
Unburned brick	6.6	6.9	9.5	10.2

When comparing concrete and lime plaster structure, it can be stated that for first 120 minutes concrete has a higher sorption potential, and the confidence interval is below the confidence interval of lime plaster. From the 120th minute, the results are almost identical and the intervals overlap. If the last of the measured typical building materials, gypsum board, is added for comparison, its dynamic sorption properties are even better. Its very narrow confidence interval is just below the lower limit of the confidence interval of previous materials (Fig. 110).

When measuring clay plaster, if we assume no erroneous measurements, and the confidence interval is so wide, the following can be stated: In the worst possible composition of clay plasters, it may happen that the sorption properties of common building materials are comparable to those of clay plasters. In

the narrow upper limit of the clay plaster interval, the assumed values of intervals overlap (Fig. 111). However, this condition never occurs in the case of unburned bricks or rammed earth structure.

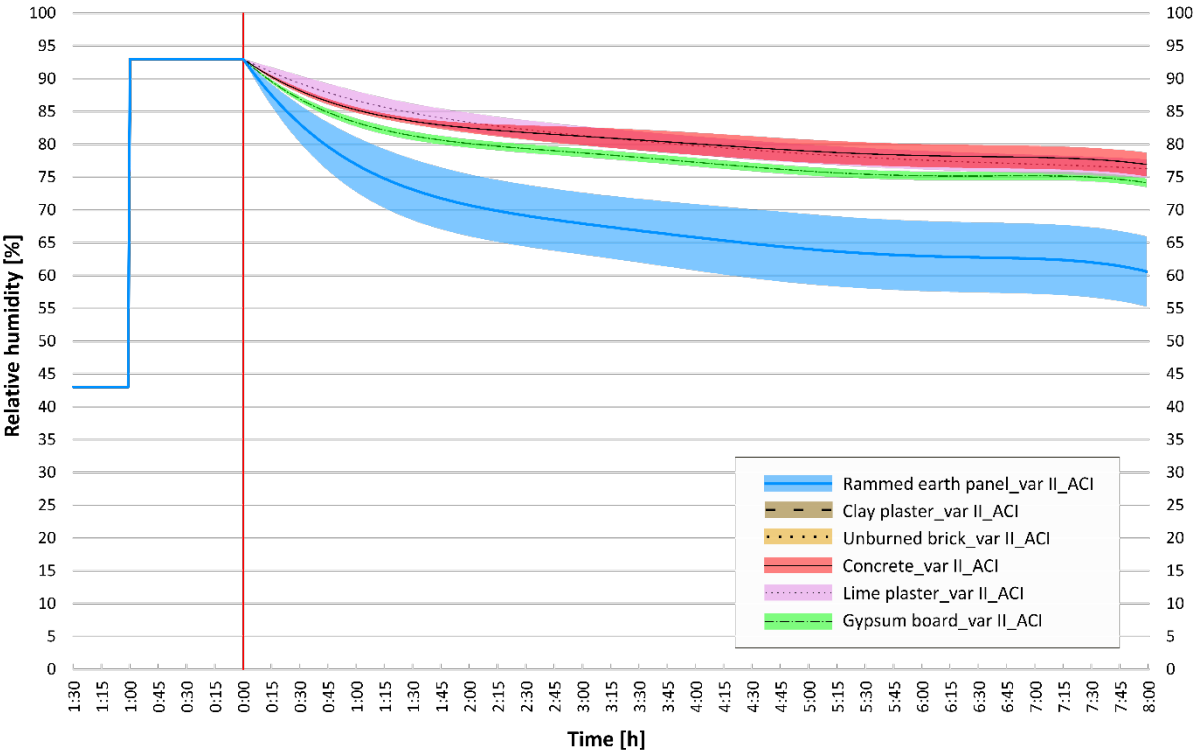

Fig. 110 Comparison of adjusted confidence intervals var II: rammed earth panel, gypsum board, concrete, lime plaster

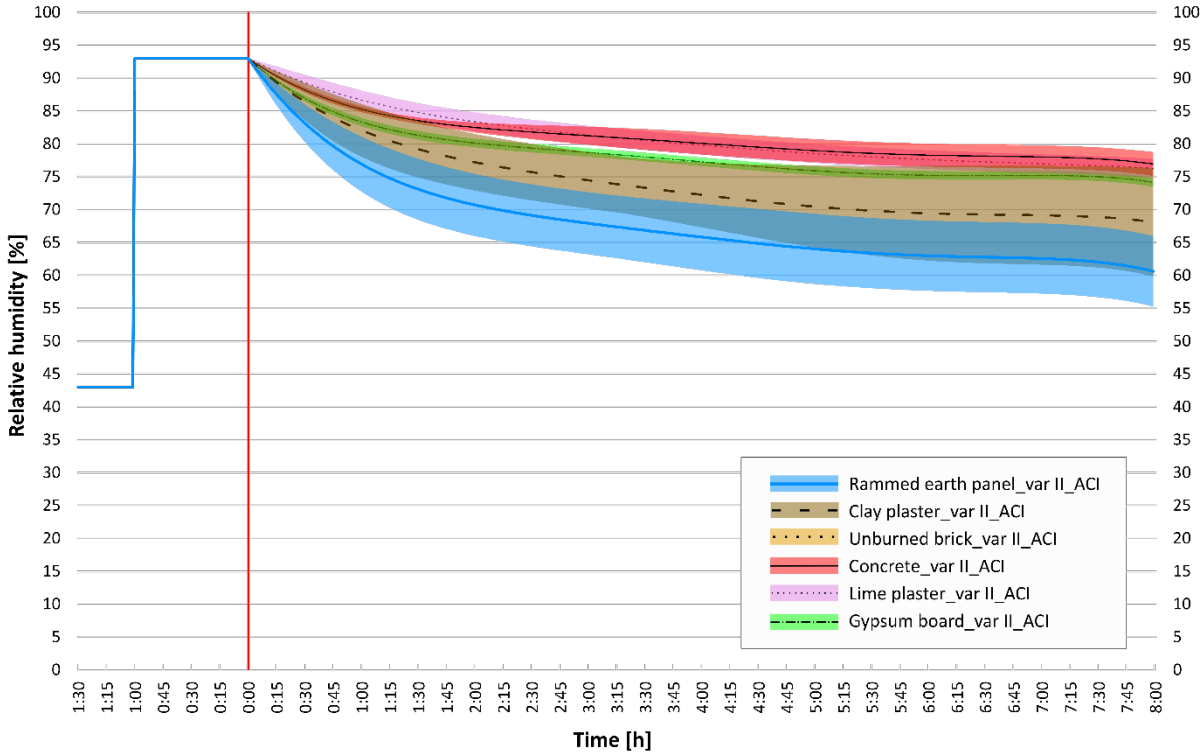

Fig. 111 Comparison of adjusted confidence intervals var II: rammed earth panel, clay plaster, gypsum board, concrete, lime plaster

As expected, when comparing clay materials, rammed earth panel has the best sorption properties. It can be observed that the confidence intervals overlap – the upper half of rammed earth panel to the lower half of clay plaster. The results show that the sorption potential of the unburned bricks is roughly between that of clay plaster and the rammed earth (Fig. 112).

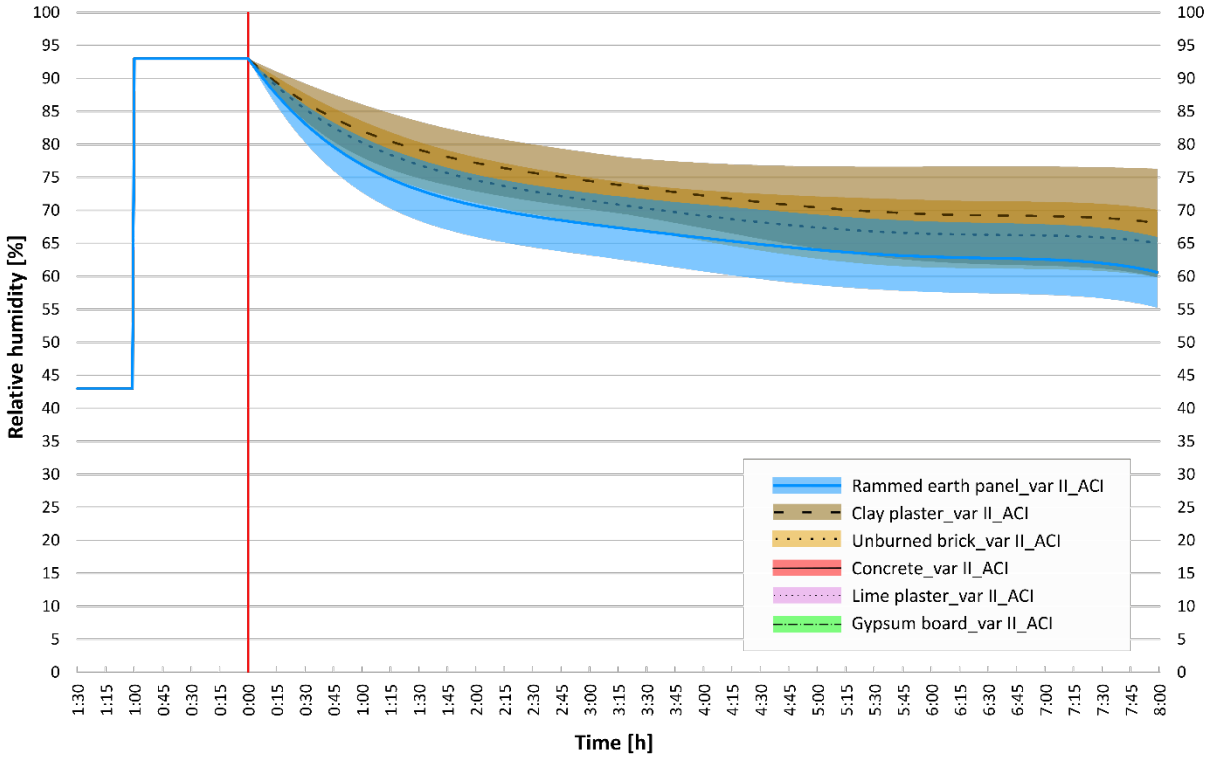

Fig. 112 Comparison of adjusted confidence intervals_var II: rammed earth panel, unburned brick, clay plaster

6.2.3 Analysis of dynamic behaviour

The last evaluation of the experiment was on the resulting slope of the tangent of the regression curve of mean values. This analysis reveals the dynamic potential of sorption properties.

The slope of the tangent (the first derivative of the regression curve function) was determined at each minute interval. The evaluation was performed for all selected building structures in both variants of the experiment. The result is the arithmetic mean of each structure.

It should be emphasized that the regression curves do not have as significant a dynamic onset as the measured experimental values. However, it should be noted that the determination of the regression curves was performed according to the same methodology, so that some distortion (reduction of the slope of the tangent in the first minutes of observation) may result from the same error for all structures.

Results of var I

The dynamic course of the behaviour of structures (Fig. 113) can be divided according to the observation time into the following intervals:

- 0–30 minutes: Thirty minutes after the start of the observation, the dynamic potential has a half value.
- 30–90 minutes: Desorption is suspended in the next 60 minutes; interestingly, the dynamic desorption potential is the same for all structures after 75 minutes from the start of the observation.

- 90–420 minutes: The dynamic behaviour of all structures is the same, the value of the slope of the tangent is less than 0.017 (conversion to degree < 1 °), i.e. it is an almost constant state.
- 420–480 minutes: The values of the slope of the tangent in this interval cannot be used for analysis because the regression curves in this interval allow for the potential trend of other data (i.e. observations longer than 8 hours). The regression curves rise significantly in this interval, even when they do not follow the laws of physics. It would be better to find a more accurate regression curve, but it is extremely time consuming and, for the purposes of this work, this curve is sufficient. Dynamic behaviour is especially important at the beginning of observation.

Looking at these data, it is clear that the clay structures (rammed earth, unburned brick, and clay plaster) have the highest desorption potential from the beginning of the observation, followed by gypsum board and lime plaster. Concrete structure has half the dynamic potential as clay materials.

Results of var II

The analysis of the dynamic adsorption behaviour (Fig. 114) can be divided into five time intervals from the beginning of the observation:

- 0–60 minutes: Sixty minutes after the start of the observation, the dynamic potential has a half value.
- 60–120 minutes: In another 60 minutes, the dynamic potential drops by another 1/3; this is the last significant dynamic part.
- 120–300 minutes: The properties of dynamic adsorption of selected materials are grouped as follows: clay structures; concrete and gypsum board; and lime plaster
- 300–420 minutes: Identical dynamic properties of all materials. The value of the slope of the tangent is less than 0.017 (conversion to degree < 1 °), i.e. it is almost constant.
- 420–480 minutes: The values of the slope of the tangent in this interval cannot be used for analysis for the same reason as the same interval in var I. In this case, the regression curves decrease.

The results of this analysis show that the highest dynamic adsorption potential is obtained with rammed earth. Other clay materials (unburned brick and clay plaster) and gypsum board follow. Concrete structure has half the dynamic potential of rammed earth. According to the results, lime plaster has the lowest dynamic adsorption.

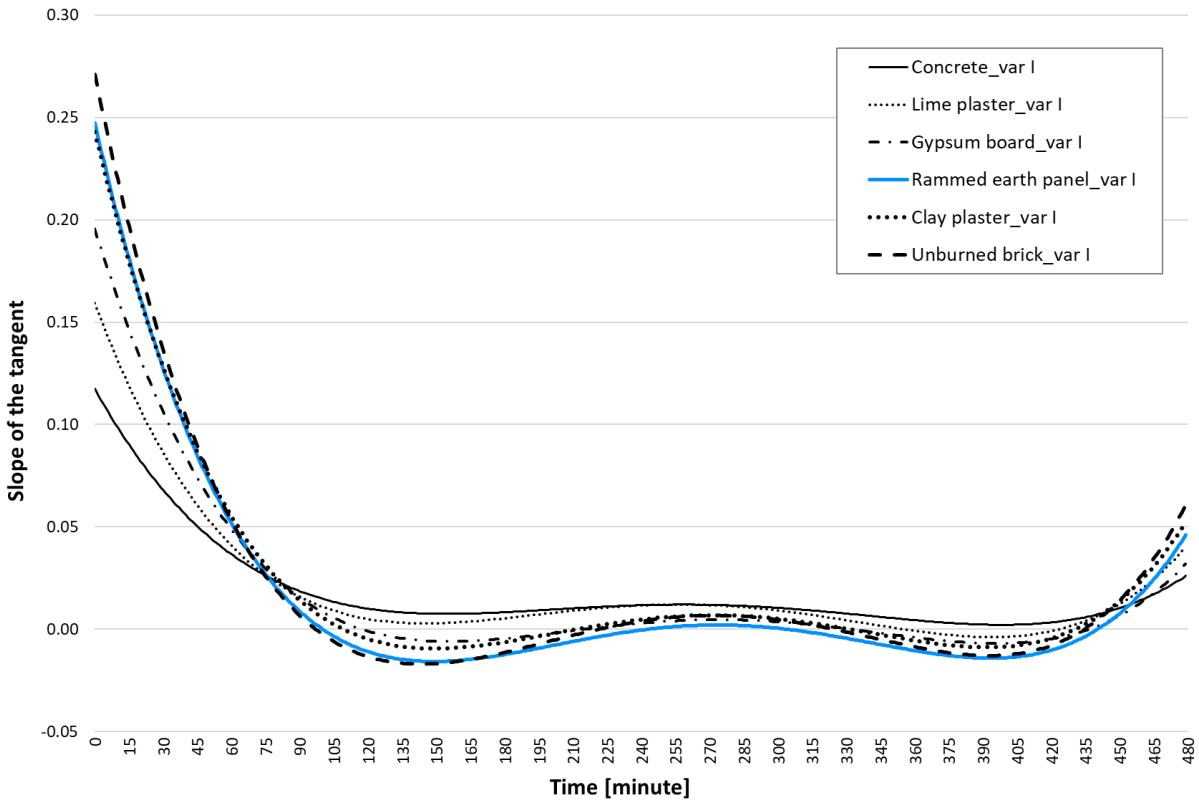

Fig. 113 Slope of the dynamic desorption tangent (var I)

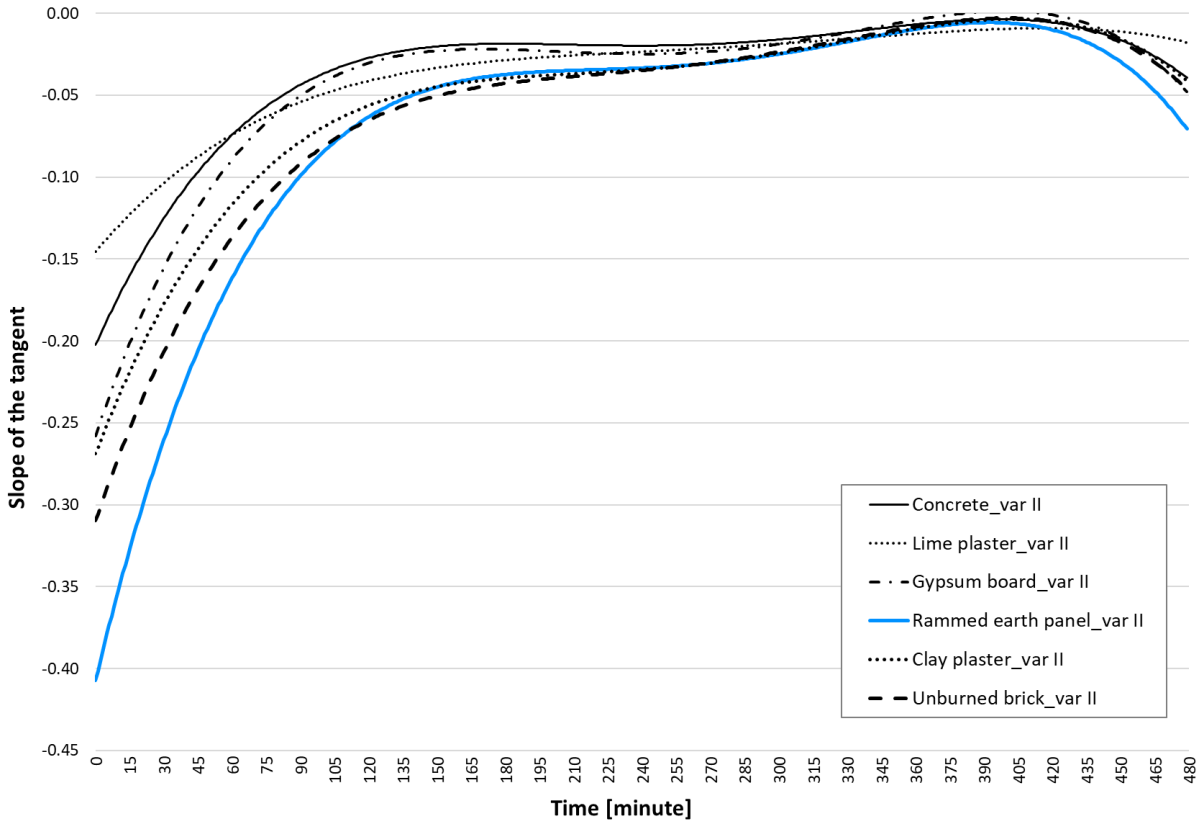

Fig. 114 Slope of the dynamic adsorption tangent (var II)

7 Discussion and conclusions

This chapter provides a comprehensive evaluation of the issues solved.

A large set of measured sorption isotherms can be used to evaluate individual building materials, but can also serve as a basis for advanced mathematical models of moisture. The methodology for dynamic sorption tests developed within the thesis was found sufficient to assess different structures and provides valuable results.

High potential of natural porous materials such as natural clays in the form of clay plasters, clay boards, unburned bricks, or rammed earth panels for moisture buffering was proved by the performed tests.

Principals of passive moisture buffering can be used in modern sustainable construction to help maintain the quality of the internal microclimate by allowing an appropriate level of relative humidity with zero operating energy and reduced operating costs.

The results are valuable for further research in this field and prove the use of "environmentally active" materials.

7.1 Measurement conclusions

Steady state and dynamic experiments were performed. The usefulness and suitability of the tests performed were taken into consideration.

Outcomes of sorption properties of materials

The measurements were performed according to accepted standards in glass desiccators at constant temperature. A total of 31 different materials were measured and were classified into the following categories: rammed earth panels; clay products; and standard building materials.

After evaluating the data on the measurement of clay materials, the results are clear – they match predictions described in the literature. This means that these predictions can be confirmed and that measurements performed have been done correctly.

The breakdown of sorption properties of clay materials is as follows:

- Type and amount of clay minerals – montmorillonites have the best sorption properties, followed by illites and zeolites, with kaolinites having the worst. This disparity is due to the construction of the wafers from the individual minerals.
- Influence of sand sharpening – the effect of the sand additive (shrinkage-reducing sharpening) is evident. The more sand contained in the clay mixture, the worse its sorption properties are. The reason is the low ability of sand grains to bind air humidity due to their minimal porosity and specific surface.
- Influence of chemical stabilization – chemical stabilization of the clay mixture (by adding lime or cement) will improve its mechanical properties but, at the same time, significantly worsen its sorption properties. This is caused by chemical bonds inside the material. It is recommended to limit this method of stabilization, as it lowers the materials sorption potential and increases its carbon footprint.

- Influence of the drying method – it has been reported in the literature and confirmed in these experiments that chemical changes can occur in clay materials at temperatures above 60 °C, which, among other things, negatively affect the sorption properties.

The comparison of clay materials with commonly used materials was completely surprising and showed that the sorption properties of some clay materials can be overrated. The low sorption potential of tested clay plaster and clay board due to the high amount of shrink reducing sand is striking. This sorption potential is at a similar level to concrete mixtures. Poor ability to absorb moisture by ceramic blocks is also evident.

The results also confirmed the original assumption that a higher sand content reduces the sorption capacity of unburned clay products. In case of the Claygar clay mixture used, consisting mainly of hydroslides and kaolinite with a small admixture of montmorillonite, the addition of 10 % sand lessened the sorption properties of the clay mixture by 12 %. The addition of 30 % sand deteriorates clay sorption by up to 25 %, illite by up to 30 %, and conversely for kaolinite by only 11 %.

Compared to the selected reference material from rammed earth C_S10/W10, adobe brick and unfired brick (commercial product) have a 40–45 % lower sorption potential. Experiments show that clay plasters and clay panels have about 20–35 % worse adsorption potential versus concrete. On the other hand, adobe or unburned brick have a 2.5–2.8 times higher sorption capacity. In this respect, rammed earth has a greater potential for moisture buffering in the interior than, for example, clay plasters, in which about 60 % to 75 % of sand is present (to reduce shrinkage cracks and improve workability).

The addition of 5 % lime to the clay mixture lowers the sorption potential by up to 43 % compared to the original composition without chemical stabilization. When stabilizing 5 % of cement, the reduction in sorption capacity is about 40 %. The results show that after the addition of 10 % sand and 5 % of cement or lime (mixture C_S10/W10_cem and C_S10/W10_lim) to the clay mixture, the sorption potential is still more than twice as good as concrete and up to 8 times better than gypsum board.

Experimentally verified results of sorption properties of unfired clay provide a very good precondition for its use as an effective tool for stabilizing the humidity microclimate. The measured adsorption and desorption curves can be described by mathematical functions that can be further used, for example, in a zone moisture model, or to determine the moisture buffer value.

Outcomes of specific surface area

BET analysis is an advanced test of the sorption properties of a material. A lot of useful information can be read from it to understand the moisture dependence in building constructions. This is a fast and accurate measurement, and a very small sample is enough for experimental evaluation. The type of pore system significantly affects the sorption properties of the material. The larger the specific surface accessible to the water vapour molecules, the more the material can regulate air humidity.

It can be concluded from the experimental results that lime plaster and gypsum board are non-porous materials with a sorption curve Type 2 according to IUPAC. Clay plaster and concrete have similarly shaped sorption isotherms. Their shape corresponds to Type 2 or Type 4. Hysteresis is negligible. These materials can be declared as macroporous or non-porous materials or that there is a minimum number of mesopores. The sorption curve of unburned brick is classified as Type 4 with clear hysteresis. It is a partially mesoporous material. Material from the rammed earth panel has a clear character: very porous with high hysteresis. According to IUPAC, it is a Type 4 isotherm, typical of mesoporous adsorbents. The pores of the material are open on both sides. The shape of the hysteresis loop corresponds to Type H3, which corresponds with slit pores.

Compared to the rammed earth panel C_S10/W10, the specific surface area of unburned brick is smaller by 62 %, of gypsum board by 80 %, of concrete by 82 %, of clay plaster by 90 %, and of lime plaster by 94 %.

Outcomes of sorption properties of building structure

To gather reliable and valid results of the behaviour of the complete structures, the appropriate testing method was developed. The main idea of the dynamic sorption test was to simulate real situations and behaviours of building structures in physical conditions.

The proposed test method was based on the following situations: the internal environment and the tested structure were in an equilibrium state, followed by an intensive increase of relative humidity for a period of one hour (someone was taking a shower or bath, cooking, drying clothes, etc.). After that, two scenarios were possible:

- var I: The humid air was ventilated and the indoor environment returned to its original relative humidity at equilibrium. Subsequently, it was observed how much moisture was absorbed in the structure by how the internal humidity in the chamber increased, dictated by the desorption potential of the building structure;
- var II: The humid air was not ventilated and it was observed how the relative humidity in the climatic chamber decreased, which determined the potential of the tested building structure to moderate the moisture peaks and to absorb the moisture from the environment (adsorption potential of the building structure).

It is highly dependent on the ratio of the exposed area A of the material and the volume of the experimental space V. This A/V ratio was 0.473 $m^2 \cdot m^{-3}$.

The results of the var I experiment (dynamic desorption test) are not so conspicuous. The most pronounced dynamic event occurs in the first hour of the observation. Clay materials quickly desorb the adsorbed moisture back into the interior. The course of RH is very similar for all clay structures. The RH value peaks in about 90-120 minutes. Non-clay structures have worse dynamic predictions, especially concrete and lime plaster which rise only slightly, compared to clay materials, to about 50 % relative humidity. The gypsum board clearly shows characteristics between clay and non-clay materials.

Differences in the behaviour of the test samples regarding humidity absorption and decreasing the peak (dynamic adsorption test, var II) are apparent. As expected, rammed earth panel has the highest potential, followed by uncovered unburned blocks, unburned blocks with clay plaster, and gypsum board. The ceramic blocks with lime plaster and concrete structure have the lowest dynamic sorption potential. After eight hours of observation at a given A/V ratio, the rammed earth panel reduces the relative humidity in the interior by 34 %, unburned brick by about 30 %, and clay plaster by 27 %. The decrease in relative humidity of non-clay structures after eight hours is 17–20 %.

The amount of water consumed during wetting in the dynamic experiments corresponds to the ability of the structure to absorb moisture. The experiment with rammed earth consumed the most water, followed by unburned brick, and then clay plaster and common building materials. To maintain the same relative humidity in the chamber, the rammed earth panel consumed 2.7 times more water than clay plaster and other common structures.

Another point of evaluation may be the time during which the RH increases from 45 % to 50 % (var I): with clay structures taking approx. 35 minutes; gypsum board 70 minutes; lime plaster 180 minutes; and concrete 270 minutes.

It is also possible to show the time needed to reduce the relative humidity from 95 % to 80 % (var II): rammed earth panel take 40 minutes; unburned brick 60 minutes; clay plaster 80 minutes; gypsum board 130 minutes; concrete and lime plaster approx. 240 minutes.

The dynamic desorption experiment (var I) has not been appropriately designed. Mechanical ventilation has a great effect on the internal environment and overwhelms the sorption potential of porous building materials. The main significance of this experiment occurred in the first 60 minutes after ventilation/initiation of observation.

However, the lower informative value of this experiment does not mean that porous structures do not have significance in buildings with controlled mechanical ventilation. These materials can reduce fluctuation peaks of relative humidity in the indoor environment. This can reduce the operating energy consumption. Sorption potential is also relevant in the event of a power failure.

7.2 Analysis of sorption properties

Before using any regression model, it is always recommended to plot a simple scatter diagram to know the type of relationship that exists between specific variables. A simple linear model may not always be the best choice and it makes sense to consider polynomial regression with a degree of the polynomial $m > 1$.

The statistical evaluation of the dynamic sorption properties measured on six building structures (concrete; lime plaster; gypsum board; rammed earth panel; clay plaster; unburned brick) was performed in the following steps:

- smoothing individual observations by use of regression analysis;
- evaluating the accuracy of the regression model used by testing hypotheses and choosing suitable regression curves;
- determining the confidence interval.

Comparisons of data were performed by the statistical analysis described above. The data are the result of only three repeated measurements with a reliability factor $\alpha = 0{,}1$ determined.

The boundary conditions significantly affect the resulting confidence interval. For a more accurate evaluation more measurements would be needed, but the chosen number was sufficient for the presentation of the results. The number of repetitions of measurements was determined with respect to the time and cost of the experiments and their impact on statistical analysis.

In addition, the results may be skewed due to error, but these errors are expected and the data have been evaluated accordingly.

The final regression curves do not have as significant a dynamic onset as the measured experimental values at the initial point of observation and the several minutes that follow. The determination of the regression curves was performed according to the same methodology, so that some distortion (reduction of the slope of the tangent in the first minutes of observation) is subject to the same error for all structures.

Comparison of adjusted confidence interval

The main conclusion of the dynamic experiments performed is in the graphical comparison of adjusted confidence intervals of moisture response results of selected building structures. The adjusted confidence intervals of the dynamic desorption (var I) and adsorption (var II) experiments, which were performed on the six structural compositions, were shown and compared.

The trend of the results is obvious – the conventional building structures have homogeneous properties, and their confidence intervals are very narrow, while clay structures have inhomogeneous dynamic sorption properties, and their confidence interval is therefore wider.

It is not appropriate to analyse the results of the dynamic desorption test (var I) in this way. The methodology of this experiment is not adapted for such data analysis. The individual intervals overlap

and there is no clearly definable conclusion. In contrast, the dynamic adsorption experiment (var II) is appropriate and well shows the measured results.

This experiment showed that the rammed earth structure again has the best sorption properties. Its potential in water vapour adsorption is unrivalled. The unburned brick structure has a slightly less dynamic sorption potential, and the confidence interval is similarly large. However, the rammed earth panel production is noticeably more complicated than that of the structure of the unburned brick wall. This raises the question about the efficiency of unburned bricks and if its lower sorption potential is offset by its less laborious production, and thus in lower final prices.

In terms of dynamic sorption properties, the selected common building materials (concrete, lime plaster, gypsum board) cannot compete with rammed earth and unburned brick structures. The only question is how the clay plaster will fare in this comparison. The resulting confidence interval of this material has a large deviation, probably due to one erroneous measurement. The evaluation of the structure of clay plaster therefore is inconclusive.

Analysis of dynamic behaviour

This evaluation of the dynamic experiment was performed on the basis of the slope of the tangent of the regression curve of mean values. The slope of the tangent (the first derivative of the regression curve function) was determined at each minute point. The evaluation was performed for all selected building structures in both variants of the experiment (var I and var II). The result is the arithmetic mean of each structure. This analysis better illustrates the dynamic potential of adsorption and desorption properties.

The dynamic course of desorption properties of building structures (var I) can be divided according to the observation time into four intervals: 0th–30th–90th–420th–480th minute. In the first interval, the dynamic desorption potential is the greatest, and after thirty minutes it is halved. At the 75th minute, the dynamic desorption potential of all selected structures is the same. From the 90th minute, the dynamic behaviour of all structures is the same, the value of the slope of the tangent is less than 0.017 (conversion to degree < 1 °), i.e. it is an almost constant state.

The dynamic course of adsorption properties (var II) was divided into five time intervals: 0th–60th–120th–300th–420th–480th minute. The first interval is again the most dynamic. The dynamic potential is halved after 60 minutes. In the second interval, the dynamic potential drops by another 1/3 and is the last significant dynamic interval. In the third interval, the properties of dynamic adsorption of selected materials are grouped into: clay structures; concrete and gypsum board; and lime plaster. From the 300th minute, the dynamic behaviour of all structures is the same; the value of the slope of the tangent is less than 0.017 (conversion to degree < 1 °), an almost constant state.

The evaluation of the slope of the tangent was very useful. This confirmed the expected and measured conclusions about the sorption properties of porous materials without steady state. It was verified that the highest dynamic potential is for rammed earth panel, followed by clay structures (unburned brick and clay plaster), which are followed, as expected, by commonly used building structures such as gypsum board, concrete, and lime plaster.

7.3 General conclusions

The process of adsorption and desorption of air moisture into the structure of the porous material is complex. The analysis is more complicated for clay materials because the properties and behaviour of clay minerals also come into play. Therefore, clay structures cannot be easily quantified and their properties accurately declared. The resulting clay-based materials are often unique with their properties dependent on the source of the raw material and its exact mineralogical composition. It is therefore

difficult to compare the results of experiments across scientific teams if the materials studied have no information on their exact composition.

The results of the experiment show the potential of using unfired clay as an environmentally active material for regulation or stabilization of the microclimate's internal humidity.

A relatively interesting conclusion comes from a comparison of selected building materials (three clay and three non-clay building structures) by the type of experiment performed and subsequent analysis of the results. In all analyses, the structure of rammed earth had the best properties for water vapour sorption. This was followed by unburned brick which was 2nd place in all evaluations except the dynamic experiment of desorption properties, when it shared first place with rammed earth and clay plaster. Order of materials now becomes variable. According to the dynamic experiments, clay plaster is in third place, while according to the results of sorption isotherms, concrete is 3rd, and according to BET analysis, it is gypsum board that is 3rd. Lime plaster was almost always last on the imaginary ladder. Fourth place in the dynamic experiments was occupied by gypsum board, while in BET analysis, fourth goes to concrete.

It is very interesting that the results of the BET analysis (sorption isotherms and specific surface area) do not exactly correspond to the results of dynamic sorption. This proves that the sorption of water vapour in building structures is a very complex problem.

Lessons from experiments

For scientific conclusions, it is important to evaluate experimental data using statistical methods. Such an evaluation may show a different view of the measured and published data.

This is all more important when evaluating data on inhomogeneous materials such as clay structures. These materials have a wide dispersion of the resulting properties, and therefore it is necessary to take this fact into account and evaluate the data correctly. The variance of the results can be significant depending on the statistical methods used.

Use of experimental data

A considerable amount of experimental data about the properties of building materials and building structures was measured in this work. Experimental data, in this case sorption isotherms, can be used for mathematical modelling. It is suitable for modelling the humidity behaviour of a zone or just the course of moisture in the structure/material.

The results of the medium-dimensional dynamic test can be used for further research and verification of the properties of other designed building structures. It can be used to evaluate the humidity response of the indoor environment to changes in relative humidity when using porous building materials.

Sorption properties and potential of clay materials

As expected, the sorption properties of rammed earth structures are excellent. Thanks to production technology, they can contain significantly more clay minerals than other clay structures and, thus, the highest sorption potential. Of course, this is also related to the porosity and the specific surface area of the material. The main research was on a structure made of rammed earth developed at the Faculty of Civil Engineering CTU in Prague as a prefabricated load-bearing panel. The sorption properties of similar structures strongly depend on the type and amount of clay mineral used in the structure.

The commercial product of unburned bricks achieved very good sorption results. In all experiments performed, in terms of the quality of the properties, it was just behind the rammed earth structure. The material must have a good source of soil that contains a large amount of clay minerals. A considerable advantage of an unburned brick structure is easier production compared to rammed earth technology and thus lower final cost. From an economic point of view, therefore, this structure has the greatest influence on the problematic adsorption and desorption of water vapour from the air. The biggest

disadvantage, however, is the aesthetics. Rammed earth is a much more valuable structure in terms of design. It would therefore be appropriate to expand the market for unburned bricks but also to focus on their appearance, as this material should be used as unplastered, fair-face brickwork.

The last of the group of clay materials was a detailed examination of clay plaster. As mentioned several times above, clay plasters are sometimes overrated for their properties. Although natural clay has excellent sorption properties, in practical use, clay plasters contain a certain amount of sand primarily to minimize shrinkage. Typical clay plasters contain 60–75 % of sand which rapidly diminishes the sorption ability. Such a high amount of sand means that the sorption properties of clay plaster can be on par with traditional building materials. This is shown by the results of sorption isotherms. However, dynamic experiments have shown that clay plasters still have a greater sorption potential than selected standard non-clay building structures.

However, it is necessary to look at the properties of building structures comprehensively. In addition to excellent sorption properties, clay materials also have low CO_2 emissions, are suitable for negative ion remediation, and are recyclable, etc. In terms of internal environment and environmental quality, they make very high-quality structures.

This thesis was focused only on sorption properties; other parameters are not part of this research.

Operating energy savings passive systems, e.g. by using clay materials

Compared to the technical solution of indoor microclimate conditioning in the form of forced ventilation, regulation, and intelligent control, environmentally active materials are not comparably efficient and at the same time they are not so dynamic in terms of their control. On the other hand, they are sufficiently robust and immune to extreme situations (black out, failure of the device or its parts, incorrect steering settings, etc.). With an optimal and conceptual building design, these materials can significantly reduce and, ideally, completely replace the mechanical systems for managing the quality of the indoor environment and the energy required for their operation.

At the same time, this passive solution brings other benefits for the environment – a favourable microclimate; heat and humidity accumulation of massive clay constructions (reduction of heat loss, reduction of the risk of overheating in summer, moisture buffering); discharge of negative ions in the interior; use of natural, low carbon and easily recyclable materials; etc.

The proof is shown in the examples of projects abroad and in our country, where unburned clay materials stabilize the humidity of the indoor environment. These materials can be significant, for example, in the reconstruction of prefabricated panel houses, where low humidity is generally a problem, or in archival buildings, where it is necessary to maintain a stable microclimate even in the event of power failure.

Continuation of research

Current research can continue on several fronts. For selected materials, it is possible to measure other thermal humidity parameters such as diffusion resistance, thermal conductivity, or specific heat capacity. This would add a wealth of information on these building products.

Another useful parameter would be MBV. Based on these results, it would be possible to compare the measurement procedures with other research institutes and add information about the dynamic properties of selected structures, especially clay materials. These values are still very rarely measured.

It would be very useful to create a single-zone moisture transport model that would correspond to the designed and performed dynamic sorption experiments. Based on such a model and measured data, the model could be verified and used for more complex modelling of sorption processes. This would help to better understand and describe the complex processes of water vapour transport in clay materials.

References

[1] United Nations, "Sustainable Development Goals," *United Nations Sustainable Development*, 2015. https://www.un.org/sustainabledevelopment/ (accessed Jul. 16, 2020).

[2] European Commission, "Green Deal," 12 2019. https://eur-lex.europa.eu/legal-content/EN/TXT/?qid=1588580774040&uri=CELEX:52019DC0640 (accessed Jul. 21, 2020).

[3] J. Růžička, "Influence of Way of Stabilization of Unburned Bricks on Mechanical Physical Properties." CZECH TECHNICAL UNIVERSITY IN PRAGUE, 2006.

[4] F. Havlík, "Development and Experimental Verification of Mechanical-physical Properties of Pre-formed Rammed Earth Wall Panel." CZECH TECHNICAL UNIVERSITY IN PRAGUE, 2017.

[5] N. E. Klepeis, "A Resource for Assessing Exposure to Environmental Pollutants." The National Human Activity Pattern Survey, 2001, [Online]. Available: https://indoor.lbl.gov/sites/all/files/lbnl-47713.pdf.

[6] G. Clausen, Ed., *Ventilation, good indoor air quality and rational use of energy*. Luxembourg: Office for Official Publications of the European Communities, 2003.

[7] Ing. Hana Doležílková, Ph.D., "Kvalita vnějšího a vnitřního vzduchu," *TZB-info*. https://vetrani.tzb-info.cz/vnitrni-prostredi/6486-kvalita-vnejsiho-a-vnitrniho-vzduchu (accessed Oct. 06, 2020).

[8] World Health Organization Regional Office for Europe, "Sick building syndrome." [Online]. Available: https://www.wondermakers.com/Portals/0/docs/Sick%20building%20syndrome%20by%20WHO.pdf.

[9] A. Lajčíková, "Syndrom nemocných budov." 2006, [Online]. Available: http://www1.szu.cz/chpnp/pages/education/syndrom_nemocnych_budov.pdf.

[10] Centrum pasivního domu, "Indoor air quality." https://www.pasivnidomy.cz/kvalita-vnitrniho-prostredi/t384 (accessed Jul. 22, 2020).

[11] M. V. Jokl, "Thermal Comfort and Optimum Humidity Part 1," *Acta Polytech.*, vol. 42, no. 1, Art. no. 1, Jan. 2002, doi: 10.14311/302.

[12] prof. Ing. Karel Kabele, CSc., Ing. Zuzana Veverková, PhD., Ing. Pavla Dvořáková, PhD., "Vnitřní prostředí budov," *ASB Portal*, Jun. 26, 2015. https://www.asb-portal.cz/stavebnictvi/technicka-zarizeni-budov/vetrani-a-klimatizace/vnitrni-prostredi-budov (accessed Oct. 08, 2020).

[13] I. Juhásová Šenitková, M. Kraus, P. Machová, D. Skulinová, M. Flimel, and Wydawnictwo Sztafeta, *Budovy a prostředí: adresná identifikace, analýza výskytu a metodologie optimalizace vybraných složek vnitřního prostředí budov : vědecká monografie*. Stalowa Wola – Polska: Wydawnictwo Sztafeta Sp. z o.o., 2018.

[14] M. Pinterić, *Building Physics: from physical principles to international standards*. Cham: Springer, 2017.

[15] M. Jokl, *Teorie vnitřního prostředí budov (Indoor Environmental Quality)*, 2. ed. Prague: CTU in Prague, 1991.

[16] "ANSI/ASHRAE Standard 55: Thermal Environmental Conditions for Human Occupancy." ASHRAE Headquarters: Atlanta, GA, US, 2013, Accessed: Oct. 09, 2020. [Online]. Available: ISSN 1041-2336.

[17] A. Korjenic, H. Teblick, and T. Bednar, "Increasing the indoor humidity levels in buildings with ventilation systems: Simulation aided design in case of passive houses," *Build. Simul.*, vol. 3, no. 4, pp. 295–310, Dec. 2010, doi: 10.1007/s12273-010-0015-2.

[18] Centrum pasivního domu, "Kvalita vnitřního prostředí – Pasivnidomy.cz." https://www.pasivnidomy.cz/kvalita-vnitrniho-prostredi/t384?chapterId=1832 (accessed Oct. 09, 2020).

[19] M. Kraus, "Hygrothermal Analysis of Indoor Environment of Residential Prefabricated Buildings," *IOP Conf. Ser. Mater. Sci. Eng.*, vol. 245, p. 042071, Oct. 2017, doi: 10.1088/1757-899X/245/4/042071.

[20] Mgr. Hana Bednaříková, "Voda a vzduch." [Online]. Available: ISSN 1802-4785.

[21] M. Krus, *Moisture transport and storage coefficients of porous mineral building materials*. Stuttgart: Fraunhofer IRB Verlag, 1996.

[22] ENLIST Chemistry Workshop, University of Illinois, 2010, "Structure of Water," 2010. http://butane.chem.uiuc.edu/pshapley/Enlist/Labs/WaterStruc/Teachers.html (accessed Oct. 15, 2020).

[23] M. Hakala, K. Nygård, S. Manninen, L. G. M. Pettersson, and K. Hämäläinen, "Intra- and intermolecular effects in the Compton profile of water," *Phys. Rev. B*, vol. 73, no. 3, p. 035432, Jan. 2006, doi: 10.1103/PhysRevB.73.035432.

[24] L. Svoboda, *Stavební hmoty*. Bratislava: Jaga, 2004.

[25] Anatol Malijevský, Josef P. Novák, Stanislav Labík, and Ivona Malijevská, *Breviář fyzikální chemie*, ÚFCH VŠCHT., vol. 2001. ÚFCH VŠCHT, 2001.

[26] DOKA IZOL, s.r.o., "Jak může vlhkost cestovat stavební konstrukcí?" https://www.dokaizol.cz/ (accessed Apr. 28, 2021).

[27] PAVLÍK Z., "Secondary effects on material properties characterising water vapour transport assessedby the cup method," *Staveb. Obz.*, vol. 2013, no. 07.

[28] John Straube, "BSD-138: Moisture and Materials," *Building Science Corporation*. https://www.buildingscience.com/documents/digests/bsd-138-moisture-and-materials (accessed Oct. 16, 2020).

[29] K. Y. Foo and B. H. Hameed, "Insights into the modeling of adsorption isotherm systems," *Chem. Eng. J.*, vol. 156, no. 1, pp. 2–10, Jan. 2010, doi: 10.1016/j.cej.2009.09.013.

[30] S. Airaksinen, *Role of excipients in moisture sorption and physical stability of solid pharmaceutical formulations*. 2005.

[31] J. Krňanský, "Úvaha k interpretaci faktoru difúzního odporu kapilárně pórovitých materiálů," *izolace.cz*, Jun. 05, 2009. https://www.izolace.cz/clanky/uvaha-k-interpretaci-faktoru-difuzniho-odporu-kapilarne-porovitych-materialu/ (accessed Oct. 22, 2020).

[32] J. Pechoušek, "Měření plochy povrchu pevných látek a určování jejich porozity metodou sorpce plynu," p. 19.

[33] IUPAC, "REPORTING PHYSISORPTION DATA FOR GAS/SOLID SYSTEMS with Special Reference to the Determination ofSurface Area and Porosity," *Pure App Chem*, vol. 1985, no. 57, pp. 603–619, 1985.

[34] V. Kumar *et al.*, "Characterization of adsorption site energies and heterogeneous surfaces of porous materials," *J. Mater. Chem. A*, vol. 7, Feb. 2019, doi: 10.1039/C9TA00287A.

[35] M. Thommes *et al.*, "Physisorption of gases, with special reference to the evaluation of surface area and pore size distribution (IUPAC Technical Report)," *Pure Appl. Chem.*, vol. 87, no. 9–10, pp. 1051–1069, Oct. 2015, doi: 10.1515/pac-2014-1117.

[36] M. B. Yahia, Y. B. Torkia, S. Knani, M. A. Hachicha, M. Khalfaoui, and A. B. Lamine, "Models for Type VI Adsorption Isotherms from a Statistical Mechanical Formulation:," *Adsorpt. Sci. Technol.*, Apr. 2013, Accessed: Oct. 23, 2020. [Online]. Available: https://journals.sagepub.com/doi/10.1260/0263-6174.31.4.341.

[37] R. Bulánek, *The Surface Phenomena on Solids*, 1. Univerzita Pardubice.

[38] IUPAC, "Recommendations for the Characterization of Porous Solids," *Pure & App!. Chem.*, vol. 1994, no. 66. pp. 1739–1758, 1994, doi: 10.1515/iupac.66.0925.

[39] M. M. Dubinin and A. A. Isirikyan, “Micropore structures of charcoal adsorbents,” *Bull. Acad. Sci. USSR Div. Chem. Sci.*, vol. 29, no. 1, pp. 6–10, Jan. 1980, doi: 10.1007/BF00951867.

[40] J. Kodikara, S. L. Barbour, and D. G. Fredlund, “Changes in clay structure and behaviour due to wetting and drying,” *Consol. Knowl. Proc. 8th Aust. N. Z. Conf. Geomech. Hobart Febr. 1999*, pp. 179–185, Dec. 1999.

[41] B. Zdravkov, J. Čermák, M. Šefara, and J. Janků, “Pore classification in the characterization of porous materials: A perspective,” *Open Chem.*, vol. 5, no. 2, pp. 385–395, Jun. 2007, doi: 10.2478/s11532-007-0017-9.

[42] J. Solař, *Odstraňování vlhkosti: sanace vlhkého zdiva*. Praha: Grada, 2013.

[43] M. Keppert, “Pore size distribution of building materials – characterisation and importance.” CTU in Prague, Accessed: Oct. 29, 2020. [Online]. Available: https://docplayer.cz/176655565-Ing-martin-keppert-ph-d.html.

[44] “ISO 9277:2010 Determination of the specific surface area of solids by gas adsorption — BET method.” https://www.iso.org/obp/ui/#iso:std:iso:9277:ed-2:v1:en (accessed Oct. 27, 2020).

[45] S. Brunauer, P. H. Emmett, and E. Teller, “Adsorption of Gases in Multimolecular Layers,” *J. Am. Chem. Soc.*, vol. 1938, no. 60, pp. 309–319, Feb. 1938, doi: 10.1021/ja01269a023.

[46] G. Minke, *Building with Earth – Design and Technology for a Sustainable Architecture*, 2., vol. 2009. .

[47] M. Hall and D. Allinson, “Analysis of the hygrothermal functional properties of stabilised rammed earth materials,” *Building and Environment*, vol. 44, no. 9, pp. 1935–1942, 2009, doi: https://doi.org/10.1016/j.buildenv.2009.01.007.

[48] S. Liuzzi, M. R. Hall, P. Stefanizzi, and S. P. Casey, “Hygrothermal behaviour and relative humidity buffering of unfired and hydrated lime-stabilised clay composites in a Mediterranean climate,” *Build. Environ.*, vol. 61, pp. 82–92, Mar. 2013, doi: 10.1016/j.buildenv.2012.12.006.

[49] M. Saidi, A. S. Cherif, B. Zeghmati, and E. Sediki, “Stabilization effects on the thermal conductivity and sorption behavior of earth bricks,” *Constr. Build. Mater.*, vol. 167, pp. 566–577, Apr. 2018, doi: 10.1016/j.conbuildmat.2018.02.063.

[50] H. Cagnon, J. E. Aubert, M. Coutand, and C. Magniont, “Hygrothermal properties of earth bricks,” *Energy Build.*, vol. 80, pp. 208–217, Sep. 2014, doi: 10.1016/j.enbuild.2014.05.024.

[51] L. Randazzo, G. Montana, A. Hein, A. Castiglia, G. Rodonò, and D. I. Donato, “Moisture absorption, thermal conductivity and noise mitigation of clay based plasters: The influence of mineralogical and textural characteristics,” *Appl. Clay Sci.*, vol. 132–133, pp. 498–507, Nov. 2016, doi: 10.1016/j.clay.2016.07.021.

[52] S. Liuzzi *et al.*, “Hygrothermal properties of clayey plasters with olive fibers,” *Constr. Build. Mater.*, vol. 158, pp. 24–32, Jan. 2018, doi: 10.1016/j.conbuildmat.2017.10.013.

[53] T. Ashour, A. Korjenic, and S. Korjenic, “Equilibrium moisture content of earth bricks biocomposites stabilized with cement and gypsum,” *Cem. Concr. Compos.*, vol. 59, pp. 18–25, May 2015, doi: 10.1016/j.cemconcomp.2015.03.005.

[54] F. El Fgaier, Z. Lafhaj, C. Chapiseau, and E. Antczak, “Effect of sorption capacity on thermo-mechanical properties of unfired clay bricks,” *J. Build. Eng.*, vol. 6, pp. 86–92, Jun. 2016, doi: 10.1016/j.jobe.2016.02.011.

[55] F. McGregor, A. Heath, A. Shea, and M. Lawrence, “The moisture buffering capacity of unfired clay masonry,” *Build. Environ.*, vol. 82, pp. 599–607, 2014, doi: 10.1016/j.buildenv.2014.09.027.

[56] F. McGregor, A. Heath, E. Fodde, and A. Shea, “Conditions affecting the moisture buffering measurement performed on compressed earth blocks,” *Build. Environ.*, vol. 75, pp. 11–18, May 2014, doi: 10.1016/j.buildenv.2014.01.009.

[57] I. Vitázek and J. Havelka, “Sorption isotherms of agricultural products,” *Res. Agric. Eng.*, vol. 60, no. Special Issue, pp. S52–S56, Dec. 2014, doi: 10.17221/35/2013-RAE.

[58] Carsten Rode Pedersen, “COMBINED HEAT AND MOISTURE TRANSFER IN BUILDING CONSTRUCTIONS.” Technical University of Denmark, Sep. 1990.

[59] Carsten Rode, "Moisture Buffer Value of Building Materials," *Symp. Heat-Air-Moisture Transp. Meas. Build. Mater.*, vol. 2006, 2006.

[60] S. Roels and H. Janssen, "A Comparison of the Nordtest and Japanese Test Methods for the Moisture Buffering Performance of Building Materials," *J. Build. Phys.*, vol. 30, no. 2, pp. 137–161, Oct. 2006, doi: 10.1177/1744259106068101.

[61] V. Cascione, D. Maskell, A. Shea, P. Walker, and M. Mani, "Comparison of moisture buffering properties of plasters in full scale simulations and laboratory testing," *Constr. Build. Mater.*, vol. 252, p. 119033, Aug. 2020, doi: 10.1016/j.conbuildmat.2020.119033.

[62] D. Maskell, A. Thomson, P. Walker, and M. Lemke, "Determination of optimal plaster thickness for moisture buffering of indoor air," *Build. Environ.*, vol. 130, pp. 143–150, Feb. 2018, doi: 10.1016/j.buildenv.2017.11.045.

[63] T. Padfield, "The Role of Absorbent Building Materials in Moderating Changes of Relative Humidity." Technical University of Denmark, 1998.

[64] T. Mitamura, C. Rode, and J. Schultz, "Full-scale testing of indoor humidity and moisture buffering in building materials," Accessed: Mar. 12, 2021. [Online]. Available: https://users.encs.concordia.ca/~raojw/crd/reference/reference001349.html.

[65] M. Salonvaara, T. Ojanen, A. Holm, and H. M. Künzel, "Moisture Buffering Effects on Indoor Air Quality— Experimental and Simulation Results," p. 11.

[66] L. H. Mortensen, C. Rode, and R. H. Peuhkuri, "Full scale tests of moisture buffer capacity of wall materials," in *Proceedings of the 7th Symposium on Building Physics in the Nordic Countries*, 2005, pp. 662–669, Accessed: Apr. 20, 2020. [Online]. Available: https://orbit.dtu.dk/en/publications/full-scale-tests-of-moisture-buffer-capacity-of-wall-materials.

[67] V. Cascione, D. Maskell, A. Shea, and P. Walker, "A review of moisture buffering capacity: From laboratory testing to full-scale measurement," *Constr. Build. Mater.*, vol. 200, pp. 333–343, Mar. 2019, doi: 10.1016/j.conbuildmat.2018.12.094.

[68] B. K. Kreiger and W. V. Srubar, "Moisture buffering in buildings: A review of experimental and numerical methods," *Energy Build.*, vol. 202, p. 109394, Nov. 2019, doi: 10.1016/j.enbuild.2019.109394.

[69] P. Walker, Ed., *Rammed earth: design and construction guidelines*. Watford: BRE Bookshop, 2005.

[70] A. Heringer, L. B. Howe, and M. Rauch, *Upscaling earth: material, process, catalyst*. 2019.

[71] A. Weismann, K. Bryce, and R. Main, *building with cob: a step-by-step guide*. Cambridge: Green Books, 2013.

[72] T. Krahn, *Essential rammed earth construction: the complete step-by-step guide*. 2019.

[73] R. Niemeyer, *Der Lehmbau und seine praktische Anwendung*, Unveränd. Nachdr. d. Originalausg. aus dem Jahre 1946. Staufen bei Freiburg/Br: Ökobuch-Verl, 1992.

[74] O. Kapfinger and M. Rauch, *Rammed Earth*. Basel ; Boston: Birkhäuser, 2001.

[75] C. Ziegert, *Lehmwellerbau: Konstruktion, Schäden und Sanierung*. Stuttgart: Fraunhofer IRB Verl, 2003.

[76] R. Rael, *Earth architecture*, 1. paperback ed. New York, N.Y: Princeton Architectural Press, 2009.

[77] H. Houben and H. Guillaud, *Earth construction: a comprehensive guide*. London: Intermediate Technology Publ, 1994.

[78] I. Žabičková, *Hliněné stavby*. Brno: ERA, 2002.

[79] P. Suske, *Hlinené domy novej generácie.* Bratislava: Alfa, 1991.

[80] "Engineering Classification of Earth Materials," in *National Engineering Handbook*, United States Department of Agriculture, 2012.

[81] "ISO 14688-1:2002," *ISO*. https://www.iso.org/cms/render/live/en/sites/isoorg/contents/data/standard/02/52/25260.html (accessed Oct. 30, 2020).

[82] "Sieve analysis," *Wikipedia*. Oct. 14, 2020, Accessed: Oct. 30, 2020. [Online]. Available: https://en.wikipedia.org/w/index.php?title=Sieve_analysis&oldid=983436803.

[83] J. Jamila and M. ZOUKAGHE, "EVOLUTION OF EXPANSIVE SOILS STRUCTURE WITH DIFFERENT SOLICITATIONS AND EFFECT OF SOME PARAMETERS ON SWELLING PROPERTIES – REVIEW ARTICLE," *Theor. Appl. Sci.*, vol. 37, pp. 68–77, May 2016, doi: 10.15863/TAS.2016.05.37.14.

[84] Torraca G., *Porous building materials – materials science for architectural conservation*. Rome, Italy: ICCROM, 2005.

[85] D. Liu *et al.*, "High-pressure adsorption of methane on montmorillonite, kaolinite and illite," *Appl. Clay Sci.*, vol. 85, pp. 25–30, Nov. 2013, doi: 10.1016/j.clay.2013.09.009.

[86] V. ŠUCHA, *Íly v geologických procesoch*. Bratislava: Univerzita Komenského Bratislava, 2001.

[87] G. Segonzac, "The transformation of clay minerals during diagenesis and low-grade metamorphism: A review," *Sedimentology*, vol. 15, pp. 281–346, Feb. 2011, doi: 10.1111/j.1365-3091.1970.tb02190.x.

[88] "HERZOG & DE MEURON." https://www.herzogdemeuron.com/index.html (accessed Apr. 29, 2021).

[89] "Adam Rujbr Architects." http://www.ararchitects.cz/cs/reference/detail/174?kategorie=top-reference (accessed Feb. 28, 2021).

[90] "Klimareferat der Vereinten Nationen, D-53113 Bonn › Dachverband Lehm e.V." https://www.dachverband-lehm.de/bauwerke/unfccc-klimareferat-der-vereinten-nationen-bonn (accessed Feb. 28, 2021).

[91] "Sluňákov," *Sluňákov*. https://slunakov.cz/ (accessed Apr. 29, 2021).

[92] "EN ISO 12571 (2013) Hygrothermal performance of building materials and products. Determination of hygroscopic sorption properties." .

[93] A. Carotenuto and M. Dell'Isola, "An experimental verification of saturated salt solution-based humidity fixed points," *Int. J. Thermophys.*, vol. 17, no. 6, pp. 1423–1439, Nov. 1996, doi: 10.1007/BF01438677.

[94] L. Greenspan, "Humidity fixed points of binary saturated aqueous solutions," *J. Res. Natl. Bur. Stand. Sect. Phys. Chem.*, vol. 81A, no. 1, p. 89, Jan. 1977, doi: 10.6028/jres.081A.011.

[95] "EN 772-13 (2001) Methods of test for masonry units – Part 13: Determination of net and gross dry density of masonry units (except for natural stone)." .

[96] Comet System, s.r.o., "COMET S3120." Comet System, [Online]. Available: https://www.cometsystem.cz/pdf/s3120.

[97] A&D, "A&D – GX-400 – Precision Balance." https://www.affordablescales.com/and/gx-s/gx-400.asp# (accessed Nov. 11, 2020).

[98] "3 Flex General Interest | Micromeritics." https://www.micromeritics.com/3-Flex-General-Interest.aspx (accessed Aug. 11, 2020).

[99] I. Mills, International Union of Pure and Applied Chemistry, and International Union of Pure and Applied Chemistry, Eds., *Quantities, units, and symbols in physical chemistry*, 2nd ed. Oxford ; Boston : Boca Raton, Fla: Blackwell Scientific Publications ; CRC Press [distributor], 1993.

[100] J. Růžička, J. Diviš, K. Staněk, and J. Richter, "The influence of natural clays and earthen structures on relative humidity of internal microclimate," Weimar, 2016, vol. 2016.

[101] K. Gertis and H. Erhorn, "Wohnfeuchte und Wärmebrücken," *Heiz. LüftungKlima Haustech.*, vol. 36, no. 3, pp. 130–135, 1985.

[102] Heluz, "Technický list – Heluz." [Online]. Available: https://www.heluz.cz/files/12080_20-Technicky-list-CZ.pdf.

[103] Cemix, "Technický list – Cemix." [Online]. Available: https://www.cemix.cz/produkty/zdici-malta-5-mpa#soubory.

[104] Hasit, "Technický list – Hasit jádrová omítka." [Online]. Available: https://www.hasit.cz/produkty/detailseite/hasit-666-kalkputz-299953.

[105] Hasit, "Technický list – Hasit vápenný štuk." [Online]. Available: https://www.hasit.cz/produkty/detailseite/hasit-160-fein-kalkputz-424218.

[106] X. P. s.r.o, "HELUZ NATURE Energy 12/25 | HELUZ." https://www.heluz.cz/cs/vyrobek/heluz-nature-energy-12-25-1 (accessed Aug. 26, 2020).

[107] "Přilnavostní nátěr – Picas." https://www.picas.cz/prilnavostni-nater/ (accessed Aug. 26, 2020).

[108] "Picas ECONOM – hrubá – Picas." https://www.picas.cz/picas-econom-hruba/ (accessed Aug. 26, 2020).

[109] "Hliněná omítka jemná – Picas." https://www.picas.cz/jemna-econom/ (accessed Aug. 26, 2020).

[110] ROTRONIC, "ROTRONIC – Main Catalogue_Measurement devices for relative humidity, temperature, CO2 and differential pressure." [Online]. Available: file:///C:/Users/divisja4/AppData/Local/Temp/productattachments_files_r_o_rotronic_england_catalogue_v16_low.pdf.

[111] WEISS, "Climate Test Chambers WK3 WKS3." weisstechnik, [Online]. Available: https://weiss-na.com/wp-content/uploads/Climate-Test-Chambers-WK3-WKS3-1.pdf.

[112] V. Dupač and M. Hušková, *Pravděpodobnost a matematická statistika*. Praha: Karolinum, 1999.

[113] GUM, Ed., *Guide to the expression of uncertainty in measurement*, 1st ed. 2008. Genève, Switzerland: International Organization for Standardization, 2008.

[114] A. D. Aczel, *Complete Business Statistics*, 7 th. 2009.

[115] "ČSN ISO 3534-1." Statistics – Vocabulary and symbols – Part 1: General statistical terms and terms used in probability, Winter 2010.

[116] "ČSN ISO 3534-2." Statistics – Vocabulary and symbols – Part 2: Applied statistics, 9 2010.

[117] "ČSN ISO 3534-3." Statistics – Vocabulary and symbols – Part 3: Design of experiments, 12 2019.

[118] H. Akaike, "A new look at the statistical model identification," *IEEE Trans. Autom. Control*, vol. 19, no. 6, pp. 716–723, Dec. 1974, doi: 10.1109/TAC.1974.1100705.

[119] E. Ostertagová, "Modelling using Polynomial Regression," *Procedia Eng.*, vol. 48, pp. 500–506, Jan. 2012, doi: 10.1016/j.proeng.2012.09.545.

List of tables

List of figures